

**Department of Chemical Engineering**

**Formation and Characteristics of Glucose Oligomers during the  
Hydrolysis of Cellulose in Hot-Compressed Water**

**Yun Yu**

**This thesis is presented for the Degree of  
Doctor of Philosophy  
of  
Curtin University of Technology**

**December 2009**

**Declaration**

To the best of my knowledge and belief this thesis contains no material previously published by any other person except where due acknowledgement has been made.

This thesis contains no material which has been accepted for the award of any other degree or diploma in any university.

Signature:.....

Date:.....

To my beloved family

**ABSTRACT**

Energy production from fossil fuels results in significant carbon dioxide emission, which is a key contributor to global warming and the problems related to climate change. Biomass is recognized as an important part of any strategy to address the environmental issues related to fossil fuels usage for sustainable development. The carbohydrates in lignocellulosic biomass mainly exist as cellulose and hemicellulose. These materials must be broken down through hydrolysis for the production of desired biomass extracts (e.g. sugar products), which can then be converted into ethanol. Developing efficient hydrolysis processes is essential to producing biomass extracts of desired properties. Due to its unique physical and chemical properties, hot compressed water (HCW) may be utilized as both solvent and reactant simultaneously in various applications including hydrolysis. So far, there has been a lack of fundamental understanding of biomass and cellulose hydrolysis in HCW. The present study aims to characterize the formation of glucose oligomers in the primary liquid products, and to bring some new insights into the reaction mechanisms of cellulose hydrolysis in HCW.

The specific objectives of this research include the development of a new sampling and analytical method to characterise the glucose oligomers in the liquid products, to investigate the formation of precipitate from fresh liquid products, to understand the primary reactions on the surface of reacting cellulose particle during hydrolysis in HCW at various temperatures, to study the significant differences in hydrolysis behavior of amorphous and crystalline portions within microcrystalline cellulose, to investigate the evolution of primary liquid products with conversion, and to study the effect of ball milling on the hydrolysis of microcrystalline cellulose in HCW. To accomplish these objectives, a semicontinuous reactor system was developed and set up to carry out the experiments of the hydrolysis of various cellulose samples in HCW. The liquid samples were characterised by a number of analytical instruments, including the introduction of a new technique to analyse the glucose oligomers in the liquid sample.

First of all, this study shows the presence of a wide range of glucose oligomers with the degree of polymerizations (DPs) up to 30 and their derivatives in the fresh liquid products, which is produced from cellulose hydrolysis in HCW using a semicontinuous reactor system at 280 °C and 20 MPa, by a high performance anion exchange chromatography with pulsed amperometric detection (HPAEC-PAD). None of those oligomers can be detected by a high performance liquid chromatography with evaporative light scattering detector (HPLC-ELSD) that however can detect glucose oligomers with DPs up to 6 after the liquid solutions are concentrated by 25 times via vacuum evaporation at 40 °C, during which a large amount of precipitate was formed. While quantitative analysis of the glucose oligomers with DPs > 5 cannot be done due to the lack of standards, that of the glucose oligomers from glucose (DP = 1) to cellopentaose (DP = 5) using both HPAEC-PAD and HPLC-ELSD are in good agreement, suggesting that these low-DP glucose oligomers do not contribute to the precipitate formation.

Secondly, the study of a set of purposely-designed precipitation experiments indicates that the precipitation starts as the fresh liquid sample is collected and is fast during the initial 8 hours, levels off as the precipitation time increases further and completes after 120 hours (5 days). Based on a new approach developed for the quantification of glucose oligomers retention during the precipitation process, it is found that the contribution of glucose oligomers to precipitate formation increases with DP. The higher the DP is, the lower the solubility of the glucose oligomer is. The glucose oligomers from glucose to cellopentaose and their derivatives (DPs = 1-5) contribute little to the precipitate formation, which explains why HPLC-ELSD can correctly analyze these glucose oligomers in the concentrated solutions prepared by vacuum evaporation. The glucose oligomers and their derivatives with DPs > 5, which are soluble in HCW but become supersaturated in the solutions under ambient conditions, are responsible for precipitate formation. Most (but not all) of the glucose oligomers and their derivatives with DPs > 16 contribute to the precipitate formation as tiny peaks of these glucose oligomers are still shown in the chromatograms, suggesting that these glucose oligomers have very low (but non-zero) solubilities in ambient water. The retentions of glucose oligomers and their derivatives increase substantially with the DP decreasing from 16 to 6, indicating that less of these lower-

DP oligomers contribute to the precipitate formation. To avoid the effect of precipitation on oligomer analysis, the fresh liquid products must be analyzed immediately after sample collection.

Thirdly, this study reports the experimental results on the primary liquid products from the hydrolysis of microcrystalline cellulose in HCW at 10 MPa and 230-270 °C using a semicontinuous reactor system under optimised reaction conditions. The primary liquid products contain glucose oligomers and their derivatives with a wide range of degrees of polymerization (DPs) from 1 to a maximal DP, which increases with temperature from 23 at 230 °C, to 25 at 250 °C then to 28 at 270 °C. Temperature also has a significant influence on the distribution of glucose oligomers in the primary liquid products. The results suggest that the hydrolysis reactions proceed on the surface of reacting cellulose particles via the cleavage of the accessible glycosidic bonds within the structure of microcrystalline cellulose in a manner with randomness. Thermal cleavage of glycosidic bonds seems also to occur on the accessible surface of the reacting cellulose particles in a similar manner. The randomness of these reactions seems to be temperature dependent and is likely related to the change in the accessibility of glycosidic bonds as results of the cleavage of hydrogen bonds in the structure of microcrystalline cellulose. The hydrolysis reactions seem also to be accompanied by other parallel reactions (e.g. cross-linking reactions), which may affect the primary liquid products as well, particularly at high temperatures. The post hydrolysis of primary liquid products has a high glucose yield of ~80% on a carbon basis, suggesting that combining HCW and enzymatic hydrolysis may be a promising technology for sugar recovery from lignocellulosic feedstocks.

Fourthly, this study finds that the reactivity of microcrystalline cellulose exhibits a considerable reduction in the initial stage during hydrolysis in HCW, due to the presence of amorphous structure in microcrystalline cellulose. Further analysis of the liquid products obtained at various temperatures suggests that amorphous portion within microcrystalline cellulose contains some short glucose chain segments hinged with crystalline cellulose via weak bonds (e.g. hydrogen bonds). These short chain segments are reactive components responsible for the formation of C4-C13 in the

primary liquid products during hydrolysis in HCW at temperatures as low as 100 °C. The minimal temperature for breaking the glycosidic bonds in those short chain segments to form glucose monomer from amorphous portion within microcrystalline cellulose is ~150 °C. However, the minimal temperature at which glucose monomer starts to be produced from the crystalline portion within microcrystalline cellulose is around 180 °C, apparently due to the limited accessibility of the glycosidic bonds in the crystalline portion to HCW as results of the strong intra- and inter-molecule hydrogen bonding networks. The differences of chain length and hydrogen bonding pattern between amorphous and crystalline cellulose also greatly affects the distribution of glucose oligomers in their liquid products during hydrolysis in HCW. Generally, amorphous cellulose produces more glucose mono- and oligomers at the same hydrolysis temperature, but the selectivity ratios of glucose oligomers in the primary liquid products from amorphous and crystalline portions do not show a monotonic trend with DP, at least partly resulting from the presence of shorter glucose chain segments in amorphous portion within the microcrystalline cellulose.

Fifthly, this study demonstrates the dynamic evolution of the specific reactivity and primary liquid products with conversion during the hydrolysis of both amorphous and crystalline cellulose in HCW. The results suggest the dynamic changes in cellulose structure occur during conversion, and strongly depend on reaction temperature. Results from a set of purposely-designed two-step experiments further confirm at least two mechanisms which may be responsible for such structural changes. One is the selective consumption of the reactive components within the intrinsically heterogeneous cellulose at early conversions. This mechanism dominates during the hydrolysis of at low temperatures, e.g. 180-200 °C for amorphous cellulose and 230 °C for microcrystalline cellulose. The other is the combined effects of various parallel reactions during hydrolysis in HCW, including cleavage of hydrogen bonds, degradation reactions and cross-linking reactions. Enhanced hydrogen bond cleavage increases the production of glucose oligomers. However, parallel degradation reactions and cross-linking reactions decrease the selectivities of glucose oligomers. The effect of cross-linking increases significantly with temperature and becomes dominant at high temperature, leading to a structural

condensation hence a reduction in the specific reactivity of cellulose and the selectivities of glucose oligomers in the primary liquid products.

Sixthly, this study investigates the effect of ball milling as a pretreatment method on microcrystalline cellulose hydrolysis in HCW. Ball milling leads to a considerable reduction in cellulose particle size and crystallinity therefore a significant increase in the specific reactivity during hydrolysis in HCW. It is found that crystallinity is the dominant factor in determining the hydrolysis reactivity of cellulose in HCW while particle size only plays a minor role. Ball milling also significantly influences the distribution of glucose oligomers in the primary liquid products of hydrolysis. Ball milling increases the selectivities of glucose oligomers at low conversions. At high conversions, the reduction in chain length plays an important role in glucose oligomer formation since cellulose samples become more crystalline. An extensive ball milling completely converts the crystalline cellulose into amorphous cellulose, leading to a significant increase in the formation of high-DP glucose oligomers. It seems that ball milling is a good strategy for improving cellulose hydrolysis reactivity in HCW.

Overall, the present research has provided valuable information for the fundamental understanding of the mechanisms of cellulose hydrolysis in HCW. The development of a sampling and analytical method makes it possible to characterise the glucose oligomers in the liquid products and understand the formation of precipitate in the liquid products. The primary liquid products of cellulose hydrolysis in HCW, which were firstly reported in this field, are of great importance to elucidate the primary hydrolysis reactions of cellulose hydrolysis in HCW. The structural differences between amorphous and crystalline cellulose, as well as the evolution of structural changes with conversion during hydrolysis in HCW were also revealed. This study further estimated the effect of ball milling on the improvement in the performance of cellulose hydrolysis in HCW.



## ACKNOWLEDGEMENTS

I gratefully acknowledge the CIRTS scholarship received from Curtin University of Technology for my PhD research, which is financially supported by the Australian Research Council through its Discovery Project Program (Grant DP0559636).

I would like to express my deepest gratitude to my supervisor, Professor Hongwei Wu, for providing me the opportunity for this research and for his invaluable advice, guidance, support, patience, inspiration as well as devotion in supervision during the course of this research. Without him, my PhD research would not be possible.

I am deeply grateful to my co-supervisor, Associate Professor Xia Lou, and my thesis committee chairperson, Professor Moses Tade, for their advice, assistance, and help as thesis committee members.

I am indebted to my beloved family, for their support, encouragement and understanding during my 4 years of PhD study overseas. Most importantly, I would like to express my greatest appreciation to my wife for her love, support and encouragement. The birth of our daughter brings me so much joy and happiness.

Special thanks go to Dr. Peter Grayling (Western Australian Department of Environment and Conservation) for his advice and assistance in the HPLC analysis. I would like to express my appreciation to Ms. Karen Haynes, as well as Mr. Zeno Zhang and Ms. Ann Carroll, for their laboratory assistances. Dr. Fujun Tian, Dr. Kongvui Yip, Mr. Qiang Fu, Mr. Xiangpeng Gao, Ms. Yi Li, Ms. Hanisom Abdullah, Mr. William Hendrawinata in our research group, my friend Mr. Chao Li, as well as all my other colleagues in Department of Chemical Engineering, are thanked for their help in various ways. Thanks also go to the staff members from Department of Chemical Engineering for their assistances, and the staff from Department of Applied Physics for guidance in SEM and XRD analyses.

---

## LIST OF PUBLICATIONS

### Journal Papers

- [1] **Yun Yu**, Xia Lou, Hongwei Wu. Some Recent Advances in Hydrolysis of Biomass in Hot-Compressed Water and Its Comparisons with Other Hydrolysis Methods, *Energy & Fuels* **2008**, 22: 46-60.
- [2] **Yun Yu**, John Bartle, Chun-Zhu Li, Hongwei Wu. Mallee Biomass as a Key Bioenergy Source in Western Australia: Importance of Biomass Supply Chain, *Energy & Fuels* **2009**, 23: 3290-3299.
- [3] **Yun Yu**, Hongwei Wu. Characteristics and Precipitation of Glucose Oligomers in the Fresh Liquid Products Obtained from the Hydrolysis of Cellulose in Hot-Compressed Water, *Ind. Eng. Chem. Res.* **2009**, 48: 10682-10690.
- [4] **Yun Yu**, Hongwei Wu. Understanding the Primary Liquid Products of Cellulose Hydrolysis in Hot-Compressed Water at Various Reaction Temperatures, *Energy & Fuels*, **2010**, 24: 1963-1971.
- [5] **Yun Yu**, Hongwei Wu. Significant Differences in the Behavior of Amorphous and Crystalline Portions within Microcrystalline Cellulose during Hydrolysis in Hot-Compressed Water, *Ind. Eng. Chem. Res.*, DOI: 10.1021/ie901925g. Published Online: March 2, 2010.
- [6] **Yun Yu**, Hongwei Wu. Evolution of Primary Liquid Products and Evidence of in Situ Structural Changes in Cellulose with Conversion during Hydrolysis in Hot-Compressed Water, *Ind. Eng. Chem. Res.*, DOI: 10.1021/ie902020t. **in press**.

### Submitted Journal Papers

- [1] **Yun Yu**, Hongwei Wu. Effect of Ball Milling on the Hydrolysis of Microcrystalline Cellulose in Hot-Compressed Water, *AIChE Journal*, **submitted**.

### Conference Papers

- [1] **Yun Yu**, John Bartle, Hongwei Wu. Production of Mallee Biomass in Western Australia: Life Cycle Greenhouse Gas Emissions. *CHEMECA 2008*, September 28 - October 1, 2008, Newcastle City Hall, Newcastle, Australia.

- [2] **Yun Yu**, Hongwei Wu. Hydrolysis of Cellulose in Hot-Compressed Water under Continuous-Flow Reaction Conditions. *12th Aisa Pacific Confederation of Chemical Engineering Congress (APCCChE 2008)*, August 4-6, 2008, Dalian, China.
- [3] **Yun Yu**, John Bartle, Hongwei Wu. Modelling of Production and Transport of Mallee Biomass in Western Australia. '*Bioenergy Australia 2007*' Conference, November 26-28, 2007, Gold Coast International Hotel, Surfers Paradise, Queensland, Australia.
- [4] **Yun Yu**, Hongwei Wu. Economic Viability of Ethanol Production from Mallee Biomass in Western Australia. *CHEMECA 2007*, September 23-26, 2007, Sofitel Melbourne, Victoria, Australia.
- [5] **Yun Yu**, Xia Lou, Hongwei Wu. Biomass Hydrolysis for Sugar Recovery: a Review. *CHEMECA 2007*, September 23-26, 2007, Sofitel Melbourne, Victoria, Australia.
- [6] **Yun Yu**, Xia Lou, Hongwei Wu. Hydrolysis of Biomass in Hot-Compressed Water and its Comparisons with Other Hydrolysis Methods. *International Conference on Bioenergy Outlook2007: Issues, Advances and Opportunities in Biomass Energy*, April 26-27, 2007, Singapore.

**TABLE OF CONTENTS**

**Declaration.....I**

**ABSTRACT ..... III**

**ACKNOWLEDGEMENTS.....VIII**

**LIST OF PUBLICATIONS.....IX**

**TABLE OF CONTENTS.....XI**

**LIST OF FIGURES ..... XVII**

**LIST OF TABLES .....XXIII**

**CHAPTER 1 INTRODUCTION ..... 1**

    1.1 Background and Motive ..... 1

    1.2 Scope and Objectives ..... 3

    1.3 Thesis Outline ..... 3

**CHAPTER 2 LITERATURE REVIEW ..... 5**

    2.1 Introduction ..... 5

    2.2 Biomass Components..... 5

        2.2.1 Cellulose..... 6

        2.2.2 Hemicellulose..... 9

        2.2.3 Lignin ..... 9

        2.2.4 Other Components ..... 10

    2.3 Biomass Hydrolysis in Hot-Compressed Water ..... 11

        2.3.1 Properties of HCW ..... 11

        2.3.2 Cellulose Hydrolysis in HCW..... 14

            2.3.2.1 Mechanisms of Cellulose Hydrolysis in HCW ..... 14

            2.3.2.2 Mechanisms of Glucose Decomposition in HCW ..... 17

        2.3.3 Factors Influencing Cellulose Hydrolysis in HCW ..... 20

            2.3.3.1 Feedstock Property..... 20

            2.3.3.2 Reactor Configuration..... 21

2.3.3.3 HCW Property.....	22
2.3.3.4 Heating Rate.....	23
2.3.3.5 Catalyst.....	24
2.3.4 Hemicellulose Hydrolysis in HCW.....	24
2.3.5 Lignocellulosic Biomass Hydrolysis in HCW.....	26
2.3.6 Sugar Recovery.....	29
2.3.7 Reaction Kinetics of Model Compounds and Biomass Hydrolysis in HCW .....	31
2.3.8 Modelling of Model Compounds and Biomass Hydrolysis in HCW.....	34
2.4 Comparisons with Other Biomass Hydrolysis Technologies.....	34
2.4.1 Acid Hydrolysis.....	34
2.4.1.2 Dilute Acid Hydrolysis.....	35
2.4.1.2 Concentrated Acid Hydrolysis.....	35
2.4.2 Alkaline Hydrolysis.....	36
2.4.3 Enzymatic Hydrolysis.....	36
2.4.4 Comparison.....	38
2.5 Conclusions and Research Gaps.....	39
2.6 Research Objectives of the Present Study.....	40
<b>CHAPTER 3 METHODOLOGY AND ANALYTICAL TECHNIQUES.....</b>	<b>42</b>
3.1 Introduction.....	42
3.2 Methodology.....	42
3.2.1 Characteristics and Precipitation of Glucose Oligomers in the Fresh Liquid Products.....	44
3.2.2 Primary Liquid Products at Various Reaction Temperatures.....	44
3.2.3 Different Behaviors between Amorphous and Crystalline Portions within Microcrystalline Cellulose.....	45
3.2.4 Evolution of Primary Liquid Products and Evidence of in situ Structure Changes with Conversion.....	45
3.2.5 Hydrolysis of Pretreated Microcrystalline Cellulose by Ball Milling.....	45
3.3 Experimental.....	46
3.3.1 Raw Material.....	46
3.3.2 Sample Preparation.....	46

3.3.3 Reactor System.....	48
3.3.4 Precipitation of Fresh Liquid Products .....	52
3.3.5 Post Hydrolysis .....	52
3.4 Instruments and Analytical Techniques .....	52
3.4.1 High-Performance Liquid Chromatography with Evaporative Light Scattering Detector (HPLC-ELSD).....	52
3.4.2 High-Performance Anion Exchange Chromatography with Pulsed Amperometric Detection (HPAEC-PAD).....	54
3.4.3 Total Organic Carbon (TOC) Analysis .....	57
3.4.4 Specific Reactivity Analysis .....	58
3.4.5 X-ray Diffraction (XRD) Analysis.....	59
3.4.6 Particle Size Analysis.....	59
3.4.7 Scanning Electron Microscope (SEM) Analysis .....	59
3.5 Summary .....	60
 <b>CHAPTER 4 CHARACTERISTICS AND PRECIPITATION OF GLUCOSE OLIGOMERS IN THE FRESH LIQUID PRODUCTS.....</b>	
<b>61</b>	
4.1 Introduction .....	61
4.2 Analysis of Glucose Oligomers in the Liquid Products.....	63
4.2.1 HPLC-ELSD Analysis .....	63
4.2.2 HPAEC-PAD Analysis .....	63
4.2.3 Comparison between HPLC-ELSD and HPAEC-PAD Analysis .....	65
4.3 Precipitation of Glucose Oligomers from the Fresh Liquid Products.....	67
4.3.1 TOC Analysis.....	67
4.3.2 HPAEC-PAD Analysis .....	68
4.3.2.1 Development of a Method for Quantifying the Retention of Glucose Oligomers after Precipitation .....	68
4.3.2.2 Retention of Glucose Oligomers after Precipitation .....	70
4.3.2.3 Effect of Initial Concentration on the Retention of Glucose Oligomers after Precipitation .....	73
4.4 Characterization of Precipitate.....	74
4.5 Further discussion .....	75
4.6 Conclusions .....	77

---

<b>CHAPTER 5 PRIMARY LIQUID PRODUCTS AT VARIOUS REACTION TEMPERATURES .....</b>	<b>80</b>
5.1 Introduction .....	80
5.2 Identification of Reaction Conditions to Obtain the Liquid Products with Minimized Secondary Reactions.....	83
5.2.1 Cellulose Conversion at Various Flow Rate .....	83
5.2.2 Development of a Method for Comparing the Selectivity of Glucose Oligomers.....	84
5.2.3 Selectivity Ratios of Glucose Oligomers at Various Flow Rates .....	85
5.3 Effect of Sample Loading on the Liquid Products of Cellulose Hydrolysis in HCW .....	87
5.4 Effect of Reaction Temperature on the Primary Liquid Products of Cellulose Hydrolysis in HCW.....	88
5.4.1 HPAEC-PAD Chromatograms of Primary Liquid Products at Various Temperatures.....	88
5.4.2 Comparison of the Selectivity of Glucose Oligomers in the Primary Liquid Products.....	94
5.5 Glucose Yield Recovered via Post Hydrolysis .....	95
5.6 Conclusions .....	96
 <b>CHAPTER 6 DIFFERENT BEHAVIORS BETWEEN AMORPHOUS AND CYRSTALLINE PORTIONS WITHIN MICROCRYSTALLINE CELLULOSE .....</b>	 <b>98</b>
6.1 Introduction .....	98
6.2 Specific Reactivity of Cellulose during Hydrolysis in HCW .....	100
6.3 Heterogeneity in the Structures of Microcrystalline Cellulose.....	101
6.4 Hydrolysis Behavior of the Amorphous Portion within Microcrystalline Cellulose.....	103
6.4.1 Amorphous Portion within Raw Microcrystalline Cellulose .....	103
6.4.2 Amorphous Portion within Pretreated Microcrystalline Cellulose .....	106
6.5 Hydrolysis of the Crystalline Portion within Microcrystalline Cellulose in HCW .....	108

6.6 Comparisons between the Hydrolyses of the Amorphous and Crystalline Portions within Microcrystalline Cellulose.....	111
6.7 Conclusions .....	112
<b>CHAPTER 7 EVOLUTION OF PRIMARY LIQUID PRODUCTS AND EVIDENCE OF IN SITU STRUCTURAL CHANGES WITH CONVERSION</b>	<b>114</b>
7.1 Introduction .....	114
7.2 XRD Analysis of Microcrystalline and Amorphous Samples .....	115
7.3 Evolution of Specific Reactivity as a Function of Conversion during the Hydrolysis of Cellulose in HCW .....	116
7.3.1 Hydrolysis of Amorphous Cellulose.....	116
7.3.2 Hydrolysis of Microcrystalline Cellulose .....	116
7.4 Evolution of Primary Liquid Products as a Function of Conversion during the Hydrolysis of Cellulose in HCW. ....	118
7.4.1 Hydrolysis of Amorphous Cellulose.....	118
7.4.2 Hydrolysis of Microcrystalline Cellulose .....	119
7.5 Effect of in Situ Pretreatment on the Evolution of Specific Reactivity and Primary Liquid Products with Conversion.....	123
7.5.1 Pretreatment of Amorphous Cellulose .....	123
7.5.2 Pretreatment of Microcrystalline Cellulose .....	124
7.6 Conclusions .....	128
<b>CHAPTER 8 EFFECT OF BALL MILLING ON THE HYDROLYSIS OF MICROCRYSTALLINE CELLULOSE</b> .....	<b>130</b>
8.1 Introduction.....	130
8.1 Changes in Cellulose Structure due to Ball Milling.....	131
8.1.1 Change in Particle Size Distribution.....	131
8.1.2 Change in X-ray Diffraction Pattern.....	132
8.2 Effect of Ball Milling on the Evolution of Specific Reactivity of Cellulose during Hydrolysis in HCW. ....	133
8.2.1 Cellulose Conversion .....	133
8.2.2 Evolution of Specific Reactivity .....	134



8.3 Dominant Role of Crystallinity in Cellulose Reactivity during Cellulose Hydrolysis in HCW .....	135
8.4 Comparisons between the Primary Liquid Products Produced from the Raw and Ball-Milled Cellulose during Hydrolysis in HCW .....	137
8.4.1 Comparisons of IC Chromatograms.....	137
8.4.2 Comparisons of Selectivities of Glucose Oligomers in the Primary Liquid Products.....	138
8.5 Further Discussion on Mechanisms of Cellulose Hydrolysis in HCW .....	141
8.6 Conclusions .....	143
<b>CHAPTER 9 CONCLUSIONS AND RECOMMENDATIONS .....</b>	<b>145</b>
9.1 Introduction .....	145
9.2 Conclusions .....	145
9.2.1 Characteristics and Precipitation of Glucose Oligomers in the Fresh Liquid Products.....	145
9.2.2 Primary Liquid Products at Various Reaction Temperatures .....	147
9.2.3 Different Behaviors between Amorphous and Crystalline Portions within Microcrystalline Cellulose .....	148
9.2.4 Evolution of Primary Liquid Products and Evidence of in Situ Structural Changes with Conversion .....	149
9.2.5 Effect of Ball Milling on the Hydrolysis of Microcrystalline Cellulose.	150
9.3 Recommendations .....	151
<b>REFERENCES.....</b>	<b>154</b>

**LIST OF FIGURES**

Figure 1-1: Thesis map..... 4

Figure 2-1: Typical plant cell wall arrangement<sup>69</sup> ..... 6

Figure 2-2: Chemical structure of cellulose with intrachain and interchain hydrogen-bonded bridging<sup>71</sup> ..... 8

Figure 2-3: The structures of p-coumaryl alcohol, coniferyl alcohol and sinapyl alcohol<sup>27</sup> ..... 10

Figure 2-4: Partial structure of a hardwood lignin molecule<sup>90</sup> ..... 10

Figure 2-5: Selected properties of water at high temperature and high pressure.<sup>68</sup> IP: ionic product, expressed as  $\log[\text{H}_3\text{O}^+][\text{OH}^-]$ ;  $\epsilon$ : relative dielectric constant, a higher  $\epsilon$  reduces the activation energy of a reaction with a transition state of higher polarity compared to the initial state;  $\rho$ : density, defined as mass per unit volume..... 12

Figure 2-6: Temperature and pressure dependence of water density.<sup>45</sup> Region I: 773-973 K; Region II: 647-773 K; Region III: below 647 K..... 13

Figure 2-7: Proposed reaction mechanism of microcrystalline cellulose in subcritical and supercritical water.<sup>44</sup> 1) Swelled (or Dissolved) cellulose; 2) cellooligosaccharides; 3) glucose; 4) erythrose; 5) glycolaldehyde; 6) fructose; 7) glyceraldehyde; 8) dihydroxyacetone; 9) pyruvaldehyde; 10) 5-HMF; 11) 2-furfural; 12) glucopyranosyl-erythrose; 13) glucopyranosyl-glycolaldehyde; 14) anhydro-cellooligosaccharides; 15) levoglucosan. .... 15

Figure 2-8: Proposed reaction scheme in hot-compressed water<sup>51,93,129</sup> ..... 17

Figure 2-9: Main reaction pathways of glucose and fructose in hot-compressed water<sup>44</sup> ..... 18

Figure 2-10: Simple reaction pathways of glucose reaction<sup>137</sup> ..... 19

Figure 2-11: Schematic diagrams of typical biomass conversion system using hot-compressed water<sup>54</sup>. (a) batch-type; (b) flow-type..... 21

Figure 2-12: Main reaction pathways of D-xylose in hot-compressed water<sup>159</sup> ..... 26

Figure 3-1: Research Methodology.....	43
Figure 3-2: Two-step experiments including pretreatment and further hydrolysis. (a) for amorphous cellulose; (b) for crystalline cellulose.....	47
Figure 3-3: Schematic diagram of the experimental apparatus used in this study. 1. Water reservoir; 2. HPLC pump; 3. infrared image furnace; 4. reactor; 5. sintered stainless steel filter; 6. thermocouple; 7. cooling unit; 8. back pressure regulator; 9. liquid product collector.....	49
Figure 3-4: Reactor used in this study.....	50
Figure 3-5: The time-dependence of the reactor inlet and outlet temperatures during furnace heating period. (a) Final temperature: 250 °C, water flow rate: 10 ml/min; (b) Time-dependence of reactor outlet temperature for different setting temperatures. ....	51
Figure 3-6: Calibration curves for glucose and cellobiose by HPLC-ELSD.....	53
Figure 3-7: Typical HPLC-ELSD chromatogram of liquid sample collected during hydrolysis in HCW at 280 °C, 10MPa, and 10 ml/min. (a) without concentration; (b) with concentration. ....	54
Figure 3-8: Diagram of the pulse sequence for carbohydrate detection <sup>215</sup> .....	55
Figure 3-9: IC chromatogram of the standards of C1-C5 with concentration of 0.5 mg/L.....	56
Figure 3-10: Calibration curves for C1-C5 standards by HPAEC-PAD.....	57
Figure 3-11: Calibration curve for TOC analysis .....	58
Figure 4-1: Comparison of liquid samples from cellulose hydrolysis in HCW by HPLC-ELSD. (a) without concentration; (b) with concentration .....	64
Figure 4-2: Typical IC chromatogram of liquid products from cellulose hydrolysis in hot-compressed water.....	65
Figure 4-3: Comparison between HPLC-ELSD and HPAEC-PAD on quantitative analysis of glucose and cellobiose .....	66
Figure 4-4: Retention of carbon in the liquid during precipitation (TOC data). (a) carbon concentration in the liquid; (b) retention of carbon in the liquid. ....	68
Figure 4-5: Peak height changes of glucose oligomers after dilution.....	71

Figure 4-6: Comparison of glucose oligomers in the sample after precipitation for different times. Black: fresh sample; red: after settling for 2 hours; blue: after settling for 4 hours; pink: after settling for 8 hours; yellow: after settling for 1 day; green: after settling for 2 days.....	71
Figure 4-7: Retention of glucose oligomers in the liquid during precipitation based on peak height .....	72
Figure 4-8: Effect of dilution on the retention of glucose oligomers during precipitation. Solid: with dilution 2 times; Open: without dilution .....	74
Figure 4-9: SEM of cellulose and precipitate recovered from cellulose hydrolysis in HCW. (a) cellulose; (b) precipitate .....	75
Figure 4-10: X-ray diffraction pattern of cellulose and precipitate from cellulose hydrolysis in HCW. (a) cellulose; (b) precipitate .....	76
Figure 5-1: Effect of water flow rate on cellulose conversion during hydrolysis in HCW at various temperatures. ....	84
Figure 5-2: Effect of water flow rate on the selectivity of glucose oligomers in the fresh liquid products collected during cellulose hydrolysis at various reaction temperatures. (a) 280 °C; (b) 270 °C; (c) 250 °C; (d) 230 °C .....	86
Figure 5-3: Effect of sample loading on glucose oligomers in the fresh liquid products produced from cellulose hydrolysis in HCW at various temperatures (Pressure: 10MPa). (a) 230 °C, water flow rate: 20 ml min <sup>-1</sup> ; (b) 250 °C, water flow rate: 40 ml min <sup>-1</sup> ; (c) 270 °C, water flow rate: 40 ml min <sup>-1</sup> .....	89
Figure 5-4: HPAEC-PAD chromatograms of the primary liquid products of cellulose hydrolysis in HCW, obtained under optimised reaction conditions. (a) 270 °C; (b) 250 °C; (c) 230 °C .....	91
Figure 5-5: Selectivity of C1-C5 in the primary liquid products produced from cellulose hydrolysis in HCW at various temperatures (Pressure: 10 MPa) .....	92
Figure 5-6: Effect of reaction temperature on the selectivity of glucose oligomers in the primary liquid products (Pressure: 10 MPa) .....	94
Figure 5-7: Glucose yields after post hydrolysis for primary liquid samples produced from cellulose hydrolysis in HCW under various conditions .....	96

Figure 6-1: Model of microcrystalline cellulose that consists of crystalline and amorphous structures <sup>73</sup> .....	99
Figure 6-2: Cellulose conversion during hydrolysis in HCW at 200 and 230 °C ....	101
Figure 6-3: Specific reactivity of cellulose during hydrolysis in HCW at 200 and 230 °C.....	101
Figure 6-4: X-ray diffraction pattern of raw cellulose sample.....	102
Figure 6-5: IC chromatograms of primary liquid products from amorphous portion within microcrystalline cellulose during hydrolysis in HCW. (a) 100-150 °C; (b) 150-180 °C. ....	104
Figure 6-6: IC chromatograms of primary liquid products from pretreated amorphous cellulose during hydrolysis in HCW .....	107
Figure 6-7: IC chromatograms of primary liquid products from crystalline portion within microcrystalline cellulose during hydrolysis in HCW.....	109
Figure 6-8: IC chromatograms of primary liquid products from amorphous and crystalline cellulose during hydrolysis in HCW at 230 °C .....	110
Figure 6-9: Selectivity ratios of glucose oligomers in the primary liquid products from amorphous and crystalline cellulose during hydrolysis in HCW at 230 °C .....	110
Figure 7-1: X-ray diffraction patterns of raw and ball milled 7-hour cellulose samples .....	116
Figure 7-2: Evolution of specific reactivity of amorphous cellulose during hydrolysis in HCW at 180 – 200 °C, 10 MPa.....	117
Figure 7-3: Evolution of specific reactivity of microcrystalline cellulose during hydrolysis in HCW at 230 – 270 °C, 10 MPa.....	117
Figure 7-4: Evolution of primary liquid products of amorphous cellulose during hydrolysis in HCW at 180 – 200 °C, 10 MPa. (a) 180 °C; (b) 190 °C; (c) 200 °C .....	120
Figure 7-5: Evolution of primary liquid products of microcrystalline cellulose during hydrolysis in HCW at 230 – 270 °C, 10 MPa. (a) 230 °C; (b) 250 °C; (c) 270 °C .....	122

Figure 7-6: Effect of in situ pretreatment of amorphous cellulose at 190 and 200 °C on the evolution of specific reactivity during hydrolysis in HCW at 180 °C, 10 MPa .....	124
Figure 7-7: Effect of in situ pretreatment of amorphous cellulose at 190 and 200 °C on the evolution of primary liquid product during hydrolysis in HCW at 180 °C, 10 MPa .....	124
Figure 7-8: Effect of in situ pretreatment of microcrystalline cellulose at 250 and 270 °C on the evolution of specific reactivity during hydrolysis in HCW at 230 °C, 10 MPa .....	126
Figure 7-9: Effect of in situ pretreatment of microcrystalline cellulose on the evolution of primary liquid products during the subsequent hydrolysis in HCW at 230 °C, 10 MPa. (a) 250 °C for 10 min; (b) 270 °C for 5 min .....	126
Figure 7-10: Effect of in situ pretreatment of microcrystalline cellulose at 200 °C for 4 hours on the evolution of specific reactivity during hydrolysis in HCW at 230 °C, 10 MPa.....	127
Figure 7-11: Effect of in situ pretreatment of microcrystalline cellulose at 200 °C for 4 hours on the evolution of primary liquid products during the subsequent hydrolysis in HCW at 230 °C, 10 MPa.....	128
Figure 8-1: Particle size distributions of various cellulose samples .....	132
Figure 8-2: X-ray diffraction patterns of various cellulose samples.....	133
Figure 8-3: Conversions vs time of various cellulose samples during hydrolysis in HCW at 230 °C.....	133
Figure 8-4: Specific reactivities of various cellulose samples during hydrolysis in HCW at 230 °C.....	134
Figure 8-5: Comparisons of cryogenic ball milled sample with raw and 4 hr ball milled samples. (a) particle size distribution; (b) X-ray diffraction pattern; (c) conversion vs time; (d) specific reactivity .....	136
Figure 8-6: IC chromatograms of primary liquid products from raw and cryogenic ball milled samples at 30% conversion during hydrolysis in HCW at 230 °C	138
Figure 8-7: IC chromatograms of primary liquid products from raw and ball milled samples at 30% conversion during hydrolysis in HCW at 230 °C .....	138

Figure 8-8: Selectivity ratios of glucose oligomers in the primary liquid products from various cellulose samples during hydrolysis in HCW at 230 °C. (a) at conversion of 15%; (b) at conversion of 30%; (c) at conversion of 60%..... 139

---

**LIST OF TABLES**

Table 2-1: Typical lignocellulosic biomass compositions (% dry basis)<sup>26,28,30</sup> ..... 7

Table 2-2: Properties of water under different conditions<sup>36,38</sup> ..... 13

Table 2-3: Results on sugar recovery by biomass hydrolysis in hot-compressed water  
..... 30

Table 2-4: Summary of kinetic parameters obtained from literatures ..... 33

Table 2-5: Comparisons of different hydrolysis methods<sup>28,31</sup> ..... 38

Table 5-1: Characteristics of various reactor systems for cellulose/biomass hydrolysis  
in HCW ..... 81

Table 8-1: The relative crystallinity index for raw and ball milled samples ..... 132



## CHAPTER 1 INTRODUCTION

### 1.1 Background and Motive

Energy production from fossil fuels produces significant carbon dioxide emission, which is a key contributor to global warming and the problems related to climate change.<sup>1</sup> Renewable energy, particularly biomass, is therefore becoming increasingly important for sustainable development. Biomass contributes ~12% of global primary energy supply, and up to 40~50% in many developing countries.<sup>2</sup> According to the analysis carried out by the United National Conference on Environment and Development, biomass will potentially supply about half of the world primary energy consumption by the year 2050.<sup>3</sup> Therefore, biomass is recognized as an important part of any strategy to address the environmental issues related to fossil fuels usage.<sup>4,5</sup>

Biomass growth captures and condenses solar energy into chemical energy as carbohydrates through photosynthesis reactions of carbon dioxide and water.<sup>6</sup> If the non-renewable energy inputs, such as fossil fuel usage associated with fertilizer consumption, harvest and transport etc. during biomass production process, can be minimized or eliminated, biomass for fuels can be carbon neutral or close to carbon neutral in its lifecycle. In Australia, mallee biomass is a byproduct of dryland salinity management and complements food production.<sup>7-10</sup> Due to its super energy performance, economically competitiveness and carbon neutrality over its production life cycle,<sup>11-13</sup> mallee biomass is a truly second generation renewable feedstock<sup>14,15</sup> and has recently attracted significant R&D on its utilisation.<sup>16-22</sup>

The carbohydrates in lignocellulosic biomass mainly exist as cellulose and hemicellulose. These materials must be broken down through hydrolysis for the production of desired biomass extracts (e.g. sugar products), which can then be

converted into ethanol.<sup>23</sup> Developing efficient hydrolysis processes is essential to producing biomass extracts of desired properties. Available technologies for biomass hydrolysis include dilute acid hydrolysis,<sup>24-26</sup> concentrated acid hydrolysis,<sup>26,27</sup> alkaline hydrolysis<sup>27,28</sup> and enzymatic hydrolysis.<sup>26,29,30</sup> Acid hydrolysis technologies have a long industrial history but lead to high operating costs and various environmental and corrosion problems.<sup>28,31</sup> Enzymatic hydrolysis is not commercialized yet but is recognized to be the most promising hydrolysis technology.<sup>31</sup> The past two decades have also witnessed the research and development on biomass hydrolysis in hot-compressed water (HCW).<sup>32-35</sup> Due to its unique physical and chemical properties,<sup>36-38</sup> HCW may be utilized as both solvent and reactant simultaneously in various applications for biomass utilization including lignocellulosic biomass pretreatment,<sup>39,40</sup> hydrothermal degradation for bio-oil production,<sup>41,42</sup> supercritical water gasification,<sup>43-45</sup> subcritical water hydrolysis and liquefaction<sup>35,38,46</sup> and material synthesis.<sup>47,48</sup>

So far, there has been a lack of fundamental understanding of biomass and cellulose hydrolysis in HCW. For example, an adequate sampling procedure and analytical technique is required to characterise various sugars in the liquid products which may comprise glucose oligomers with a wide range DP. The formation of precipitate from cellulose or biomass hydrolysis in HCW has been found, but no one has clearly explained the formation of precipitate from the fresh liquid products during hydrolysis in HCW. Moreover, due to the constraints of experimental conditions, most of the past studies were not able to separate the primary hydrolysis reactions on the surface of reacting cellulose particles from the secondary reactions of the primary hydrolysis products in the aqueous phase. Therefore, the liquid products are typically not the primary liquid products from hydrolysis. Besides, it is well known that amorphous and crystalline cellulose have distinct structure, but little study has reported their behaviors during hydrolysis in HCW. Therefore, a fundamental study is of great importance to understand the above unknown questions during biomass and cellulose hydrolysis in HCW, and promote the application of this green technology for biomass utilisation.

## 1.2 Scope and Objectives

The present study aims to fundamentally understand the mechanism of cellulose hydrolysis in HCW, and characterize the formation of glucose oligomers in the primary liquid products. With the development of a method to characterise the glucose oligomers in the liquid products, the present study tries to explain the formation of precipitate from fresh liquid products, to understand the primary reactions involved in the hydrolysis of cellulose in HCW, to study the different behaviors of amorphous and crystalline portions during hydrolysis, to investigate the evolution of primary liquid products with conversion during hydrolysis, and to study the hydrolysis behaviors of pretreated cellulose samples by ball milling.

## 1.3 Thesis Outline

There are a total of 9 chapters in this thesis including this chapter. Each chapter is outlined as follows, and the thesis structure is schematically shown in the thesis map (Figure 1-1):

Chapter 1 introduces the background and objectives of the current research;

Chapter 2 reviews the existing understandings in the literature on biomass and cellulose hydrolysis, finally leading to the identification of gaps and determination of specific objectives for the current research;

Chapter 3 presents the methodology employed to achieve the research objectives, along with explanations of the experimental equipments used;

Chapter 4 develops a method for analysing the liquid products obtained from cellulose hydrolysis in HCW, and investigates the precipitate formation from the liquid products;

Chapter 5 understands the primary liquid products of cellulose hydrolysis in HCW at various temperatures;

Chapter 6 examines the significant differences in the behavior of amorphous and crystalline portions within microcrystalline cellulose during hydrolysis in HCW;

Chapter 7 reveals the evolution of primary liquid products during hydrolysis with the evidence of in situ structural changes;

Chapter 8 studies the effect of ball milling on the hydrolysis of microcrystalline cellulose in HCW; and

Chapter 9 concludes the present study and recommends several areas/aspects for further research.

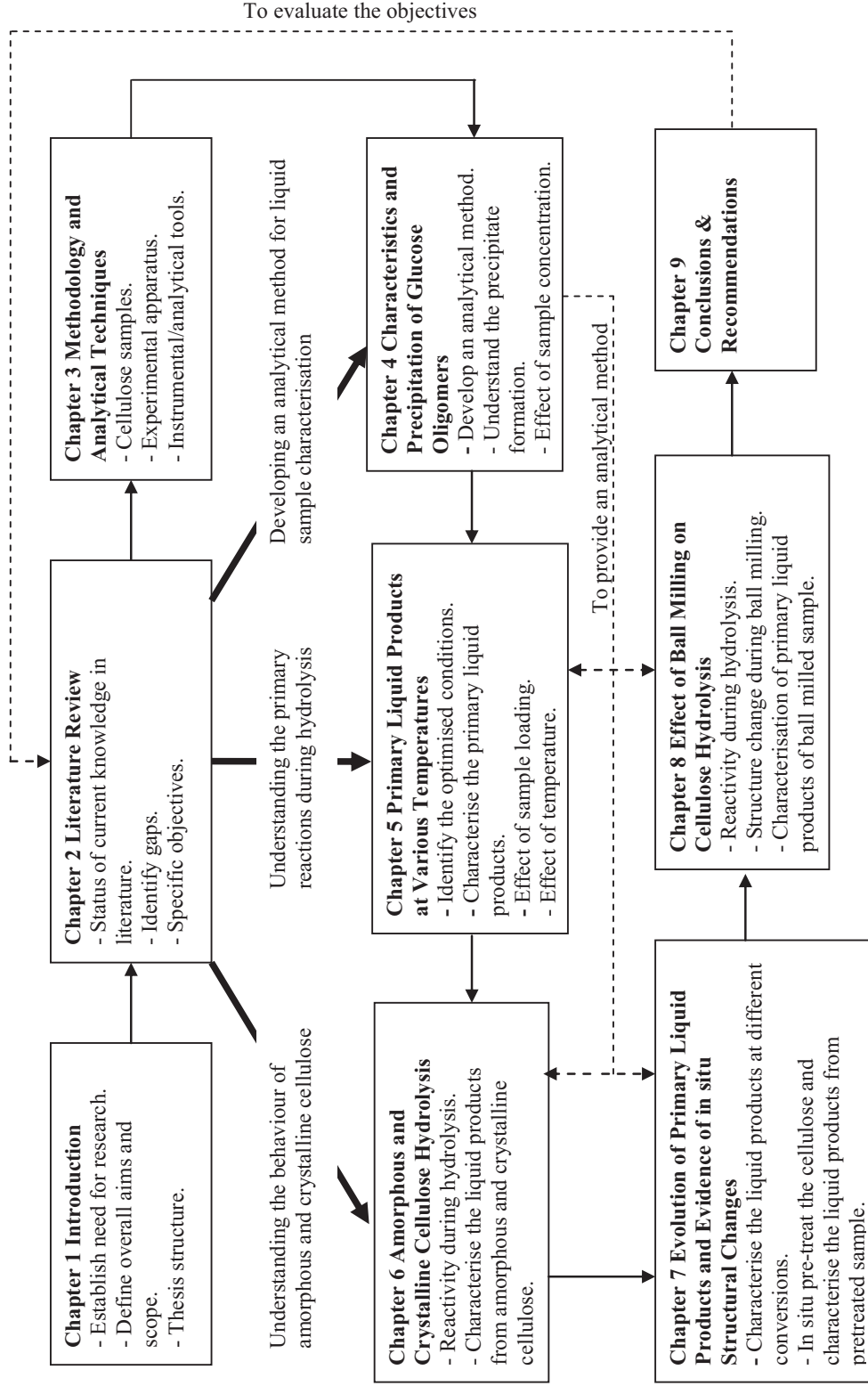


Figure 1-1: Thesis map

## CHAPTER 2 LITERATURE REVIEW

### 2.1 Introduction

In the past twenty years, there has been significant research in using HCW as a hydrolysis media for sugar recovery.<sup>32,34,35,44,49-66</sup> Due to its unique physical and chemical properties,<sup>36-38</sup> HCW may be utilized as both solvent and reactant simultaneously in various applications for biomass utilization including lignocellulosic biomass pretreatment,<sup>39,40</sup> hydrothermal degradation for bio-oil production,<sup>41,42</sup> supercritical water gasification,<sup>43-45</sup> subcritical water hydrolysis and liquefaction<sup>35,38,46,67</sup> and material synthesis.<sup>48,68</sup> It is the objective of this chapter to review the up-to-date research progress on biomass hydrolysis in HCW and to evaluate its future applications, with a focus on HCW at subcritical conditions.

This review first gives a brief introduction on biomass and its main components. A detailed overview on hydrolysis in HCW then follows, covering model compounds (cellulose and hemicellulose) and lignocellulosic biomass materials. Key factors determining the sugar recovery during biomass hydrolysis in HCW are also discussed. The chapter then briefly reviews the current status of other biomass hydrolysis technologies, such as acid hydrolysis, alkaline hydrolysis and enzymatic hydrolysis. The advantages, disadvantages, typical operation conditions, products properties and application potentials of these technologies, together with hydrolysis using HCW are then summarized. Key research gaps on hydrolysis in HCW are then identified, assisting in defining the scope of the present study.

### 2.2 Biomass Components

Biomass may be classified into four main categories: agriculture, forest, municipal solid wastes and others such as fast-growing plants, short-rotation crops, herbage plants and ocean biomass.<sup>69,70</sup> Photosynthesis reactions during biomass production

leads to the formation of key biomass components, such as cellulose and/or hemicellulose (see Figure 2-1), which consists of various numbers of sugar building blocks, represented as  $(\text{CH}_2\text{O})_x$  in a polymer form.<sup>69</sup> Typical wood plants consist of approximately 40~50% cellulose, 20~30% hemicellulose, 20~28% lignin and some percentages of other substances including minerals and organic extractives. The contents of various components in common biomass are summarized based on data in the literature<sup>26,28,30</sup> and listed in Table 2-1. This section only gives a brief introduction of various components in biomass. Further details can be found in the literature.<sup>26,28,30</sup>

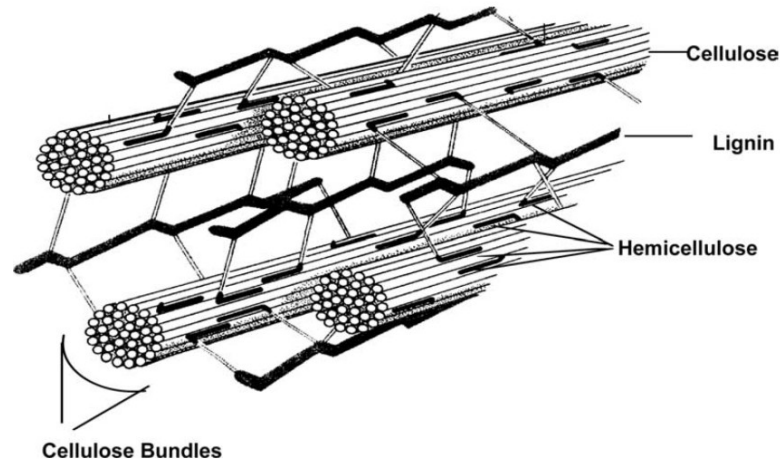


Figure 2-1: Typical plant cell wall arrangement<sup>69</sup>

### 2.2.1 Cellulose

Cellulose is the most abundant organic material on earth, with an annual production of over 50 billion tonnes.<sup>27</sup> As shown in Figure 2-2, it is a skeletal polysaccharide with a glucose monomer unit and  $\beta$ -1,4 glycoside linkages.<sup>71</sup> The basic repeating unit of cellulose polymer consists of two glucose anhydride units, called a cellobiose unit. Cellulose can be considered as a condensation polymer of glucose, like starch, but the links between the glucose monomers are slightly different. Cellulose has an average molecular weight range of 300,000~500,000, depending on the length of the cellulose chain,<sup>26,28</sup> which is often quantified by the degree of polymerization (DP). Values for the DP range from 7000~10,000 for wood, to as high as 15,000 for cotton. Cellulose is insoluble in water due to its low-surface-area crystalline form held together by hydrogen bonds. The degree of crystallinity of cellulose varies with their

origin and treatment. Cotton (70% crystalline) is more ordered than wood, which in turn is more ordered than regenerated cellulose (40% crystalline). Strong acids and alkalis can swell and disperse, or even dissolve the cellulose, breaking up the highly ordered crystallites.<sup>72</sup>

Table 2-1: Typical lignocellulosic biomass compositions (% dry basis)<sup>26,28,30</sup>

Lignocellulosic	Cellulose	Hemicellulose	Lignin	Ash
<b>Hard woods</b>				
White poplar	49.0	25.6	23.1	0.2
European birch	48.5	25.1	19.4	0.3
White willow	49.6	26.7	22.7	0.3
<b>Soft woods</b>				
White spruce	44.8	30.9	27.1	0.3
Monterey pine	41.7	20.5	25.9	0.3
Douglas fir	42.0	23.5	27.8	0.4
<b>Agricultural</b>				
Corn stover	37.1	24.2	18.2	5.2
Sugarcane	39.0	24.9	23.1	3.7
Wheat straw	44.5	24.3	21.3	3.1
<b>Other Wastes</b>				
Newspaper	40-55	25-40	18-30	NA
Waste papers	60-70	10-20	5-10	NA
Sorted refuse	60	20	20	NA

It is well known that microcrystalline cellulose contains both the amorphous and crystalline portions, because a cellulose microfibril is formed by several microcrystals hinged together and surrounded by amorphous cellulose.<sup>73</sup> Crystalline cellulose, in contrast to amorphous cellulose, has different intermolecular hydrogen bonding links at the C-6 position.<sup>74,75</sup> Sufficient evidences in the literature<sup>73-80</sup> demonstrate the significant structural differences between the amorphous and crystalline cellulose, mainly in the chain length of cellulose and hydrogen bonding patterns. While the crystalline consists of well-packed long cellulose chains side by side via strong hydrogen bonds, the amorphous cellulose can have the length of the rigid chain segments as short as the order of one cellobiose unit.<sup>74</sup> It was also found that the chains in amorphous cellulose were held together by isotropic intermolecular hydrogen bonds linked to the hydroxyl groups at C-2 and C-3 positions, resulting in

randomly distributed domain.<sup>76</sup> While the crystalline cellulose is known to have a preferred orientation,<sup>79,80</sup> the chains of amorphous cellulose are typically bent and twisted backbones and the molecules are in a random coil conformation.<sup>75,77,78</sup>

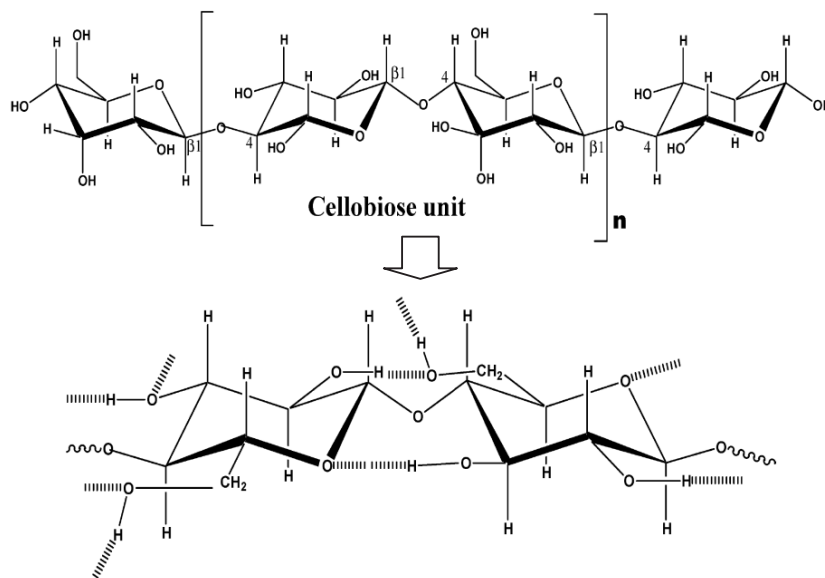


Figure 2-2: Chemical structure of cellulose with intrachain and interchain hydrogen-bonded bridging<sup>71</sup>

Crystalline cellulose has six known polymorphs (I, II, III<sub>I</sub>, III<sub>II</sub>, IV<sub>I</sub> and IV<sub>II</sub>), and they can interconvert.<sup>81</sup> Cellulose I has parallel arrangement of chains, and it is the only polymorph that occurs naturally. It was found also that native cellulose exists as a mixture of two crystalline forms I <sub>$\alpha$</sub>  and I <sub>$\beta$</sub> , which have triclinic and monoclinic unit cells, respectively.<sup>79,80</sup> Bacterial or algal cellulose are essentially cellulose I <sub>$\alpha$</sub>  whereas cellulose from tunicates or animal cellulose is mostly of the cellulose I <sub>$\beta$</sub>  form.<sup>79,80</sup> Cellulose I <sub>$\alpha$</sub>  is thermodynamically less stable, as shown by its conversion to cellulose I <sub>$\beta$</sub>  by annealing at 260 °C.<sup>82</sup> In both crystalline forms, cellobiose is the repeating unit with strong intramolecular hydrogen bonding from O-3 to the preceding ring O-5, whereas the intermolecular hydrogen bonding and packing of the crystal are slightly different in two forms.<sup>79,80</sup> Cellulose II is converted by mercerization or solubilization regeneration of native or other celluloses.<sup>83</sup> Cellulose II has thermodynamically more stable structure with an antiparallel arrangement of the strands and some intersheet hydrogen bonding. Cellulose III<sub>I</sub> and III<sub>II</sub> can be prepared from cellulose I and II, respectively, by treatment with liquid or



supercritical ammonia or some amines,<sup>84-86</sup> where cellulose IV<sub>I</sub> and IV<sub>II</sub> can be obtained from heating III<sub>I</sub> and III<sub>II</sub>, respectively, to 206 °C in glycerol.<sup>87</sup>

### 2.2.2 Hemicellulose

Compared to cellulose, hemicellulose consists of various polymerized monosaccharides including five-carbon sugars (usually xylose and arabinose), six-carbon sugars (galactose, glucose and mannose), 4-O-methyl glucuronic acid and galacturonic acid residues. It exists in association with cellulose in the cell wall.<sup>71,72</sup> The most abundant building block of hemicellulose in hardwoods is xylan (a xylose polymer), which consists of xylose monomer units linked at the 1 and 4 positions. Hemicellulose is usually branched with DP ranging from less than 100 to about 200 units.<sup>27</sup> Due to its structure and branched nature, hemicellulose is amorphous and relatively easy to hydrolyse to its monomer sugars compared to cellulose.

### 2.2.3 Lignin

Lignin is a three-dimensional, highly branched, polyphenolic substance that consists of an irregular array of variously bonded “hydroxyl-” and “methoxy-” substituted phenylpropane units.<sup>88,89</sup> The three general monomeric phenylpropane units exhibit the *p*-coumaryl, coniferyl, and sinapyl structure (Figure 2-3). As a necessary component for plant to be classified as woody, lignin is an amorphous cross-linked resin, serving as a cement between the wood fibers and a stiffening agent within the fibers.<sup>27</sup> Lignin is often associated with the cellulose and hemicellulose materials making up lignocellulose compounds, which must be broken down to make the cellulose or hemicellulose accessible to hydrolysis.<sup>72</sup> Lignin has an amorphous structure, which leads to a large number of possible interlinkages between individual units. Ether bonds predominate between lignin units, unlike the acetal functions found in cellulose and hemicellulose. Covalent linking also exists between lignin and polysaccharides, which strongly enhances the adhesive bond strength between cellulose fibers and its lignin “potting matrix”. Figure 2-4 illustrates some typical lignin chemical linkages in a small section of the lignin polymer.<sup>90</sup>

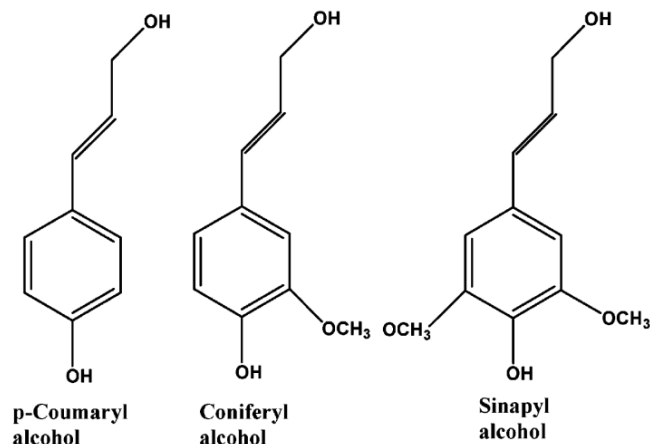


Figure 2-3: The structures of p-coumaryl alcohol, coniferyl alcohol and sinapyl alcohol<sup>27</sup>

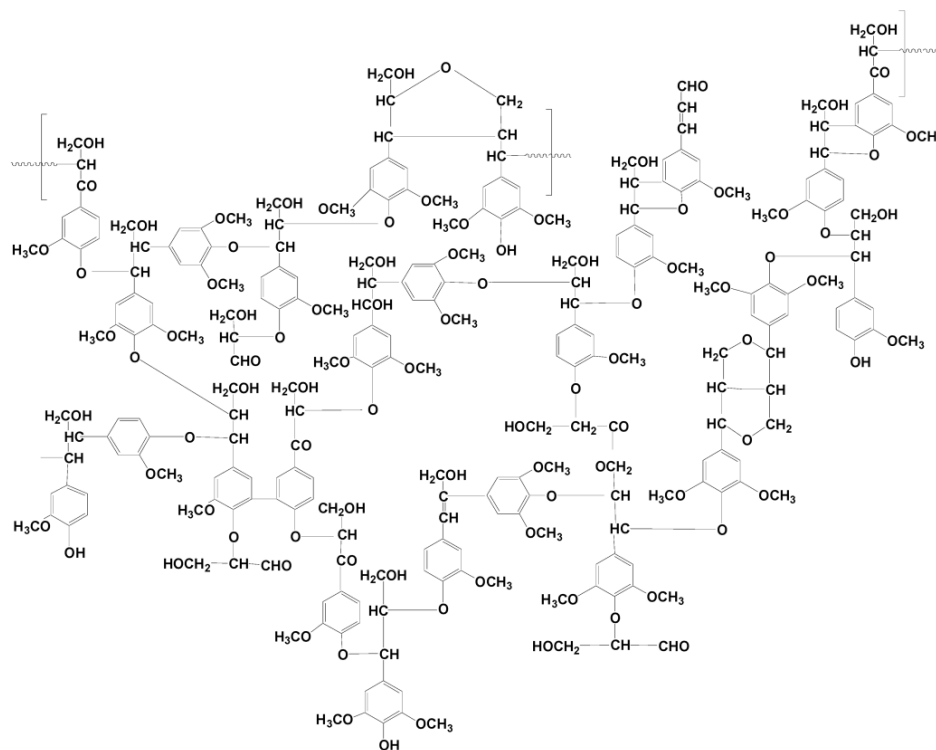


Figure 2-4: Partial structure of a hardwood lignin molecule<sup>90</sup>

### 2.2.4 Other Components

Biomass may also contain a wide range of organic extractives which can be extracted using polar or nonpolar solvents. Example extractives include fats, waxes, alkaloids, proteins, phenolics, simple sugars, pectins, mucilages, gums, resins, terpenes, starches, glycosides, saponins, and essential oils. Extractives function as

intermediates in metabolism, as energy reserves, and as protective agents against microbial and insect attack. Biomass also contains a small content of inorganic species such as potassium, sodium, calcium etc., as a result of nutrients uptake during its growth.

### 2.3 Biomass Hydrolysis in Hot-Compressed Water

In the last two decades, there have been strong research interests in utilizing hot-compressed water (HCW) as a solvent and reaction medium<sup>68</sup> for biomass conversion. Hydrolysis in HCW for sugar recovery from biomass is a relatively recent development. A number of studies have been carried out to investigate hydrolysis performance,<sup>32,33,35,55,91</sup> reaction mechanisms<sup>34,35,92-95</sup> and kinetics<sup>34,65,95-101</sup> and to develop mathematical models.<sup>65,101-105</sup> These studies focused mainly on the biomass model compounds (cellulose and hemicellulose) and various lignocellulosic biomass materials. An overview on the developments will be given after the discussion of HCW properties.

#### 2.3.1 Properties of HCW

HCW can be generally described as water at temperature above 150 °C and various pressures. Depending on the temperature and pressure, HCW may exhibit exciting physical and chemical properties. As shown in Figure 2-5, adapted from the literature,<sup>68</sup> the not too low relative dielectric constant in the subcritical state can enhance ionic reaction, suitable for a variety of synthesis or some degradation reactions. In the supercritical state, HCW exhibits the properties of a non-polar solvent, suitable for C-C bond formation or even organometallic-catalyzed reactions, yet the structure of a single water molecule remains to be polar molecule that can interact with ions. Compared to ambient water, HCW also has a higher compressibility. Depending on temperature and pressure, HCW supports either free radical or ionic reactions. At high densities below the critical temperature or in supercritical water at very high pressures, ionic reactions dominate; at high temperatures and low densities, free-radical reactions are superior.<sup>68,106,107</sup>

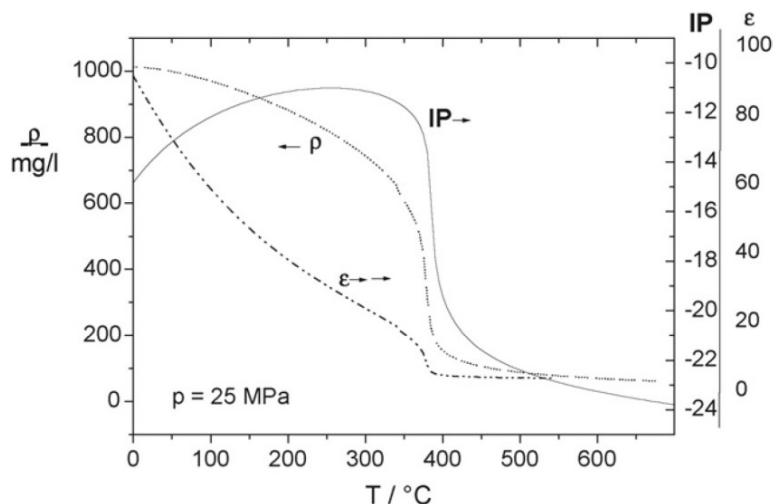


Figure 2-5: Selected properties of water at high temperature and high pressure.<sup>68</sup> IP: ionic product, expressed as  $\log[\text{H}_3\text{O}^+][\text{OH}^-]$ ;  $\epsilon$ : relative dielectric constant, a higher  $\epsilon$  reduces the activation energy of a reaction with a transition state of higher polarity compared to the initial state;  $\rho$ : density, defined as mass per unit volume.

Table 2-2 summarizes the properties of sub- and supercritical water.<sup>36,38</sup> Subcritical water is water that is in a state under a pressurized condition at temperatures above its boiling point under ambient pressure and below the critical point ( $T_c = 374\text{ }^\circ\text{C}$ ,  $p_c = 22.1\text{ MPa}$ ,  $\rho_c = 320\text{ kg/m}^3$ ).<sup>38</sup> Subcritical water remains in aqueous phase and has properties different from ambient water: a low relative dielectric constant and a large ion product. Dielectric constant of liquid water decreases with increasing temperature.<sup>37</sup> At temperature from 550 to 650 K, the dielectric constant becomes as low as those of polar organic solvents such as pyridine and tetrahydrofuran.<sup>108</sup> The ionic product of water is maximized at temperatures between 500 and 600 K depending on the pressure. In this temperature range, the ionic product is greater by 1 to 2 orders of magnitude than that at ambient temperature and even greater than that at temperature above 647 K.<sup>109</sup> Thus, sub-critical water could act as acid and/or base catalysts for reactions such as hydrolysis of ether and/or ester bonds, and also as a solvent for extraction of low molecular-mass products.

Table 2-2: Properties of water under different conditions<sup>36,38</sup>

Fluid	Ordinary	Subcritical	Supercritical water	
Temperature $T$ (°C)	25	250	400	400
Pressure $p$ (MPa)	0.1	5	25	50
Density $\rho$ (gcm <sup>-3</sup> )	1	0.80	0.17	0.58
Dielectric constant $\epsilon$	78.5	27.1	5.9	10.5
$pK_w$	14.0	11.2	19.4	11.9
Heat capacity $c_p$ (kJkg <sup>-1</sup> K <sup>-1</sup> )	4.22	4.86	13.0	6.8
Dynamic viscosity $\eta$ (mPas)	0.89	0.11	0.03	0.07
Heat conductivity $\lambda$ (mWm <sup>-1</sup> K <sup>-1</sup> )	608	620	160	438

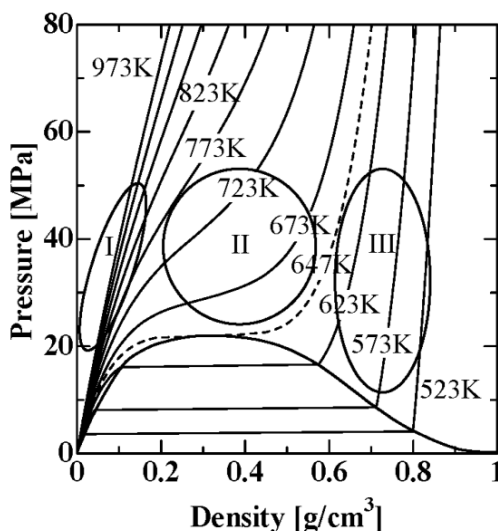


Figure 2-6: Temperature and pressure dependence of water density.<sup>45</sup> Region I: 773-973 K; Region II: 647-773 K; Region III: below 647 K.

Supercritical water is above the critical temperature of 647 K. It is compressible and the properties depend strongly on the pressure. Supercritical water is miscible with light gases and small organic compounds, and its dielectric constant varies in the range of 3.7~19.72, which has an influence on the rate of reactions with a polar activated complex.<sup>110</sup> Employing a supercritical water reaction environment provides an opportunity to conduct chemistry in a homogeneous phase that would otherwise occur in a heterogeneous phase under more conventional conditions.<sup>111</sup> It also offers the possibility of shifting dominant reaction mechanisms from those of free-radical to

those of ionic through manipulating the water density.<sup>112</sup> The water density varies greatly with temperature and pressure as shown in Figure 2-6.

### 2.3.2 Cellulose Hydrolysis in HCW

As one of the main components in biomass, cellulose is often used as a model compound as a good starting point for the more complex biomass materials in various studies.<sup>28,34,35,52,53,59,91,94,97,98,101,102,113-117</sup> Bobleter et al<sup>28,113</sup> was the first to study the biomass hydrothermal process using HCW. A conclusion was made based on their study that the hydrothermolysis has a reaction mechanism comparable to acid hydrolysis. For non-catalyzed hydrothermal degradation of cellulose (215~219 °C), the cellulose hydrolysis rate is much lower than that of acid hydrolysis and the glucose yield is also lower.<sup>113</sup> A number of later studies<sup>46,50,52,53,109,114,115,117-121</sup> show that ether and ester undergo rapid hydrolysis in near-critical or supercritical water even without any catalysts. A summary of the research progress on cellulose hydrolysis in HCW is given below.

#### 2.3.2.1 Mechanisms of Cellulose Hydrolysis in HCW

A good understanding on fundamental reaction mechanisms is a key to improve the reaction performance, the control of the reactions and the design of the reactors. Sasaki et al<sup>34,35,52</sup> investigated the hydrolysis and decomposition of cellulose in the temperature range of 290~400 °C with the residence time less than 14 s. Lü et al<sup>91</sup> carried out the research of cellulose decomposition for temperature below 290 °C and longer residence time (30~96 s). The results of those studies showed that the main products of cellulose decomposition in HCW were glucose, fructose, erythrose, dihydroxyacetone, glyceraldehyde, pyruvaldehyde, and oligomers (cellobiose, cellotriose, cellotetraose, cellopentaose, and cellohexaose). The oligomers will precipitate from the fresh liquid products when settling the sample at room temperature for a while. However, it is unclear if these products are the primary liquid products from cellulose hydrolysis in HCW, because there has no study so far to report the primary reactions occur on the reacting cellulose surface during cellulose hydrolysis in HCW, due to the difficulty to minimize the secondary reactions of primary liquid products. It is also not clear how the detailed secondary decomposition reactions of primary liquid products happen in the HCW.

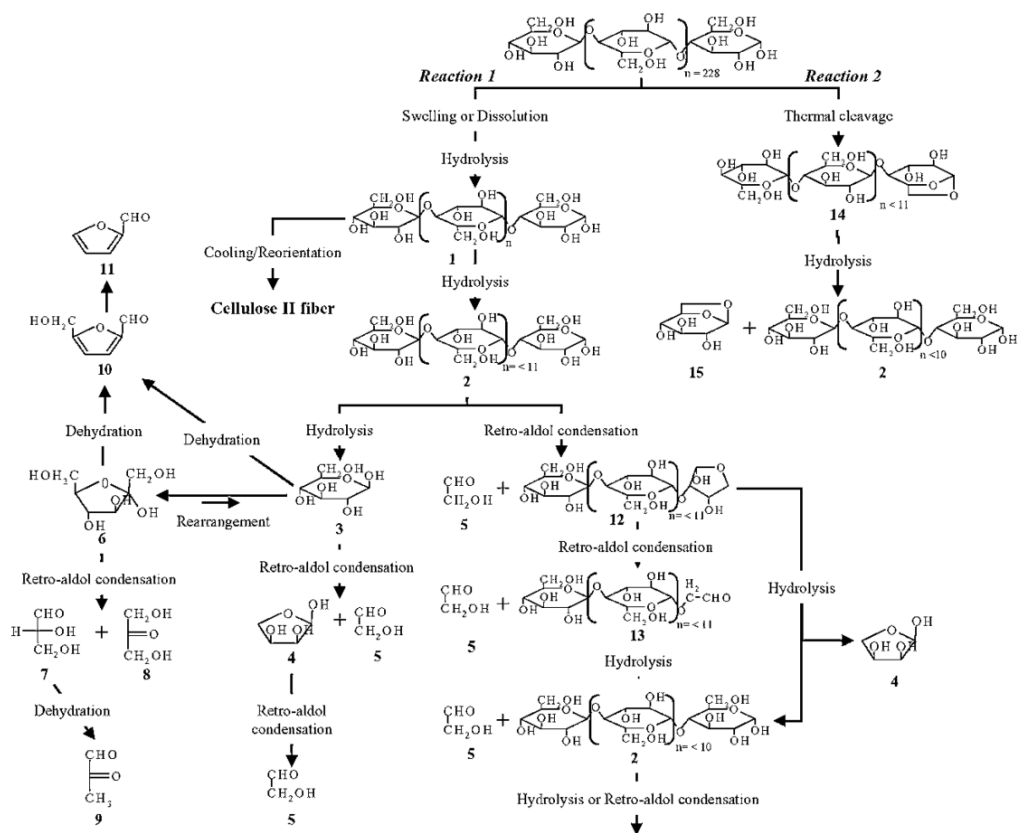


Figure 2-7: Proposed reaction mechanism of microcrystalline cellulose in subcritical and supercritical water.<sup>44</sup> 1) Swelled (or Dissolved) cellulose; 2) celooligosaccharides; 3) glucose; 4) erythrose; 5) glycolaldehyde; 6) fructose; 7) glyceraldehyde; 8) dihydroxyacetone; 9) pyruvaldehyde; 10) 5-HMF; 11) 2-furfural; 12) glucopyranosyl-erythrose; 13) glucopyranosyl-glycolaldehyde; 14) anhydro-cellulooligosaccharides; 15) levoglucosan.

Through the kinetic and mechanistic studies of these products and cellulose model compounds (cellobiose, cellotriose and cellopentaose), the main pathways have been elucidated,<sup>35,44</sup> as summarized in Figure 2-7. Cellulose is depolymerized mainly by the two reaction pathways: (1) dehydration of reducing-end glucose via pyrolytic cleavage of the glycosidic bond in cellulose (or partly retro-aldol reaction) and (2) hydrolysis of the glycosidic bond via swelling and dissolution of cellulose. The former takes place as the temperature increases and the pressure decreases, while the latter becomes predominant in high density regions in near- and supercritical water.<sup>44</sup>

The reactions of microcrystalline cellulose in subcritical and supercritical water require an extra step to break down the cellulose crystallite. Sasaki et al.<sup>34,35,52</sup> has proposed that when a crystallite is taken up, cellulose molecules in the crystallite line up in parallel and form intermolecular hydrogen bond networks among the molecules. In subcritical water, the crystallite is hydrolyzed at the surface region without swelling or dissolving. Therefore, the overall conversion rate of microcrystalline cellulose is slow and there is no cellulose II crystal formed in the residue. In contrast, in near- and supercritical water, the crystallite can swell or dissolve around the surface region to form amorphous-like cellulose molecules. These molecules are inactive, so they can be easily hydrolyzed to lower DP celluloses and celooligosaccharides. Some of the hydrolysate can pass from the polymer phase to water phase by cleavage of their hydrogen bond networks, while others remain on the crystallite surface of the residue. The liberated portion in the water phase is further hydrolyzed to water-soluble saccharides, or crystallized as water-insoluble cellulose II after the reaction. On the other hand, the amorphous-like portion remaining in the polymer phase is hydrolyzed to water-soluble saccharides, or swells further or dissolves and moves from the polymer phase to the water phase. As a consequence, the overall conversion rate of microcrystalline cellulose can become faster than that in near- and subcritical water.<sup>34</sup> This can also be supported by a recent finding by Deguchi et al.<sup>122,123</sup> By performing in situ polarized microscopic observation, it was found that crystalline cellulose underwent transformation to an amorphous state in HCW at 320 °C and 25 MPa, which was followed by complete dissolution. This finding shows that the hydrolysis of cellulose in HCW is determined by the unique properties of cellulose that arise from the extensive networks of hydrogen bonds among the cellulose chains in the crystal.<sup>123</sup> In HCW at higher temperatures (supercritical state), the hydrogen bonding networks seem to break significantly, therefore leading to the fast reaction of cellulose hydrolysis.

Minowa and co-workers<sup>51,93,124-128</sup> also investigated the reaction mechanism of cellulose in HCW using an autoclave reactor with the temperature range of 200~350 °C and pressure up to 3 MPa. In absence of catalysts, cellulose was slightly decomposed over 200 °C to produce water-soluble products, which include



dominantly sugar products. This indicated that hydrolysis was the primary step of cellulose decomposition. Then cellulose was decomposed quickly around 250 °C to form not only water-soluble products, but also gas, oil and char. Over 300 °C, char production continued, although no cellulose was left in the reactor, and sugars and oil were decomposed. Char was the main final product obtained with a yield of 60% on carbon basis. A gas yield of 10% was produced with mostly CO<sub>2</sub> and a small amount of CO. Based on these results, the authors proposed a reaction scheme,<sup>51,124</sup> as shown in Figure 2-8. To confirm the hydrolysis is the first step, glucose was used as a starting feedstock. The product distribution of gas, oil and char at different reaction temperatures were almost the same as that for cellulose, indicating a similar degradation scheme.<sup>43,51,93</sup>

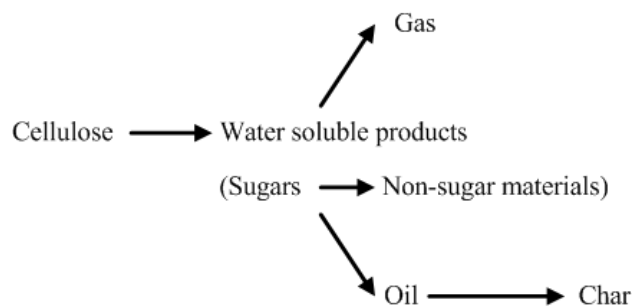


Figure 2-8: Proposed reaction scheme in hot-compressed water<sup>51,93,129</sup>

### 2.3.2.2 Mechanisms of Glucose Decomposition in HCW

Sugars are the most important hydrolysis products of biomass for subsequent conversion to produce transport fuels, such as ethanol. However, sugars, e.g. glucose, may be easily decomposed to form stable products such as 5-hydroxymethyl furfural (5-HMF) in HCW. Mechanisms of sugar decomposition in HCW were studied previously, with or without a catalyst.<sup>98,130-142</sup> Sasaki and Kabyemela<sup>98,132-134</sup> conducted a series of fundamental studies on kinetics of glucose decomposition in HCW and found that the main products of glucose decomposition were fructose, erythrose, glycolaldehyde, dihydroxyacetone, glyceraldehyde, 1,6-anhydroglucose, and pyruvaldehyde. The primary reactions of glucose were found to be as follows (also illustrated in Figure 2-9): (1) glucose isomerization into fructose via keto-enol tautomerisation, (2) glucose dehydration into 1,6-anhydroglucose, and (3) glucose

decomposition into aldehyde and ketone via retro-aldol condensation. Further, (4) dehydration of the tautomerization intermediate and fructose produce 5-HMF. Dehydration (C-O bond splitting) and retro-aldol condensation (namely C-C bond breaking) were found to be the key reactions. The contribution of retro-aldol condensation became predominant at higher temperatures (673~773 K), while that of dehydration reaction became significant at lower temperatures (523~623 K).<sup>98,132</sup> This reaction mechanism can typically be applied to the reaction that proceeds in a rapid heat-flow apparatus. As summarized recently by Watanabe,<sup>112</sup> at higher temperature and low water density, radical reactions are likely to happen; on the other hand, ionic reactions mainly occur at lower temperature and high water density.

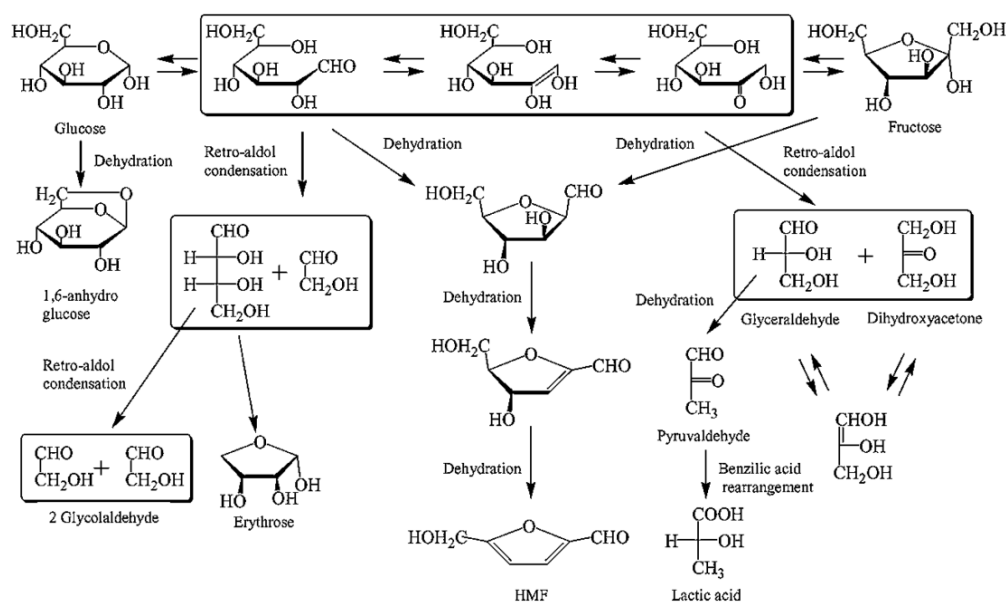


Figure 2-9: Main reaction pathways of glucose and fructose in hot-compressed water<sup>44</sup>

In addition to reaction conditions (temperature, pressure, or water density), additives (acid or base) may also influence glucose reactions especially at low temperatures. It was reported that the retro-aldol condensation was favored under alkali conditions<sup>143</sup>, and an acid catalyst was effective to enhance the dehydration reactions.<sup>144-147</sup> Homogeneous acid and base additives such as sulfuric acid (H<sub>2</sub>SO<sub>4</sub>) and sodium hydroxide (NaOH) are commonly used to change the acidic or basic atmosphere. The addition of alkali promoted isomerisation and retro-aldol condensation reactions of

glucose, while the addition of acid promoted the dehydration reaction of glucose. As homogeneous additives have environmental implications, Watanabe and co-workers<sup>139,141,142</sup> studied the influence of heterogeneous acid and base additives such as metal oxides on the glucose reactions. They found that the addition  $ZrO_2$  also promotes isomerisation of glucose and fructose and thus  $ZrO_2$  can be considered to be a base catalyst for glucose. Anatase  $TiO_2$  also promotes isomerisation and dehydration into HMF, indicating the existence of both base and acid sites on the surface.

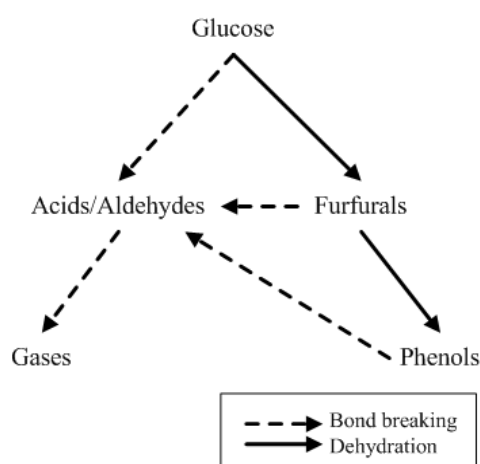


Figure 2-10: Simple reaction pathways of glucose reaction<sup>137</sup>

Sinag and co-workers<sup>135-137</sup> studied glucose decomposition in supercritical water. A relatively simple reaction mechanism was proposed as shown in Figure 2-10. Glucose converts into furfurals and acids/aldehydes in parallel. Further conversion of furfurals leads to acids/aldehydes and phenol formation. Acids and aldehydes are precursors of the gaseous compounds. Furfural forms through dehydration, and further dehydration of furfural gives phenols. In contrast, acids and aldehydes are produced by bond-breaking reactions. Such a simple mechanism is very useful to estimate the predominance of the two pathways (dehydration and bond breaking) from the yields of the key compounds such as furfurals, acids, aldehydes, phenols, and gaseous products.

### 2.3.3 Factors Influencing Cellulose Hydrolysis in HCW

Several factors might have significant influence on cellulose hydrolysis in HCW. These factors are classified as a) feedstock property; b) reactor configuration; c) HCW property; d) time-temperature history experienced by reacting particle; and e) catalyst and other additive.

#### 2.3.3.1 Feedstock Property

Natural celluloses such as cotton, ramie, etc., vary from one to another in their characteristics depending on their origins. As shown in section 2.2.1, microcrystalline cellulose generally consists of amorphous and crystalline portions, and there are six known polymorphs even for crystalline cellulose. These variations would lead to different water accessibilities of the materials. Saka et al<sup>148</sup> used semi-batch type reaction system under the conditions of a temperature of 500 °C and pressure of 35 MPa, in order to study the supercritical water hydrolysis of celluloses with different chemical compositions and the degrees of crystallinity. It is found that the difference in crystallographic nature of cellulose has little influence on the pattern of cellulose hydrolysis. However, the glucose yields were different between cellulose I (32%) and cellulose II (48%), when treated in supercritical water for 10 s. Pretreatment of cellulose samples to improve water accessibility seems to play an important role in hydrolysis. The hydrolysis reactions in supercritical water proceed slightly faster in starch than cellulose due to the fact that starch is in a more amorphous state with less hydrogen bonding, while celluloses are composed of crystalline microfibrils with numerous hydrogen bonds.

However, hydrolysis in HCW at low temperatures could be different, since high temperature could break the hydrogen bonds very fast to transform crystalline to amorphous structure,<sup>122,123</sup> leading to little difference of the hydrolysis behavior of crystalline and amorphous cellulose in HCW. Another study which carried out the studies of cellulose and chitin hydrolysis in HCW at 300-400 °C under pressure of 15-30 MPa, found that the different hydrolysis reactivities of cellulose and chitin could be due to the different intra- and intermolecular hydrogen bonding structures.<sup>149</sup> These results indicate that hydrogen bonding plays an importance role

for hydrolysis at lower temperatures. Further studied are required to study the behaviour of cellulose of various structures during hydrolysis in HCW.

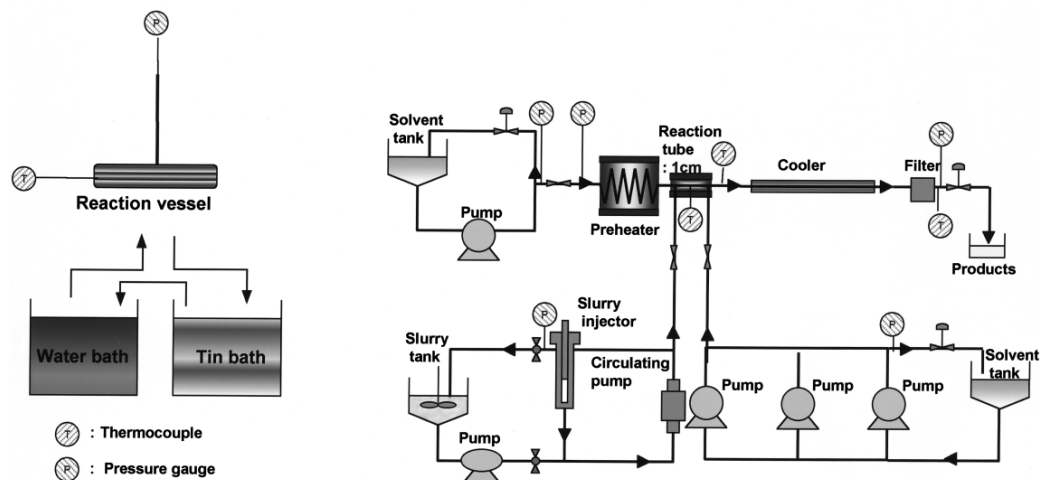


Figure 2-11: Schematic diagrams of typical biomass conversion system using hot-compressed water<sup>54</sup>. (a) batch-type; (b) flow-type.

### 2.3.3.2 Reactor Configuration

Typical reactor systems used for cellulose and/or biomass hydrolysis in HCW include batch, semicontinuous and continuous reactor systems.<sup>32,33,35,50-52,54-56,65,66,101,114,150</sup> Typical batch-type and flow-type reactor are shown in Figure 2-11. In batch-type reactor system, the hydrolysis products experience a long residence time therefore glucose easily decomposes.<sup>51,93,129</sup> A flow-type (semicontinuous or continuous) reactor system makes it possible to shorten the heating, treating and cooling times therefore reduces the degradation of sugar products. Ehara et al<sup>54</sup> also compared the cellulose conversion using both a batch-type and a flow-type reactor systems. The flow-type system produced a higher yield of hydrolysates, including some sugar oligomers, which will precipitate from fresh liquid sample after settling a while. The yield of glucose could not be increased by subcritical treatment using the batch-type system because the crystalline structure of cellulose cannot be decrystallized under subcritical conditions of water. A two-step treatment, which consists of supercritical water treatment and subsequent subcritical treatment using a flow-type reactor, was then proposed to address these issues. With the two-stage treatment, i.e. a 0.1 s supercritical water treatment followed by a subsequent 30 s subcritical water treatment, the yield of hydrolyzed products was successfully

increased and reached 66.8% for 30.1 s.<sup>55</sup> The combined supercritical and subcritical water technology for cellulose and biomass hydrolysis in HCW was further studied by Zhao et al. to find the optimised reaction conditions to achieve a high sugar yield.  
62-64

Therefore, the characteristics of biomass extracts obtained depend strongly on the reactor system used. For example, in a batch system, sugar yields are typically low while oil and char yields are high, apparently due to the extensive secondary reactions of the primary hydrolysis products.<sup>51</sup> A semicontinuous or continuous reactor system may potentially reduce the degradation of reaction intermediates in the liquid phase. For example, it was reported previously<sup>53</sup> that the liquid products contain mainly oligosaccharides in a semicontinuous reactor system, but only glucose oligomers up to cellopentaose were indentified in the liquid products. The fresh liquid sample from biomass hydrolysis was clear but after settling for a while, precipitate appeared from the liquid products. It is believed that such precipitate is mainly formed from the precipitation of glucose oligomers which are soluble in HCW but have much lower solubilities or even insoluble in water at room temperature.<sup>52</sup> However, it is still not clear about the size of glucose oligomers in the liquid products. It is also unknown which glucose oligomers are responsible for precipitate formation.

### 2.3.3.3 HCW Property

As shown in section 2.3.1, the properties of HCW significantly change with reaction conditions, therefore greatly affecting the cellulose hydrolysis in HCW. The reaction rate and the product distribution in the liquid products largely depend on the reaction temperature during cellulose hydrolysis in HCW, while the effect of pressure on cellulose hydrolysis reaction in HCW is not clear so far. Generally, the increase of reaction temperature significantly accelerates the cellulose conversion, from several hours in the subcritical water to a few seconds in the supercritical water. However, the detailed mechanisms at various temperatures are still not fully understood so far, due to the lack of knowledge on primary reactions at various temperatures during cellulose hydrolysis in HCW. Higher temperatures also favour to produce the oil and

char, resulting from the severe secondary decomposition reactions of primary liquid products.

Ogihara et al.<sup>151</sup> used the diamond anvil cell (DAC) to carry out the direct visual observation of the dissolution of microcrystalline cellulose in water, and the results showed that cellulose particle dissolution is water density dependent. The dissolution temperatures changed systematically with density and showed a minimum temperature of dissolution at densities around 800 kg/m<sup>3</sup>. Cellulose particles noticeably swelled when heating at densities from 600 to 800 kg/m<sup>3</sup>. The swelling probably increases the water accessibility to parts of the cellulose particle, which causes the temperature at which cellulose becomes homogeneous with water to decrease with density from 500 to 800 kg/m<sup>3</sup>. At high water densities (>900 kg/m<sup>3</sup>), the dissolution temperatures increased and approached those at the lower densities (500 kg/m<sup>3</sup>). At high temperature and low water density, radical reactions are likely to take place; on the other hand, ionic reactions mainly occur at low temperature and high water density.<sup>112</sup> In particular, for ionic reactions, water density is the most important controlling factor in the absence of a catalyst. However, water density of the saturated liquid phase cannot be changed significantly with pressure below the critical point compared to the supercritical region.

#### 2.3.3.4 Heating Rate

Heating rate also affects the biomass hydrolysis. For a batch type reactor, a high heating rate shortens the residence time of the biomass resulting in reduced degradation of glucose product, therefore leading to a high production yield of glucose. Fang et al.<sup>124</sup> studied cellulose decomposition mechanism without catalysts in a DAC coupled with optical and infrared microscopy in subcritical water. It was found that the main product for non-catalytic decomposition of cellulose was solid residue at 350 °C. Using low heating rates (e.g. 0.18 °C/s), the reaction occurs mostly under heterogeneous conditions. These compounds probably decompose further to water-insoluble residues at high temperatures. Using higher heating rates (>2.2 °C/s), reaction (hydrolysis and decomposition) can occur in a homogeneous phase. Reaction mechanisms of cellulose under homogeneous and heterogeneous conditions are very different as evident by the formation of “glucose char” in the

former or the formation of “cellulose char” in the latter. The effect of heating rate on product distribution during cellulose hydrolysis was further experimentally studied and mathematically modelled by Kamio et al.<sup>105</sup>

### 2.3.3.5 Catalyst

Under subcritical condition of water, additives are needed to control ionic reactions. However, apart from acids and alkalis, very few catalysts have been found to be efficient to improve the sugar yield during cellulose or biomass hydrolysis in subcritical water. A study demonstrated that metal catalyst  $\text{CuSO}_4$  can reduce the corrosion problem while keeping high yield of glucose for cellobiose hydrolysis in HCW.<sup>152,153</sup> It is unknown whether  $\text{CuSO}_4$  can be used to improve the glucose yields for cellulose or lignocellulosic biomass in subcritical water.

Recently, solid acid catalysts have been used for hydrolysis of cellulose into glucose.<sup>154,155</sup> It was found that solid acid catalyst, such as sulfonated activated-carbon ( $\text{AC-SO}_3\text{H}$ ), for the hydrolysis of cellulose with  $\beta$ -1,4-glycosidic bonds can achieve a glucose selectivity higher than 90% on a carbon basis at 423 K,<sup>154</sup> but the reaction rate is slow. It requires a hydrolysis time of at least 24 hours. For starch, the  $\text{AC-SO}_3\text{H}$  catalyst can obtain a glucose yield higher than 90%. Another catalyst using amorphous carbon bearing with  $\text{SO}_3\text{H}$ ,  $\text{COOH}$  and  $\text{OH}$  groups even converts all the cellulose into glucose and oligomers within 3 hours at 373 K, and achieves a total sugar yield of 68%,<sup>155</sup> indicating that the hydrothermal process with the solid acid catalyst is promising for the efficient production of glucose from cellulose.

### 2.3.4 Hemicellulose Hydrolysis in HCW

A previous study<sup>49</sup> showed that HCW can solubilize hemicellulose completely from whole biomass. Six woody and four herbaceous biomass samples were washed with compressed liquid water for 0~15 min at 200~300 °C, and 40~60% of the sample mass was solubilized. In all case, 100% of the hemicellulose was solubilized, of which 90% (on average) was recoverable as monomeric sugar. Current hemicellulose hydrolysis models were mostly built based on the knowledge of cellulose hydrolysis.<sup>156,157</sup> For xylan fraction in hemicellulose, it was proved that most of the xylose released into solution was in oligomeric form in HCW, and the xylooligomer was



then decomposed to yield xylose monomer.<sup>58,156</sup> Longer holding times might increase xylose monomer recovery at the expense of decreasing the total yield since xylose may be further converted to furfural and other degradation products.

Kumar and Wyman<sup>158</sup> studied the selectivity of xylooligomer (with DPs from 2-5) depolymerization to monomer at 160 °C with and without the addition of acid. It was found that the yield of xylose from xylooligomers increased with acid concentration, but decreased with increasing the xylooligomer DP. All the xylooligomers decomposed at a higher rate compared to xylose monomer, and the decomposition rate constant increased with DP from 2 to 5. They also found that, the lower DP oligomers of 2 and 3 can directly degrade to unknown compounds in the absence of acid, but that direct degradation is minimized by the presence of acid. On the contrary, the higher oligomers of DP 4 and 5 exhibited negligible losses to degradation products. Therefore, it seems the direct degradation reactions only occur for lower oligomers such as xylobiose and xylotriose. Further experiments are needed to conduct the experiments at various temperatures to clarify the reaction mechanism and elucidate the reaction pathways for decomposition of xylooligomers.

Hemicellulose contains five-carbon sugars (usually xylose and arabinose) and six-carbon sugars (galactose, glucose and mannose). Kumar and Wyman<sup>158</sup> also found that the xylose decomposition depends on the xylose concentration, especially at low concentrations of acid. Xylose degradation was found to follow the first-order kinetics, with the rate depending on the acid concentration and temperature.<sup>158</sup> Sasaki et al<sup>159</sup> have also clarified the reaction mechanisms of xylose, a monomer of xylan (model compound of hemicelluloses), in HCW and proposed the main reaction pathways as shown in Figure 2-12. Kinetic study on this reaction demonstrated that the contribution of retro-aldol condensation and dehydration to the overall decomposition rate were consistent with that in the case of glucose in supercritical water. Some other hemicellulose-derived sugars, such as glucose, mannose, galactose, and arabinose were studied by Srokol et al<sup>138</sup> through the hydrothermal reaction at 340 °C and 27.5 MPa. No qualitative differences were found in the products formed from the six-carbon sugars, although the amounts of the various compounds and their rates of formation depended strongly on the nature of the

starting sugars. The decomposition products of arabinose were mainly glycolaldehyde and 2-furaldehyde, which are also same as the main products of xylose. It can be concluded that the decomposition mechanisms of hemicellulose-derived sugars (including five-carbon sugars and six-carbon sugars) are similar in HCW.

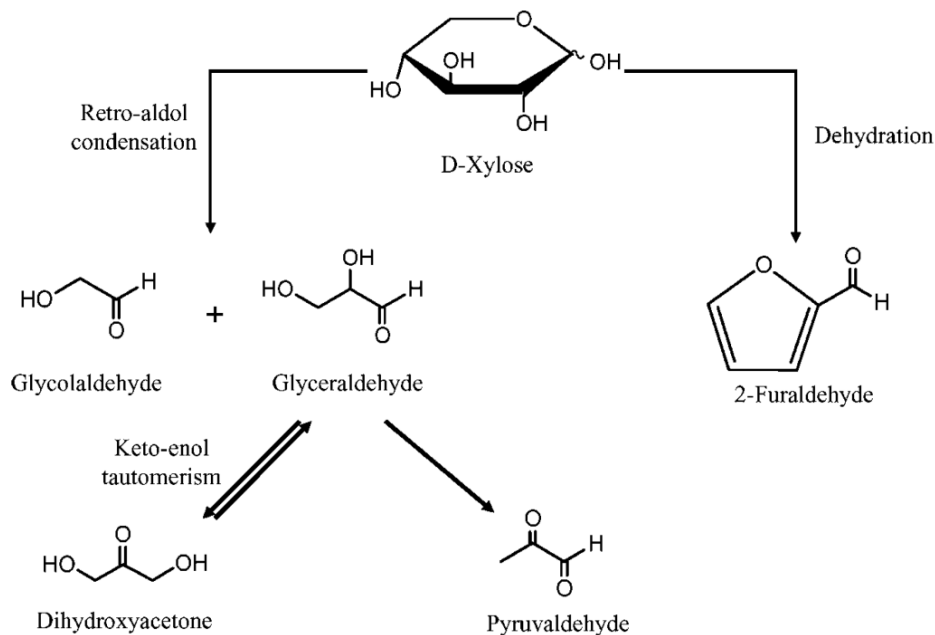


Figure 2-12: Main reaction pathways of D-xylose in hot-compressed water<sup>159</sup>

### 2.3.5 Lignocellulosic Biomass Hydrolysis in HCW

The majorities of the previous<sup>32,33,56,110,160</sup> studies on lignocellulosic biomass hydrolysis in HCW were focused on the hydrolysis behavior and characterisation of the compounds in the liquid products. Not much work has been done so far on the detailed reaction mechanisms of lignocellulosic biomass during the hydrolysis in HCW due to complex nature of biomass materials. Kobayashi et al.<sup>161</sup> tried to understand the mechanisms of biomass hydrolysis in HCW by characterising the solid residues obtain from HCW treatment of woody biomass. It was found that the characteristics of solid residue changed drastically depending on the reaction temperature. For example, cellulose crystallinity decreased with increasing reaction temperature, and the physical characteristics of solid residue, such as particle shape, particle size, and pore size distribution, also changed dramatically. Dehydration of

woody component was found to be one of the important factors during HCW treatment.

For the hydrolysis of lignocellulosic biomass, knowledge of the component fractionation is very important for efficient utilization of lignin, hemicellulose and cellulose. In general, because of its branched structure and lower DP, hemicellulose is more susceptible to hydrolysis than cellulose. Ando et al.<sup>32</sup> studied the decomposition behavior of plant biomass in HCW and found that hemicellulose decomposition commences at 180 °C while cellulose decomposition would not start until temperature is over 230 °C. Lignin was extracted by HCW at relatively low temperatures and flowed out with decomposed products of hemicellulose. However, for biomass materials which has a large amount of lignin, such as Japan cedar (33% lignin), a significant amount of lignin remained in the reactor after the effluence of cellulose. Therefore, it is important to develop processes for separating the components of biomass and improving the sugar recovery. Since the decomposition of hemicellulose starts at a lower temperature (180 °C) than that of cellulose (230 °C)<sup>32</sup> and the degradation of glucose rapidly increases at temperatures higher than 230 °C,<sup>96,103,162,163</sup> the degradation of glucose would be unavoidable if hemicellulose and cellulose are hydrolyzed together.

Because of the complicated reaction pathways of hydrothermal reactions, it is relatively difficult to optimize HCW hydrolysis process for lignocellulosic biomass. Mochidzuki et al.<sup>99,100</sup> used the liquid-phase thermogravimetric measuring system to investigate the reaction kinetics of biomass-based unutilized materials in HCW. According to the optimised conditions for biomass decomposition, a two-step treatment was proposed, leading to a remarkable improvement in the yield of water-soluble organics, especially sugars, and a prevention of unwanted side-reactions of hemicelluloses.<sup>99</sup> Two-stage hydrolysis in HCW has become important to solve the problem associated with different hydrolysis characters of cellulose, hemicellulose and lignin and to improve the biomass conversion and sugar recovery.<sup>33,99,164</sup> To achieve a high sugar yield, continuous flow type reactors are favoured and the hydrolysis products need to be cooled down rapidly to minimize further degradation of sugars. A preferred approach is to recover hemicellulose-derived sugars first at

180~200 °C, followed by an increase in temperature to over 230 °C for the recovery of glucose from the solid residue. It was reported that at 180~200 °C, close to 100% of the hemicellulose can be solubilized of which 80~90% is recoverable as monomeric sugars.<sup>49,165,166</sup>

A recent work done by Lu et al<sup>164</sup> conducted the two-step hydrolysis of Japanese beech at 230 °C and 10 MPa as the first stage treatment for 15 min and at 270 °C and 10 MPa as the second stage treatment for 15 min. It was found that the hemicellulose and lignin were hydrolysed in the first stage, while the crystalline cellulose was hydrolysed in the second stage. The total treatment can solubilize 95.6% of the Japanese beech with 4.4% remaining in the water-soluble residue mainly consisting of lignin. According to the liquid analysis, the main products in the first stage hydrolysis are xylose and xylo-oligosaccharides from hemicellulose, and monomeric guaiacyl and syringyl units and their dimeric condensed-type units from lignin. Products from the second stage hydrolysis are mainly glucose and cello-oligosaccharides.<sup>164</sup>

Recently, hydrolysis in HCW was also found to be a promising technology for lignocellulosic biomass pre-treatment to produce sugars by enzymatic hydrolysis. During the pretreatment process in HCW, it is necessary to remove lignin, recover fermentable sugars from hemicellulose, make the residue more digestible by enzyme for the subsequent enzymatic hydrolysis.<sup>39,66,167-175</sup> Therefore, an optimised condition is required to efficiently recover the fermentable sugars (e.g., xylose, glucose, arabinose, etc.) from hemicellulose, leaving the biomass residue rich in cellulose for further enzymatic hydrolysis to recover glucose.

In summary, due to the heterogeneous structure, it is more difficult to recover sugar products from lignocellulosic biomass. A two-stage strategy is suitable, since hydrolysis at lower temperatures can recover most of the sugars (mainly oligomers) from hemicellulose and avoid the further degradation of these sugars. Cellulose hydrolysis in HCW needs a relatively high temperature which would accelerate the degradation of the sugar products. An appropriate catalyst to facilitate cellulose hydrolysis at relatively low temperatures is desirable.

### 2.3.6 Sugar Recovery

Recent results of sugar recovery from the hydrolysis of model compounds and various biomass materials in HCW are summarized in Table 2-3. It can be seen that in comparison with cellulose, starch hydrolysis is higher in both conversion and sugar yield due to its relatively weaker structure. Sugar recovery is also low for the hydrolysis of lignocellulosic biomass in HCW. This is mainly due to the complex structure of lignocellulosic biomass. Another reason is that most of the hydrolysis studies were carried out using batch reactors that require prolonged residential time of hydrolysis products in a reactor during the heating-up and cooling-down processes, resulting in degradation of the sugar products.

A high sugar yield is only possible when the exposure time of sugar products to the high temperature is minimized. A continuous flow type reactor with a rapid heating or cooling control is preferable. Sakaki<sup>114</sup> obtained a glucose yield of 40% from cellulose using a continuous flow type reactor under even near-critical water conditions. Hashaiekh et al.<sup>33</sup> studied the two-stage hydrothermal dissolution of willow in HCW using a continuous flow type reactor. A 95% dissolution of willow was achieved, and the glucose recovery was 20% on a carbon basis. Considering that willow has a 50% cellulose, a 20% of glucose recovery is encouraging for lignocellulosic biomass. However, using the flow type (semicontinuous or continuous) reactor system generally produces a large portion of sugar oligomers in the liquid products, therefore further treatment process is required to convert these sugar oligomers into monomer, i.e., by enzymes. Therefore, a combined HCW and enzymatic hydrolysis technology is suitable for fermentable sugar production from lignocellulosic biomass. More systematic R&D activities are needed to optimize the process and conditions of the combined HCW and enzymatic hydrolysis technology to further improve the sugar recovery from lignocellulosic biomass.

Table 2-3: Results on sugar recovery by biomass hydrolysis in hot-compressed water

Feedstock	Reactor type	Reaction condition	Sugar yield (wt%)	Conversion (wt%)	Literature
Starch	Batch	0.1 MPa, 200 °C, 30 min	69.5%	93.6%	Nagamori and Funazukuri <sup>176</sup>
		0.1 MPa, 220 °C, 10 min	66.8%	96.1%	
		0.1 MPa, 240 °C, 10 min	24.3%	72.3%	
Cellulose	Batch	25 MPa, 400 °C, 15 s	34%	100%	Adschiri et al <sup>50</sup>
		25 MPa, 320 °C, 1 min	20%	100%	
		25 MPa, 300 °C, 7 min	18%	100%	
		25 MPa, 250 °C, 60 min	12%	100%	
		10 MPa, 250 °C, 13 min	40%	80%	
Cellulose	Batch	380 °C, 10 s	40% for oligo sugars, 24% for hexoses	NA	Mochidzuki et al <sup>100</sup> Zhao et al <sup>62</sup>
Rice husk (cellulose 40%, hemicellulose 19%)	Batch	380 °C 16 s + 280 °C 44s	39.5% for hexoses		Zhao et al <sup>64</sup>
		10 MPa, 250 °C, 13 min	4%	36%	Mochidzuki et al <sup>100</sup>
	Semi-batch	10 MPa, 260 °C, 8 min	NA	37.9%	
		10 MPa, 260 °C, 11 min	5%	44%	
		10 MPa, 260 °C, 18 min	NA	43.2%	
		10 MPa, 200 °C, 18 min + 260 °C, 8 min	NA	50%	
		10 MPa, 200 °C, 18 min + 260 °C, 11 min	30%	62.2%	
		10 MPa, 200 °C, 18 min + 260 °C, 18 min	NA	60.4%	
		9.8 MPa, 180 °C, 20 min + 180-285 °C, 21 min + 285 °C, 7 min	NA	97.1%	Ando et al <sup>12</sup>
		250 °C, 150 s	5.3%	26.6%	Goto et al <sup>60</sup>
Bamboo	Flow	300 °C, 30 s	4.2%	48.3%	
		200 °C, 15 min	11.5%	48%	
		10 MPa, 230 °C + 310 °C	20% for glucose	95%	Hashaikeh et al <sup>33</sup>
Chinquapin	Batch	384 °C 17 s + 280 °C 27 s	27.4% for hexoses	NA	Zhao et al <sup>63</sup>
Japan cedar	Batch	384 °C 19 s + 280 °C 54 s	6.7% for hexoses	NA	
Rabbit food (cellulose 16%)	Batch	200 °C, 7min	94.4% for oligo- and monomer		Miyazawa and Funazukuri <sup>177</sup>
Willow (cellulose 50%)	Semi-continuous	200 °C, 60min	22.8% mannose, 11.7% galactose		
Corn stalks	Batch				
Wheat straw	Batch				
Guar gum	Batch				

### 2.3.7 Reaction Kinetics of Model Compounds and Biomass Hydrolysis in HCW

Several studies<sup>65,92,95,97,98,101,103,120,132,133,162</sup> were carried out to obtain reaction kinetics of model compounds and biomass decomposition in HCW. Sasaki et al.<sup>34,35</sup> investigated the kinetics of cellulose hydrolysis in HCW and found the reaction rates of cellulose hydrolysis could be controlled by manipulating the temperature and pressure in HCW without catalysts. The hydrolysis rates under supercritical conditions are much faster than those under subcritical conditions due to the swelling of cellulose under supercritical conditions. Due to the complexity of cellulose hydrolysis reactions, Sasaki and Kabyemela<sup>95</sup> selected cellobiose as the starting material to study its decomposition kinetics in HCW. This significantly simplified the reaction system as cellobiose decomposition involves only two main reactions (hydrolysis and retro-aldol condensation). With decreasing pressure of near- or supercritical water, the contribution of hydrolysis to the overall cellobiose decomposition rate decreased and that of retro-aldol condensation greatly increased. The rate of retro-aldol condensation could be expressed as a first-order reaction rate law while the hydrolysis rate was a second-order reaction (first-order reaction of the water concentration).

A number of studies<sup>97,98,103,120,132,133,162</sup> have been conducted on the kinetics of glucose decomposition in HCW. Recent results by Matsumura et al.<sup>103</sup> indicate that the reaction order of glucose decomposition varies from unity to lower values as temperature increases from 448 to 673 K, primarily due to the shift of reaction mechanisms from ionic to radicalic. As shown in Figure 2-9, glucose decomposition consists of a series of parallel reactions. The controlling steps of the global hydrolysis reaction strongly depend on temperature, although the detailed kinetics of each individual reaction is still unknown.

Sasaki et al.<sup>35</sup> also compared the decomposition rate of cellobiose, glucose and cellulose in HCW. At low temperatures, the glucose or oligomer decomposition rate is much faster than the cellulose decomposition rate. This would lead to a low glucose yield for cellulose hydrolysis in subcritical water. At around the critical point, the cellulose decomposition rate increases rapidly by more than an order of magnitude and becomes faster than the glucose decomposition rate. This leads to a

high yield of hydrolysis products in supercritical water. However, the reaction is very difficult to control due to the short reaction time. Leaching of the reactor material or nickel alloy has also been reported.<sup>120</sup>

Few studies can be found in the open literature on the kinetics of hemicellulose decomposition in HCW. Mochidzuki et al.<sup>99,100</sup> designed a novel liquid-phase thermogravimetry to investigate the reaction kinetics of hemicellulose and cellulose from some plant biomass-based solid wastes. Kinetic analysis indicated that the global decomposition reactions of hemicellulose and cellulose in HCW have activation energies of 85~150 kJ/mol and 130~220 kJ/mol, respectively. Although the reaction activation energy exhibited a considerable wide range depending on the origin of the biomass used, the activation energy of cellulose decomposition is always higher than that of hemicellulose decomposition.

Table 2-4 summaries the limited kinetic data on the decomposition of various model compounds in HCW, collected from the literature.<sup>34,35,91,92,95,99-101,103,178,179</sup> It can be seen that the values of activation energy of hemicellulose, cellobiose and glucose decomposition in HCW are lower than that of cellulose decomposition. There is still considerable scope to improve by further research in order to obtain sufficient kinetic data. There has been little work done on the impacts of the water pressure on the decomposition of those model compounds and their reaction kinetics. There are also no kinetic data available in the literature for lignocellulosic biomass hydrolysis in HCW, yet such data are of great importance to future practical reactor design. To improve sugar yield, catalysts seem to be inevitable to facilitate cellulose hydrolysis at low temperatures so that sugar decomposition is minimized. Kinetic data of such catalytic reactions are also essential.



Table 2-4: Summary of kinetic parameters obtained from literatures

Reaction	Reactor type	Pressure (MPa)	Temperature (°C)	Residence time	Activation energy (kJ/mol)	Frequency factor	Literature	Other notes
Cellulose decomposition	Continuous flow-type	30	290-400	0.02-13.1 s	136 <sup>a</sup>	$7.28 \times 10^{6a}$	Sasaki et al <sup>35</sup>	Microcrystalline cellulose
	Continuous flow-type	25	240-310	0.5-1.6 min	147		Lü et al <sup>91</sup>	Microcrystalline cellulose
	Continuous flow-type	20-25	240-310	0-3 min	147.9	$5.32 \times 10^{12}$	Rogalinski et al <sup>101</sup>	Microcrystalline cellulose
	Semi-batch	25	200-400		190		Adschiri et al <sup>20</sup>	Dried cellulose powder
	Batch	10	250-300		215	$2.33 \times 10^{18}$	Mochizuki et al <sup>99</sup>	Microcrystalline cellulose
	Batch	10	250-300		180	$5.9 \times 10^{14}$	Mochizuki et al <sup>100</sup>	Cellulose in rice husk
	Batch	10	250-300		150	$1.2 \times 10^{12}$	Mochizuki et al <sup>100</sup>	Cellulose in old newspaper
Hemicellulose decomposition	Batch	10	250-300		100	$7.4 \times 10^8$	Mochizuki et al <sup>100</sup>	Hemicellulose in rice husk
	Batch	10	250-300		96	$4.4 \times 10^8$	Mochizuki et al <sup>100</sup>	Hemicellulose in spent malt
Cellobiose hydrolysis	Continuous flow-type	25-40	325-400	0.01-0.54 s	91 <sup>b</sup>	$2.83 \times 10^{7b}$	Sasaki et al <sup>95</sup>	
	Continuous flow-type	25-40	300-400	0.02-2 s	108.6		Kabyemela et al <sup>92</sup>	
Cellobiose pyrolysis	Continuous flow-type	25-40	325-400	0.01-0.54 s	122.6	$1.26 \times 10^{10}$	Sasaki et al <sup>95</sup>	
	Continuous flow-type	25-40	300-400	0.02-2 s	121		Kabyemela et al <sup>92</sup>	
					110		Bobleter and Pape <sup>179</sup>	
Glucose decomposition	Continuous flow-type	25	175-400	0.11-382.5 s	121	$1.33 \times 10^{11}$	Matsumura et al <sup>103</sup>	
	Continuous flow-type	25-40	300-400	0.2-2 s	96	$2.57 \times 10^{11c}$	Kabyemela et al <sup>98</sup>	
		25			88		Amin et al <sup>178</sup>	
		25			121		Bobleter and Pape <sup>179</sup>	

<sup>a</sup> Calculated from given data in Sasaki et al<sup>35</sup>. <sup>b</sup> Calculated from given data in Sasaki et al<sup>95</sup>. <sup>c</sup> Calculated from given data in Kabyemela et al<sup>98</sup>.

### 2.3.8 Modelling of Model Compounds and Biomass Hydrolysis in HCW

Due to the complexity of hydrolysis reactions in HCW and the lack of reaction kinetic data, few modelling studies have been carried out for predicting biomass hydrolysis in HCW. Recently, Kamio et al.<sup>102,104,105</sup> assumed a simplified reaction model for cellulose hydrolysis in HCW based on three processes: (1) conversion of cellulose particle to oligosaccharides, (2) conversion of oligosaccharides to monosaccharides and pyrolysis products, and (3) conversion of monosaccharides to pyrolysis products. Based on kinetic data obtained from experiments, the model gives a reasonable prediction. However, the largest oligosaccharide considered in their mathematical model is cellotriose, which is much smaller than that found in the experiments.<sup>54,55</sup> Certainly, more sophisticated models need to be developed, considering the complex structure of lignocellulosic biomass and the decomposition reaction mechanisms of different biomass components. To establish a mathematical model, the primary reactions of cellulose and biomass during hydrolysis in HCW have to be fundamentally understood. However, so far little work has been done to investigate the primary hydrolysis reactions, which are separated from secondary decomposition reactions of primary hydrolysis products, during cellulose and biomass hydrolysis in HCW.

## 2.4 Comparisons with Other Biomass Hydrolysis Technologies

This section gives an overview on the current status and up-to-date progress of other biomass hydrolysis technologies including acid hydrolysis, alkaline hydrolysis and enzymatic hydrolysis, followed by a detailed comparison of these hydrolysis technologies and biomass hydrolysis in HCW.

### 2.4.1 Acid Hydrolysis

Both dilute acid hydrolysis and concentrated acid hydrolysis are commonly used. The dilute acid process is conducted under high temperature and pressure, and has a reaction time at a scale of up to minutes, facilitating continuous processing. The concentrated acid process uses relatively mild conditions, with a much longer reaction time.

### 2.4.1.2 Dilute Acid Hydrolysis

It has been known for over 150 years that cellulose can be converted to glucose by dilute acid hydrolysis, which is feasible at a commercial scale and capable of providing a maximum glucose yield of 50%.<sup>27</sup> Higher glucose yields are possible for shorter reaction time at higher temperatures, but the process efficiency becomes low due to heat transfer limitations and glucose degradation at high temperatures. Countercurrent shrinking bed reactor technologies have been successful in achieving >90% glucose yield from cellulose.<sup>26,180,181</sup>

During dilute acid hydrolysis, lignocellulosic biomass is converted to sugars, which may be further degraded to other products, typically furfural. Hemicellulose-derived sugars (five-carbon sugars) degrade more rapidly than cellulose-derived sugars (six-carbon sugars). One way to decrease sugars degradation and maximize sugars yields during biomass hydrolysis is to implement a two-stage process. The first stage is operated under mild conditions to recover five-carbon sugars, while the second stage is optimized to recover six-carbon sugars.<sup>24,26,182</sup>

In recent years, treating lignocellulosic biomass with dilute sulfuric acid has been viewed primarily as a pretreatment step for subsequent processing, such as enzymatic hydrolysis. Conventional dilute acid cellulose hydrolysis has been unpopular, because sugars decompose under conditions which are required for cellulose hydrolysis, i.e., high temperature and low pH.<sup>181</sup>

### 2.4.1.2 Concentrated Acid Hydrolysis

This method uses concentrated sulphuric acid to disrupt the hydrogen bonding between cellulose chains, converting it to a completely amorphous state. Cellulose is decrystallized and forms homogeneous gelatine with the acid. As the cellulose is extremely susceptible to hydrolysis at this point, diluting with water at modest temperatures provides complete and rapid hydrolysis to glucose.<sup>26</sup> Compared with dilute acid hydrolysis, concentrated acid hydrolysis leads to little sugar degradation and give sugar yields approaching 100%. However, environment and corrosion problems, and the high cost of acid consumption and recovery present major barriers to economic success.<sup>183</sup>

### 2.4.2 Alkaline Hydrolysis

During alkaline hydrolysis, the  $\text{OH}^-$  ion attacks the anomeric carbon atom, thus cleaving the ether bridge. With the uptake of water and liberation of the  $\text{OH}^-$  ion, glucoses are formed. Experimental results for the cleavage of glycosidic bonds in water-soluble carbohydrates prove that alkaline hydrolysis has the highest reaction rates, followed by acid hydrolysis and finally hydrothermal degradation.<sup>28</sup> However, it is difficult to obtain a high yield of sugar by alkaline hydrolysis because monomeric and dimeric carbohydrates, such as glucose, fructose or cellobiose, are severely attacked by alkalis at temperatures below 100 °C. Organic acids are also formed during hydrolysis, so the alkali consumption by acid formation is also a problem. Alkaline hydrolysis can be used for pretreatment of lignocellulosic biomass, being saponification of intermolecular ester bonds crosslinking xylan hemicellulose and other components, e.g. lignin and other hemicelluloses.<sup>30</sup> Dilute NaOH treatment of lignocellulosic biomass causes swelling, leading to an increase in internal surface area, a decrease in crystallinity, separation of structural linkages between lignin and carbohydrates, and disruption of lignin structure.<sup>184</sup>

### 2.4.3 Enzymatic Hydrolysis

Enzymatic hydrolysis is based on the same principles of biomass microbial decomposition as an integral part of the global carbon cycle. Research on the mechanism of the microbial degradation of cellulose has provided the conceptual framework for an enzymatic conversion plant.<sup>27</sup> Reese et al<sup>185</sup> firstly suggested that an enzyme known as *C1* decrystallizes the cellulose, followed by a consortium of hydrolytic enzymes, known as *Cx* which breaks down the cellulose to sugar. Further research revealed that enzymes work in a more sophisticated way. There are three major classes of cellulase enzymes: (1) endoglucanases, which act randomly on soluble and insoluble glucose chains; (2) exoglucanases, which include glucanhydrolases that preferentially liberate glucose monomers from the end of the cellulose chain and cellobihydrolases that preferentially liberate cellobiose from the end of the cellulose chain; (3)  $\beta$ -glucosidases, which liberate *D*-glucose from cellobiose dimmers and soluble cellodextrins.<sup>26</sup> These enzymes work together synergistically in a complex interplay for efficient decrystallization and hydrolysis of native cellulose.

At present, an economically viable enzymatic hydrolysis process for lignocellulosic materials are hindered by several technical problems: (1) although a high yield (75~95%) of glucose can be potentially achieved, enzymatic hydrolysis reactions are much slower than acid hydrolysis, requiring days rather than hours or minutes for completion; (2) lignocellulose is difficult to be converted into sugars by enzymes due to its high crystallinity, low surface area and heterogeneous nature, as well as cellulose protection by lignin and sheathing by hemicelluloses.<sup>30,186</sup> An effective pretreatment step seems to be necessary to break the lignin seal and reduce cellulose crystallinity; (3) cellulase enzymes are expensive to produce and have a very low specific cellulase activity; (4) The hydrolysis reactions also suffer from end-product inhibition by sugar and time-dependent loss of cellulase activity; and (5) thermal inactivation limits the efficiency of cellulase recycling.<sup>29,183</sup> In spite of these disadvantages, enzymatic hydrolysis is promising for ethanol production from lignocellulosic biomass due to its ability to produce high yield of relatively pure glucose without generation of glucose degradation products and mild reaction conditions.<sup>183</sup>

A major breakthrough came in October 2004 and reduced the cost of cellulose-digesting enzymes to 10~18 US cents/gal of ethanol from the enzyme's 5 US\$/gal cost in 2001.<sup>187</sup> They created genetically modified organisms that produce large amounts of cellulase enzymes that digest cellulose efficiently. Previous studies<sup>39,40,186,188-192</sup> also investigated the performance of various pretreatment options based on the use of a single feedstock, common analytical methods, and a consistent approach to data interpretation. The pretreatment methods considered were uncatalyzed steam explosion, treatment in liquid hot water or pH-controlled hot water, flow through liquid hot water or dilute acid, flow-through acid, treatment with lime, and treatment with ammonia. Sasaki et al<sup>116</sup> also reported that enzymatic hydrolysis of the solubilized cellulose, which was the product of cellulose pretreatment in supercritical water, can achieve two or three orders of magnitude faster reaction rate with high sugar yield and selectivity.

Another important process improvement is the introduction of simultaneous saccharification and fermentation, which combines the cellulase enzymes and

fermenting microbes in one vessel to improve the ethanol production economics.<sup>193-196</sup> The technology has been improved to include the co-fermentation of multiple sugar substrates, i.e. simultaneous saccharification of both cellulose (to glucose) and hemicellulose (to xylose) and co-fermentation of both glucose and xylose by genetically engineered microbes in the same broth.<sup>197</sup>

Table 2-5: Comparisons of different hydrolysis methods<sup>28,31</sup>

Hydrolysis	Conditions	Glucose yield <sup>a</sup>	Advantages & Disadvantages
Concentrated Acid	30-70% H <sub>2</sub> SO <sub>4</sub> 40 °C 2-6 h	90%	A: High sugar recovery High reaction rate D: Environmental and corrosion problems High cost for acid recovery
Dilute Acid	<1% H <sub>2</sub> SO <sub>4</sub> 215 °C 3 min	50-70%	A: High sugar recovery Very high reaction rate D: Environmental and corrosion problems Sugar decomposition at elevated temperature High utility cost for elevated temperature High operating cost for acid consumption
Alkaline	18% NaOH 100 °C 1 h	30%	A: High reaction rate D: Low sugar yield Sugar decomposition by alkali attack
Enzymatic	Cellulase 70 °C 1.5 days	75→95%	A: High yield of relatively pure sugar Mild environmental conditions No environmental and corrosion problems D: Pretreatment of biomass required High cost of cellulase enzymes Low hydrolysis rate
Hot-Compressed Water	150-250 °C 10-25 MPa 0-20 min	<40%	A: No environmental and corrosion problems Low maintenance cost Relatively high reaction rate D: Relatively low sugar yield

<sup>a</sup> During cellulose hydrolysis.

#### 2.4.4 Comparison

Table 2-5 makes a comparison of the process conditions and performance of various hydrolysis methods. Dilute acid hydrolysis achieves a sugar yield of 50~70%. At present, enzymatic hydrolysis can obtain a sugar yield of 75~85% and a projected yield of 85~95% with further research. Although acid processes are matured technologies, enzymatic processes have comparable costs and the potential of future

cost reductions as technology improves.<sup>31</sup> HCW technology is considered to be a green technology. However, the current sugar yield is still low for biomass hydrolysis in HCW hence further research is needed. Each method has its own advantages and disadvantages. It is of great importance to choose a suitable method for biomass of different types. For example, the concentrated acid may be favored when there is significant variability in feedstock characteristics, such as municipal solid waste (MSW).

## 2.5 Conclusions and Research Gaps

Lignocellulosic biomass materials are cheap feedstocks for ethanol production. The key challenge is to develop hydrolysis technologies which are capable of recovering sugars effectively and efficiently. Hydrolysis in HCW can be used as a pre-hydrolysis or pretreatment technology for lignocellulosic biomass to recover hemicellulose-derived sugars. The high xylose recovery (88~98%) and no acid or chemical catalyst required in HCW hydrolysis process make it very attractive economically and environmentally. At present, hydrolysis in HCW achieves a low sugar yield, primarily due to the concurrent competing degradation of sugar products during hydrolysis. Further R&D is needed to improve sugar recovery from lignocellulosic biomass using HCW technology, including:

- (1) Systematic study to gain fundamental understanding on the detailed reaction mechanisms of cellulose hydrolysis under various HCW conditions. This first requires the development of an analytical technique to characterise the glucose oligomers with a wide range of degree of polymerization. Then, the primary liquid products from cellulose hydrolysis in HCW with minimization of secondary reactions have to be obtained and characterised to facilitate the understanding of primary reactions. The structure evolution of cellulose during hydrolysis in HCW needs to be understood as well for efficient production of sugar from cellulose.
- (2) Understanding of the different behaviors of cellulose of various structures (e.g., amorphous and crystalline cellulose, cellulose of various polymorphs) during hydrolysis in HCW. To obtain a high sugar yield, pre-treatment of cellulose or additions of various additives (such as solid catalysts in<sup>154</sup> and<sup>155</sup>) are required to reduce the reaction temperature to minimize the degradation of sugar products.

- (3) Systematic study to gain fundamental understanding on the detailed reaction mechanisms of lignocellulosic biomass hydrolysis under various HCW conditions, considering its heterogeneous structures. The introduction of suitable phase modifiers,<sup>198</sup> may enhance the sugar yield, facilitate the effective and efficient separation of sugars from other degradation products in the biomass extracts and potentially realize co-production of sugars and other chemicals.
- (4) Development of a two-stage hydrolysis strategy, which uses a flow-type reactor to recover hemicellulose-derived sugars and cellulose-derived sugars separately in HCW for enhancing total sugar yields from lignocellulosic biomass.<sup>33,164</sup> Future research is needed to develop suitable catalysts (such as solid catalysts in Refs 154 and 155) to facilitate cellulose hydrolysis at relatively low temperatures in order to minimize the decomposition of sugar products.
- (5) Collection of sufficient reaction kinetic data on the decomposition of model compounds and lignocellulosic biomass in HCW under various conditions. Such kinetic data are essential to reactor design.
- (6) Development of mathematical models for biomass decomposition in HCW, predicting the composition of biomass extracts, process effectiveness and efficiency under various conditions, when different biomass feedstock are used.

HCW technology can find other useful applications in fractionation<sup>165,166</sup> of biomass materials, i.e. selective extraction of various components from biomass. It is also suitable to convert lignocellulosic biomass into extracts for the further production of other biofuels, e.g. bio-hydrogen and/or bio-alkanes by aqueous-phase reforming<sup>72,199-210</sup> or oils through liquefaction processes.<sup>211</sup> One potential technology is to develop an integrated hydrolysis and catalytic aqueous reforming process so that the desired sugar products produced from hydrolysis can be in-situ catalytically reformed to produce hydrogen-rich gas. By adjusting reaction conditions, the in-situ catalytic reforming may be optimized so that the further degradation reactions of sugars are minimized.

## 2.6 Research Objectives of the Present Study

The above literature review has identified various research gaps in the field. However, it is impossible to carry out complete research to address all of those



research gaps. Therefore, this thesis focuses on a systematic investigation on the hydrolysis of cellulose in HCW under various conditions.

The main objectives of this thesis are listed as follows:

- (1) To develop an analytical method for characterising the liquid products obtained from cellulose hydrolysis in HCW, and investigate the precipitate formation from the liquid products.
- (2) To identify the optimised conditions to obtain the primary liquid products from cellulose hydrolysis in HCW, and understand the primary liquid products at various temperatures.
- (3) To examine the significant differences in the behavior of amorphous and crystalline portions within microcrystalline cellulose during hydrolysis in HCW.
- (4) To investigate the evolution of primary liquid products with conversion during hydrolysis in HCW at various temperatures, with the evidence of in situ structural changes.
- (5) To study the behaviors of pretreated microcrystalline cellulose samples by ball milling during hydrolysis in HCW.

## CHAPTER 3 METHODOLOGY AND ANALYTICAL TECHNIQUES

### 3.1 Introduction

This chapter describes the overall research methodology employed to achieve the thesis objectives (outlined in Chapter 2), and the experimental and analytical techniques used in this thesis. The detailed procedures for accomplishing the objectives will be given accordingly in each chapter.

### 3.2 Methodology

Cellulose sample preparation, such as sieving, grinding, etc., was first carried out. Hydrolysis of various cellulose samples in HCW was then conducted using a semicontinuous reactor system, which was developed based on the one used in a previous study<sup>37</sup> on coal degradation in sub-critical water. The solid sample, such as raw and pretreated cellulose samples, precipitate after drying, were characterised by a number of analytical instruments, such as SEM, XRD and particle size analysis, while the liquid samples were mainly characterised by total organic carbon (TOC) analyser, high performance liquid chromatography with evaporative light scattering detector (HPLC-ELSD), high performance anion exchange chromatography with pulsed amperometric detection (HPAEC-PAD).

As shown in Figure 3-1, the overall methodology to achieve the objectives in Chapter 2, will be explained in the following sections. In this research, most experiments or analytical analysis were repeated to ensure reproducibility of results.

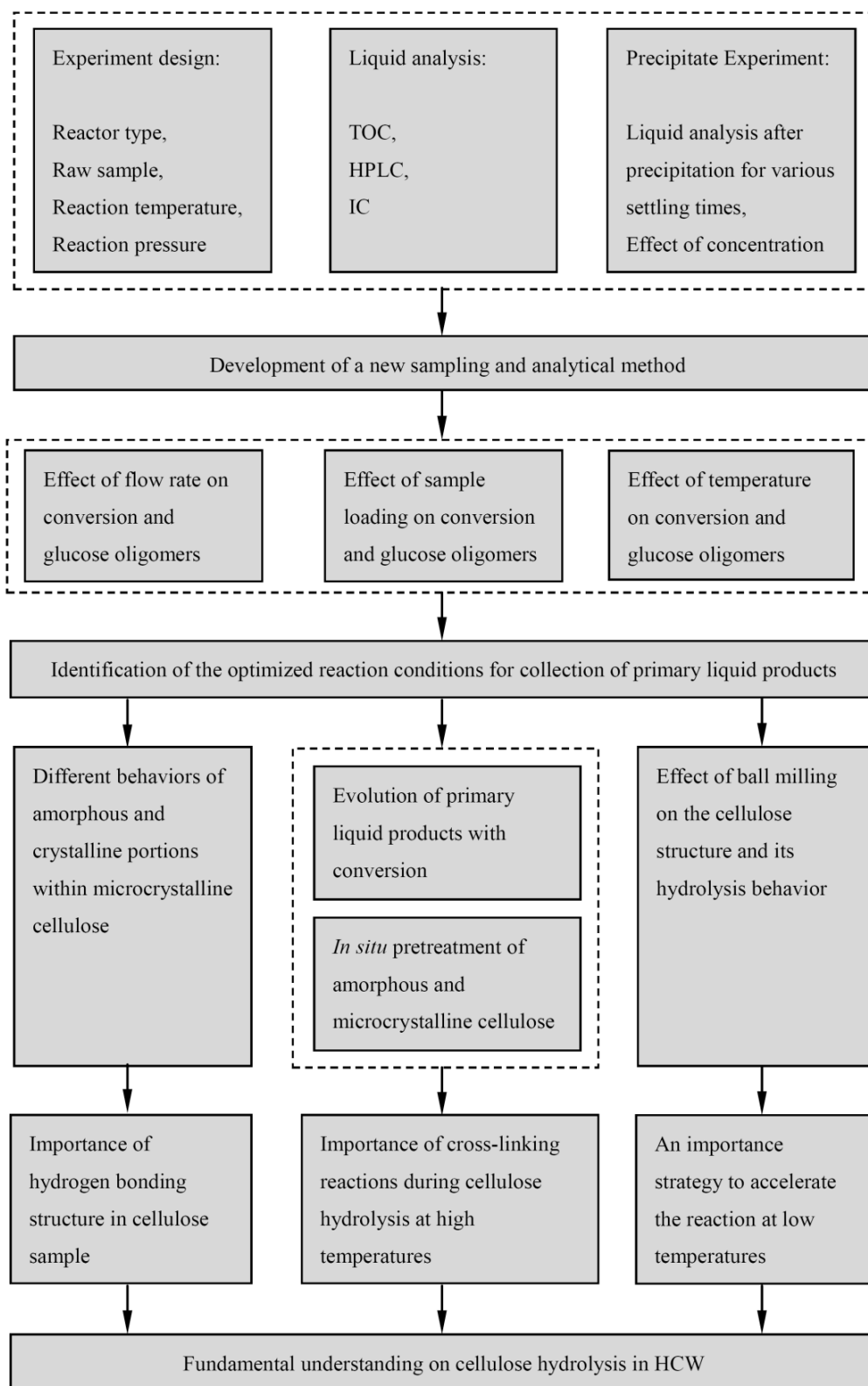


Figure 3-1: Research Methodology

### **3.2.1 Characteristics and Precipitation of Glucose Oligomers in the Fresh Liquid Products**

In this study, an analytical technique for characterising the glucose oligomers in the liquid products of cellulose hydrolysis in HCW was firstly developed. A liquid sample with a high load of glucose oligomers was obtained at a high reaction temperature and characterised by HPLC-ELSD and HPAEC-PAD. In order to understand the formation of precipitate in the fresh liquid products, the liquid samples settled for various precipitation times were analysed by HPAEC-PAD to determine the retention of glucose oligomers in the liquid sample. Then, according to the study in this chapter, a new sampling and analytical method was summarised and used in the whole research included in this thesis.

### **3.2.2 Primary Liquid Products at Various Reaction Temperatures**

In this study, the liquid products collected at various flow rates but the same conversion from cellulose hydrolysis in HCW were characterised by HPAEC-PAD using the sampling and characterisation method developed in section 3.2.1 (Chapter 4). Then the extents of secondary reactions at various flow rates were further estimated by comparing the selectivities of glucose oligomers in the liquid samples, based on a newly-developed method in this section. The effect of sample loading on the selectivities of glucose oligomers was also investigated. Then the optimised reaction condition (flow rate, sample loading, etc.) to achieve the minimization of secondary reactions of primary liquid products at various temperatures can be identified.

The distributions of glucose oligomers in the primary liquid products at various temperatures were then compared to understand the effect of temperature on the formation of glucose oligomers during cellulose hydrolysis in HCW. The primary liquid products collected under various hydrolysis conditions were also subjected to post hydrolysis to analyze the neutral glucose yield, aiming to investigate the possibility of using HCW to break down the long-chain cellulose into short-chain glucose oligomers of various DPs for further fermentation to produce bioethanol.

### **3.2.3 Different Behaviors between Amorphous and Crystalline Portions within Microcrystalline Cellulose**

To understand the differences in the hydrolysis behaviors of amorphous and crystalline cellulose in HCW, the primary liquid products from amorphous and crystalline cellulose were collected at low temperatures ( $< 230$  °C) for characterising the glucose oligomers in the primary liquid products by HPAEC-PAD, following the sampling and characterisation method in section 3.2.1 (Chapter 4). The sample which contains crystalline cellulose only was prepared by pretreating the raw cellulose sample at low temperatures (e.g., 200 °C) sufficient long to remove the amorphous portion. The start temperature of amorphous and crystalline cellulose during hydrolysis in HCW also can be obtained by this study.

### **3.2.4 Evolution of Primary Liquid Products and Evidence of in situ Structure Changes with Conversion**

To study the structure changes of amorphous and crystalline cellulose samples during hydrolysis in HCW, the primary liquid products at different conversions were collected for HPAEC-PAD analysis, following the sampling and characterisation method in section 3.2.1 (Chapter 4). Comparisons of the selectivity of each glucose oligomer in various liquid products are made according to a method developed in section 3.2.2 (Chapter 5).

Apart from experiments at various temperatures, another set of novel two-step experiments were also conducted. Each of those experiments consists of two steps, i.e. a pretreatment step and a subsequent hydrolysis step in HCW. The evolution of specific reactivity and primary liquid products obtained from the two-step experiments were then compared with that of hydrolysis of the raw amorphous sample at 180 °C directly at the same overall conversion levels (considering the conversions during both pretreatment and hydrolysis steps). Similar experiments and comparisons were also done for the microcrystalline cellulose.

### **3.2.5 Hydrolysis of Pretreated Microcrystalline Cellulose by Ball Milling**

To study the hydrolysis behavior of ball milled samples in HCW, the properties (e.g., particle size, crystallinity, etc.) of cellulose samples after ball milling were analysed

first. Then, hydrolysis experiments for ball milled samples were carried out in the semicontinuous reactor system, and the primary liquid products for various ball milled samples at same conversion were characterised by HPAEC-PAD, following the sampling and characterisation method in section 3.2.1 (Chapter 4). The glucose oligomers in the primary liquid products from various ball milled samples were further compared with those for raw sample at same conversion, according to a method developed in section 3.2.2 (Chapter 5), to understand the formation of glucose oligomers for various ball milled samples.

### 3.3 Experimental

#### 3.3.1 Raw Material

Microcrystalline cellulose (Avicel PH-101, Degree of Polymerization: ~250) was purchased from Sigma-Aldrich for experiments. According to the manufacturer, this microcrystalline cellulose is prepared by acidic hydrolysis (hydrochloric acid) of  $\alpha$ -cellulose rich wood pulp. The cellulose sample was sieved and the size fraction of 75~106  $\mu\text{m}$  was used in all the experiments to ensure the cellulose sample is homogeneous.

#### 3.3.2 Sample Preparation

In Chapter 6, in order to obtain cellulose containing crystalline portion only, a pre-treatment was also carried out to remove the amorphous portion within microcrystalline cellulose by treating in HCW at 200 °C for 4 hours, because the reactivity of cellulose remains unchanged with increasing conversion after 4-hour treatment at 200 °C. To remove the reactive part within amorphous cellulose, the raw sample was treated in HCW at 180 °C for 10 min.

In Chapter 7, the in situ pretreated samples were required to understand the structure change of cellulose during hydrolysis in HCW. For amorphous cellulose (Figure 3-2a), the sample was firstly pretreated at 190 or 200 °C in HCW for 5 mins then in situ cooled down to 180 °C for continuous hydrolysis reactions in HCW. The evolution of specific reactivity and primary liquid products obtained from the two-step experiments were then compared with that of hydrolysis of the raw sample at 180 °C directly at the same overall conversion levels (considering the conversions

during both pretreatment and hydrolysis steps). Similar experiments and comparisons were also done for the microcrystalline cellulose (Figure 3-2b), which was pretreated in HCW at 200 °C for 4 hours, or 250 and 270 °C for 5 or 10 mins then in situ increased or cooled to 230 °C for subsequent hydrolysis reactions. It should be noted that the temperature of reactor outlet will require ~5 min to stabilize when the reactor inlet temperature reaches 230 °C. Then, the liquid products can be collected to compare with raw cellulose sample at the same overall conversions. Generally, the pre-treatment at high temperatures cannot be too long, because the reaction at high temperatures is too fast, while it requires a long time for reaction at low temperatures to achieve the same conversion.

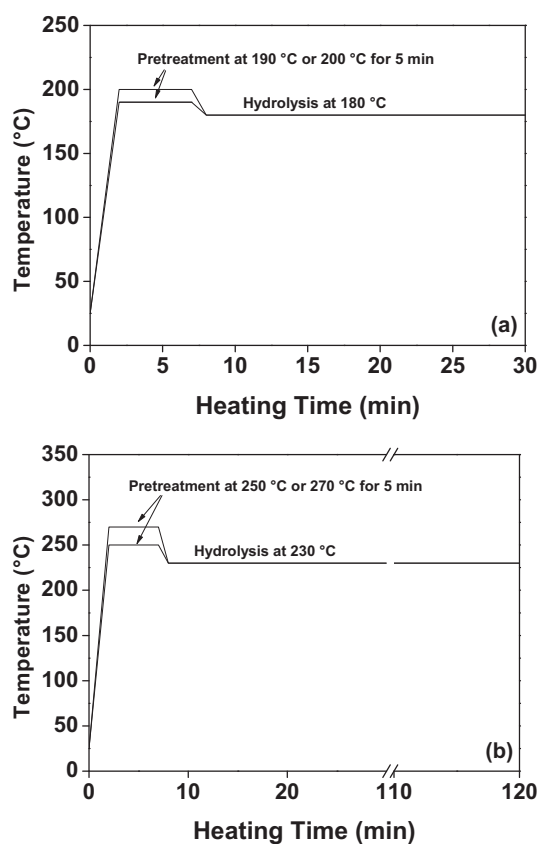


Figure 3-2: Two-step experiments including pretreatment and further hydrolysis. (a) for amorphous cellulose; (b) for crystalline cellulose

In Chapter 8, the ball milled samples were prepared using a laboratory ball mill (Retsch Mixer Mill MM400), in order to study the behaviors of ball milled cellulose samples during hydrolysis in HCW. Briefly, ~2 g cellulose sample was charged into

the grinding cell and the ball mill operated at a grinding frequency 15 Hz with a 15 mm ball size. Various grinding times (1–7 hrs) were used for preparing the sample with different contents of crystalline cellulose. Cryogenic ball milling was also used to prepare a sample with particle size reducing significantly but little change on hydrogen bonding structure. The grinding cell was cooled with liquid nitrogen for 10 min to make sample become embrittled prior to grinding in the ball mill, in order to achieve a considerable reduction of size in a short milling time (e.g., 2 min).

### 3.3.3 Reactor System

In the previous studies, three types of reactor systems were typically used, i.e. batch,<sup>51,54,57,60,61</sup> semicontinuous<sup>32,33,50,53,56</sup> and continuous reactor systems.<sup>35,52,54,55</sup> In a batch reactor system,<sup>51,54,57,60,61</sup> feedstock solid particles are mixed with HCW in the reactor. The residence time of the reacting solid is long; so are the liquid products, leading to their extensive degradation hence low sugar yields and high oil and char yields. In a semicontinuous reactor system,<sup>32,33,50,53,56</sup> HCW flows through a bed of feedstock particles; while the reacting particles remain in the reactor, the liquid products are rapidly swept out. In a continuous reactor system,<sup>35,52,54,55</sup> the slurry of feedstock particles and HCW flows through the reactor together. Therefore, the residence times of liquid products in semicontinuous and continuous reactor systems are short, resulting in much less degradation compared to a batch reactor system hence the observed high sugar yields.<sup>54,55</sup> One key difference between semicontinuous and continuous reactor systems is that the contact between liquid products and reacting particles in a semicontinuous reactor system is minimized while that is continuous in a continuous reactor system. A continuous reactor system is also typically required to operate at high temperatures and pressures in order to achieve a high conversion of the feedstock within a short residence time.<sup>34</sup>

Compared to other reactor systems, the semicontinuous reactor system has some unique features which are suitable for our research to investigate the primary liquid products from cellulose hydrolysis in HCW. These features include:

- long residence time of reacting solid and short residence time of liquid products.
- minimized contact between liquid products and reacting solid residue.



- minimization of the secondary decomposition reactions of primary liquid products in the aqueous phase.
- high yields of mono- and oligo-saccharides, and low yields of oil and char.
- operation at both low and high reaction temperatures

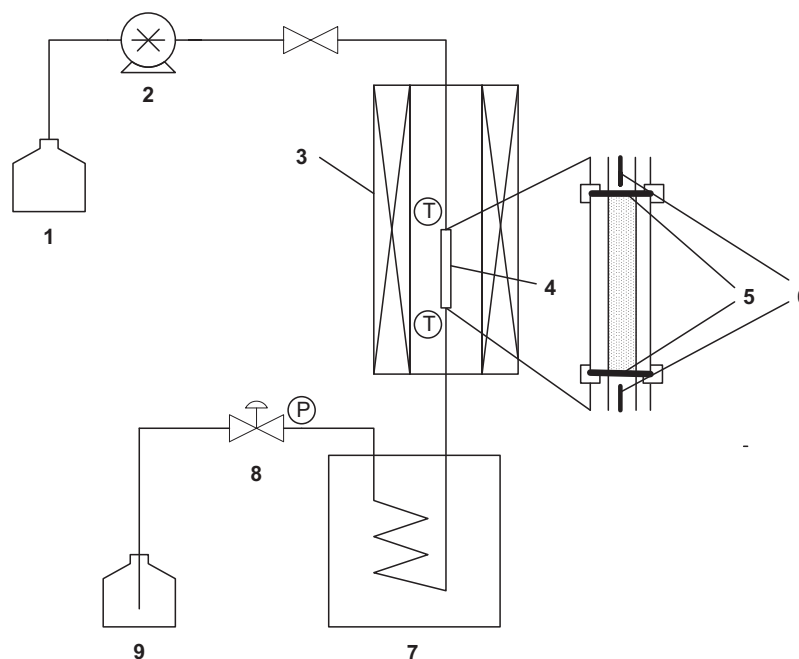


Figure 3-3: Schematic diagram of the experimental apparatus used in this study. 1. Water reservoir; 2. HPLC pump; 3. infrared image furnace; 4. reactor; 5. sintered stainless steel filter; 6. thermocouple; 7. cooling unit; 8. back pressure regulator; 9. liquid product collector

A schematic diagram of the semicontinuous reactor system used in the present study is shown in Figure 3-4. This system was developed based on the one used in a previous study<sup>37</sup> on coal degradation in sub-critical water. It mainly includes a HPLC pump to deliver the deionized water, an infrared image furnace to heat the reactor, two thermocouples to monitor the reaction temperature, a cooling unit to quench the liquid product quickly, and a back pressure regulator to control the reaction pressure. As shown in Figure 3-5, the reactor used in this study actually consists of a double male union (Part Number: SS-4-VCR-6-DM), two filter gaskets (Part Number: SS-4-

VCR-2-.5M, pore size: 0.5  $\mu\text{m}$ ), two tube adapter glands (Part Number: SS-4-VCR-3-4TA) and two female nuts (Part Number: SS-4-VCR-1) from Swagelok.

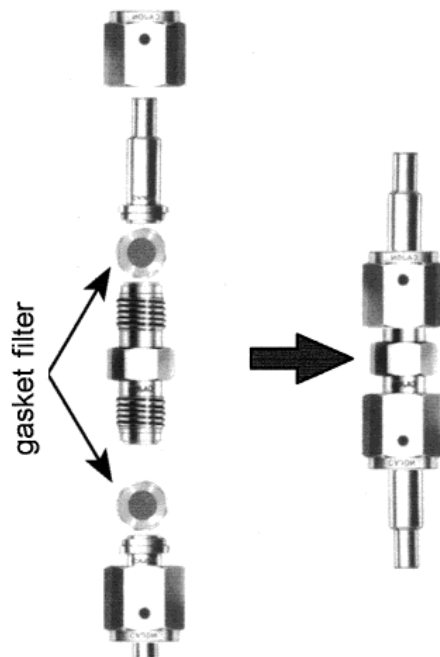


Figure 3-4: Reactor used in this study

In each experiment, a small amount of cellulose was loaded in a SUS316 stainless steel tubular reactor cell (see Figure 3-4), which was sandwiched by a pair of sintered stainless steel gasket filters at its both ends. The reactor cell was then placed inside an infrared gold image furnace (ULVAC-RIKO INC., Japan), which is capable of rapid heating. Before heating, deionised water was delivered by a HPLC pump (Alltech, Model 627) and flowed through the reactor cell at a pre-set flow rate. The reactor cell was then rapidly heated to the reaction temperature within 2 minutes and held at the reaction temperature for a desired period. The reactor cell temperature was controlled with a thermocouple, the tip of which was located right above the reactor cell. Another thermocouple was located right below the reactor cell to monitor the reactor outlet temperature. The temperature profiles of reactor inlet and outlet are shown in Figure 3-5. Generally, the reactor inlet temperature is similar as the furnace setting temperature, while the reactor outlet temperature will stabilize in  $\sim 2$  min after the inlet temperature achieves the setting value at the water flow rate of

10 ml/min. At a higher water flow rate, the stabilization time can be shortened. Pressure in the reactor was controlled using a back-pressure regulator.

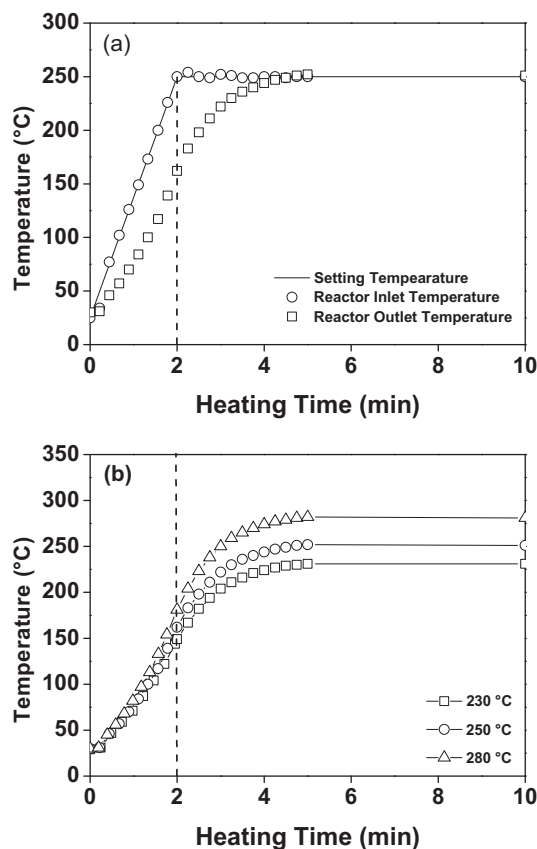


Figure 3-5: The time-dependence of the reactor inlet and outlet temperatures during furnace heating period. (a) Final temperature: 250 °C, water flow rate: 10 ml/min; (b) Time-dependence of reactor outlet temperature for different setting temperatures.

The liquid products were quickly quenched using an ice water bath and collected periodically. Carbon balance in the liquid products is also ~100% at 280 °C so that little gaseous product was formed during hydrolysis. It should be noted that there are ~4 min lag between the reactor outlet and sample collection point. Depending on reaction temperature, experiments were carried out at various water flow rates (10–40 ml min<sup>-1</sup>) and sample loadings (7.5–60 mg). In all experiment, a reaction pressure of 10 MPa was used.

### 3.3.4 Precipitation of Fresh Liquid Products

For precipitation experiments, in order to obtain a liquid sample with a high concentration of glucose oligomers, the liquid hydrolysis products were produced from the hydrolysis of cellulose in HCW at 280 °C and 20 MPa. The liquid products collected under such reaction conditions form a large yield of precipitate under ambient conditions. Then the same fresh liquid product was firstly divided into 10 samples of the same volume. These liquid samples were then settled for a precipitation time (2 to 144 hours). Once the precipitation time was reached, the liquid sample was then filtered using a syringe filter (0.45 µm, PVDF) to remove the the water-insoluble portion then immediately analyzed by the HPLC-ELSD or HPAEC-PAD. In this study, repeated cellulose hydrolysis experiments were carried out in order to produce fresh samples under the same reaction condition for subsequent analysis and precipitation experiments. The precipitate samples after settling for at last one week were also collected by centrifugal separation and dried at 50 °C for subsequent characterization by SEM and XRD.

### 3.3.5 Post Hydrolysis

Post hydrolysis experiments were conducted to determine the total neutral glucose content in a liquid product by converting all the glucose oligomres into monomer using acid hydrolysis following a NREL method.<sup>212</sup> Briefly, sulphuric acid (72%) was added to the liquid products and the acid concentration was adjusted to 4%. The liquid sample was then treated in an autoclave for 1 h at 121 °C. After neutralization of the sulphuric acid in the sample, the glucose content was analysed by HPAEC-PAD using an isocratic method, which elutes 100 mM NaOH only with a flow rate of 0.5 ml min<sup>-1</sup>. The glucose standards at different concentrations were also prepared to correct for losses due to the degradation of glucose during acid hydrolysis.

## 3.4 Instruments and Analytical Techniques

### 3.4.1 High-Performance Liquid Chromatography with Evaporative Light Scattering Detector (HPLC-ELSD)

The liquid sample was first analysed by high performance liquid chromatography with evaporative light scattering detector (HPLC-ELSD), which is much more sensitive than the traditional refractive index (RI) or low-wavelength ultraviolet (UV)

detectors.<sup>213</sup> Following a method detailed elsewhere,<sup>214</sup> the HPLC-ELSD was equipped with a Prevail carbohydrate ES column (250 × 4.6 mm) packed with 5- $\mu$ m spherical polymer beads coated with proprietary bonding material. The precolumn cartridge (7.5 × 4.6 mm) and the analytical column were obtained from Alltech. HPLC-grade acetonitrile and water mixture was used as mobile phase, and a Hewlett Packard 1050 instrument with Alltech ELSD 3300 detector was used for sugar detection.

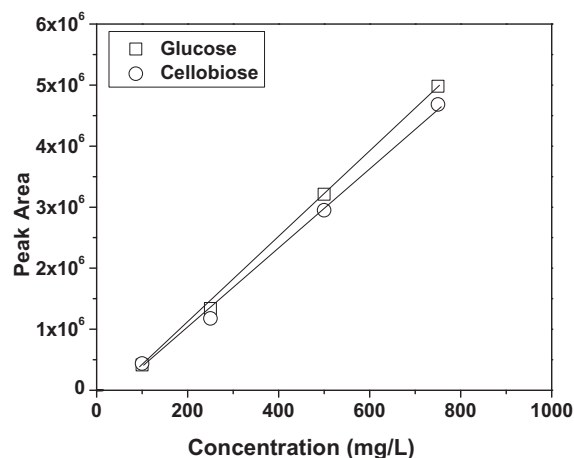


Figure 3-6: Calibration curves for glucose and cellobiose by HPLC-ELSD

Although the HPLC-ELSD is more sensitive compared to other detectors, we only can identify the sugar peaks with concentrations higher than 10 mg/L. Quantitative analysis of C1-C5 with large concentrations (e.g., > 100 mg/L) can be also made by HPLC-ELSD according to the standard curves. Figure 3-6 shows the standard curves for glucose and cellobiose with concentration range of 100-750 mg/L by HPLC-ELSD. However, due to the low concentration of liquid sample collected in our experiment, we cannot directly identify any sugar peaks in the fresh sample. The liquid sample was then concentrated by vacuum evaporation to increase concentrations of the glucose oligomers for HPLC-ELSD analysis. In order to avoid the decomposition of glucose oligomers, the vacuum evaporation was conducted at a low temperature (40 °C). After 25 times of concentration, the HPLC-ELSD could finally identify the peaks of glucose oligomers with DPs up to 6 (see Figure 3-7) in the liquid solutions.

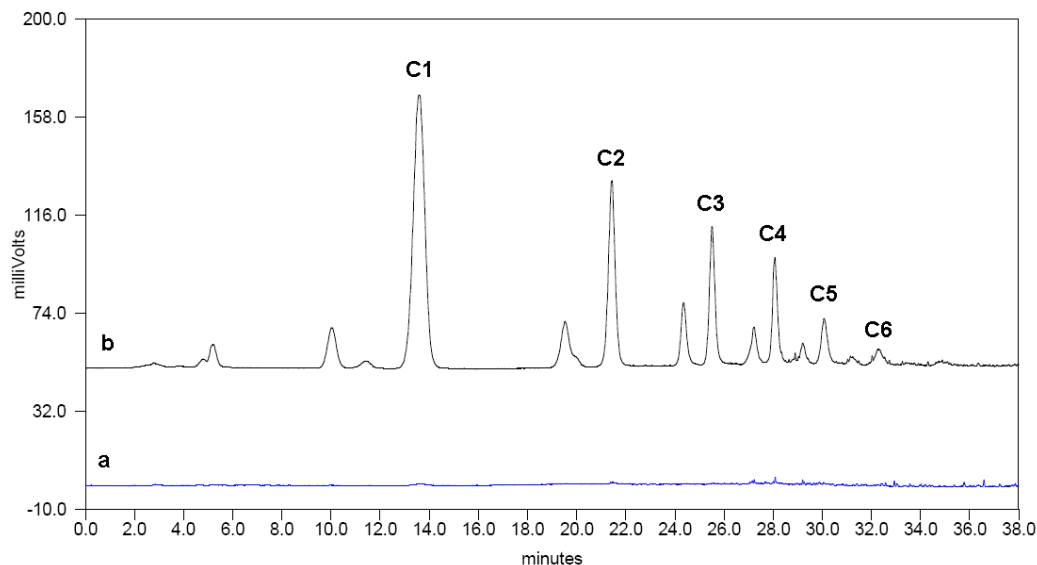


Figure 3-7: Typical HPLC-ELSD chromatogram of liquid sample collected during hydrolysis in HCW at 280 °C, 10MPa, and 10 ml/min. (a) without concentration; (b) with concentration.

#### 3.4.2 High-Performance Anion Exchange Chromatography with Pulsed Amperometric Detection (HPAEC-PAD)

The liquid sample was further analysed by a high performance anion exchange chromatography with pulsed amperometric detection (HPAEC-PAD), which permits the direct analysis of carbohydrate at low-picomole levels without requiring derivatization.<sup>215</sup> Basically, carbohydrates are detected by measuring the electrical current generated by their oxidation at the surface of a gold electrode. The products of this oxidation reaction also poison the surface of the electrode, which means that it has to be cleaned between measurements. This is accomplished by first raising the potential to a level sufficient to oxidize the gold surface. This will cause desorption of the carbohydrate oxidation products. The electrode potential is then lowered to reduce the electrode surface back to gold.<sup>215</sup> The sequence of the potentials is illustrated in Figure 3-8.

Pulsed amperometric detection thus employs a repeating sequence of three potentials. Current from carbohydrate oxidation is measured at the first potential,  $E_1$ . The second,  $E_2$ , is a more positive potential that oxidizes the gold electrode and cleans it of products from the carbohydrate oxidation. The third potential,  $E_3$ , reduces the gold

oxide on the electrode surface back to gold, thus permitting detection during the next cycle at  $E_1$ . The three potentials are applied for fixed durations referred to as  $t_1$ ,  $t_2$ , and  $t_3$ . The step from one potential to the next produces a charging current that is not part of the analyte oxidation current, so the analyte oxidation current is measured after a delay that allows the charging current to decay. The carbohydrate oxidation current is measured by integrating the cell current after the decay. Current integration over time is charge, so the detector response is measured in coulombs. Since the oxidation of the sugars at the electrode is catalyzed by the electrode surface, the amperometric response of a class of compounds is controlled primarily by the dependence of the catalytic surface state on the electrode potential and not on the redox potentials of the compounds themselves. More details on pulsed amperometric detection can be found elsewhere.<sup>215,216</sup>

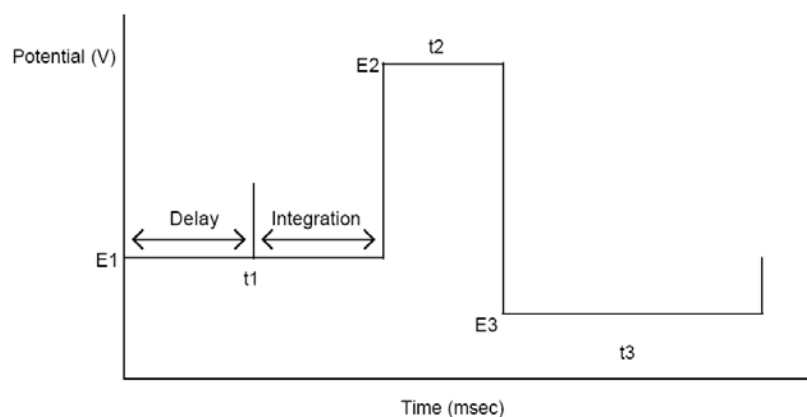


Figure 3-8: Diagram of the pulse sequence for carbohydrate detection<sup>215</sup>

The HPAEC-PAD analysis in this study was carried out using a Dionex ICS-3000 ion chromatography (IC) system equipped with a CarboPac PA200 analytical column ( $3 \times 250$  mm) and guard column ( $3 \times 50$  mm). The analysis follows a gradient method which consists of eluting 20-225 mM NaOAc over 30min with a flow rate of 0.5 ml/min, according to Curve 6 (100 mM NaOH throughout) based on the detection wave form from a Dionex technical note.<sup>216</sup>

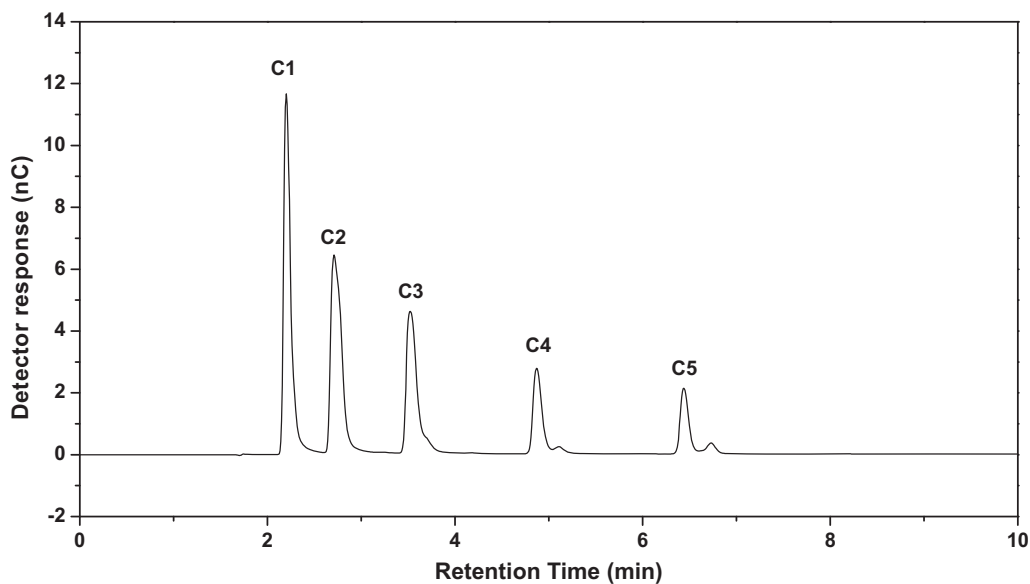


Figure 3-9: IC chromatogram of the standards of C1-C5 with concentration of 0.5 mg/L

At present, sugar standards are only available for glucose oligomers with DPs up to 5 (i.e., glucose, cellobiose, cellotriose, cellotetraose, and cellopentaose). These sugar standards were purchased from Sigma-Aldrich and used to quantitatively analyze glucose oligomers with DPs up to 5 in the liquid samples based on their calibration curves. Typical IC results for glucose with DP of 1-5 is shown in Figure 3-9, it is found that HPAEC-PAD is sensitive enough to analyse the glucose oligomers in the water with concentrations of 0.5 mg/L, but quantitative analysis can only be made for glucose oligomers with DPs up to 5. However, glucose oligomers with DPs > 5 could only be qualitatively analysed, due to the lack of standards for higher-DP glucose oligomer. The identification of glucose oligomers with DPs > 5 is based on their sequences shown in the IC chromatogram. Even the current standards of C4 and C5 are not 100% pure (e.g., ~90% for C4, ~85% for C5), because small peaks near C4 and C5 can be found in the IC chromatogram. The calibration curves for C1 to C5 based on peak height for the standards C1 to C5 using HPAEC-PAD are shown in Figure 3-10. It is found that the calibration curves are only linear up to particular concentrations for C1 to C5, respectively. For quantitative analysis, necessary dilution of sample may be required to ensure the sample concentration is within the linear response range of the HPAEC-PAD detection system. Detailed application of



HPAEC-PAD for the characterization glucose oligomers in the liquid sample collected from hydrolysis in HCW will be discussed in Chapter 4.

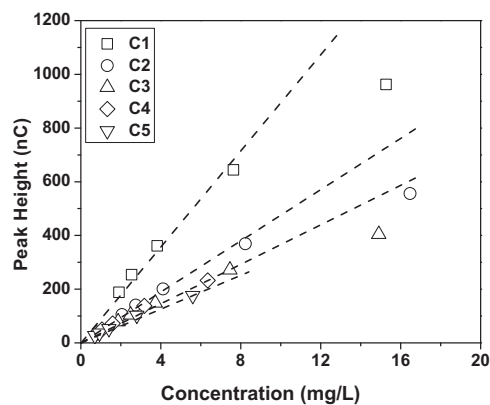


Figure 3-10: Calibration curves for C1-C5 standards by HPAEC-PAD.

### 3.4.3 Total Organic Carbon (TOC) Analysis

The total organic carbon of the liquid samples was analyzed using a total organic carbon (TOC) analyzer (Shimadzu TOC-V<sub>CPH</sub>), which uses the 680 °C combustion catalytic oxidation method.<sup>217</sup> The TOC analyser not only employs the most powerful wet oxidation reagent (peroxodisulfuric acid) but also adds a combination of UV radiation and heating to further enhance oxidation performance. The high-sensitive non-dispersive infrared detector achieves the ultrahigh sensitivity measurement with a detection limit of 0.5 µg/L. Generally, the sample is injected via the sample pre-treatment/injection system into the combustion tube, which is filled with catalyst. The carbon in the sample is oxidised to carbon dioxide and water. After removing the moisture and halides that may damage the detection cell, the gas then enters the sample side of the non-dispersive infrared detector (NDIR), where the carbon dioxide is detected. The NDIR signal is converted to a peak profile, and the peak area is calculated. In our study, the carbon concentration in the liquid sample is measured based on the calibration curve shown in Figure 3-11. Generally, the sample will be injected three times, and the average value will be reported as the final result.

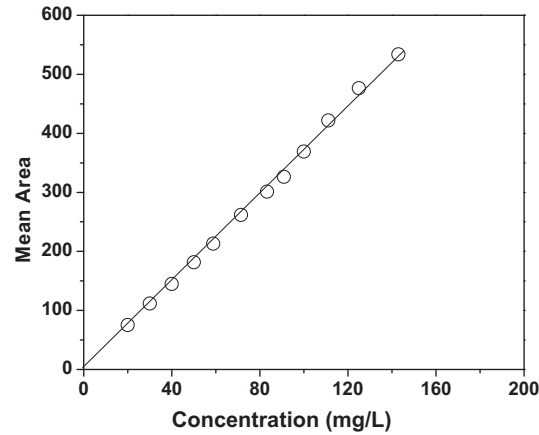


Figure 3-11: Calibration curve for TOC analysis

### 3.4.4 Specific Reactivity Analysis

The total carbon contents liquid samples were analysed using a TOC analyzer (Shimadzu TOC-V<sub>CPH</sub>). The conversion level  $X$  of cellulose at a reaction time  $t$ , on a carbon basis, is calculated as

$$X = \frac{C_t}{C_0} \quad \text{Equation (3-1)}$$

where  $C_0$  is total carbon of the initial sample loaded into the reactor and  $C_t$  is the total carbon converted from the sample after a reaction time  $t$ . The value of  $C_t$  can be calculated from the sum of all carbon collected from the hydrolysis reactions commence at  $t = 0$ , i.e.

$$C_t = \sum V_i c_i \quad \text{Equation (3-2)}$$

where  $V_i$  is the total liquid volume between two sampling intervals and  $c_i$  is the carbon concentration of that liquid. It should be noted that for the two-step experiments, the overall conversion  $X$  consists of both the pretreatment and hydrolysis steps. The specific reactivity  $R$  of cellulose, on a carbon basis, was then determined as

$$R = -\frac{1}{C} \frac{dC}{dt} \quad \text{Equation (3-3)}$$

where  $C$  is the carbon content in the remaining cellulose at a reaction time  $t$  during hydrolysis in HCW. The liquid samples were collected every 5 min so that the

specific reactivity calculated is actually an average reactivity of cellulose during the collection time.

### 3.4.5 X-ray Diffraction (XRD) Analysis

X-ray diffraction (XRD) analysis was used to qualitatively identify the amorphous and crystalline portions in cellulose. The analysis was carried out using a Bruker AXS D8 Advance x-ray diffractometer. The diffracted intensity of Cu K $\alpha$  radiation was measured in a  $2\theta$  range from  $10^\circ$  to  $30^\circ$ .

Based the XRD results, relative crystallinity of the solid residues were then calculated according to Segal's method<sup>218</sup>

$$x_c = \frac{I_{(200)} - I_{am}}{I_{(200)}} \quad \text{Equation (3-4)}$$

where  $I_{(200)}$  and  $I_{am}$  are the intensities of the 200 peak ( $2\theta = 22.7^\circ$ ) and the amorphous peak ( $2\theta = 18^\circ$ ), respectively.  $I_{(200)}$  represents both crystalline and amorphous material while  $I_{am}$  represents amorphous material only.

### 3.4.6 Particle Size Analysis

Raw and ball milled cellulose samples were analyzed using a laser-diffraction particle size analyzer (Malvern Mastersizer2000) to determine the distribution of particle size. The sample was mixed with sodium hexametaphosphate solution (10% w/v) to aid dispersion of fine particles before loading into the measuring chamber. Repeated measurements were done and the standard error is <1%.

### 3.4.7 Scanning Electron Microscope (SEM) Analysis

The morphology of raw cellulose and precipitate samples were characterised using a Zeiss EVO 40XVP scanning electron microscopy (SEM). The sample was coated with gold using a vacuum sputter-coater to provide a conductive medium for the analysis.

### 3.5 Summary

Microcrystalline cellulose sample was used in the present research. The cellulose sample was sieved and the size fraction of 75~106  $\mu\text{m}$  was used in all the experiments to ensure the cellulose sample is homogeneous. Raw cellulose sample was pretreated to obtain the samples with different structures for understanding the mechanisms of cellulose hydrolysis in HCW.

Hydrolysis of cellulose in HCW was carried out using a semicontinuous reactor system, which allows the liquid products to be rapidly swept out of the reactor system, quenched by an ice water bath and collected for analysis, while the reacting solid sample remains in the reactor. This minimizes the secondary decomposition reactions of glucose oligomers in the aqueous phase, therefore suitable for our research to investigate the primary liquid products from cellulose hydrolysis in HCW.

Analytical or instrumental analyses were carried out on the cellulose and liquid product samples for chemical and physical characterisations, including total organic carbon analysis by TOC analyzer, glucose oligomers analysis by HPLC-ELSD and HPAEC-PAD, morphological characterisation by SEM, identification of amorphous and crystalline cellulose by XRD, etc.

## CHAPTER 4 CHARACTERISTICS AND PRECIPITATION OF GLUCOSE OLIGOMERS IN THE FRESH LIQUID PRODUCTS

### 4.1 Introduction

Typical reactor systems used for cellulose and/or biomass hydrolysis in HCW include batch, semi-continuous and continuous reactor systems.<sup>32,33,35,50-52,54-56,65,66,101,114,150</sup> It was found that the characteristics of biomass extracts obtained depend strongly on the reactor systems used. For example, in a batch system, sugar yields are typically low while oil and char yields are high, apparently due to the extensive secondary reactions of the primary hydrolysis products.<sup>51</sup> A semi-continuous or continuous reactor system may potentially reduce the degradation of reaction intermediates in the liquid phase. For example, it was reported previously<sup>53</sup> that the liquid products contain mainly oligosaccharides in a semi-continuous reactor system, but only glucose oligomers up to cellopentaose were indentified in the liquid products. The fresh liquid sample from biomass hydrolysis was clear but after settling for a while, precipitate appeared from the liquid products. It is believed that such precipitate is mainly formed from the precipitation of glucose oligomers which are soluble in HCW but have much lower solubilities or even insoluble in water at room temperature.<sup>52</sup> However, it is still not clear about the size of glucose oligomers in the liquid products. It is also unknown which glucose oligomers are responsible for precipitate formation.

The low solubilities of glucose oligomers particularly those with high degree of polymerizations (DPs) mean there are significant challenges in the identification and analysis of these products in the liquid hydrolysis products, due to both their low concentration and their continuous precipitation after sample collection. For example,

it was reported in previous studies<sup>32,52,53,56</sup> that high performance liquid chromatography (HPLC) systems using traditional refractive index (RI) or low-wavelength ultraviolet (UV) detectors can only detect limited and typically overlapped peaks for glucose oligomers. Attempts were also made to use matrix-assisted laser desorption/ionization time-of-flight mass spectrometry (MALDI-TOFMS) to identify glucose oligomers in liquid products and the technique successfully identified the presence of oligomers with DPs up to 12 in the liquid products of cellulose decomposition in HCW.<sup>54,55,150</sup> However, it is still unknown if there are other high-DP glucose oligomers present in the liquid products but unidentified. Little knowledge is available on the effect of precipitation on the compositions of glucose oligomers in the liquid hydrolysis products.

Recently, with HPLC systems, an evaporative light scattering detector (ELSD) is reported to be more sensitive than RI or low-wavelength UV detection, and has the capability of detecting carbohydrates to low nanogram levels.<sup>213</sup> An improved chromatographic technique, known as high performance anion exchange chromatography with pulsed amperometric detection (HPAEC-PAD), was also used to characterize xylan oligomers in the products from xylan hydrolysis in HCW.<sup>58</sup> The HPAEC-PAD permits the direct analysis of carbohydrate at low-picomole levels without derivatization.<sup>215</sup> Therefore, these advanced techniques may provide additional capacities for characterizing glucose oligomers in the liquid products obtained from the hydrolysis of cellulose and/or biomass in HCW. Such knowledge on glucose oligomers in the liquid products is essential to understanding hydrolysis mechanisms therefore the development of advanced technologies to convert these glucose oligomers to monomers for subsequent ethanol production.

Therefore, it is the objective of this chapter to use the two analytical techniques (i.e., HPLC-ELSD and HPAEC-PAD) for determining the distribution of the glucose oligomers in the liquid products from cellulose hydrolysis in HCW. A systematic experimental program has been carried out to investigate the precipitation of glucose oligomers, due to the development of a new method for analyzing the glucose oligomers in the liquid products of cellulose hydrolysis in HCW.

## 4.2 Analysis of Glucose Oligomers in the Liquid Products

### 4.2.1 HPLC-ELSD Analysis

Figure 4-1 presents the data obtained from the HPLC-ELSD analysis of the fresh liquid products immediately collected after the experiments. It is surprising to see that the HPLC-ELSD results (see Figure 4-1a) show no apparent sugar peaks, indicating that the concentrations of glucose oligomers in the liquid products are too low to be analyzed by the HPLC-ELSD. The liquid sample was then concentrated by vacuum evaporation in order to increase concentrations of the glucose oligomers for analysis. In order to avoid the decomposition of glucose oligomers, the vacuum evaporation was conducted at a low temperature (40 °C). After 25 times of concentration, the HPLC-ELSD could finally identify the peaks of glucose oligomers with DPs up to 6 (see Figure 4-1b) in the liquid solutions. No peaks of glucose oligomers with DPs > 6 are shown in the HPLC-ELSD chromatogram. It is also noteworthy that while the fresh liquid sample was clear, coincidentally, during the concentration of fresh liquid product by vacuum evaporation, a significant amount of precipitate (white color) was also formed and observed in the concentrated liquid sample but filtered before the concentrated sample was injected into the HPLC-ELSD for analysis. Take it together, the results in Figure 4-1b and the observation of precipitate indicate that the concentrations of the glucose oligomers with DPs > 6 are still too low in the concentrated liquid sample to be detected by the HPLC-ELSD and obviously part of these glucose oligomers in the fresh liquid products contributed to precipitate formation during vacuum concentration.

### 4.2.2 HPAEC-PAD Analysis

The fresh liquid sample was also directly analyzed using the HPAEC-PAD, immediately after sample collection without being concentrated. As shown in Figure 4-2, the HPAEC-PAD successfully detected glucose oligomers with a wide range of DP in the fresh sample without being concentrated. Figure 4-2 clearly shows that the liquid products from cellulose hydrolysis in HCW can actually contain various high-DP glucose oligomers (with DPs up to 30 in this sample), which are well separated and clearly identified. Compared to the HPLC-ELSD analysis of the fresh sample (Figure 4-1a), the results show that HPAEC-PAD offers excellent sensitivity in the analysis of glucose oligomers in the fresh liquid products. The results also clearly

demonstrate the presence of a wide range of high-DP glucose oligomers, which cannot be detected by the HPLC-ELSD analysis (for either fresh or concentrated samples, see Figure 4-1) and has not been reported previously. The highest DP of glucose oligomer in liquid products from cellulose hydrolysis in HCW was reported to be 12, identified by MALDI-TOFMS in previous studies.<sup>23-25</sup> The differences in the glucose oligomers identified in Figure 4-1b by HPLC-ELSD, those in Figure 4-2 by HPAEC-PAD and those in previous studies may be due to two reasons. One is that the analytical instruments are not capable of analyzing or sensitive enough to detect these high-DP glucose oligomers. The other is that the liquid sample was not analyzed immediately so that at least part of these high-DP glucose oligomers already precipitated before analysis.

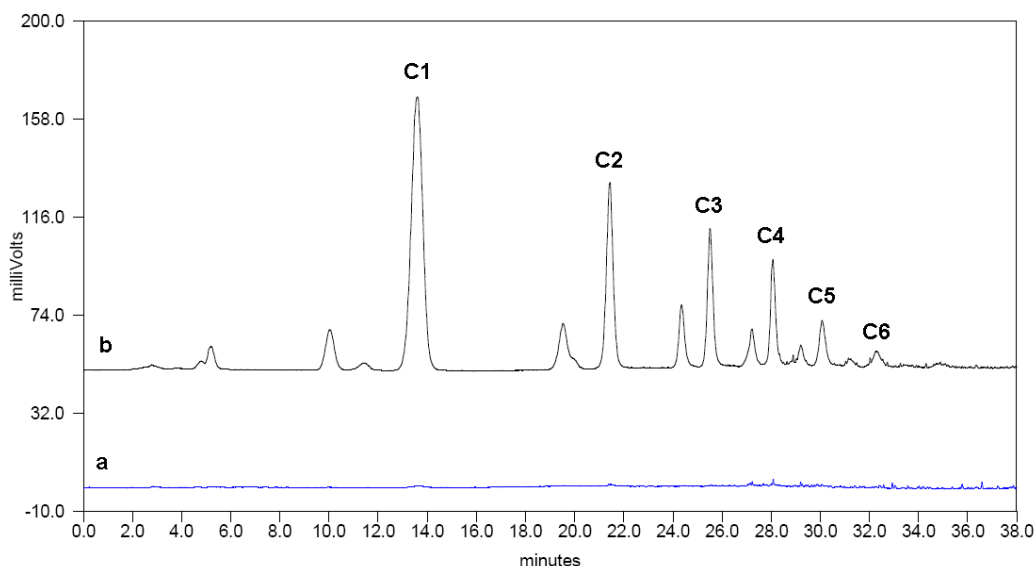


Figure 4-1: Comparison of liquid samples from cellulose hydrolysis in HCW by HPLC-ELSD. (a) without concentration; (b) with concentration

It should also be noted in both Figure 4-1b by HPLC-ESLD analysis and Figure 4-2 by HPAEC-PAD analysis that some compounds were also detected as small peaks near the peaks of glucose oligomers. The exact forms of these compounds are unknown. However, Kabyemela et al<sup>92</sup> studied the cellobiose (C2) decomposition in HCW and found that cellobiose was decomposed to glucosyl-erythrose and glucosyl-glycolaldehyde by HCW treatment. The decomposition of glucose at the reducing end of cello-oligosaccharide to levoglucosan, erythrose and glycolaldehyde was further proved using MALDI-TOFMS by Ehara and Saka.<sup>55</sup> Therefore, it is likely



that these small peaks near the glucose oligomers peaks in our results are the glucose oligomer derivatives with the glucose at the reducing end of glucose oligomers decomposed to levoglucosan, erythrose and glycolaldehyde. It is also possible that these compounds are directly produced from cellulose hydrolysis via thermal cleavage.<sup>44</sup>

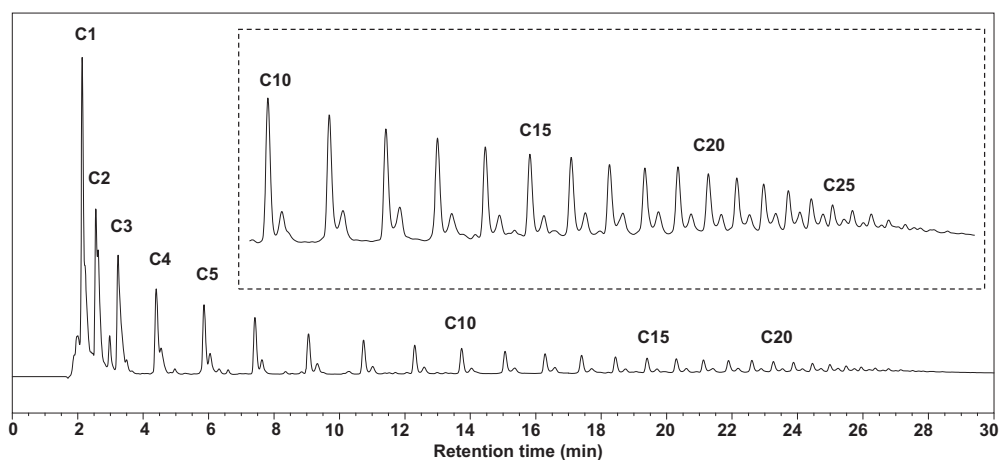


Figure 4-2: Typical IC chromatogram of liquid products from cellulose hydrolysis in hot-compressed water

#### 4.2.3 Comparison between HPLC-ELSD and HPAEC-PAD Analysis

Further efforts were then taken to compare the results by HPLC-ELSD and HPAEC-PAD for quantitative analysis of glucose oligomers with DPs up to 5. Quantitative analysis of glucose oligomers with DPs > 5 were not carried out due to the lack of standards. In a previous study which used HPAEC-PAD for the quantitative analysis of xylooligomers in aqueous solutions, Yang and Wyman<sup>58</sup> calculated the concentrations of xylooligomers with DPs > 5 based on their peak heights, using the ratio of peak height for every xylooligomer compared to xylobiose same as the ratio of their concentrations. Such a method was also used in an earlier study using an ion-moderated partition (IMP) chromatography.<sup>219</sup> Preliminary analysis was then carried out in this study however a similar relationship between concentration and peak height using HPAEC-PAD could not be established for the glucose oligomers at the time of writing this paper. Therefore, no quantitative analysis was carried out for glucose oligomers with DPs > 5.

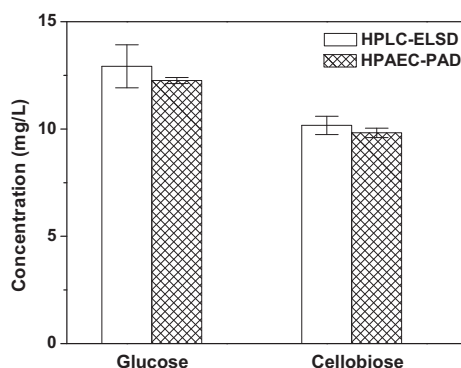


Figure 4-3: Comparison between HPLC-ELSD and HPAEC-PAD on quantitative analysis of glucose and cellobiose

For the quantitative analysis, analysis of the fresh liquid sample by HPAEC-PAD and the concentrated liquid sample by HPLC-ELSD were carried out for at least three times and Figure 4-3 presents the average concentrations of glucose and cellobiose together with their error bars. It should be noted that for HPAEC-PAD analysis necessary dilution of the fresh liquid sample was done prior to analysis in order to ensure the concentrations of glucose oligomers be within the linear response range of the HPAEC-PAD detection system (see discussion in next section). Results in Figure 4-3 are also calculated as those in the fresh liquid sample, taking into account the concentration factor in the concentrated liquid sample for HPLC-ELSD analysis. Figure 4-3 clearly shows that the results from HPLC-ELSD and HPAEC-PAD analyses are in good agreement, indicating that the glucose and cellobiose concentrations in the liquid products are ~12.5 and ~10 mg/L (ppm), respectively. The two instruments showed similar results for cellotriose, cellotetraose, and cellopentaose. There are several important conclusions which can be drawn from these results: (1) as the liquid sample for HPLC-ELSD analysis was concentrated by 25 times, the similar results obtained from the analyses using HPLC-ELSD and HPAEC-PAD indicate that there was little precipitation of the low-DP glucose oligomers (with DPs up to 5) during the vacuum concentration of the fresh liquid product; (2) both HPLC-ELSD and HPAEC-PAD can be used for quantitative analysis of low-DP glucose oligomers (with DPs up to 5); (3) the analytical error of HPLC-ELSD analysis is larger than that of HPAEC-PAD, possibly due to the poor

sensitivity of HPLC-ELSD and the errors introduced during the concentration process of the fresh liquid sample via vacuum evaporation. These conclusions are significant but it is still unknown which glucose oligomers are responsible for the precipitate formation from the fresh liquid sample. To clarify this important point, a set of experiments was then designed and carried out to investigate the precipitation behavior of glucose oligomers.

### **4.3 Precipitation of Glucose Oligomers from the Fresh Liquid Products**

#### **4.3.1 TOC Analysis**

For the set of precipitation experiments, the fresh liquid products collected from the hydrolysis experiments was immediately divided into 10 samples of the same volume. These liquid samples were then settled for various precipitation times (2 to 144 hours). Once a precipitation time was reached, one of the liquid samples was immediately filtered to remove the precipitate and the filtered liquid sample was immediately analyzed. While the liquid sample collected right after the hydrolysis experiment was clear, it is interesting to note that after settling at room temperature for about 1 hour, the sample was no longer clear, indicating that the precipitation had already started. This was the reason that the fresh liquid products and each liquid sample must be analyzed immediately after sample collection. Figure 4-4 presents the retention of the total (water-soluble) carbon in the liquid sample as a function of precipitation time, calculated based on the TOC data. It can be seen in Figure 4-4 that as a result of precipitation, the total water-soluble carbon in the liquid decreases with precipitation time. The precipitation was fast during the initial 8 hours but leveled off as the precipitation time increases further. After 120 hours (5 days) precipitation, ~70% of total carbon remained as water-soluble portion in the liquid, leading to an estimated precipitate yield ~30% on a carbon basis. The discussion on the effect of dilution on precipitation, as shown in Figure 4-4, will be discussed later.

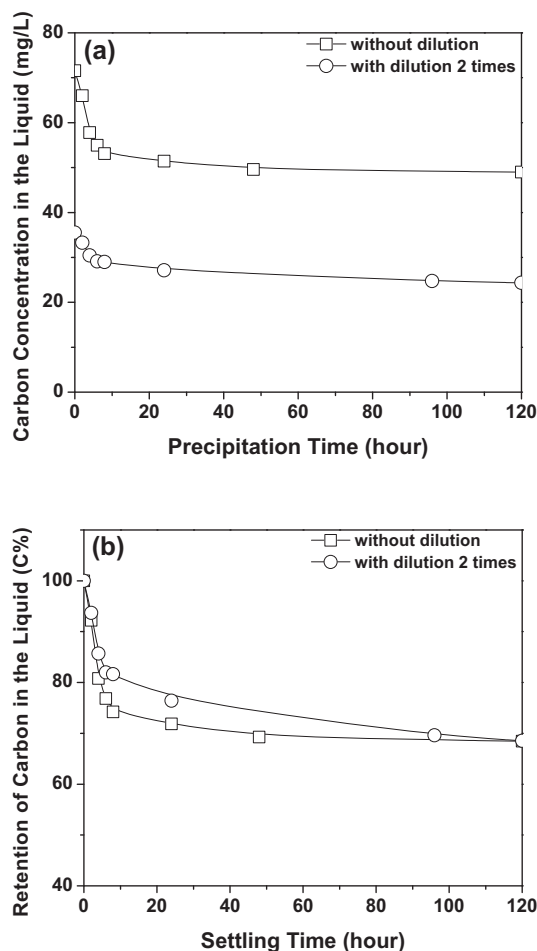


Figure 4-4: Retention of carbon in the liquid during precipitation (TOC data). (a) carbon concentration in the liquid; (b) retention of carbon in the liquid.

### 4.3.2 HPAEC-PAD Analysis

#### 4.3.2.1 Development of a Method for Quantifying the Retention of Glucose Oligomers after Precipitation

The fresh liquid product and its liquid samples after precipitation were also immediately analyzed using the HPAEC-PAD. As the quantitative determination of large-DP glucose oligomers cannot be achieved due to the lack of standards, this study has developed a new method based on direct comparisons between peak heights to quantify the retention of glucose oligomers in the liquid as a function of precipitation time. As each liquid sample has the same volume, the total liquid volume is hereby assumed as  $V_0$ . For a liquid sample after a precipitation time  $t$ , (the case of  $t = 0$  indicates the fresh liquid sample), due to the low concentrations of

glucose oligomers in the liquid, the precipitation process should lead to little change in the liquid volume. If the concentration of a glucose oligomer  $i$  in the liquid is  $G_i(t)$  and the height of the peak in the HPAEC-PAD chromatogram is  $H_i(t)$ , the total amount of glucose oligomer  $i$  in the liquid sample  $V_i(t)$  can be calculated as

$$V_i(t) = V_0 G_i(t) \quad \text{Equation (4-1)}$$

If the concentration of the glucose oligomer  $i$  is within the linear response range of the HPAEC-PAD detection system and assuming the concentration-height calibration factor is  $\alpha_i$  (which should be a constant providing the instrument operates continuously under the same condition for the analysis of all samples), we have

$$G_i(t) = \alpha_i H_i(t) \quad \text{Equation (4-2)}$$

i.e., we have

$$V_i(t) = V_0 \alpha_i H_i(t) \quad \text{Equation (4-3)}$$

Although the determination of the absolute amount of a particular glucose oligomer is not possible, the retention of glucose oligomer  $i$ ,  $\eta_i$ , after a precipitation time  $t$ , expressed as the percentage of the same glucose oligomer in the fresh liquid products can be then calculated as

$$\eta_i = \frac{G_i(t)}{G_i(0)} = \frac{\alpha_i H_i(t)}{\alpha_i H_i(0)} = \frac{H_i(t)}{H_i(0)} \quad \text{Equation (4-4)}$$

Equation (4-4) shows that the retention of any glucose oligomer after precipitation is equal to the height ratio of the peaks of that glucose oligomer in the chromatograms of the liquid sample after precipitation and the fresh liquid sample. However, it should be noted that Equation (4-4) is only valid when the concentration of glucose oligomer  $i$  is within the linear response range of the HPAEC-PAD detection system.

To test whether the concentrations of glucose oligomers are within the linear response range of the instrument detection system, the fresh liquid samples (obtained from repeated experiments under identical condition) were diluted at various dilution factors. The dilution and analysis of the diluted samples were done immediately after the collection from the fresh sample. The calibration curves for C1 to C5 based on peak height for the standards C1 to C5 using HPAEC-PAD are shown in Chapter 3 (see Figure 3-10). It is found that the calibration curves are only linear up to

particular concentrations for C1 to C5, respectively. For glucose oligomers with DPs  $> 5$ , there are no standards available. However, if Equation (4-4) holds (i.e., the concentration of a glucose oligomer is within the linear response range of the system), the peak height ratio of that glucose oligomer before and after each dilution of the liquid product should be equal to the dilution factor. Figure 4-5 shows the calculated peak height ratios of all glucose oligomers for three dilutions by 2, 4 and 8 times. It can be seen in Figure 4-5 that all glucose oligomers with DPs  $> 5$  in the liquid are found to be within the linear response range of the HPAEC-PAD detecting system. It is also interesting to see in Figure 4-5 that the glucose oligomers with DPs = 1-5 are actually not within the linear ranges in the undiluted sample (i.e., the fresh liquid sample), but become within the linear ranges after one dilution by 2 times. This is in agreement with the observed calibration curves in Figure 3-10 (see Chapter 3).

#### 4.3.2.2 Retention of Glucose Oligomers after Precipitation

After the validation, Equation (4-4) can then be directly used to calculate the retention of all glucose oligomers during precipitation based on the peak height ratios in the HPAEC-PAD chromatograms that are shown in Figure 4-6. It can be clearly seen in Figure 4-6 that the concentrations of the glucose oligomers in the water-soluble portion of the liquid reduce significantly with precipitation time. A close look of the peaks of the high-DP glucose oligomers in Figure 4-6 shows that, the peak heights of the derivatives of those high-DP glucose oligomers also reduce substantially, indicating that those derivatives also significantly contribute to the precipitate formation. Therefore, the precipitate is produced from the glucose oligomers and their derivatives due to their changes of solubilities in the water which changes from the hot-compressed condition to the ambient condition. The low-DP glucose oligomers and their derivatives seem to contribute little to the precipitate formation, indicating their solubilities in water under ambient conditions are much higher than those of higher DPs. Figure 4-6 clearly shows that the peak heights for C1-C5 and their derivatives do not change during precipitation.

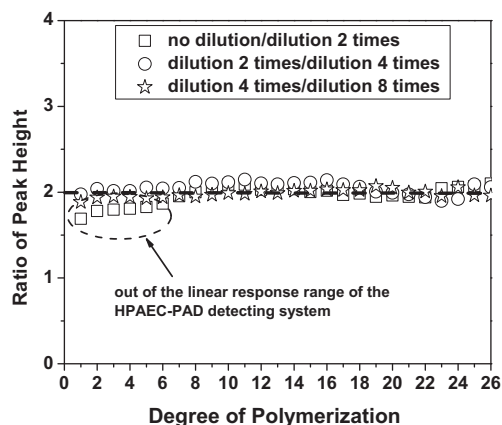


Figure 4-5: Peak height changes of glucose oligomers after dilution

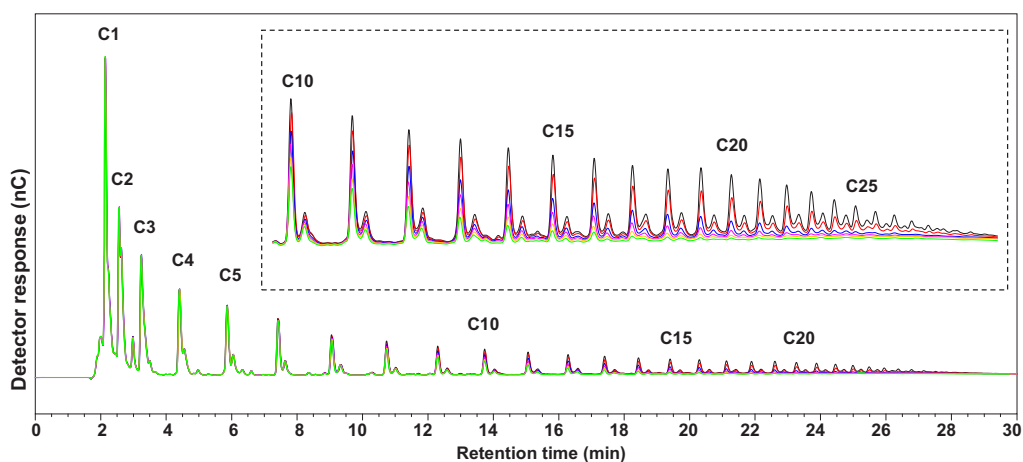


Figure 4-6: Comparison of glucose oligomers in the sample after precipitation for different times. Black: fresh sample; red: after settling for 2 hours; blue: after settling for 4 hours; pink: after settling for 8 hours; yellow: after settling for 1 day; green: after settling for 2 days

Based on Equation (4-4), calculations were then carried out using the data from the chromatograms in Figure 4-6. The results are plotted in Figure 4-7, which shows the retention of various glucose oligomers in the liquid products as a function of precipitation time of 2-144 hours. It should also be noted that similar analyses were also done for those small peaks for the derivatives of the glucose oligomers in Figure 4-6 and similar trends were observed. It should also be noted that, although the glucose oligomers with DPs up to 30 are present in the liquid as identified by the HPAEC-PAD, Figure 4-7 only shows the calculated results for the glucose oligomers

with DPs up to 26. Quantitative analysis of the peak height becomes difficult for the glucose oligomers with DPs > 26 due to those peaks being too small.

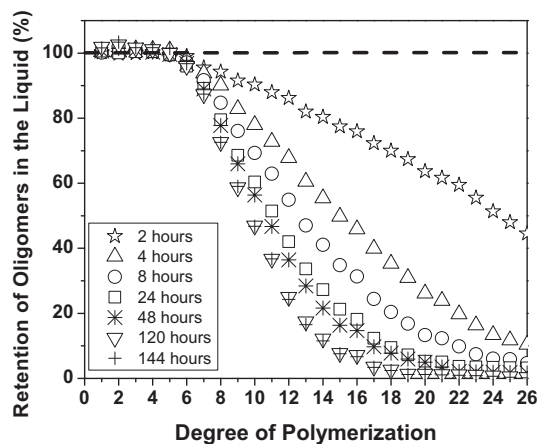


Figure 4-7: Retention of glucose oligomers in the liquid during precipitation based on peak height

It is interesting to see in Figure 4-7 that, the retentions of C1 to C5 are 100% in the liquid regardless of the precipitation time. Similar trends are also seen for their derivatives. Therefore, C1 to C5 and their derivatives contribute little to the precipitation formation and only the glucose oligomers with DPs > 5 contribute to the precipitate formation. This explains why the results of C1-C5 in the concentrated liquid sample by HPLC-ELSD are in good agreement with those in the fresh liquid products by HPAEC-PAD, as shown in Figure 4-3. The data also clearly demonstrate that the glucose oligomers with DPs > 5 and their derivatives are soluble in HCW but become supersaturated in the solutions under ambient conditions after sample collection, leading to the formation of precipitate in the solutions. At the same precipitation time, glucose oligomers with higher DPs precipitate faster than those with lower DPs. For example, after 2-hour precipitation, ~36% of C20 already precipitated while only ~10% of C10 did.

Figure 4-7 also shows that the precipitation kinetics of glucose oligomers is fast initially and slows down after 8 hours, in agreement with the TOC data in Figure 4-4. After precipitation for 120 hours (i.e., 5 days), no further precipitation of glucose oligomers occurred, indicating that all the glucose oligomers with DPs > 5 reach



their respective saturation levels in the solutions. It should be noted that after reaching their saturations, most of the glucose oligomers and their derivatives with DPs > 16 had precipitated. However, not all of these glucose oligomers had precipitated because tiny peaks of these glucose oligomers can still be observed in the chromatograms in Figure 4-6, indicating that these glucose oligomers may be of very low (but not zero) solubilities in ambient water. The retentions of glucose oligomers with DPs of 6-16 in the liquid samples after precipitation increase substantially with decreasing DP, indicating less percentage of lower-DP glucose oligomers originally present in the fresh liquid products contributed to the precipitate formation. Therefore, Figure 4-7 clearly shows the solubility of glucose oligomers decreases with DP. It is also worthwhile to point out that based on the TOC data in Figure 4-4, completion of precipitation has led to a total of ~30% reduction in the total carbon of the liquid products, such reduction is therefore all due to the precipitation of glucose oligomers with DPs > 5 and their derivatives.

#### **4.3.2.3 Effect of Initial Concentration on the Retention of Glucose Oligomers after Precipitation**

The effect of initial concentrations of the glucose oligomers and their derivatives in the liquid products on precipitation was also investigated. To do so, the starting liquid sample was diluted by a factor of two before precipitation experiments commenced. The precipitation behavior of the diluted liquid samples was then compared to that of the undiluted liquid sample as shown in Figures 4-4 and 4-8. It can be seen in Figure 4-4b that, compared to the undiluted sample, the 2-time diluted sample led to initial higher total carbon retention in the liquid but the same ultimate carbon retention after precipitation for 120 hours. Figure 4-8 further presents the effect of dilution of liquid sample on the retention of glucose oligomers, indicating that reduced initial concentrations of the glucose oligomers in the liquid products delayed the precipitation process of those precipitable glucose oligomers. After the same precipitation time, the glucose oligomers in the diluted sample are always more than those in the undiluted sample. For example, after 2-hour settling, ~36% of C20 in the undiluted liquid product contributes to precipitate formation in comparison to only 20% for the diluted sample.

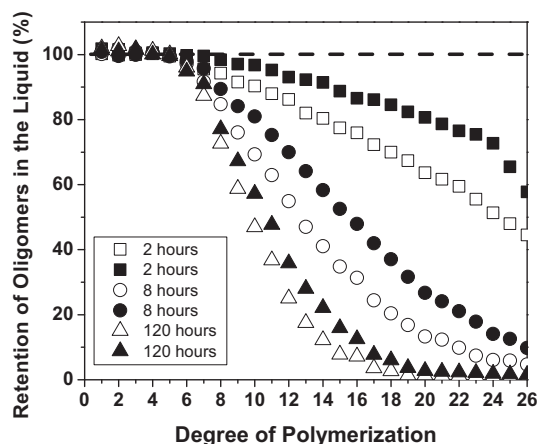


Figure 4-8: Effect of dilution on the retention of glucose oligomers during precipitation. Solid: with dilution 2 times; Open: without dilution

#### 4.4 Characterization of Precipitate

In this study, the precipitate after complete precipitation was collected by centrifugal separation and dried. The crystallized precipitate was manually crushed to small pieces, and characterized by XRD and SEM. It is shown in the previous section that the precipitate is formed from the glucose oligomers with DPs  $> 5$  and their derivatives. However, after the precipitate was dried, the glucose oligomers and their derivatives have been recrystallized, as shown in Figure 4-9b. The crystallized precipitate has a smooth surface but rough structure inside the crystal, indicating that the crystallized precipitate does not maintain their original phases. Also, the crystallized precipitate loses the fiber structure as raw cellulose (see Figure 4-9a). Further XRD analysis (see Figure 4-10b) shows that the crystallized precipitate has the diffraction pattern of cellulose II, which is different from that for raw cellulose (see Figure 4-10a). It is known that the cellulose II is usually prepared by regeneration of the solvated cellulose<sup>94</sup>. Similar finding was also observed in the precipitate formed from the extracts of wood in HCW<sup>56</sup>. Furthermore, some chemical reactions between the small organic molecules and the glucose oligomer derivatives may also lead to the precipitate formation. Further experimental study is required to clearly understand the precipitation process, including the nucleation and crystal growth during precipitation. Our current results prove that the glucose oligomers, which are mainly responsible for precipitate formation, experience crystallization after drying. Therefore, in order to study the original phase of precipitate, the

precipitate should not be dried as it would lead to the recrystallization of the glucose oligomers and their derivatives in the precipitate to form cellulose II.

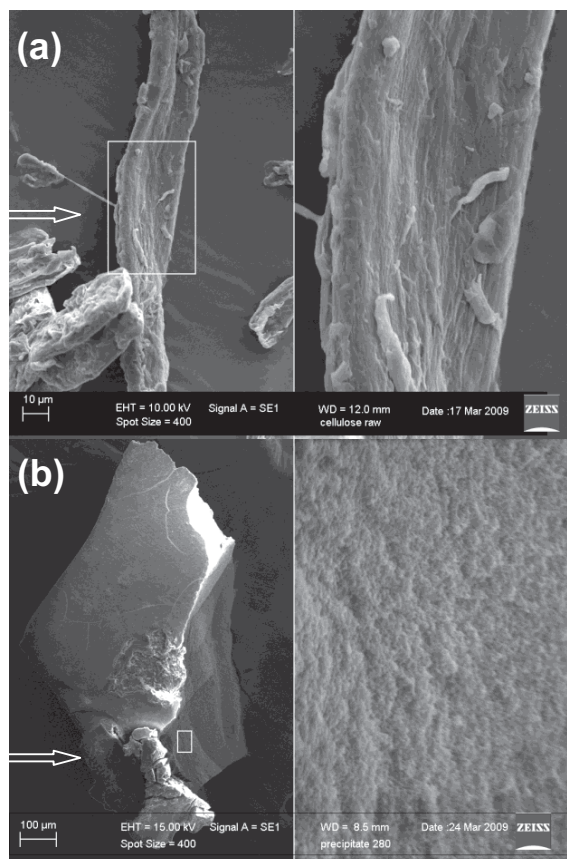


Figure 4-9: SEM of cellulose and precipitate recovered from cellulose hydrolysis in HCW. (a) cellulose; (b) precipitate

#### 4.5 Further discussion

The results obtained in this study clearly demonstrate that the liquid products from cellulose hydrolysis in HCW can be supersaturated for the glucose oligomers with DPs > 5 and their derivatives in the water under hot-compressed condition. Due to the changes of their solubilities in the water from hot-compressed condition to ambient condition, the precipitation of the glucose oligomers with DPs > 5 and their derivatives commences within one hour after the liquid products are collected from the hydrolysis of cellulose in HCW. Therefore, care must be taken in the analysis of glucose oligomers in the liquid products and the design of experiments during cellulose or biomass hydrolysis in HCW.

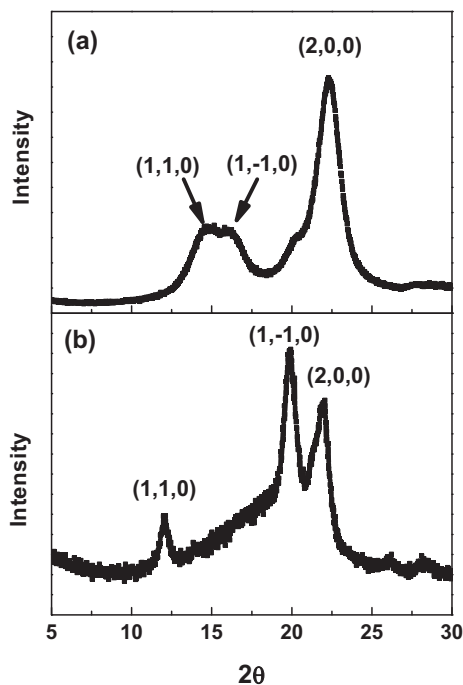


Figure 4-10: X-ray diffraction pattern of cellulose and precipitate from cellulose hydrolysis in HCW. (a) cellulose; (b) precipitate

Clearly, the fresh liquid product must be analyzed immediately after it is collected, otherwise the analysis will underestimate the concentrations of the glucose oligomers with DPs > 5 as results of potential precipitation. While a HPLC-ELSD is incapable of analyzing glucose oligomers with DPs > 6 because those compounds have low concentrations below the instrument detection limits as results of their low solubilities, HPAEC-PAD is indeed a powerful tool for the determination of glucose oligomer distribution in the liquid products of cellulose hydrolysis in HCW, with an excellent sensitivity.

This study has then developed a new approach using an HPAEC-PAD for the analysis of glucose oligomers. It is important to note that in order to use such an approach, the analysis of liquid samples of various dilutions (e.g., the one in this study) must be done to check and ensure that the concentrations of the glucose oligomers in the liquid samples are within the linear response range of the HPAEC-PAD detection system. If the concentration is too high, necessary dilution of the

sample is required. For the analysis of glucose oligomers with DPs > 5, due to the lack of standards, the new approach proposed in this study based on relative peak height ratio can be very useful for quantitatively estimating the retention of those glucose oligomers during precipitation.

It is also important to note that complete precipitation of large-DP glucose oligomers can not be reached until the liquid sample is settled for sufficient long time. This study shows that in order to investigate the precipitation behavior of the liquid products and calculate the ultimate precipitate yield, it is important to settle the sample for at least 5 days before the liquid and precipitate are separated for further analysis. A precipitation time of 12-24 hours, which were typically used in the previous studies,<sup>52,53,55,94</sup> is not sufficiently long to reach complete precipitation.

Finally, the data in this paper also indicates that a semi-continuous reactor system is a good option for studying the fundamental reaction mechanisms for cellulose/biomass hydrolysis in HCW. On one hand, such a reactor system achieves the advantages of a continuous reactor system for the minimization of the secondary reactions of the primary hydrolysis products in the aqueous phase (such reactions are extensive in a batch reactor system). On the other hand, a semi-continuous reactor system also effectively separates the reacting cellulose materials and the liquid hydrolysis product via rapidly sweeping the liquid products out of the reactor system. This enables the collection of partially-hydrolyzed cellulose samples with minimized contamination of the glucose oligomers which may potentially precipitate and deposit on the surface of the partially-hydrolyzed cellulose particles.

#### 4.6 Conclusions

In this study, a high performance anion exchange chromatography with pulsed amperometric detection (HPAEC-PAD) was employed to determine the distribution of the glucose oligomers in liquid products collected from the hydrolysis of cellulose in HCW using a semi-continuous reactor system. The fresh liquid products were collected from the experiments and analyzed immediately. The HPAEC-PAD chromatogram clearly demonstrates the presence of a wide range of glucose oligomers (with DPs up to 30) and their derivatives.

However, due to their low concentrations, none of those glucose oligomers in the fresh liquid products could be detected by a HPLC-ELSD. HPLC-ELSD was able to detect glucose oligomers with DPs up to 6 in the liquid solutions after being concentrated by 25 times via vacuum evaporation at 40 °C, during which a large amount of precipitate was also formed. Quantitative analysis was only carried out for analyzing glucose oligomers up to cellopentaose (DP = 5) as the standards for glucose oligomers with DPs > 5 are unavailable. The concentrations of glucose oligomers from glucose to cellopentaose analysed by both HPAEC-PAC and HPLC-ELSD were in good agreement, suggesting that these low-DP glucose oligomers do not contribute to the precipitate formation.

A set of experiments were then designed to identify the glucose oligomers responsible for precipitate formation. The results show that precipitation started as the fresh sample was collected. The precipitation was fast during the initial 8 hours but leveled off as the precipitation time increases further. The precipitation process did not complete until after 120 hours (5 days). A new approach was then developed to quantify the retention of various glucose oligomers during the precipitation process based on the ratio of each glucose oligomers' peak heights in the HPAEC-PAD chromatograms of the liquid samples after and before precipitation.

The results clearly demonstrate that the glucose oligomers with DPs > 5 and their derivatives, which are soluble in HCW but become supersaturated in the solutions at ambient solutions, are responsible for precipitate formation. The contribution of glucose oligomer to the precipitate formation clearly increases with DP as the solubility of glucose oligomer increases with decreasing DP. Most but not all of the glucose oligomers and their derivatives with DPs of 17 and more contribute to the precipitate formation as tiny peaks of these glucose oligomers could still be observed in the chromatograms, suggesting that these glucose oligomers have very low (but non-zero) solubilities in ambient water. The retentions of glucose oligomers increase substantially with the DP decreasing from 16 to 6, indicating that less percentage of lower-DP glucose oligomers contributed to the precipitate formation. The glucose oligomers from glucose (DP = 1) to cellopentaose (DP = 5) and their derivatives

contribute little to the precipitate formation. The results indicate that the fresh liquid products from cellulose hydrolysis in HCW must be analyzed immediately after sample collection in order to avoid the effect of precipitation on oligomer analysis.

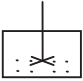

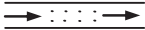
## CHAPTER 5 PRIMARY LIQUID PRODUCTS AT VARIOUS REACTION TEMPERATURES

### 5.1 Introduction

Cellulose and hemicelluloses, which are the two major carbohydrates in lignocellulosic biomass, are responsible for the formation of various sugars and their derivatives in the liquid products from the hydrolysis or pyrolysis of these materials.<sup>17,23,34</sup> The past two decades have witnessed significant research efforts in using hot-compressed-water (HCW). Three types of reactor systems were typically used for cellulose and biomass hydrolysis in HCW, i.e. batch,<sup>51,54,57,60,61</sup> semicontinuous<sup>32,33,50,53,56,66</sup> and continuous reactor systems,<sup>35,52,54,55,65,101</sup> as summarised in Table 5-1. In a batch reactor system,<sup>51,54,57,60,61</sup> feedstock solid particles are mixed with HCW in the reactor. The residence time of the reacting solid is long; so are the liquid products, leading to their extensive degradation hence low sugar yields and high oil and char yields. In a semicontinuous reactor system,<sup>32,33,50,53,56,66</sup> HCW flows through a bed of feedstock particles; while the reacting particles remain in the reactor, the liquid products are rapidly swept out. In a continuous reactor system,<sup>35,52,54,55,65,101</sup> the slurry of feedstock particles and HCW flows through the reactor together. Therefore, the residence times of liquid products in semicontinuous and continuous reactor systems are short, resulting in much less degradation compared to a batch reactor system hence the observed high sugar yields.<sup>54,55</sup> One key difference between semicontinuous and continuous reactor systems is that the contact between liquid products and reacting particles in a semicontinuous reactor system is minimized while that is continuous in a continuous reactor system. A continuous reactor system is also typically required to operate at high temperatures and pressures in order to achieve a high conversion of the feedstock within a short residence time.<sup>34</sup>



Table 5-1: Characteristics of various reactor systems for cellulose/biomass hydrolysis in HCW

	Batch <sup>51,54,57,60,61</sup>	Semicontinuous <sup>32,33,50,53,56,66</sup>	Continuous <sup>35,52,54,55,65,101</sup>
<b>Reactor system</b>			
<b>Operation mode</b>	Feedstock particles are mixed with HCW in the reactor. Reacting particles and liquid products remain in the reactor during hydrolysis	HCW flows through a bed of feedstock particles. Reacting particles remain in the reactor while liquid products are rapidly swept out of the reactor	Slurry of feedstock particles and HCW is pumped through the reactor. Reacting particles flow with the liquid products which is rapidly swept out of the reactor
<b>Liquid residence time</b>	Long	Short	Short
<b>Solid residence time</b>	Long	Long	Short
<b>Contact between reacting solid particles and</b>	Continuous and long contact time	Minimised	Continuous but short contact time
<b>Liquid products</b>	High yields of degradation products, oil	High yield of mono- and oligo-sugars	High yield of mono- and oligo-sugars
<b>Pressure</b>	Various	Various	Typically high
<b>Temperature</b>	Various	Various	Typically high

Therefore, the large volume of previous work in the open literature has provided sufficient evidence that the characteristics of liquid products strongly depend on the reactor systems used. It is clear that the secondary reactions of the hydrolysis products in the aqueous phase can be significant, particularly in a batch reactor system. To understand the fundamental hydrolysis mechanisms of cellulose or biomass in HCW, it is therefore critical to obtain thorough knowledge on the primary liquid products without (or with minimised) secondary reactions in the aqueous phase. This requires the hydrolysis experiments to be purposely-designed and carried out under adequate reactor configurations and proper reaction conditions where secondary reactions of the primary products are proven to be minimised. Unfortunately, no previous studies on cellulose/biomass hydrolysis in HCW in the open literature have experimental proofs to demonstrate that such conditions were achieved.

Apart from the required experimental design and conditions to ensure that the liquid products collected are indeed primary products, two additional key reasons make it very hard to know if the knowledge obtained on the liquid products in the past studies truly represents that of the primary liquid products. One is that there is a lack of an adequate analytical technique which is capable of characterising sugars in the liquid products which may comprise glucose oligomers with a wide range of degrees of polymerization (DPs). It is known that the conventional systems for sugar analysis such as HPLC-RI,<sup>34,53,56</sup> HPLC-UV<sup>53</sup> or even the latest HPLC-ELSD as tested in Chapter 4 are only capable of analysing lower-DP sugars (with DPs up to 6). The other is the fact that the settling of the fresh liquid products collected from experiments forms a large quantity of precipitate.<sup>34,53,56</sup> According to the study in Chapter 4, the precipitation of glucose oligomers in the fresh hydrolysis products is continuous and will not complete until 5 days so that the compositions of the liquid products change continuously with time. Therefore, a proper procedure for sample collection and analysis must be in place before the primary liquid products of cellulose/biomass hydrolysis in HCW can be confidently characterised.

Research progress in Chapter 4 also has established a new method for characterizing the glucose oligomers in the fresh liquid products of cellulose hydrolysis in HCW using a high performance anion exchange chromatography with pulsed amperometric detection (HPAEC-PAD). It was clearly demonstrated that the fresh liquid products must be analysed immediately after collection. The newly established method in Chapter 4 is capable of characterizing the glucose oligomers of a wide range of DPs and their derivatives in the fresh liquid products obtained at 20 MPa and 280 °C, although it is still unknown whether those fresh liquid products are the primary hydrolysis products under the reaction conditions.

A semicontinuous reactor system was utilised and further developed, which provides an opportunity to minimize secondary reactions of the liquid products of hydrolysis in the aqueous phase, through the optimisation of reaction conditions. Such research progress opens the possibility for the collection of the primary liquid products of cellulose/biomass hydrolysis in HCW. The collected fresh primary liquid products can then be analysed by our newly established method for characterising glucose

oligomers and their derivatives based on the HPAEC-PAD technique, enabling to obtain the essential knowledge on the primary liquid products of cellulose/biomass hydrolysis in HCW under various conditions.

Therefore, the key objectives of this chapter are to obtain the primary liquid products of cellulose hydrolysis in HCW under various conditions, and investigate the effect of hydrolysis reaction temperature on the distribution of glucose oligomers in the primary liquid products. The primary liquid products collected under various hydrolysis conditions were also subjected to post hydrolysis to analyze the neutral glucose yield, aiming to investigate the possibility of using HCW to break down the long-chain cellulose into short-chain glucose oligomers of various DPs for further fermentation to produce bioethanol.

## **5.2 Identification of Reaction Conditions to Obtain the Liquid Products with Minimized Secondary Reactions**

### **5.2.1 Cellulose Conversion at Various Flow Rate**

To obtain the primary liquid products of cellulose hydrolysis in HCW, the residence time of the primary liquid products must be short enough to minimize the secondary reactions. Therefore, a series of experiments were performed to investigate the effect of residence time on the liquid products. In our reactor system, the residence time can be adjusted by varying the water flow rate in the range of 10–40 mL min<sup>-1</sup>, which corresponds to residence times of ~1 s to ~4 s. Additionally, it is known that the decomposition of sugar products can be very fast at high temperatures, e.g., the completion decomposition of glucose only requires < 5 s at reaction temperatures of > 300 °C.<sup>103</sup> Therefore, this study carefully selected the hydrolysis temperature in the range of 230–280 °C.

Figure 5-1 shows the effect of flow rate on cellulose conversion at various hydrolysis temperatures, based on total carbon in the liquid products. Figure 5-1 clearly shows that the water flow rate has little influence on cellulose conversion. This is an interesting observation. Generally speaking, the primary hydrolysis reactions occur on the surface of cellulose particles, and the glucose oligomers, as part of the hydrolysis products, will only enter into the aqueous phase after being dissolved in

HCW. The overall cellulose conversion may be dependent on how much such glucose oligomers products can be dissolved in HCW. It is possible that the dissolution of the glucose oligomers with high DPs may be limited by their solubilities in HCW. Therefore, it is expected that the conversion may increase with flow rate, because of the increase of soluble oligomers with a larger amount of water. For example, previous studies<sup>58,220</sup> reported the increase in xylan removal with flow rate for corn stover; however, this influence was determined to be effective only for the low flow rates  $< 10 \text{ mL min}^{-1}$ .<sup>220</sup> However, this is not the case for cellulose hydrolysis in this study as shown in Figure 5-1. Therefore, Figure 5-1 suggests that the solubilities of the primary hydrolysis products in HCW do not seem to be a limiting factor, even at a flow rate of  $10 \text{ ml min}^{-1}$ , possibly because of the small sample loading in the reactor. Therefore, in this study, at the same sample loading, it is reasonable to assume that the primary products should be similar during hydrolysis at various flow rates (this is further confirmed in section 3.2). This makes it possible to identify the extent of secondary reactions by comparing the selectivity changes of glucose oligomers in the liquid samples at different flow rates.

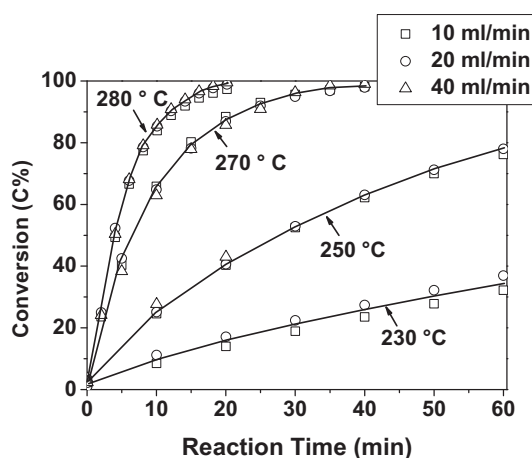


Figure 5-1: Effect of water flow rate on cellulose conversion during hydrolysis in HCW at various temperatures.

### 5.2.2 Development of a Method for Comparing the Selectivity of Glucose Oligomers

A method for comparing the selectivity changes of glucose oligomers in two liquid samples is then developed. In this study, all liquid samples were prepared for analysis within the HPAEC-PAD detector's linear response region, following the

procedure developed in the Chapter 4. If the total liquid volume of the sample is represented as  $V_0$ , the peak height of the glucose oligomer  $i$  obtained from the HPAEC-PAD chromatogram is represented as  $H_i$  and the linear concentration-height calibration factor is  $\alpha_i$ , the total amount of glucose oligomer  $i$  in one liquid sample,  $V_i$ , can be calculated as  $V_i = V_0\alpha_iH_i$ . Assuming that the carbon content for glucose oligomer  $i$  is given as  $C_i$ , and the carbon concentration of the liquid sample is given as  $C_0$ , the selectivity of glucose oligomer  $i$ ,  $S_i$ , in the liquid sample can be calculated as

$$S_i = \frac{V_i C_i}{V_0 C_0} = \frac{V_0 \alpha_i H_i C_i}{V_0 C_0} = \frac{\alpha_i H_i C_i}{C_0} \quad \text{Equation (5-1)}$$

Given that direct determinations of the selectivities of glucose oligomers with DPs > 5 are not possible, because of the lack of standards, the selectivity changes can then be evaluated via the ratio of the selectivities of a particular glucose oligomer  $i$  in two liquid samples (denoted as  $S_{i1}$  and  $S_{i2}$ , respectively):

$$\frac{S_{i1}}{S_{i2}} = \frac{\alpha_i H_{i1} C_i / C_{01}}{\alpha_i H_{i2} C_i / C_{02}} = \frac{H_{i1} / C_{01}}{H_{i2} / C_{02}} \quad \text{Equation (5-2)}$$

Equation (5-2) shows the selectivity ratio of any glucose oligomer in two different samples is the ratio of the peak height of the glucose oligomer normalised by the carbon concentration of each liquid sample. The peak heights ( $H_{i1}$  and  $H_{i2}$ ) of glucose oligomer  $i$  can be determined by the HPAEC-PAD, while the carbon concentrations ( $C_{01}$  and  $C_{02}$ ) of the liquid products can be measured by the TOC analyzer. Therefore, by comparing the selectivity change of each glucose oligomer in the fresh liquid samples at various flow rates based on Equation (5-2), it is possible to evaluate the extent of decomposition for each glucose oligomer with increasing the residence time. If the flow rate is reduced but the selectivity ratios for all the glucose oligomers remain as 1, it means that the influence of secondary reactions is effectively minimised at this or higher flow rates.

### 5.2.3 Selectivity Ratios of Glucose Oligomers at Various Flow Rates

Figure 5-2 presents the selectivity ratios of glucose oligomers in the liquid products at various hydrolysis reaction temperatures, as a function of flow rate. It can be clearly seen in Figure 5-2a that, at 280 °C, there are significant selectivity changes of glucose oligomers in the fresh liquid products when the flow rate increases from 10

mL min<sup>-1</sup> to 40 mL min<sup>-1</sup>. Even at 40 mL min<sup>-1</sup>, the data indicate that, using the current reactor system, which allows a maximum flow rate of 40 mL min<sup>-1</sup>, it is still not possible to verify whether the liquid products obtained are the primary hydrolysis products at 280 °C.

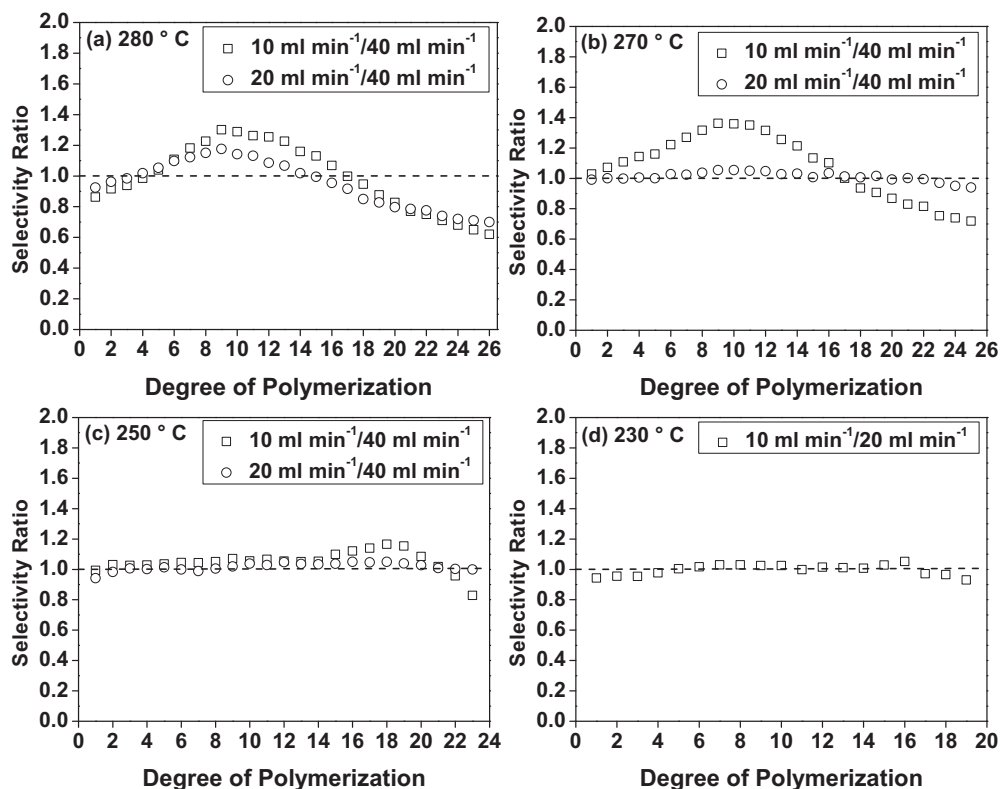


Figure 5-2: Effect of water flow rate on the selectivity of glucose oligomers in the fresh liquid products collected during cellulose hydrolysis at various reaction temperatures. (a) 280 °C; (b) 270 °C; (c) 250 °C; (d) 230 °C

Figure 5-2a also shows that a decrease in the water flow rate from 40 mL min<sup>-1</sup> to 10 mL min<sup>-1</sup> (corresponding to an increase in the residence time of liquid products from ~1 s to ~4 s) leads to significant reductions in the selectivity of glucose oligomers with DPs > 18. For example, ~40% of C26 is decomposed as a result of the residence time for secondary reactions in the aqueous phase increasing from ~1 s to ~4 s. The secondary reactions seem to shift the glucose oligomers from high DPs to low DPs, resulting in an increase in the selectivity of glucose oligomers with DPs of 5–16. The decrease in the selectivity of the lower sugars (e.g., C1–C3) with decreasing flow rate (i.e. increasing residence time) suggests that the increased production of these

lower sugars from the secondary reactions of higher-DP glucose oligomers cannot compensate the reduction caused by their own secondary reactions.

Results obtained from the experiments performed at 230, 250, and 270 °C are shown in Figure 5-2(b-d). At 270 and 250 °C, and a water flow rate of 40 mL min<sup>-1</sup>, the results clearly demonstrate that secondary reactions of all glucose oligomers in the liquid products of hydrolysis are minimised. In fact, at 230 °C, the liquid products with minimised secondary reactions can even be obtained at a lower water flow rate of 20 mL min<sup>-1</sup>. Therefore, by comparing the selectivity changes of glucose oligomers at various flow rates, the necessary reaction conditions are identified and achievable using the semicontinuous reactor system in this study for minimising the secondary reactions of liquid hydrolysis products at 230–270 °C.

### 5.3 Effect of Sample Loading on the Liquid Products of Cellulose Hydrolysis in HCW

Because the solubilities of the oligomers with high DPs may be low in HCW, further experiments were also designed and conducted to determine if there are solubility limitations for those high-DP glucose oligomers, considering different sample loadings, with other operating parameters being unchanged. Various sample loadings (7.5, 15, 30, 60 mg) are considered. All experiments were conducted under the conditions where the secondary reactions of the liquid products in the aqueous phase are minimized at 230–270 °C.

The peak height ratios of each glucose oligomer in the liquid products at different sample loadings are plotted in Figure 5-3. If the solubility of a glucose oligomer is a limiting factor, the peak height ratio of that glucose oligomer should be less than the sample loading ratio. In contrast, if solubility is not a limiting factor, the peak height ratio should be same as the sample loading ratio, e.g., a doubled sample loading should lead to a peak height ratio of 2. Indeed, this is clearly seen for all glucose oligomers in Figure 5-3, when the sample loading increases from 15 mg to 30 mg at both 230 and 250 °C. Such is the case when the sample loading increases from 7.5 mg to 15 mg at 270 °C. Therefore, the data in Figure 5-3 prove that, under those conditions, there are no solubility limitations for any of the glucose oligomers. All

the hydrolysed glucose oligomers were dissolved in the HCW under our experimental conditions.

It is interesting to note that, at 230 and 250 °C, although increasing sample loading from 15 mg to 30 mg leads to a corresponding peak height ratio of 2 for all glucose oligomers, increasing sample loading further from 30 mg to 60 mg results in the peak ratios of the glucose oligomers with high DPs (e.g., C16–C22) of > 2. Similar results were also found for hydrolysis at 270 °C when the sample loading increases from 15 mg to 30 mg, and then to 60 mg. The exact reasons for such phenomena are unknown. One of the possibilities could be due to the interactions between the liquid products and the reacting cellulose particles in the sample bed when the liquid products flow through the reactor. At a higher sample loading, such interactions would be enhanced, as result of an increased thickness of the sample bed, possibly leading to the observed changes. There could also be other unknown reasons, so that further research is certainly needed to clarify the fundamental mechanisms leading to such effect of sample loading. Nevertheless, for the purpose of this study, the data clearly demonstrate that, to obtain the primary liquid product of hydrolysis, the sample loading should be sufficiently small, to ensure that the effect of sample loading is negligible.

## **5.4 Effect of Reaction Temperature on the Primary Liquid Products of Cellulose Hydrolysis in HCW**

### **5.4.1 HPAEC-PAD Chromatograms of Primary Liquid Products at Various Temperatures**

The results in the previous two sections have shown that the primary liquid products of cellulose hydrolysis in HCW can be obtained using the semicontinuous reactor system at 230–270 °C under optimised reaction conditions. This is of significant importance to understand cellulose hydrolysis reactions in HCW. The collected primary liquid products at 230–270 °C were then immediately analysed using the HPAEC-PAD; the chromatograms are presented in Figure 5-4. Several important observations can be made in Figure 5-4.



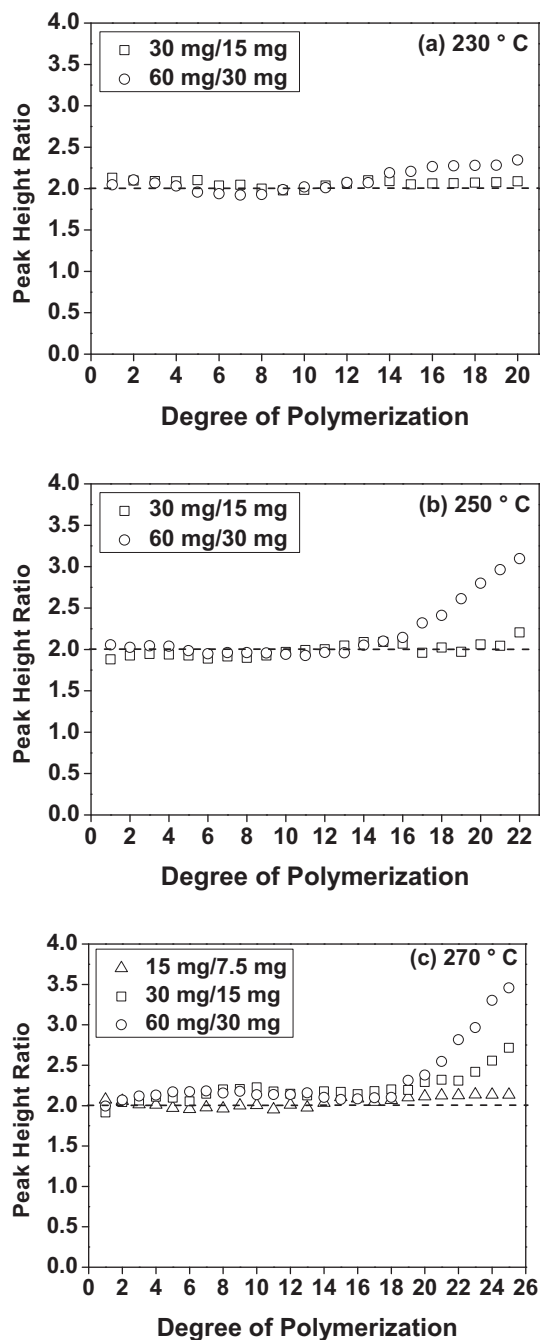


Figure 5-3: Effect of sample loading on glucose oligomers in the fresh liquid products produced from cellulose hydrolysis in HCW at various temperatures (Pressure: 10MPa). (a) 230 °C, water flow rate: 20 ml min<sup>-1</sup>; (b) 250 °C, water flow rate: 40 ml min<sup>-1</sup>; (c) 270 °C, water flow rate: 40 ml min<sup>-1</sup>

First, Figure 5-4 clearly shows that, at all temperatures, the primary liquid products of cellulose hydrolysis in HCW contain glucose oligomers with a wide range of DPs. It is interesting to see that the primary liquid products even contain a substantial amount of lower sugars, particularly glucose. This is contradictory to the common perception<sup>35,51</sup> that glucose is only produced from the secondary reactions of the dissolved high-DP oligomers in the aqueous phase. Figure 5-4 clearly shows that glucose is actually produced from the primary reactions on the surface of reacting cellulose particles. The presence of sugars with a wide range of DPs also suggests that the primary cellulose hydrolysis reactions proceed via cleavage of the glycosidic bonds (if accessible by HCW) of the long chains in a manner with a certain degree of randomness.

Second, Figure 5-4 also shows the presence of small peaks near the peaks of glucose oligomers. The exact forms of these compounds are unknown. Based on the previous studies on cellobiose decomposition,<sup>92</sup> it is likely that these small peaks near the glucose oligomers peaks are the glucose oligomer derivatives, as a result of some degradation reactions (e.g. dehydration at the reducing ends of glucose oligomers). The primary liquid products also contain various glucose oligomer derivatives with a wide range of DPs. Such an observation is also contradictory to the common perception in the literature that such derivatives are the degradation products of primary liquid products in the aqueous phase and are due to secondary reactions.<sup>44</sup> These derivatives are also actually part of the primary liquid products, indicating some thermal degradation reactions (to a much lesser extent, in comparison to primary hydrolysis reactions, because their peaks shown in the chromatograms are much smaller) actually can also occur on the surface of reacting cellulose particles prior to becoming soluble products that are stripped and dissolved into HCW. The results also suggest that such degradation reactions also proceed on the accessible sites in a manner with a certain degree of randomness.

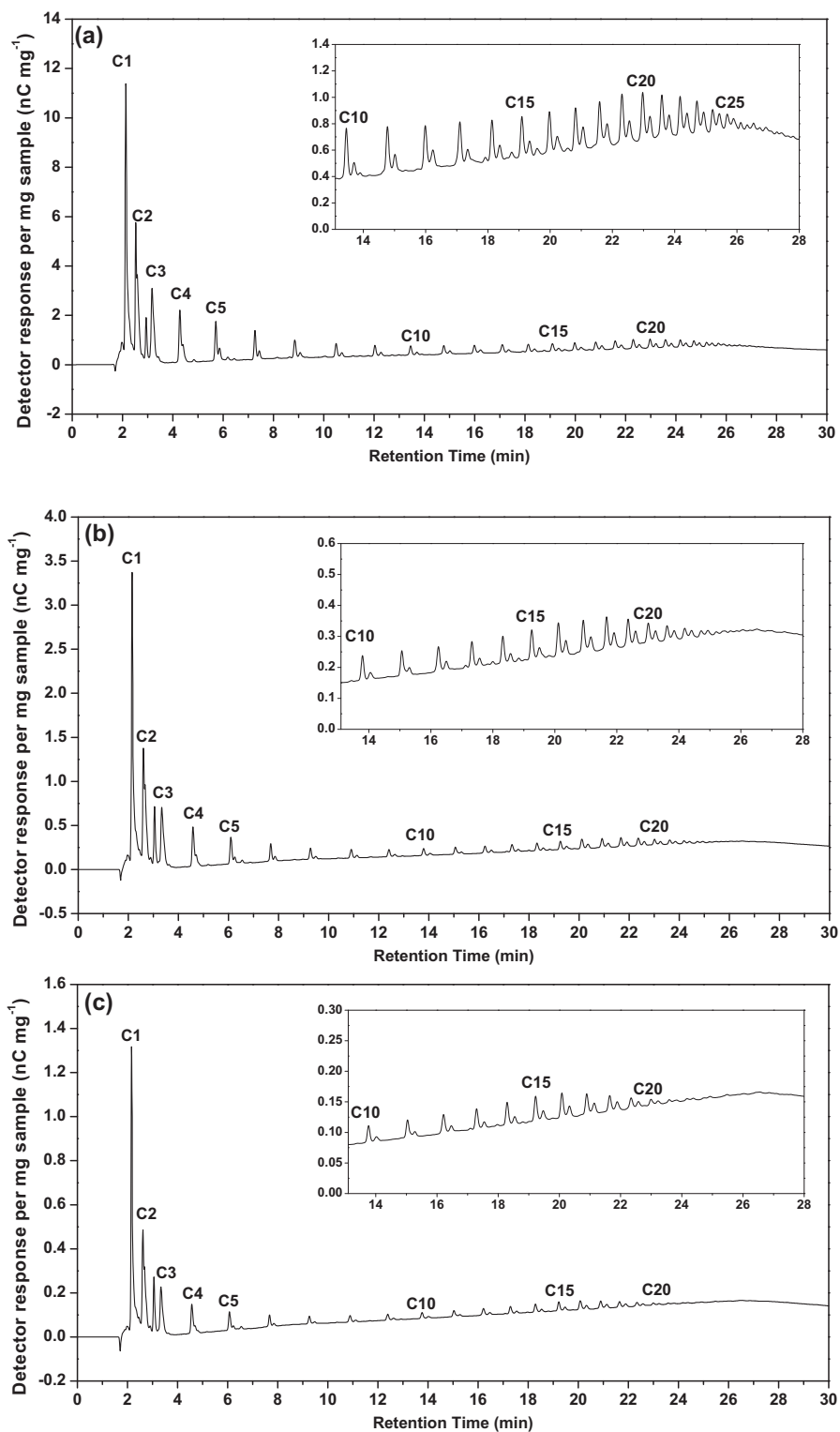


Figure 5-4: HPAEC-PAD chromatograms of the primary liquid products of cellulose hydrolysis in HCW, obtained under optimised reaction conditions. (a) 270 °C; (b) 250 °C; (c) 230 °C

Third, the reaction temperature has a significant effect on hydrolysis reactions and the formation of primary liquid products. The concentrations of all glucose oligomers and their derivatives increase with increasing reaction temperature, which is consistent with a significant increase in the overall cellulose conversion in HCW with increasing temperature, as shown in Figure 5-1. It is also interesting to note that the maximal DP of the glucose oligomer in the primary liquid product, as identified by HPAEC-PAD, also increases with reaction temperature, from 23 at 230 °C, to 25 at 250 °C, then to 28 at 270 °C. There are at least two possible reasons that may lead to this phenomenon. The first possibility is that glucose oligomers with DPs higher than the maximal DP are not soluble in the HCW at the temperature. This possibility is ruled out because, in hydrolysis experiments under same conditions but using a cellulose sample after 8 h ball milling, glucose oligomers with DPs higher than the maximal DPs are observed. The second possibility, which seems to be more likely, i.e., the primary hydrolysis reactions on the surface of the reacting cellulose particles do not produce glucose oligomers with DPs higher than the maximal DP, under the conditions.

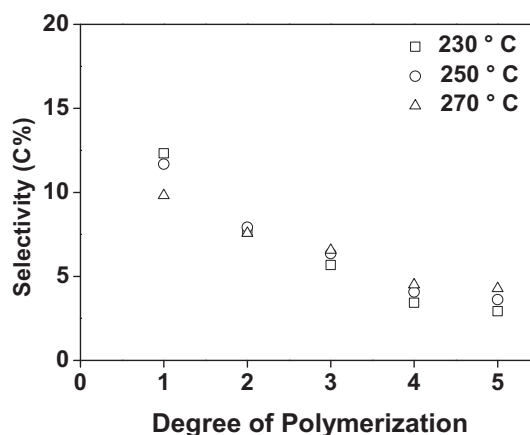


Figure 5-5: Selectivity of C1-C5 in the primary liquid products produced from cellulose hydrolysis in HCW at various temperatures (Pressure: 10 MPa)

The data in Figure 5-4 suggest that the primary hydrolysis reactions seem to proceed in a manner with some randomness on the accessible surface of the reacting cellulose particles, but such randomness also seems to be temperature-dependent. Such hydrolysis behavior may be at least partially due to the structure of microcrystalline cellulose. A single cellulose molecule is an unbranched assembly of repeating

glucose units that forms a flattened ribbon structure.<sup>221</sup> Because the production of glucose oligomers from cellulose must involve glycosidic bonds cleavage, during the hydrolysis of a single cellulose molecule, all glycosidic bonds in the chain would be accessible, so that the breaking of those glycosidic bonds would proceed in a random manner.

However, microcrystalline cellulose consists of a complex structure where in cellulose chains are stably packed side by side to form linear crystals or microfibrils via a complex network of intramolecular and intermolecular hydrogen bonds.<sup>79,80</sup> To produce glucose oligomers, hydrolysis of microcrystalline cellulose may be limited by accessibility, i.e., the glycosidic bonds between two glucose units will only be possibly attacked by HCW till at least part of the surrounding intramolecular and/or intermolecular hydrogen bonds are broken, to allow HCW to access those bonds. It is known that the ionic product of HCW increases with temperature up to  $\sim 10^{-11}$  in the temperature range from 200 °C to 300 °C, while the dielectric constant of HCW decreases with increasing temperature.<sup>68</sup> An increase in ionic product enhances the hydrolysis reactions, while a decrease in the dielectric constant of HCW can increase the solubility of glucose oligomers.<sup>47,68</sup> The population of hydrogen bonds between cellulose chains decreases with increasing temperature during cellulose hydrolysis in HCW.<sup>222</sup> The weakening/breakage of hydrogen bonding network in cellulose accelerates with increasing temperature during thermal treatment, as evidenced by infrared spectroscopy analysis.<sup>223,224</sup> At  $\sim 300$  °C, the cleavage of hydrogen bonds and other parallel reactions can even transform crystalline cellulose to an amorphous state in HCW.<sup>123</sup> Therefore, an increase in temperature would result in the chain structures within the microcrystalline cellulose being more accessible, thereby increasing the possibility to produce primary liquid products, which contain glucose oligomers with the maximal DP being increased. Under such reaction conditions, one would expect that, at a given temperature, the selectivities of the monomer or lower-DP oligomers would be higher. Because only the standards of C1–C5 are available for sugar quantification, the selectivity of C1–C5 is therefore plotted in Figure 5-5. Indeed, the data in Figure 5-5 clearly show a decreasing selectivity from C1 to C5 at all hydrolysis temperatures.

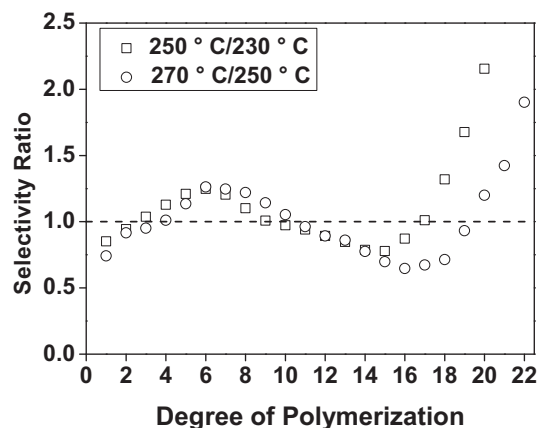


Figure 5-6: Effect of reaction temperature on the selectivity of glucose oligomers in the primary liquid products (Pressure: 10 MPa)

#### 5.4.2 Comparison of the Selectivity of Glucose Oligomers in the Primary Liquid Products

Equation (5-2) is then used to calculate the selectivity ratios of glucose oligomers in the primary hydrolysis products at various temperatures. This enables further evaluation of the effect of reaction temperature on the distribution of oligomers in the primary hydrolysis products. As shown in Figure 5-6, reaction temperature has a significant effect on the selectivity of the glucose oligomers in the primary liquid products; however, the trends are very complex. A monotonic increase in the selectivity of glucose oligomers with high-DPs is not seen. Therefore, the complexity in such trends cannot be explained alone by the increasing accessibility of glycosidic bonds as a result of increasing hydrogen bond cleavage at higher temperatures. In fact, as the temperature increases, the selectivity ratios for some glucose oligomers are  $< 1$ , suggesting that there may be other mechanisms leading to in situ changes in the structure of the reacting microcrystalline cellulose particles. For example, one possibility is the parallel cross-linking reactions during cellulose hydrolysis in HCW and increasing temperature is known to enhance these reactions during cellulose hydrolysis in HCW.<sup>225,226</sup> Detailed explanation of Figure 5-6 is only possible until the kinetic data of all of the related reactions are available, because the data in the figure are a combined outcome of these reactions.

### 5.5 Glucose Yield Recovered via Post Hydrolysis

The primary liquid products obtained under various conditions were also subjected to acid hydrolysis to determine the total neutral glucose content. As shown in Figure 5-7, the glucose yields via post hydrolysis for all the samples are very high (~80% on a carbon basis). This indicates that the glucose oligomers derivatives (i.e., those shown as small peaks near the glucose oligomer peaks in the HPAEC-PAD chromatograph) in the hydrolysis products also produce glucose during post hydrolysis; otherwise, the total neutral glucose yield would be much lower. The results also show that the effect of hydrolysis temperature on the glucose yield from the post-hydrolysis of the liquid samples collected under the reaction conditions at 230–270 °C is minor. The glucose yield recovered via post-hydrolysis also increases slightly with increasing flow rate, because of minization of the secondary reactions. Overall, even at 10 mL min<sup>-1</sup>, the secondary reaction in our reactor system seems to be small, because the neutral glucose yields are still close to 80%. In all cases, the total yields of lower sugars (C1–C5) ranges from 31–34% depending on reaction temperature and water flow rate.

These results clearly show that the liquid products from cellulose hydrolysis in HCW have a very high neutral glucose yield. It is known that effective fractionation of cellulose from biomass can be achieved by removing hemicelluloses and lignin from biomass using low-temperature HCW (~180 °C). Such results are of great importance to the potential development of a pretreatment technology for bioethanol production from cellulose that can be separated from lignocellulosic biomass. The process includes a biomass pretreatment step, a cellulose pretreatment step, an enzymatic hydrolysis step and a final fermentation step. The biomass pretreatment step uses low-temperature HCW (~180 °C) to separate lignin and hemicellulose from lignocellulosic biomass and break down hemicelluloses to oligomers and monomers. The amorphous cellulose may be partially hydrolysed during hydrolysis in low-temperature HCW. The cellulose pretreatment step employs high-temperature HCW (~270 °C) to break down long-chain microcrystalline cellulose into short-chain glucose oligomers. The enzymatic hydrolysis step converts the majority of hemicelluloses-derived oligomers and cellulose-derived oligomers into monomers (e.g., xylose and glucose). The final step is to convert various monomers into

bioethanol via fermentation. There are novel aspects of the proposed process. The process achieves clean fractionation of cellulose, lignin and hemicelluloses from biomass using low-temperature HCW, which is proven to be effective.<sup>49</sup> Additionally, it is well known that chain-end availability is a key factor limiting the reaction rate of the enzymatic hydrolysis of long-chain cellulose.<sup>227,228</sup> The breakdown of long-chain cellulose into glucose oligomers with considerably lower DPs breaks through such limitation. Therefore, compared to that of microcrystalline cellulose, the enzymatic hydrolysis of the glucose oligomers is expected to be substantially faster. It should be noted that the pretreatment technology proposed in this study uses HCW under mild conditions and is different to the pretreatment method using supercritical water (Temperature: 653 K and Pressure: 30 MPa), as summarized elsewhere.<sup>44</sup> Under those supercritical conditions, the degradation reactions are expected to be significant, the secondary reactions are inevitable and the overall reactions are rapid hence the process would be considerably more difficult to control.

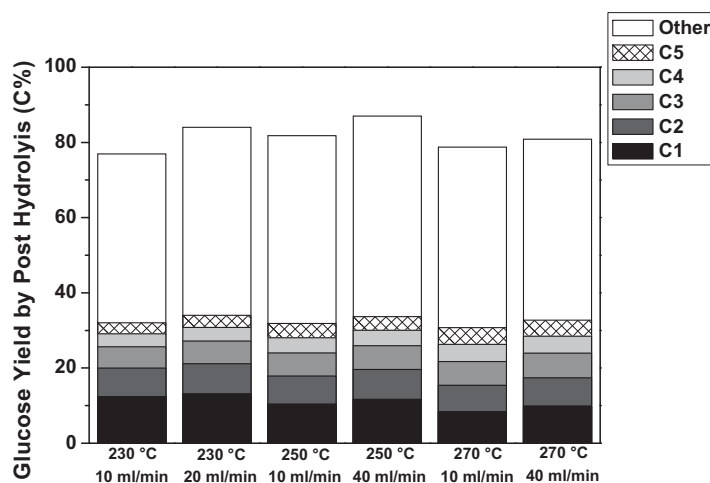


Figure 5-7: Glucose yields after post hydrolysis for primary liquid samples produced from cellulose hydrolysis in HCW under various conditions

## 5.6 Conclusions

Using a semicontinuous reactor system, this study reports data on the primary liquid products of microcrystalline cellulose hydrolysis in HCW at 10 MPa and temperatures of 230–270 °C. Reaction temperature has a significant effect on cellulose conversion and the distribution of glucose oligomers in the primary liquid products. The results of this study bring new insights into the reaction mechanisms of



cellulose hydrolysis in HCW. The primary hydrolysis reactions on the surface of reacting cellulose particles seem to proceed by the breaking of hydrogen bonds in the structure of microcrystalline cellulose and the random cleavage of the accessible glycosidic bonds in the cellulose, leading to the formation of glucose oligomers with a wide range of DPs. Thermal degradation reactions also occur randomly on the surface of cellulose particles, but to a much less extent in comparison to the primary hydrolysis reactions, leading to the production of derivatives of glucose and glucose oligomers with a wide range of DPs. The hydrolysis reactions also seem to be influenced by other parallel reactions, such as the possible cross-linking reactions during hydrolysis, leading to the change of cellulose structure. The primary liquid products may further undergo secondary reactions in the aqueous phase, depending on the reaction temperature and the residence time.

To collect primary liquid products hydrolysis, a semicontinuous reactor system is required and the reaction conditions must be optimised. The essential criteria are: (a) secondary reactions of liquid products in the aqueous phase are minimised, (b) solubility of each glucose oligomer in the liquid products is not a limiting factor, and (c) the interactions between liquid products and the reacting cellulose particle are minimized. Post hydrolysis of the primary liquid products has also shown a high glucose yield of ~80% on a carbon basis, therefore the combined HCW and enzymatic hydrolysis seems to be promising to recover sugar from lignocellulose or biomass.

## CHAPTER 6 DIFFERENT BEHAVIORS BETWEEN AMORPHOUS AND CYRSTALLINE PORTIONS WITHIN MICROCRYSTALLINE CELLULOSE

### 6.1 Introduction

In Chapter 4, a new sampling procedure and analytical method has been established for characterizing the glucose oligomers in the fresh liquid products of cellulose hydrolysis in HCW using a high-performance anion exchange chromatography with pulsed amperometric detection (HPAEC-PAD). It was clearly demonstrated that the fresh liquid products must be analysed immediately after collection to avoid the loss of high-DP glucose oligomers due to their precipitation.

Further study in Chapter 5 has successfully separated the primary hydrolysis reactions on the reacting particle surface from the secondary reactions in the aqueous phase, using a semicontinuous reactor system under optimised reaction conditions. Effects of reaction temperature on the behavior of crystalline cellulose during hydrolysis in HCW and distribution of glucose oligomers in the primary liquid products were investigated. Such progress enables the fundamental study to provide new insights into the reaction mechanisms of cellulose hydrolysis in HCW.

Microcrystalline cellulose contains both amorphous and crystalline portions as a cellulose microfibril is formed by several microcrystals hinged together and surrounded by amorphous cellulose, as illustrated in Figure 6-1.<sup>73</sup> Evidence in the literature<sup>73,75-80,229</sup> demonstrates the significant structural differences between amorphous and crystalline cellulose, mainly in the chain length of cellulose and hydrogen bonding patterns. While crystalline consists of well-packed long cellulose chains side by side via strong hydrogen bonds, amorphous cellulose can have the

length of the rigid chain segments as short as the order of one cellobiose unit.<sup>229</sup> It was also found that the chains in amorphous cellulose were held together by isotropic intermolecular hydrogen bonds linked to the hydroxyl groups at C-2 and C-3 positions, resulting in a randomly distributed domain.<sup>76</sup> While crystalline cellulose is known to have a preferred orientation,<sup>79,80</sup> the chains of amorphous cellulose are typically bent and twisted backbones and the molecules are in a random coil conformation.<sup>75,77,78</sup> Therefore, it is expected that the amorphous and crystalline portions in microcrystalline cellulose may have different behaviors during hydrolysis in HCW. The hydrolysis reactions may also exhibit significantly different reactivities, which is an important consideration in the design and operation of hydrolysis reactors. Unfortunately, little work has been done so far on these aspects.



Figure 6-1: Model of microcrystalline cellulose that consists of crystalline and amorphous structures<sup>73</sup>

Therefore, the main purpose of this chapter is to investigate the differences in the hydrolysis behavior of amorphous and crystalline structures within microcrystalline cellulose in HCW. Particularly, the primary liquid products obtained from the hydrolysis of amorphous and crystalline cellulose will be compared to understand the differences in reactivity and other reaction behaviors between amorphous and crystalline cellulose.

All experiments in this chapter were carried out at low temperatures (100-230 °C) in order to investigate the minimal temperatures at which the hydrolysis reactions of amorphous and crystalline cellulose in HCW commence. The sample which contains crystalline cellulose only was prepared by pretreating the raw cellulose sample at low temperatures (e.g., 200 °C) sufficient long to remove the amorphous portion. To understand the differences in the hydrolysis behavior of amorphous and crystalline cellulose in HCW, the primary liquid products from amorphous and crystalline cellulose were collected at low temperatures (< 230 °C) for characterising the glucose oligomers in the primary liquid products.

## 6.2 Specific Reactivity of Cellulose during Hydrolysis in HCW

Figure 6-2 presents the data on the time dependence of conversion ( $X$ ) at 200 and 230 °C. The hydrolysis reaction rate of cellulose in HCW increases significantly with reaction temperature. At 200 °C, after 1 h hydrolysis, only 10% of cellulose is converted, while at 230 °C the conversion is close to 35% on a carbon basis. The specific reactivity of cellulose is then plotted in Figure 6-3, as a function of cellulose conversion. At both temperatures, it is interesting to see that, at early stage of hydrolysis reactions, the specific reactivity is initially high and then continuously decreases until a certain conversion level  $X_c$  (10–15%), at which the specific reactivity starts to level off with further increase in conversion. Therefore, at both 200 and 230 °C, as far as hydrolysis reactions are concerned, the portion of cellulose at  $X \leq X_c$  seems to be very reactive initially but the structure of the portion of remaining cellulose becomes less and less reactive as the hydrolysis reaction progresses. At  $X > X_c$ , the remaining cellulose has a much lower but rather constant

reactivity, suggesting that from the specific reactivity point of view the structure of the remaining cellulose at  $X > X_c$  is rather similar.

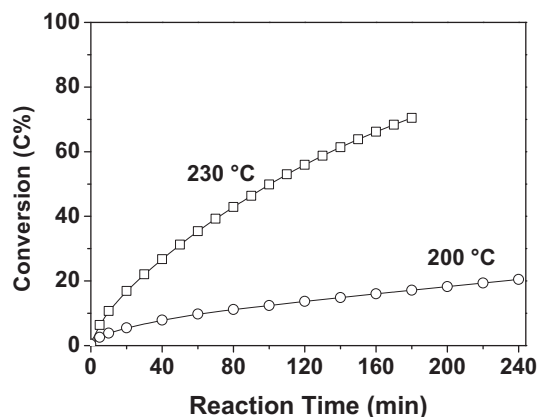


Figure 6-2: Cellulose conversion during hydrolysis in HCW at 200 and 230 °C

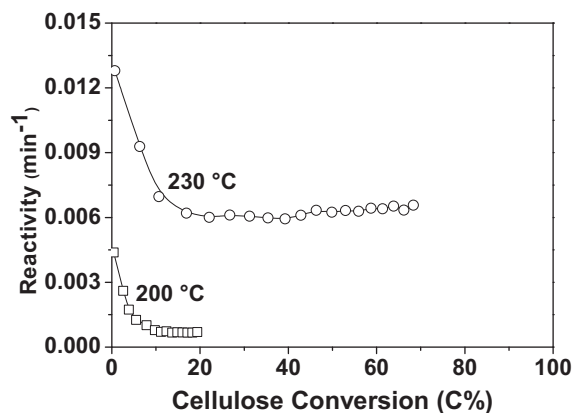


Figure 6-3: Specific reactivity of cellulose during hydrolysis in HCW at 200 and 230 °C

### 6.3 Heterogeneity in the Structures of Microcrystalline Cellulose

Microcrystalline cellulose was then further examined using X-ray diffraction (XRD) analysis, and the results are presented in Figure 6-4. It can be seen that the microcrystalline cellulose sample indeed consists of both the amorphous and crystalline structures. According to Segal's method,<sup>218</sup> the relative crystallinity index of our sample is determined to be ~0.8. In other words, the cellulose sample contains approximately 20% amorphous structure, which is similar to the conversion  $X_c$  (10% at 200 °C and 15% at 230 °C) at which the specific reactivity of cellulose starts to

level off in Figure 6-3. This is expected as the hydrolysis reactions at  $X \leq X_c$  also consume a small proportion of the crystalline structure and such conversion would also be temperature dependent. This is clearly shown in Figure 6-3 that the specific reactivity of crystalline cellulose is very low at 200 °C, but not zero, indicating that hydrolysis of crystalline cellulose in HCW already starts at 200 °C. Therefore, it is reasonable to conclude that the amorphous structure that is more reactive seems to be selectively consumed in the initial step of cellulose hydrolysis at  $X \leq X_c$ , while the more inert crystalline structure was left to be hydrolysed at higher conversions at  $X > X_c$ .

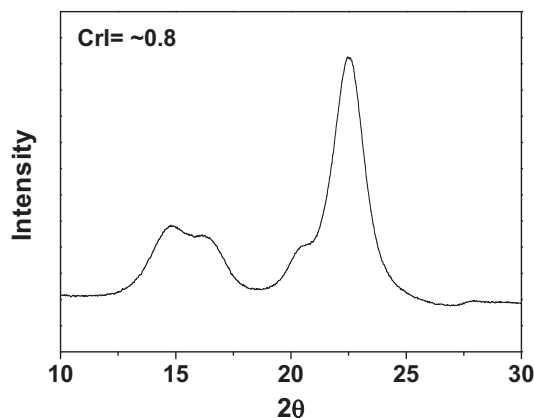


Figure 6-4: X-ray diffraction pattern of raw cellulose sample

The results in Figures 6-3 and 6-4 clearly demonstrate that the microcrystalline cellulose sample used in this study has heterogeneous structures. This is consistent with the common knowledge that microcrystalline cellulose typically contains both amorphous and crystalline structures, as illustrated in Figure 6-1.<sup>73</sup> The key structural differences between the amorphous and crystalline cellulose are in the chain length of cellulose and hydrogen bonding patterns.<sup>73,75-80,229</sup> Crystalline cellulose includes long cellulose chains which have a preferred orientation and are well-ordered and packed side by side via strong hydrogen bonds.<sup>79,80</sup> On the contrary, amorphous cellulose consists of much shorter chain segments with a wide distribution of chain lengths<sup>229</sup> hinged to the crystalline structures with much weaker hydrogen bonds. Therefore, it is not surprising that the crystalline portion would be

significantly less reactive during hydrolysis in HCW, compared to the amorphous portion within microcrystalline cellulose.

In fact, Figure 6-3 shows that even the amorphous cellulose portion itself is significantly heterogeneous, exhibiting a continuous decrease in its specific reactivity at  $X \leq X_c$ , because if the structure of amorphous cellulose is homogeneous, the reactivity of the amorphous portion within microcrystalline cellulose would be expected to decrease suddenly rather than gradually as conversion increases. The heterogeneity of amorphous cellulose structures within microcrystalline cellulose is also expected due to the structural nature of amorphous cellulose. As illustrated in Figure 6-1, the amorphous portion includes various chain segments,<sup>73</sup> which have a wide distribution of chain lengths as well as different connections of the hydrogen bonding network within the amorphous portion.<sup>229</sup> These chain segments are typically bent and twisted backbones, and the molecules are in a random coil conformation.<sup>75,77,78</sup> They hinge and surround the microcrystals of the crystalline portion via weak hydrogen bonds, resulting in randomly distributed domains<sup>76</sup> which are known to have a wide distribution of energy levels.<sup>73,75-80,229</sup> Such heterogeneous structures determine the heterogeneous behavior of the amorphous portion during hydrolysis in HCW.

## 6.4 Hydrolysis Behavior of the Amorphous Portion within Microcrystalline Cellulose

### 6.4.1 Amorphous Portion within Raw Microcrystalline Cellulose

A further set of systematic investigations needs to be designed to gain a thorough understanding of the hydrolysis behavior of the amorphous portion within microcrystalline cellulose in HCW. To do so, it is critical to carry out the experiments under the conditions where only the amorphous portion within microcrystalline cellulose participates in the hydrolysis reactions in HCW. From Figure 6-3, it is known that at 200 °C, at early conversions, the hydrolysis reactions are dominant by those of the amorphous portion and the contribution of the crystalline portion is very small. Therefore, the set of experiments was then carried out at 100–200 °C to gain fundamental knowledge on the hydrolysis behavior of the

amorphous portion in HCW. The fresh liquid samples were analysed by HPAEC-PAD immediately after collection, following the methodology described in Chapter 4.

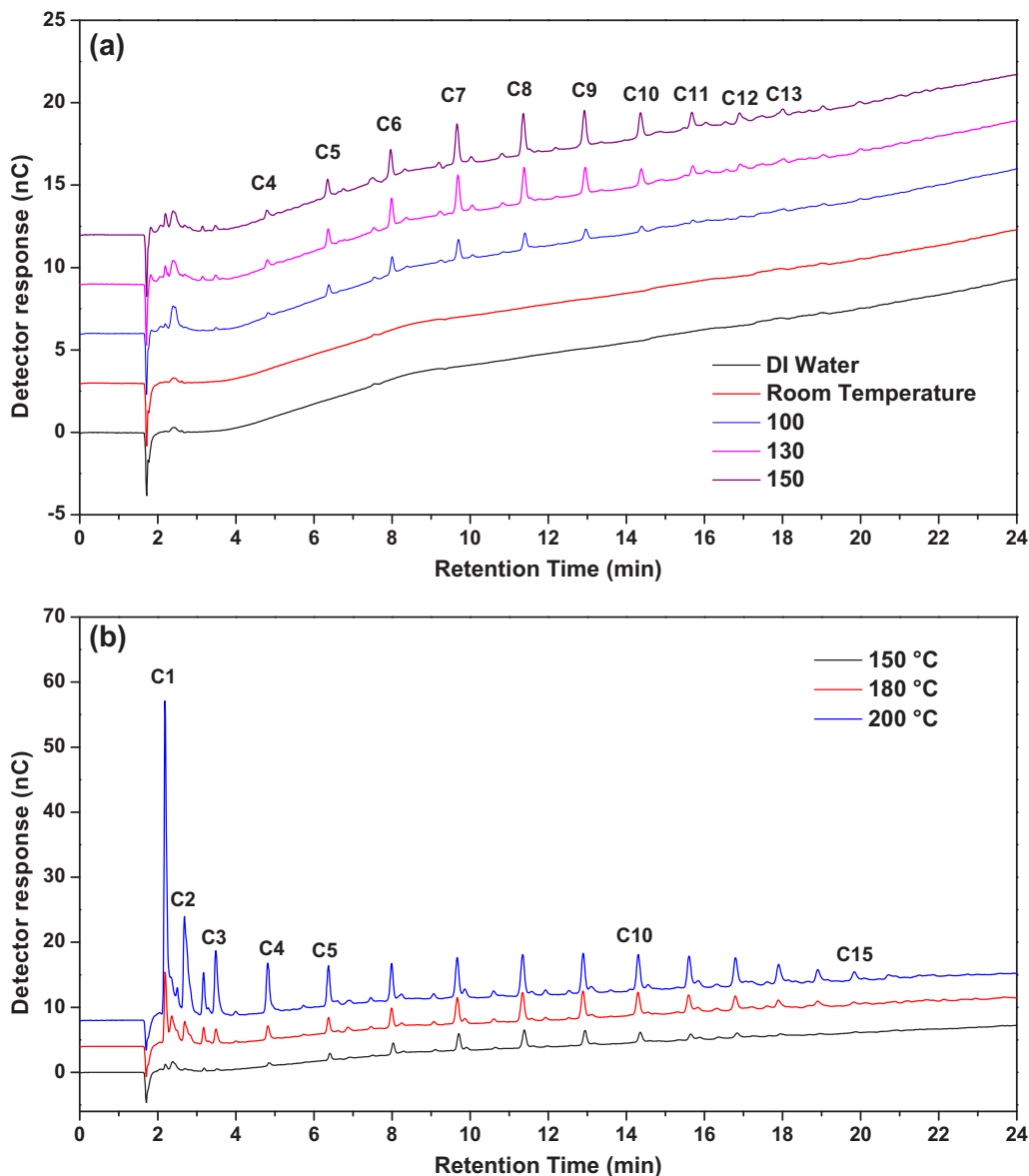


Figure 6-5: IC chromatograms of primary liquid products from amorphous portion within microcrystalline cellulose during hydrolysis in HCW. (a) 100-150 °C; (b) 150-180 °C.

Figure 6-5 presents the IC chromatograms of glucose oligomers in the primary liquid products at various temperatures, analysed by HPAEC-PAD. It is not surprising that



the carbon concentrations of liquid products, as well as the concentrations of glucose oligomers in the primary liquid products, increase with the reaction temperature. However, it is interesting to see in Figure 6-5a that, even at a temperature as low as 100 °C, various glucose oligomer peaks (C4–C13) are identified in the chromatogram of the primary liquid product via HPAEC-PAD analysis. This is surprising because the hydrolysis reactions are thought to hardly take place at such a low temperature.<sup>53</sup> Further experiments were then conducted to investigate the liquid products at room temperature and 50 °C. No peaks are present in the chromatogram of the liquid sample at room temperature; however, some very small peaks of glucose oligomers can still be seen in the liquid products at 50 °C (data not shown). The data clearly suggest that the amorphous portion contains some very reactive components which can be hydrolysed by HCW with very low temperatures. However, there are key fundamental questions to be answered:

1. Are the C4–C13 in the liquid products formed directly from the short chain segments with the same chain lengths after the connecting weak hydrogen bonds between those structures and the amorphous/crystalline cellulose are broken, or are they produced from the cleavage of glycosidic bonds of longer chain segments in the amorphous portion within microcrystalline cellulose?
2. What is the minimal temperature at which the glycosidic bonds in the chain segments start to break?

It is also surprising to see in Figure 6-5a that the low-DP glucose oligomers (C1–C3) are hardly formed at temperatures <150 °C. As one essential requirement for the formation of C1 under hydrolysis conditions is the cleavage of glycosidic bonds in at least one chain segment within amorphous cellulose, the data then suggest that the

cleavage of glycosidic bonds in any chain segment hardly happens at temperatures less than 150 °C. Figure 6-5b shows that large peaks of C1–C3 only appear in the chromatogram of the primary liquid products produced at temperatures >150 °C. Therefore, the minimal temperature required to break the glycosidic bonds in the chain segments within the amorphous portion seems to be ~150 °C. Furthermore, those glucose oligomers (C4–C13) in the primary liquid products produced from hydrolysis at temperatures < 150 °C must be the original individual chain segments hinged within microcrystalline cellulose via weak bonds (e.g., hydrogen bonds), which can be easily broken by HCW at low temperatures. Therefore, it can be proven that the short chain segments with weak hydrogen bonding connections in the amorphous portion are those reactive components responsible for the formation of C4–C13 in the primary liquid products at low temperatures.

#### 6.4.2 Amorphous Portion within Pretreated Microcrystalline Cellulose

To further prove these important conclusions, another purposely designed set of experiment was conducted. The raw cellulose sample was pretreated at 180 °C for 10 min to remove the most reactive components in the amorphous portion within the microcrystalline cellulose, since those components are believed to be responsible for the formation of C4–C13 at low temperatures. The pretreated sample was then subject to hydrolysis in HCW at desired temperatures (100–200°C). It should be noted that, due to slow reaction rate at 180 °C and the short pretreatment time, only a small proportion (<15%) of amorphous cellulose was removed during pretreatment; therefore the hydrolysis reactions of the pretreated sample at various temperatures are still dominated by those of the amorphous portion within microcrystalline cellulose. The IC chromatograms of the primary liquid products of the pretreated sample are presented in Figure 6-6. Indeed, Figure 6-6 clearly shows that no sugar peaks are seen in the IC chromatograms of the liquid products produced at hydrolysis temperatures below 150 °C while there are considerable glucose oligomers of C4–C13 produced from the raw cellulose sample under the same conditions. Furthermore, Figure 6-6 also clearly shows that the glucose (C1) peak first appears in the IC chromatograms at 150 °C, and increases gradually with further increase in the reaction temperature. Various peaks of high-DP glucose oligomers start to appear in the IC chromatograms at 160 °C. This means that those short chain segments with

weak hydrogen bonding connection can be easily removed by pretreating with HCW at 180 °C, and they only account for a small proportion (<15%) of amorphous cellulose.

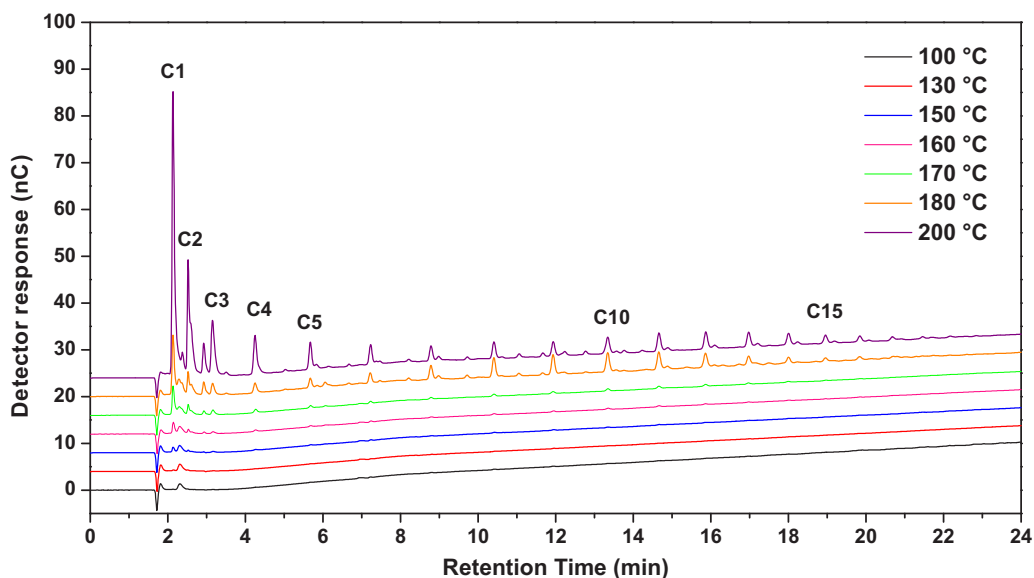


Figure 6-6: IC chromatograms of primary liquid products from pretreated amorphous cellulose during hydrolysis in HCW

These results in Figure 6-6 clearly prove that the minimal temperature required to break the glycosidic bonds in the amorphous portion within microcrystalline cellulose is 150 °C. This is consistent with the previous experimental observation<sup>113</sup> on cellobiose decomposition in HCW using a batch reactor, showing that only slight decomposition reactions of cellobiose occur at 180 °C, and hence the cleavage of glycosidic bond in cellobiose already starts at 180 °C but the reaction rate is very slow. The results in Figure 6-6 also demonstrate that the glucose oligomers (C4–C13) in the primary liquid products during hydrolysis of the amorphous portion at temperatures <150 °C (see Figure 6-5a) are indeed directly from the original individual chain segments that are hinged within the microcrystalline cellulose via weak bonds (e.g., hydrogen bonds), which can be easily broken by HCW at low temperatures. Therefore, the data suggest that the shortest chain segment in the amorphous portion is likely to be C4. There are no chain segments with only a single glucose unit in the amorphous portion within microcrystalline cellulose, in agreement

with the previous conclusion that the amorphous cellulose can have rigid chain segments as short as the order of one cellobiose unit.<sup>229</sup> Another key implication is that it is possible to develop a useful technique based on hydrolysis in HCW at low temperatures to probe the structures of amorphous cellulose. It is also noteworthy that, via TOC analysis, the concentration of total carbon of the liquid product collected from hydrolysis of the raw cellulose at 100 °C is determined to be very low, ~0.7 ppm. This demonstrates the excellent capability of HPAEC-PAD in the analysis of the glucose oligomers even in the sample with such a low concentration.

### **6.5 Hydrolysis of the Crystalline Portion within Microcrystalline Cellulose in HCW**

To study the hydrolysis of the crystalline portion within microcrystalline cellulose, it is essential to obtain a sample with the crystalline portion only. As shown in Figures 6-2 and 6-3, the amorphous portion within microcrystalline cellulose can be completely removed by treating the raw sample for a sufficiently long (4 h) at 200 °C, at which the specific reactivity of the crystalline portion is very low (but not zero), hence minimising the conversion of the crystalline cellulose structure within the sample. Therefore, using this approach, the sample containing crystalline cellulose only was prepared.

A series of experiments were then carried out to investigate the hydrolysis behavior of the crystalline portion within microcrystalline cellulose in HCW at 100–220 °C, using the prepared sample containing crystalline cellulose only. Similarly, the fresh liquid products were collected and immediately analysed by HPAEC-PAD, following the methodology described in Chapter 4. The results are presented in Figure 6-7, which shows no sugar peak in the IC chromatogram until the hydrolysis reaction temperature increases to 180 °C. This is an important observation because it suggests the minimal temperature required for the hydrolysis reactions to proceed in the crystalline portion is 180 °C, which is much higher than that (i.e., 150 °C) required for breaking the glycosidic bonds in the amorphous portion. Clearly, in the case of crystalline cellulose hydrolysis, the glycosidic bonds in the cellulose chain are not accessible, due to the strong intra- and inter-molecular hydrogen bonding

networks which prevent the glycosidic bonds in crystalline cellulose from being attacked by HCW.

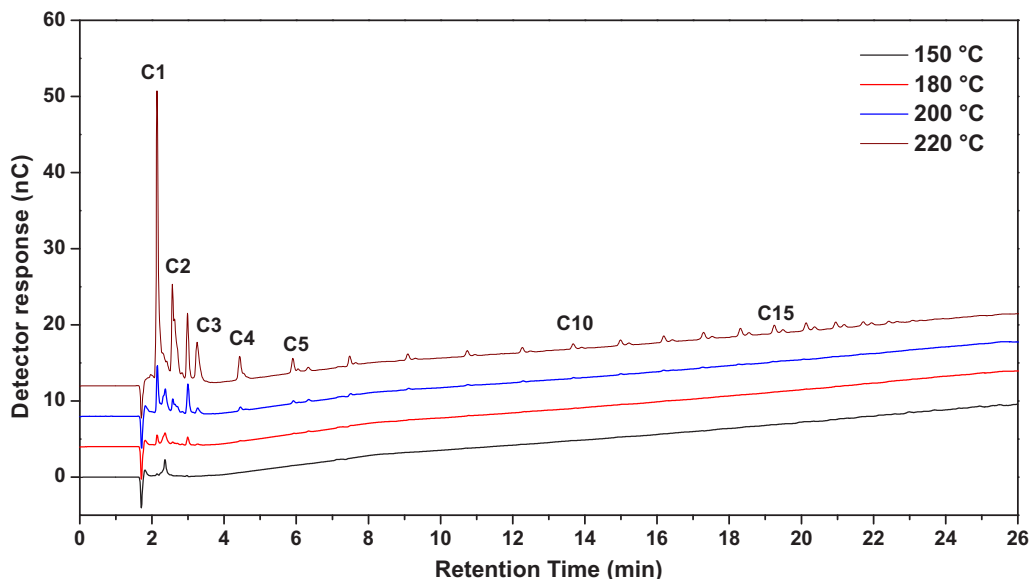


Figure 6-7: IC chromatograms of primary liquid products from crystalline portion within microcrystalline cellulose during hydrolysis in HCW

Figure 6-7 also shows that the peaks of low-DP glucose oligomers (e.g., C1–C2) first appear in the chromatogram of liquid products at 180 °C, while large-DP glucose oligomers only appear at temperatures >200 °C. As hydrolysis temperature further increases, more glucose oligomers with higher DPs are produced in the liquid products. This is completely different from those for the untreated amorphous portion within the microcrystalline cellulose, which produces substantial glucose oligomers even at 180 °C (see Figure 6-5b). It is clearly due to the significant structural differences in the amorphous and crystalline portions of microcrystalline cellulose. The crystalline portion includes long cellulose chains which lie in parallel, pack well, and are hydrogen-bonded edge to edge.<sup>79,80</sup> The strong hydrogen bonds protect the glycosidic bonds in the crystalline portion from being attacked by HCW; therefore the high-DP glucose oligomers cannot be formed until the hydrogen bonds in crystalline cellulose have been broken to make the glycosidic bonds accessible to HCW. At low temperatures, only a very small portion of hydrogen bonds is broken; therefore the hydrolysis reaction is only able to produce low-DP glucose oligomers

such as C1 and C2. As the hydrolysis temperature increases, the breakage of hydrogen bonds in the crystalline portion within microcrystalline cellulose becomes much faster, making the glycosidic bonds in these structures more accessible hence producing more high-DP glucose oligomers.

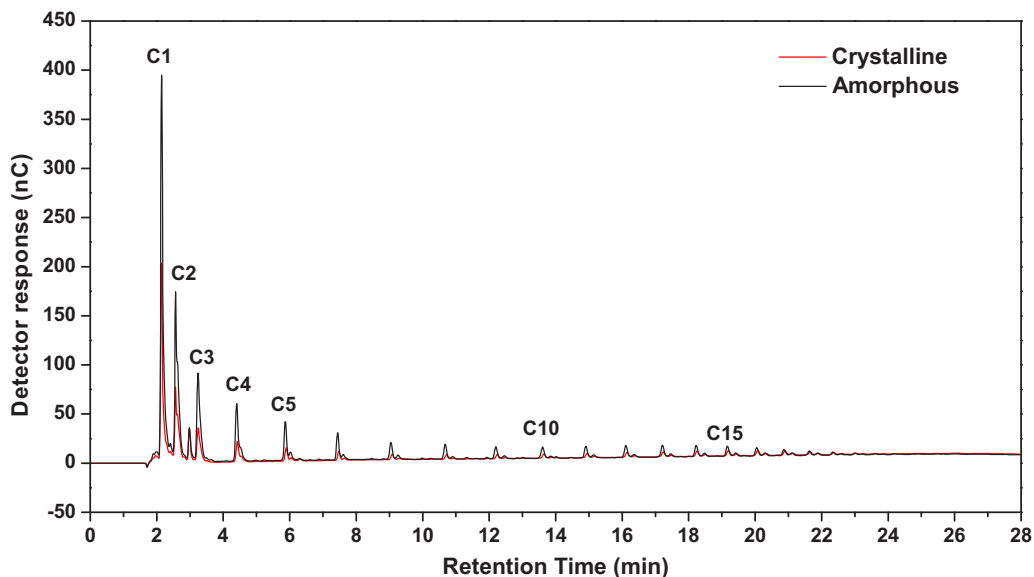


Figure 6-8: IC chromatograms of primary liquid products from amorphous and crystalline cellulose during hydrolysis in HCW at 230 °C

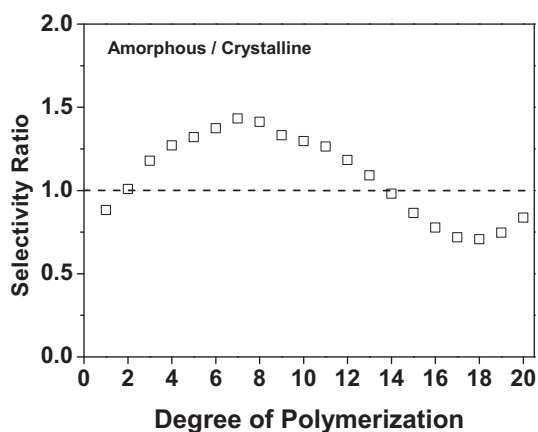


Figure 6-9: Selectivity ratios of glucose oligomers in the primary liquid products from amorphous and crystalline cellulose during hydrolysis in HCW at 230 °C

## 6.6 Comparisons between the Hydrolyses of the Amorphous and Crystalline Portions within Microcrystalline Cellulose

Further experiments were conducted to collect the primary liquid products from the amorphous and crystalline portions at the same temperature, in order to compare the differences between their primary liquid products. A temperature of 230 °C was carefully chosen for this purpose. At a lower temperature, the liquid sample with relatively high concentrations of glucose oligomers cannot be obtained from the crystalline portion because of the slow reactions, while at a higher temperature the reactions of the amorphous portion are too fast to collect the liquid sample from the amorphous portion. Figure 6-8 presents the IC chromatograms of primary liquid products collected at 5 and 30% conversions during hydrolysis of microcrystalline cellulose at 230 °C, corresponding to the primary liquid products from the amorphous and crystalline portions, respectively. It can be seen that the maximal DP of glucose oligomer in the primary liquid products from amorphous and crystalline cellulose is the same. Since amorphous cellulose is much more reactive than crystalline cellulose, the concentrations of all glucose oligomers in the liquid products from the amorphous portion are higher than those from the crystalline portion.

Based on a method described in Chapter 5, Figure 6-9 shows the selectivity ratios of glucose oligomers in the primary liquid products from the amorphous and crystalline portions during hydrolysis in HCW at 230 °C. It can be seen that the selectivities of glucose oligomers with DPs of 3–13 in the liquid products from amorphous cellulose are considerably higher than those from crystalline cellulose. Furthermore, the selectivity ratios of glucose oligomers in the primary liquid products from amorphous and crystalline cellulose do not show a monotonic trend with DP. These results are not expected because the short chain segments with weak hydrogen bonding connection responsible for C4–C13 formation at low temperatures are thought to be removed at the overall conversion of 5%, corresponding to the proportion of ~20% in the amorphous portion. In the above section, we have shown that no short chain segments are present in the amorphous portion after pretreating with HCW at 180 °C for 10 min, and <15% of the amorphous portion has been removed. However, we still found the increase of selectivities of C3–C13 in the

primary products from the amorphous portion at 230 °C, compared to those from the crystalline portion. A possible reason is that the amorphous portion may contain shorter glucose chains connected within the amorphous portion via weaker hydrogen bonds, compared to the crystalline portion. Those shorter glucose chains in the amorphous portion cannot be removed by pretreating at 180 °C, because they are connected with much stronger hydrogen bonds compared to the most reactive part in the amorphous portion, which can be removed at 180 °C. Therefore, during hydrolysis at 230 °C, amorphous portion sample collected at 5% conversion contains much more low-DP glucose oligomers (e.g., C3–C13), compared to the crystalline portion sample collected at 30% conversion. All of these results further prove that the structure of the amorphous portion within microcrystalline cellulose is heterogeneous.

### 6.7 Conclusions

This study has successfully demonstrated the significant differences in the hydrolysis behavior of the amorphous and crystalline portions within microcrystalline cellulose in HCW. Such differences are apparently due to these structural differences, such as chain length and hydrogen bonding pattern. For example, the amorphous portion is much more reactive than the crystalline portion within microcrystalline cellulose. Therefore, reaction of the amorphous portion occurs earlier, leading to the considerable reduction of reactivity of microcrystalline cellulose in the initial stage during cellulose hydrolysis in HCW, particularly at lower temperatures < 230 °C.

Furthermore, it is clearly demonstrated that the amorphous portion consists of various short chain segments with a wide range of chain lengths (as short as C4) and these short chain segments are possibly hinged in the microcrystalline cellulose via weak hydrogen bonds. Those short chain segments can be extracted or hydrolysed by HCW at relatively low temperatures (e.g., < 150 °C) without breaking the glycosidic bonds in the chain segments.

Through some purposely designed experiments, we found that the minimal temperature to break the glycosidic bonds in the amorphous portion is ~150 °C. However, the minimal temperature at which hydrolysis reactions of the crystalline



portion start is  $\sim 180$  °C, due to the strong intra- and inter-molecular hydrogen bonds which prevent the glycosidic bonds in the long cellulose chains from being accessible to HCW. An increase in the hydrolysis temperature leads to the formation of more and larger-DP glucose oligomers, apparently due to the enhanced accessibility of glycosidic bonds in the cellulose chains as results of increasing breaking of hydrogen bonds.

These structural differences also have a large influence on the distribution of glucose oligomers in the primary liquid products from amorphous and crystalline cellulose during hydrolysis in HCW. Amorphous cellulose is more reactive hence producing more glucose monomer and oligomers at the same temperature, but the selectivity ratios of glucose oligomers in the primary liquid products from amorphous and crystalline cellulose do not show a monotonic trend with DP, partly resulting from the presence of shorter glucose chains in amorphous cellulose.

## CHAPTER 7 EVOLUTION OF PRIMARY LIQUID PRODUCTS AND EVIDENCE OF IN SITU STRUCTURAL CHANGES WITH CONVERSION

### 7.1 Introduction

It is generally accepted that hydrolysis of biomass/cellulose in HCW involves complex chemical and physical process which may include primary hydrolysis on the surface of the reacting cellulose particles, the dissolution of primary hydrolysis products into HCW and the secondary decomposition reactions of primary hydrolysis products in the aqueous phase.<sup>34,44</sup> Such complex reactions are the main reasons why the characteristics of liquid products strongly depend on the configurations of reactor systems. For example, as results of extensive secondary reactions in the aqueous phase, sugars are the dominant products in semicontinuous<sup>32,33,50,53,56</sup> and continuous reactor systems,<sup>35,52,54,55</sup> while oil and/or chars are the main products in batch reactor system.<sup>51,54,57,60,61</sup>

Our studies in the chapters 4-6 provide new insights into the reaction mechanisms on cellulose hydrolysis in HCW. In chapter 4, a new sampling and analytical method was developed to characterise the glucose oligomers in the fresh liquid products via a high performance anion exchange chromatography with pulsed amperometric detection (HPAEC-PAD). In chapter 5, using a semicontinuous reactor system, a series of experiments were carefully designed to successfully obtain the primary liquid products of cellulose hydrolysis in HCW under various conditions with minimised secondary reactions in the aqueous phase. The results clearly showed that on the surface of reacting cellulose particles, hydrolysis reactions dominate to produce glucose oligomers of a wide range of degree of polymerizations (DPs) while degradation reactions do occur but in a much less extent. Both hydrolysis and

degradation reactions were found to proceed on the particle surface in parallel and in a manner of randomness that is temperature-dependent. In chapter 6, the amorphous and crystalline portions within microcrystalline cellulose also exhibit significant differences in hydrolysis behavior in HCW, due to their structural differences.

Previous experimental data also suggested that the structure of cellulose might vary with conversion as hydrolysis reactions proceed in HCW.<sup>34</sup> While hydrolysis reactions proceed, the reacting cellulose particles may also experience parallel pyrolysis and/or other reactions, which can also dynamically alter the structure of the reacting cellulose particles and hence the characteristics of hydrolysis primary liquid products. This is expected to be important in batch or semicontinuous systems in which the reacting particles experience long residence times. However, little is known on how such structural evolution influences the formation of primary liquid products as a function of conversion during the course of cellulose hydrolysis in HCW. The significance of such an effect and its dependence on reaction temperature are also unknown. Fundamentally, these are all important aspects which need to be considered in the mechanistic understanding of cellulose hydrolysis behavior in HCW, the acquisition of cellulose hydrolysis reactivity data, and the design of hydrolysis reactor systems with maximized sugar recovery.

Therefore, the key objectives of this chapter are to carry out a systematic experimental study on the evolution of primary liquid products as a function of conversion during cellulose hydrolysis in HCW at various hydrolysis temperatures. A semicontinuous reactor system same as previous chapters was employed as the reacting particles remained in the reactor during reactions, enabling the study on the possible dynamic structure evolutions. Additionally, a set of novel two-step experiments was also carried out to illustrate the importance of in situ structural changes on the evolution of cellulose specific reactivity and primary liquid products during hydrolysis in HCW, considering both crystalline and amorphous cellulose.

## 7.2 XRD Analysis of Microcrystalline and Amorphous Samples

X-ray diffraction (XRD) analysis shows the microcrystalline cellulose has a relative crystallinity index of 0.8 according to Segal's method.<sup>218</sup> A complete amorphous

cellulose sample (no crystalline peaks found in the sample's XRD pattern, see Figure 7-1) was also prepared from the microcrystalline cellulose via ball-milling for ~7 hours using a laboratory ball mill.

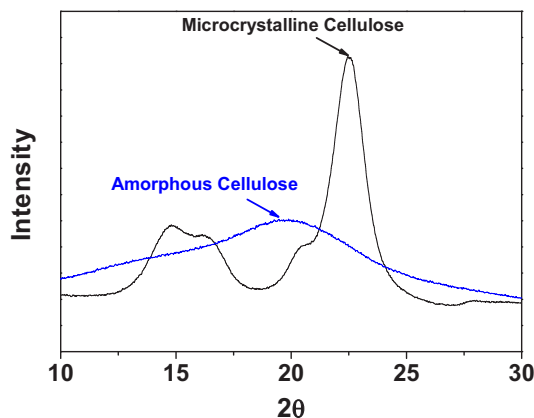


Figure 7-1: X-ray diffraction patterns of raw and ball milled 7-hour cellulose samples

### 7.3 Evolution of Specific Reactivity as a Function of Conversion during the Hydrolysis of Cellulose in HCW

#### 7.3.1 Hydrolysis of Amorphous Cellulose

Figure 7-2 presents the evolution of specific reactivity as a function of conversion during the hydrolysis of amorphous cellulose at 180–200 °C. It can be seen in Figure 2 that the specific reactivity of amorphous cellulose decreases continuously with conversion. As shown in Figure 7-1, the amorphous cellulose is completely amorphous since no crystalline peak can be found in its XRD pattern. It is well-known that amorphous cellulose has a heterogeneous structure which consists of chain segments of various chain length.<sup>73,76,229</sup> Therefore, the decrease in specific reactivity as a function of conversion in Figure 7-2 is most likely due to the selective consumption of more reactive components at early conversions during hydrolysis.

#### 7.3.2 Hydrolysis of Microcrystalline Cellulose

Figure 7-3 presents the evolution of specific reactivity as a function of conversion during the hydrolysis of microcrystalline cellulose at 230–270 °C. As discussed in chapter 6, at 230 °C there is an initial decrease in reactivity up to ~20% conversion, corresponding to the selective conversion of the amorphous portion within the microcrystalline cellulose that has a relative crystallinity index of ~0.8. After the amorphous portion is consumed, the specific reactivity of the crystalline portion

remains relatively unchanged at conversion > 20%. However, it is interesting to see that, at 250 and 270 °C, the decrease in the specific reactivity is not apparent at early conversions. It seems that, as far as specific reactivity is concerned, the structural differences between amorphous and crystalline portions within microcrystalline cellulose become less important at high temperatures. This also suggests that the strong hydrogen bonds in the microcrystalline cellulose can be broken very quickly at high temperatures. Another important point to make in Figure 7-3 is that at 270 °C, there is a significant decrease in the specific reactivity of the reacting cellulose at high conversions. Such a decrease in specific reactivity clearly indicates the structural changes within the reacting cellulose. Such structural changes seem to involve the condensation of the structures, resulting in the reacting cellulose becoming more inert (or less reactive) as the conversion increases.

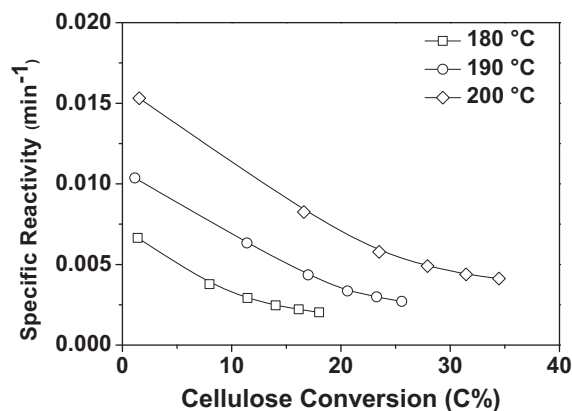


Figure 7-2: Evolution of specific reactivity of amorphous cellulose during hydrolysis in HCW at 180 – 200 °C, 10 MPa

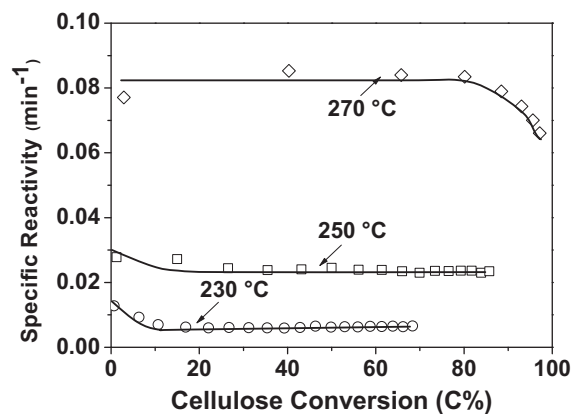


Figure 7-3: Evolution of specific reactivity of microcrystalline cellulose during hydrolysis in HCW at 230 – 270 °C, 10 MPa

#### 7.4 Evolution of Primary Liquid Products as a Function of Conversion during the Hydrolysis of Cellulose in HCW.

It is expected that the structural changes of reacting cellulose should result in the differences in the primary liquid products at various conversions. Therefore, at the same hydrolysis temperature, the primary liquid products were then collected at various conversions and compared using an index called the “selectivity ratio”. The selectivity ratio is defined in chapter 5 as the ratio between the selectivity of a glucose oligomer in two liquid products, normalised to the total carbon contents of each liquid product. Figures 7-4 and 7-5 present the selectivity ratios of glucose oligomers in the primary liquid products collected at various conversions for the hydrolysis of amorphous and microcrystalline cellulose in HCW. At a given hydrolysis temperature, if there is little structural change during conversion, the selectivity ratios for all glucose oligomers in the primary liquid products collected at various conversions should be 1. However, this is obviously not the cases in both Figures 7-4 and 7-5, which clearly show the significant changes in selectivities of glucose oligomers in the primary liquid products collected at various conversions at a given temperature. Therefore, there must be dynamic structural changes occurring in reacting cellulose particles as conversion increases during hydrolysis in HCW. A close examination of Figures 7-4 and 7-5 leads to several key observations.

##### 7.4.1 Hydrolysis of Amorphous Cellulose

For the amorphous cellulose at 180 °C, as the conversion increases, the selectivities of C3 to C13 decrease to below 1 while the lower-DP glucose oligomers (DPs < 3) and higher-DP glucose oligomers (DPs > 13) increase to above 1. The curves of the selectivity ratio have a similar shape at 190 and 200 °C. This is likely due to the heterogeneous structure of the amorphous cellulose. It is known that the chain segments of various lengths in amorphous cellulose are held together by isotropic intermolecular hydrogen bonds linked to the hydroxyl groups at the C-2 and C-3 positions,<sup>76</sup> with typically bent and twisted backbones, and the molecules are in a random coil conformation,<sup>75,77,78</sup> resulting in randomly distributed domain.<sup>76</sup> It was also found in chapter 5 that the amorphous portion with microcrystalline cellulose contains various short-length chain segments (e.g. C3–C13). For a completely amorphous cellulose sample, like the one used in this study, these short-length chain

segments are expected to be more abundant. Therefore, those short chains would be progressively removed as conversion increases, resulting in a reduction in the selectivity ratios of C3 to C13 in the primary liquid products as cellulose conversion increases and an increase in the length of chain segments within the reacting amorphous cellulose. This is clearly shown in Figure 7-4a, that the selectivities of C3 to C13 decrease with increasing conversion of amorphous cellulose at 180 °C. Additionally, with increasing conversion, the reacting particles experience longer residence times in HCW, resulting in the continuous weakening of hydrogen bonds within the amorphous cellulose. As shown in Figure 7-4a, the hydrolysis of the reacting amorphous cellulose which has longer chain sizes at increased conversions would lead to an increase in the selectivities of lower-DP glucose oligomers (DPs < 3) and higher-DP glucose oligomers (DPs > 13). The data in Figures 7-4b and 7-4c also indicate that, compared to at 180 and 190 °C, the increase in high-DP glucose oligomers is less at 200 °C, suggesting that for amorphous cellulose the other parallel reactions of the chain segments within the reacting sample to form nonsugar products seem to be apparent even at 200 °C.

#### 7.4.2 Hydrolysis of Microcrystalline Cellulose

For microcrystalline cellulose in Figure 7-5, the evolution of primary liquid products with increasing conversion follows a significantly different matter. At 230 °C, there are only small differences in the selectivities of the glucose oligomers in the primary liquid products at conversions less than 35%. Further increase in conversion leads to significant changes in the selectivity of the glucose oligomers in the primary liquid products. The selectivities of glucose oligomers with DPs of 1–14 are found to decrease significantly with conversion to be less than 1, while the selectivity of high-DP glucose oligomers (e.g., C17–C20) increases with conversion to be greater than 1. Also, the selectivity ratios of glucose oligomers larger than a certain DP (e.g., 14 at 230 °C) increases with the DP. The increasing selectivity of those high-DP glucose oligomers is possibly due to the change of hydrogen bonding. Crystalline cellulose consists of a complex network of intra- and intermolecular hydrogen bonds,<sup>79,80</sup> which can limit the accessibility of the glycosidic bonds within the chain therefore the formation of high-DP glucose oligomers. It is known that the structure of hydrogen bonds in crystalline cellulose is also drastically weakened at

temperatures  $>220$  °C.<sup>223,224</sup> Therefore, with increasing conversion, the reacting cellulose particles experience longer residence times and therefore continuous weakening of hydrogen bonds. The glycosidic bonds in cellulose residue are more accessible at higher conversions, therefore leading to an increase in the selectivity of those high-DP glucose oligomers in the primary liquid products.

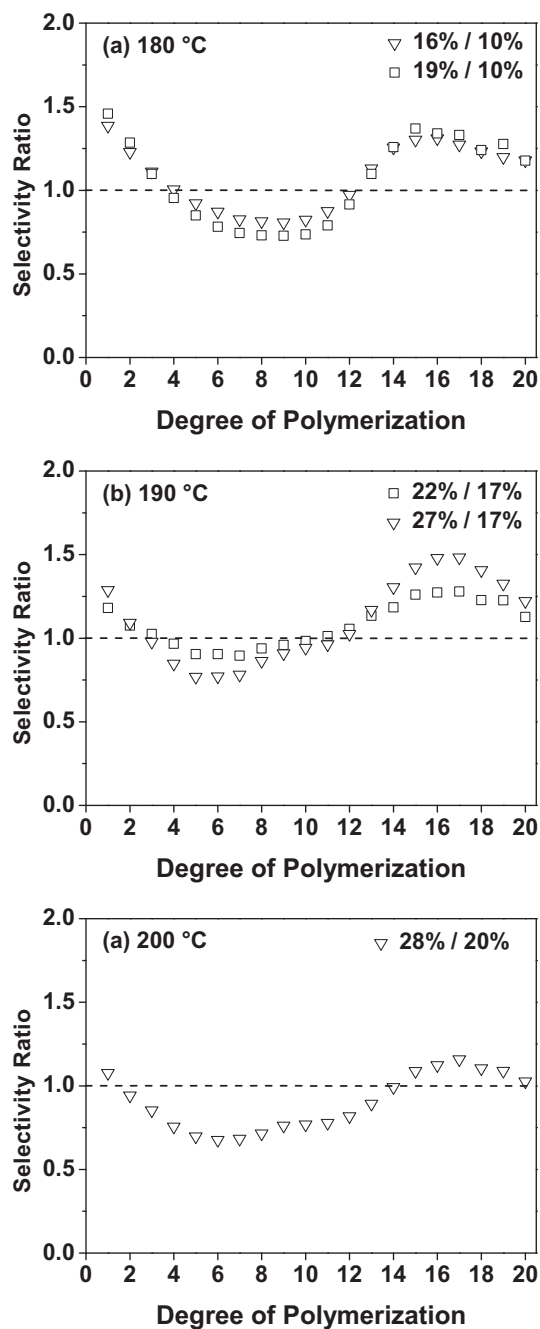


Figure 7-4: Evolution of primary liquid products of amorphous cellulose during hydrolysis in HCW at 180 – 200 °C, 10 MPa. (a) 180 °C; (b) 190 °C; (c) 200 °C



For microcrystalline cellulose, since the cleavage of accessible glycosidic bonds proceeds randomly on the surface of reacting cellulose particle during hydrolysis in HCW as we found in chapter 5, one would expect that the glucose oligomers of low DPs (e.g., 1–14 at 230 °C) should also increase at higher conversion. However, the data in Figure 7-5 show that the selectivities of those low-DP glucose oligomers actually decrease with conversion to be less than 1. Therefore, there should be other mechanisms which induce in situ changes in the structure of the reacting crystalline cellulose residue, leading to less production of those low-DP glucose oligomers. One possibility is the parallel degradation reactions during cellulose hydrolysis in HCW. Based on our study in chapter 5, parallel degradation reactions are known to occur randomly on the surface of reacting cellulose particles, albeit to much less extent in comparison to the hydrolysis reactions to produce glucose oligomers. The other possibility is the parallel cross-linking reactions<sup>225,226</sup> which condense the chain structure and lead to less production of glucose oligomers. Figure 7-5b and 7-5c show that the primary liquid products at different conversions for 250 and 270 °C have the similar trends as those for 230 °C. However, at 270 °C, the selectivity ratios of almost all glucose oligomers at higher conversions are less than 1. Although higher reaction temperature increases the cleavage of hydrogen bonding, hence increasing the accessibility of glycosidic bonds, the selectivities of high-DP glucose oligomers at 270 °C do not increase significantly, as observed at lower temperatures. It seems that the formation of glucose oligomers from reacting cellulose particle is strongly affected by the competing mechanisms for dynamic structural evolution, i.e., increasing formation of glucose oligomers due to cleavage of hydrogen bonds and decreasing formation of glucose oligomers because of degradation and cross-linking reactions. The influence of cross-linking reactions becomes dominant with increasing reaction temperature, which leads to structural condensation. Indeed, such structural condensation results in a reduction in specific reactivity at high conversions at 270 °C as shown in Figure 7-3.

Therefore, the significant variations in the compositions of the primary liquid products with conversion suggest that structural changes have taken place within the reacting cellulose as hydrolysis progresses. At least two possible mechanisms may be responsible for such structural changes. One is the intrinsic heterogeneity of cellulose which leads to the selective consumption of reactive amorphous portion at early

conversions. This is particularly apparent at low temperatures (e.g., 180–200 °C for amorphous cellulose and 230 °C for microcrystalline cellulose). The other is as results of various parallel reactions, including hydrogen bond cleavage, degradation reactions, and cross-linking reactions in HCW, which induce in situ structural changes within the reacting cellulose dynamically.

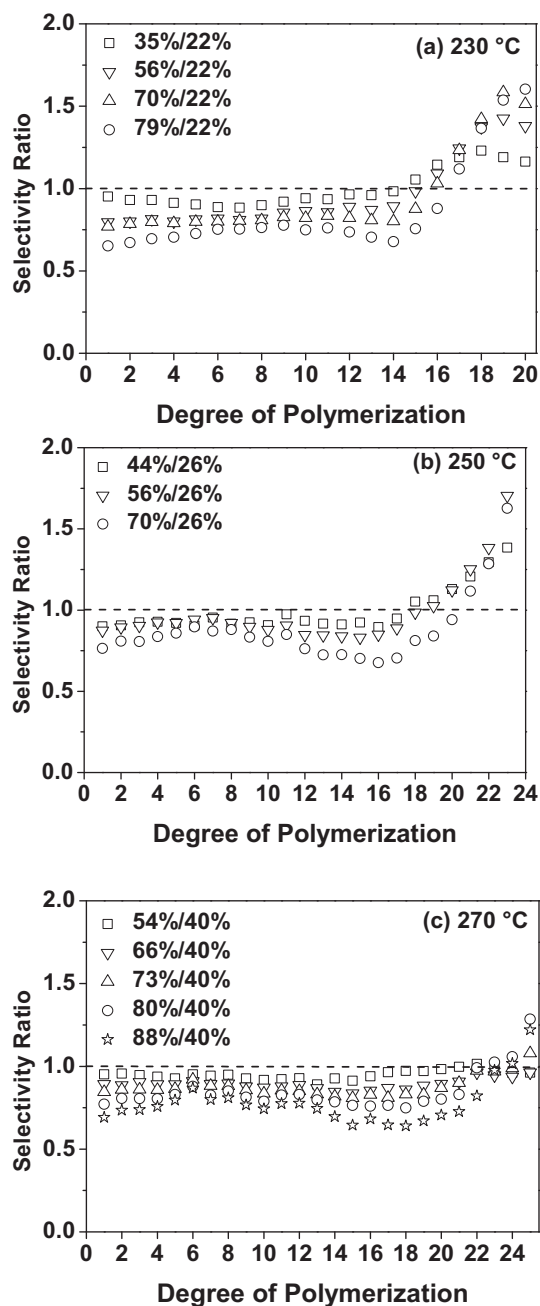


Figure 7-5: Evolution of primary liquid products of microcrystalline cellulose during hydrolysis in HCW at 230 – 270 °C, 10 MPa. (a) 230 °C; (b) 250 °C; (c) 270 °C

## 7.5 Effect of in Situ Pretreatment on the Evolution of Specific Reactivity and Primary Liquid Products with Conversion

### 7.5.1 Pretreatment of Amorphous Cellulose

An additional set of novel two-step experiments were then carried out to investigate the structural evolution during cellulose hydrolysis in HCW. The results are shown in Figures 7-6 and 7-7 for amorphous and microcrystalline cellulose, respectively. Figure 7-6 indicates that pretreatment of the amorphous cellulose at higher temperatures (190 and 200 °C) has little effect on the cellulose specific reactivity, considering the overall cellulose conversion including the pretreatment step at higher temperatures and the subsequent hydrolysis step at 180 °C. However, Figure 7-7 indicates that the pretreatment does have an effect on the glucose oligomers in the primary liquid products produced at the same overall conversion. It can be seen that pretreatment increases the selectivities of lower-DP glucose oligomers but decreases the selectivities of high-DP glucose oligomers in the primary liquid products at 180 °C. This may also be explained by the different thermochemical process which the amorphous cellulose experienced. The structure of amorphous cellulose is very reactive and is therefore prone to be influenced by pretreatment in HCW. It seems that, on the one hand, the pretreatment at 190 and 200 °C enhances the hydrogen bond weakening in the amorphous structure; therefore the selectivity of low-DP glucose oligomers is increased. On the other hand, the pretreatment at higher temperatures (e.g., 200 °C) also induced more degradation reactions of the chain segments within amorphous cellulose so that, during the subsequent hydrolysis of the pretreated cellulose at 180 °C, there are apparent reductions in the production of high-DP glucose oligomers in the primary liquid products. There is little change in the specific reactivity of amorphous cellulose as cross-linking reaction are not expected to take place at such a low temperature.

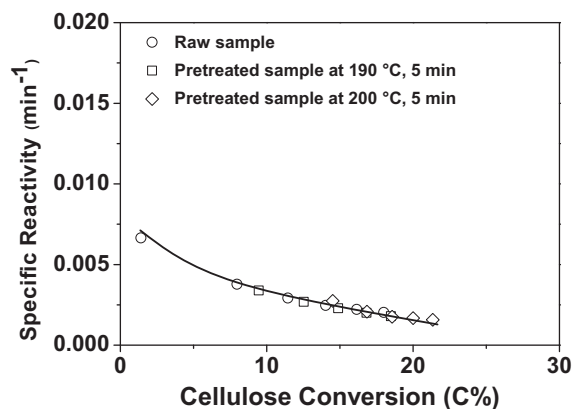


Figure 7-6: Effect of in situ pretreatment of amorphous cellulose at 190 and 200 °C on the evolution of specific reactivity during hydrolysis in HCW at 180 °C, 10 MPa

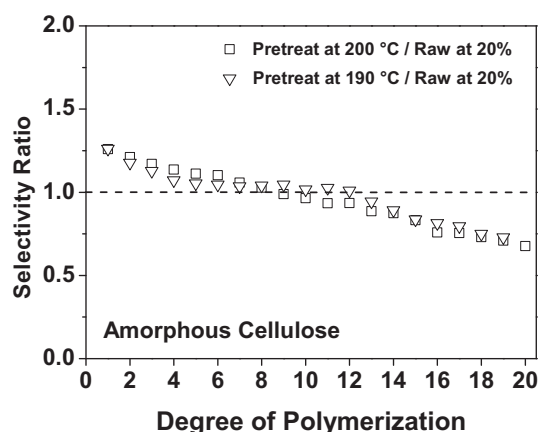


Figure 7-7: Effect of in situ pretreatment of amorphous cellulose at 190 and 200 °C on the evolution of primary liquid product during hydrolysis in HCW at 180 °C, 10 MPa

### 7.5.2 Pretreatment of Microcrystalline Cellulose

For crystalline cellulose, pretreatment at higher temperatures (250 and 270 °C) clearly has effect on the specific reactivity during the subsequent hydrolysis of the sample at 230 °C. Generally, as shown in Figure 7-8, pretreatment leads to a decrease in specific reactivity and such decrease becomes more significant at higher pretreatment temperatures (i.e., 270 °C). It is also clearly shown that at the same pretreatment temperature (i.e., 270 °C in Figure 7-9b), in comparison to a pretreatment time of 5 min, a longer pretreatment time of 10 min leads to a more significant decrease in specific reactivity of the crystalline cellulose. Accordingly, as

shown in Figure 7-9, pretreatment also leads to a decrease in the selectivities of glucose oligomers in primary liquid products to be less than 1 during the subsequent hydrolysis of the pretreated samples at 230 °C. Such a decrease becomes more significant when the pretreatment temperature increases from 250 to 270 °C. Therefore, the data in Figures 7-8 and 7-9 are in consistent with the discussion in the previous section and clearly demonstrate the significant influence of cross-linking reactions on the structure of reacting cellulose at 270 °C. Such cross-linking reactions lead to structural condensation, hence a significant reduction in specific reactivity of the pretreated sample and selectivities of glucose oligomers in the primary products during subsequent hydrolysis at 230 °C. Figure 7-9 also shows the clear evidence for the enhanced cleavage of hydrogen bonds during pretreatment as the selectivities of high-DP glucose oligomers do increase with DP, although the selectivity ratios of those glucose oligomers are  $<1$  due to the dominant effect of cross-linking reactions.

Additionally, it is interesting to note in Figure 7-8 that, during the subsequent hydrolysis at 230 °C, the specific reactivity of the pretreated samples actually increases with conversion. Accordingly, right after pretreatment, there is a significant change in the selectivities of glucose oligomers in the primary liquid products at the initial conversions during the subsequent hydrolysis of the pretreated samples. However, as conversion increases, the effect of pretreatment on the selectivity of glucose oligomers becomes much less and the selectivities of glucose oligomers become more similar to those from the hydrolysis of the raw sample. The results suggest that the effect of pretreatment seems to be limited to the outer layers of the reacting particles. It seems that the interactions between HCW and the sample did not penetrate throughout the reacting particle during pretreatment, possibly due to the short period of pretreatment time.

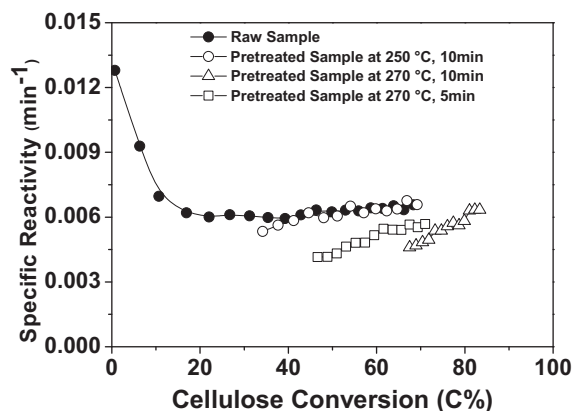


Figure 7-8: Effect of in situ pretreatment of microcrystalline cellulose at 250 and 270 °C on the evolution of specific reactivity during hydrolysis in HCW at 230 °C, 10 MPa

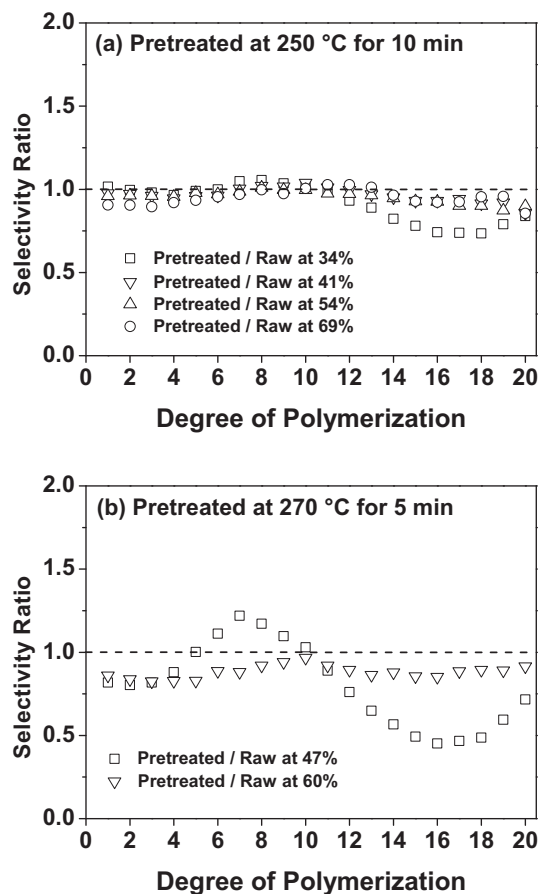


Figure 7-9: Effect of in situ pretreatment of microcrystalline cellulose on the evolution of primary liquid products during the subsequent hydrolysis in HCW at 230 °C, 10 MPa. (a) 250 °C for 10 min; (b) 270 °C for 5 min

Another experiment was then conducted to pretreat the raw cellulose for a long period (4 h) at a suitable low temperature (200 °C) and then in situ heat the pretreated sample to 230 °C for continuous hydrolysis reactions in HCW. The specific reactivity and primary liquid products were compared with those at 230 °C for raw cellulose sample in Figures 7-10 and 7-11. Despite a prolonged pretreatment at 200 °C (4 h), there is little change in the specific reactivity of the pretreated sample initially. However, after reaction at 230 °C for 3 hours, the pretreated sample actually exhibits a higher specific reactivity. The primary liquid products right after pretreatment showed a slight increase of the selectivities for low-DP glucose oligomers. With reaction proceeding further at 230 °C, the primary liquid products are almost the same as those for raw samples, until the conversion is higher than 55%. The selectivities of low-DP glucose oligomers start to decrease with conversion at higher conversions. The data in Figures 7-10 and 7-11 suggest that the cross-linking reactions are minimized as there is no reduction in the specific reactivity of the pretreated sample at 200 °C during the second step hydrolysis at 230 °C. Changes in hydrogen bonding and degradation reactions play more important roles. The slight increase of the selectivities of low-DP glucose oligomers for the in situ pretreated sample is likely due to the weakening and/or cleavage of hydrogen bonds within cellulose at 200 °C. The weakening and cleavage of hydrogen bonds seems to be mild because there is little increase in the selectivities of high-DP glucose oligomers.

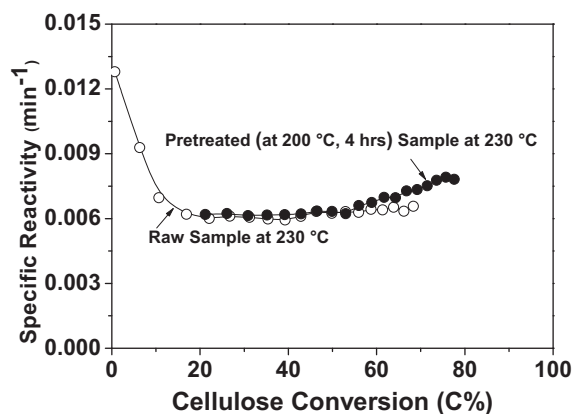


Figure 7-10: Effect of in situ pretreatment of microcrystalline cellulose at 200 °C for 4 hours on the evolution of specific reactivity during hydrolysis in HCW at 230 °C, 10 MPa

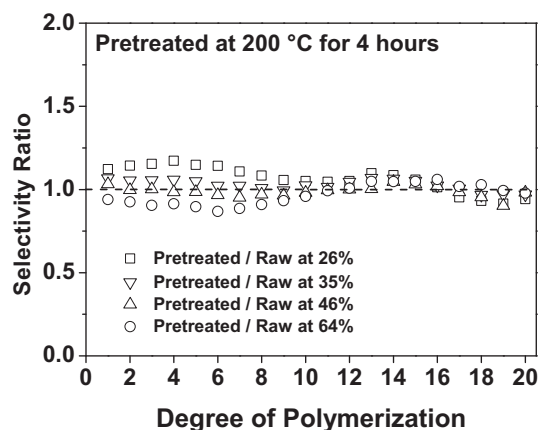


Figure 7-11: Effect of in situ pretreatment of microcrystalline cellulose at 200 °C for 4 hours on the evolution of primary liquid products during the subsequent hydrolysis in HCW at 230 °C, 10 MPa

At higher conversions, the pretreated sample shows an increase in specific reactivity but not in the selectivities of glucose oligomers. This suggests that the increase in specific reactivity at 230 °C results from the formation of nonsugar products. It is possible that as a result of prolonged reactions (it took another 70 min for the in situ pretreated sample to achieve 50% conversion), degradation reactions on the surface of reacting cellulose particles become more severe, leading to a slight increase in the formation of nonsugar products. Such a hypothesis is plausible because, even for the raw cellulose, there is also a slight increase (but less compared to the pretreated sample) in specific reactivity at conversions >55% (it takes 120 min for the raw cellulose to achieve 55% conversion), as shown in Figure 7-10. Another possibility is that the long time of pretreatment partially changes the structure of glucose chains as a result of parallel degradation reactions. Such changes lead to the formation of some partially pyrolyzed residues and hence nonsugar products.

## 7.6 Conclusions

The specific reactivity and primary liquid products dynamically evolve during the course of cellulose hydrolysis in HCW at 10 MPa and 180–270 °C, suggesting the evolution of cellulose structure during conversion. The intrinsic heterogeneity of cellulose results in the selective consumption of reactive components at early conversions at low temperatures, e.g., 180–200 °C for amorphous cellulose and 230



°C for microcrystalline cellulose. Various parallel reactions, including hydrogen bond cleavage, degradation reactions, and cross-linking reactions, also contribute to the cellulose structure evolution during hydrolysis in HCW. While enhanced hydrogen bond cleavage increases the production of glucose oligomers, degradation reactions and cross-linking reactions have the opposite effect. The effect of cross-linking reactions becomes dominant at 270 °C, resulting in a structural condensation which significantly reduces both the specific reactivity of cellulose and the selectivities of glucose oligomers in the primary liquid products.

## CHAPTER 8 EFFECT OF BALL MILLING ON THE HYDROLYSIS OF MICROCRYSTALLINE CELLULOSE

### 8.1 Introduction

Hydrolysis in HCW is an attractive way to recover sugars from cellulose or biomass,<sup>32,34,35,44,50-58,60,61,144</sup> although the mechanisms of cellulose hydrolysis in HCW are still not fully understood. The fundamental studies in Chapters 4-7 made progress to provide some new insight into the reaction mechanisms of cellulose hydrolysis in HCW. A new sampling and analytical method has been established to analyse glucose oligomers in the liquid products using a HPAEC-PAD in Chapter 4. The fresh liquid products must be analysed immediately after collection to avoid precipitation. In Chapter 5, reaction conditions were also optimised to separate the primary hydrolysis reactions on the reacting cellulose particle surface from the secondary reactions in the aqueous phase. Cleavage of hydrogen bonds becomes fast at high temperatures hence increasing the accessibility of glycosidic bonds in cellulose chain. This considerably enhances the reaction rate of hydrolysis, and alters the distribution of glucose oligomers in the primary liquid products.

Cellulose may contain both amorphous and crystalline structures, because a cellulose microfibril is generally formed by several microcrystals hinged together and surrounded by amorphous cellulose.<sup>75-78,230</sup> There are significant differences in the hydrolysis behavior of amorphous and crystalline portions within microcrystalline cellulose in HCW. As we found in Chapter 6, for the amorphous portion, as hydrogen bonds are weak, the hydrolysis reactions are limited by the cleavage of glycosidic bonds which commence at ~150 °C. The crystalline portion has a network of strong intra- and inter-molecular hydrogen bonds<sup>79,80</sup> which limit the accessibility of glycosidic bonds within the chain and hydrolysis reactions commence at ~180 °C.

Therefore, converting crystalline cellulose into amorphous cellulose can be a good strategy to substantially increase cellulose hydrolysis reactivity so a reactor can be operated under mild reaction conditions to greatly reduce the degradation of sugar products.

Amorphous cellulose usually can be prepared from microcrystalline cellulose by ball milling of crystalline cellulose.<sup>74,231</sup> The crystallinity of cellulose decreases with milling time, suggesting that the hydrogen bonds in crystalline cellulose can be weakened substantially and converted to amorphous cellulose. Zhao et al.<sup>231</sup> reported the dilute acid hydrolysis of cellulose samples by ball milling, and found that the glucose yield increased with ball milling time.

In this chapter, the key objective is to investigate the behavior of ball milled cellulose during hydrolysis in HCW. The effect of ball milling on the structure of cellulose was first investigated, followed by the behavior of ball milled cellulose during hydrolysis in HCW. Finally, the primary liquid products obtained from ball milled cellulose were characterised and compared to understand the effects of structural changes during ball milling on the formation of glucose oligomers.

## **8.1 Changes in Cellulose Structure due to Ball Milling**

### **8.1.1 Change in Particle Size Distribution**

Figure 8-1 presents the particle size distributions of the raw and ball milled cellulose samples. Under normal conditions, a 1 h ball milling of the raw cellulose sample results in a significant reduction in the particle size distribution of the cellulose sample. Further increasing ball milling time from 1 to 7 h does not lead to further size reduction, indicating that long ball milling is ineffective in reducing cellulose particle size. It is interesting to note that there is actually a slight increase in particle size, which is due to the agglomeration of fine particles as results of extensive ball milling.

### 8.1.2 Change in X-ray Diffraction Pattern

Figure 8-2 presents the X-ray diffraction patterns of the raw and ball milled cellulose samples. The crystalline peak decreases with increasing ball milling time. Further estimations of the relative crystallinity index for all samples were carried out using Segal's method.<sup>218</sup> Indeed as shown in Table 8-1, the relative crystallinity index of cellulose reduces substantially from 0.79 for the raw sample, to 0.58 for the 1 h ball-milled sample then to 0.38 for 4 h ball-milled sample. After 7 h ball-milling time, the crystalline peak disappears totally, indicating all crystalline cellulose structures are transformed into amorphous cellulose structure. The results in Figures 8-1 and 8-2 are consistent with those in the literature that mechanical ball milling of microcrystalline cellulose decreases particle size, reduces the DP of cellulose and increases the amorphous content of cellulose.<sup>19,74,231</sup> Clearly, the transformation of microcrystalline cellulose into amorphous cellulose suggests that ball milling have significantly weakened the hydrogen bonding networks within microcrystalline cellulose. Such changes are expected to have great influences on cellulose hydrolysis in HCW.

Table 8-1: The relative crystallinity index for raw and ball milled samples

samples	raw	normal ball milled			cryogenic ball milled for 2 min
		1hr	4hr	7hr	
relative crystallinity index	0.79	0.58	0.38	-	0.78

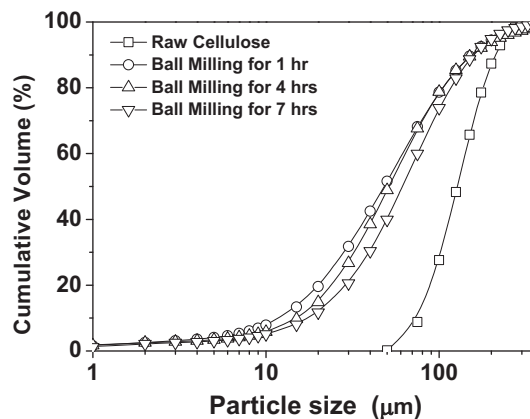


Figure 8-1: Particle size distributions of various cellulose samples

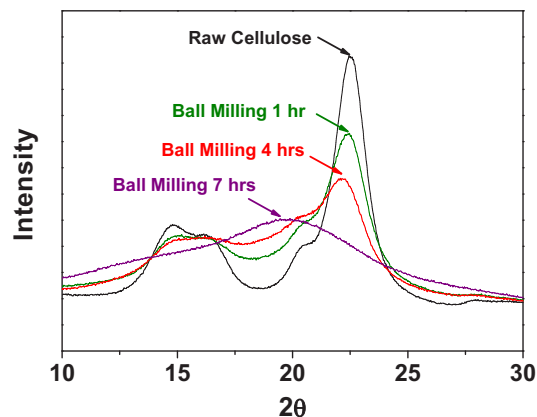


Figure 8-2: X-ray diffraction patterns of various cellulose samples

## 8.2 Effect of Ball Milling on the Evolution of Specific Reactivity of Cellulose during Hydrolysis in HCW.

### 8.2.1 Cellulose Conversion

The conversion vs time of cellulose hydrolysis in HCW at 230 °C are shown in Figure 8-3. As expected, ball milling increases the reaction rate of cellulose hydrolysis in HCW significantly. For example, while the hydrolysis of the raw sample for 2 h only achieves ~56% conversion, the 7 h ball milled sample after achieves ~80% conversion for only 1 h. This can be attributed to the changes in cellulose structure. For example, the significant weakening of hydrogen bond network during ball milling would make the microcrystalline cellulose more accessible.

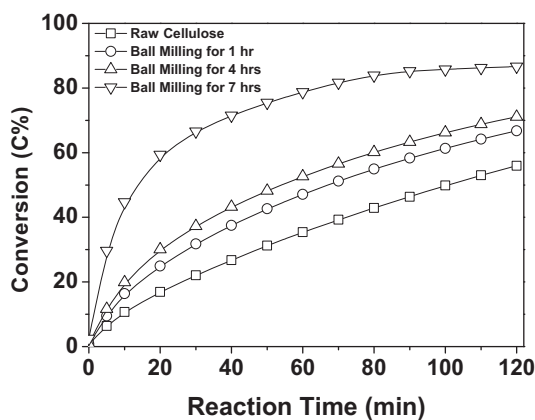


Figure 8-3: Conversions vs time of various cellulose samples during hydrolysis in HCW at 230 °C

### 8.2.2 Evolution of Specific Reactivity

The specific reactivity of various cellulose samples during hydrolysis in HCW at 230 °C is therefore plotted in Figure 8-4, from which three important observations can be made. Firstly, the specific reactivity curves of the raw cellulose and the samples after ball milling for 1 and 4 h have the same pattern, i.e. a continuous decrease till a certain conversion level  $X_c$  then levels off with further increasing conversion. The value of  $X_c$  increases with ball milling time, i.e. ~20%, ~40% and 55% for the raw cellulose and the samples after 1 and 4 h ball milling, respectively. The conversion  $X_c$  seems to be related to the sample's relative crystallinity index which partially reflects the content of crystalline portion within the cellulose samples. For amorphous cellulose, the initial hydrolysis is mainly contributed by the reactions of amorphous cellulose and a small portion of crystalline cellulose as the hydrolysis of crystalline cellulose commences at ~180 °C, based on our study in Chapter 6. Secondly, it is noteworthy that the sample after 7 h ball milling shows continuous decrease in specific reactivity with conversion, as results of its complete amorphous nature. This in turn suggests that the structure of the amorphous cellulose itself is highly heterogeneous, and as reaction progresses the remaining cellulose becomes less and less reactive. Thirdly, at the same conversion, the specific reactivity of cellulose after ball milling increases significantly with increasing ball milling time. For example, at early conversions, the specific reactivity of the 4 h ball-milled sample is twice as that of the raw sample. At higher conversions, such difference in reactivity becomes smaller because the remaining cellulose residue becomes more crystalline as hydrolysis reaction proceeds.

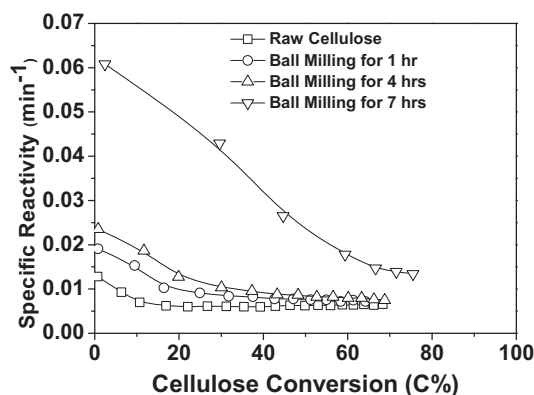


Figure 8-4: Specific reactivities of various cellulose samples during hydrolysis in HCW at 230 °C

### 8.3 Dominant Role of Crystallinity in Cellulose Reactivity during Cellulose Hydrolysis in HCW

The data in Figures 8-3 and 8-4 clearly show that mechanical ball milling is an effective method to substantially increase the specific reactivity of microcrystalline cellulose during hydrolysis in HCW. Fundamentally, this may be due to two key mechanisms. One is the structural changes due to ball milling, e.g. the destruction of hydrogen bonding networks within and the reduction of DP of the microcrystalline cellulose. The other is the substantial decrease in the cellulose particle size. However, it is still unclear which of the two mechanisms (or if both) play a dominant role in enhancing cellulose reactivity.

To clarify this important point, a new experimental method is required to separate the effect of two mechanisms. This was achieved by cryogenic ball milling of the raw cellulose at a short time of 2 min and the results are presented in Figure 8-5. Indeed, after a short milling of 2 min under cryogenic conditions, the particle size of the milled sample was reduced substantially to be even smaller than the sample which was prepared after 4 h ball milling under normal milling conditions (see Figure 8-5a). However, it is interesting to see that the cellulose sample after 2 min cryogenic ball milling has a similar crystalline pattern (see Figure 8-5b) as the raw cellulose. In fact, the relative crystallinity indices of the raw and cryogenic ball-milled samples are similar (see Table 8-1). Therefore, as shown in Figures 8-5c and 8-5d, a 2-min cryogenic ball milling leads to only a slight increase in conversion as a function of reaction time and a slight increase in the specific reactivity as a function of conversion. The data in Figure 8-5 clearly demonstrate that particle size plays only a minor role in the reaction of cellulose hydrolysis in HCW under the current condition. As the significant reduction in particle size also leads to a reduction in DP,<sup>74,231</sup> the data in Figure 8-5 also clearly suggest that any such reduction in the DP of the cellulose after 2-min cryogenic ball milling plays a minor role in cellulose reactivity during hydrolysis in HCW. Therefore, the cellulose reactivity is dominantly controlled by the cellulose's crystallinity which is an indication of the presence of strong hydrogen bonding networks. In Chapter 5, it can be known that a strong hydrogen bonding network limits the accessibility of the glycosidic bonds (by HCW) in the glucose chains within the crystalline structure. The dominant role of

crystallinity in cellulose reactivity in HCW is also clearly supported by the data in Figures 8-(1-4). It can be seen that under normal ball milling conditions, further ball milling from 1 to 7 h leads to little further reduction in particle size but significant increase in the relative crystallinity and hence the specific reactivity of cellulose sample. The minor role of particle size in the conversion and specific reactivity of cellulose during hydrolysis also clearly suggests that a shrinking-core model, which was often used for describing the reaction kinetics of cellulose hydrolysis in supercritical water,<sup>34</sup> is not applicable for modelling the overall hydrolysis reaction kinetics under conditions in this study.

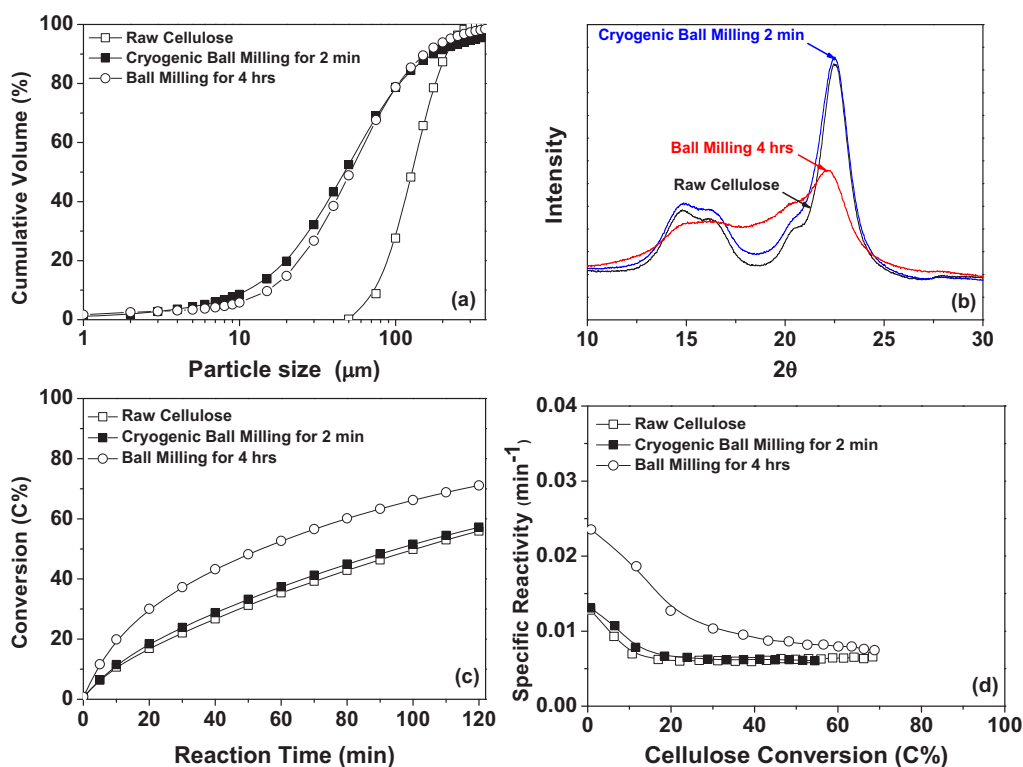


Figure 8-5: Comparisons of cryogenic ball milled sample with raw and 4 hr ball milled samples. (a) particle size distribution; (b) X-ray diffraction pattern; (c) conversion vs time; (d) specific reactivity



## 8.4 Comparisons between the Primary Liquid Products Produced from the Raw and Ball-Milled Cellulose during Hydrolysis in HCW

### 8.4.1 Comparisons of IC Chromatograms

To further understand the effect of structure change during ball milling on the formation of glucose oligomers during cellulose hydrolysis in HCW, the primary liquid products were collected from the hydrolysis of the raw and ball-milled cellulose samples at the same conversion level. The fresh liquid samples were analysed by HPAEC-PAD immediately after collection, following the methodology described in Chapter 4.

First of all, the primary liquid products between the raw cellulose and the cryogenic ball-milled sample were compared to understand the effect of particle size on the primary hydrolysis reactions occurred on the surface of cellulose. As shown in Figure 8-6, the IC chromatograms of primary liquid products collected at 30% conversion from the two samples are very similar and the maximal DP of glucose oligomers in the primary liquid products are also same (20 for both samples). This is expected because the cryogenic ball milling has little effect on the crystallinity (i.e., the hydrogen bonding networks) of the microcrystalline cellulose. However, for the samples prepared after prolonged ball milling under normal milling conditions (See Figure 8-7), there are significant differences in the IC chromatograms of the primary liquid products. The maximal DP of glucose oligomers in the primary liquid products increases with ball milling time, from 20 for the raw sample, to 22 for the ball milled 4 h sample, then to 28 for the ball milled 7 h sample. The data in Figure 8-7 are further evidence suggesting that the hydrogen bonds in crystalline glucose chains were substantially weakened and/or broken and cellulose becomes more disordered during the prolonged ball milling under normal conditions. It is also known that mechanical ball milling of microcrystalline cellulose decreases the DP of the glucose chains within the cellulose.<sup>74</sup> As results, the cellulose becomes more amorphous and the glucose chains are therefore more accessible by HCW during hydrolysis under the same condition, leading to an increase in the maximal DP of glucose oligomers in the primary liquid products. Figure 8-7 also shows that the concentrations of each glucose oligomer increase with ball milling time, such an observation is in consistence with the increase in cellulose reactivity (see Figure 8-4).

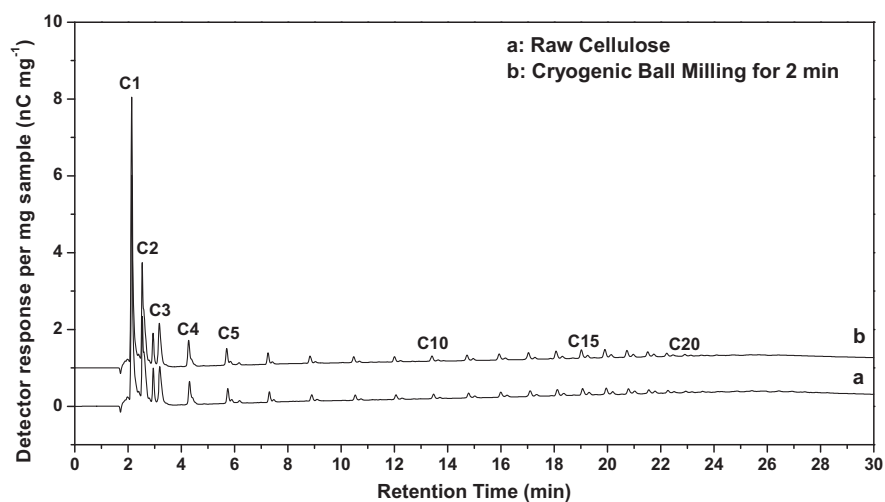


Figure 8-6: IC chromatograms of primary liquid products from raw and cryogenic ball milled samples at 30% conversion during hydrolysis in HCW at 230 °C

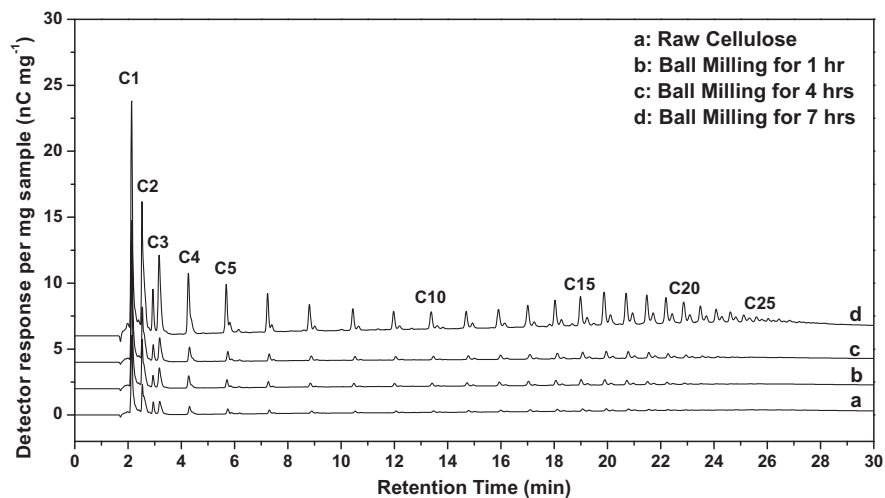


Figure 8-7: IC chromatograms of primary liquid products from raw and ball milled samples at 30% conversion during hydrolysis in HCW at 230 °C

### 8.4.2 Comparisons of Selectivities of Glucose Oligomers in the Primary Liquid Products

To understand the effect of ball milling on the distribution of glucose oligomers in the primary liquid products, further study was then conducted to compare the selectivities of glucose oligomers in the primary products of the raw cellulose and various ball-milled samples, based on a method developed in Chapter 5. The primary

liquid products at three different conversions (15%, 30% and 60%) were collected. For the 7 h ball-milled sample, only two liquid samples at 30% and 60% conversions were collected because it was difficult to collect the liquid sample at 15% conversion as results of fast reaction rate. The selectivity ratios of glucose oligomers from ball-milled samples and the raw sample are compared in Figure 8-8.

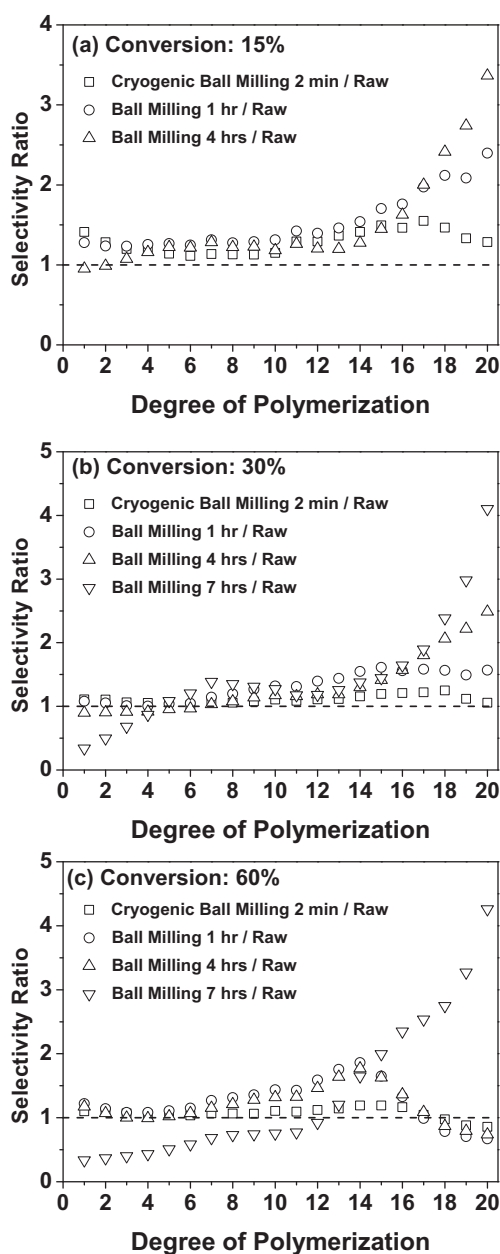


Figure 8-8: Selectivity ratios of glucose oligomers in the primary liquid products from various cellulose samples during hydrolysis in HCW at 230 °C. (a) at conversion of 15%; (b) at conversion of 30%; (c) at conversion of 60%

As shown in Figure 8-8, a 2-min cryogenic ball milling actually results in some changes in the distribution of glucose oligomers in the primary liquid products, although it leads to only slight changes in the specific reactivity (see Figure 8-5). At a low conversion (15%), the glucose oligomers have higher selectivities than those for the raw samples and the selectivity ratios for all the glucose oligomers are larger than 1. This indicates that the overall reactions favour more the production of various glucose oligomers via hydrolysis rather than the production of the sugar derivatives via degradation reactions. This is an interesting observation as it points to a way to use cryogenic milling to improve the selectivity of sugar products during hydrolysis. As discussed, the cellulose reactivity is dominantly controlled by the cellulose's crystallinity. The raw and cryogenic-ball-milled samples have similar crystallinity, i.e. similar accessibility of glucosidic bonds of the glucose chains. It is known that the significant reduction in particle size also leads to a reduction in DP.<sup>74,231</sup> Although the crystallinity is similar in comparison to the cryogenic-ball-milled the sample, the glucose chains exposing on the surface of the reacting raw cellulose is longer, leading to increased possibilities for degradation reactions therefore more sugar derivatives being produced in the primary liquid products.

At higher conversions (30% and 60%), the selectivities of the glucose oligomers of cryogenic milled sample becomes similar to those of the raw cellulose. This is mainly due to the fact that the amorphous portion has been removed so that the crystalline portion dominates the overall hydrolysis reactions. Additionally, it should also be noted that at all three conversions, there is an appreciably decrease in the selectivity ratio with DP of glucose oligomers from 16. This may be due to the significant reduction in particle size and the possible reduction in the length of glucose chains within the crystalline portion of the cellulose sample as results of ball milling, leading to a decrease in the selectivity ratio with DP for high-DP glucose oligomers.

Also illustrated in Figure 8-8, for the samples after 1 or 4 h ball milling under normal milling conditions, at conversions < 60%, the selectivities of most glucose oligomers are higher than those for raw sample and the selectivity ratio of glucose oligomers also generally increases with DP, apparently due to the increased amorphous

structures in these ball-milled samples. The relative crystallinity indices of the 1 h and 4 h ball-milled samples are 58% and 38%, respectively (see Table 8-1). Therefore, at conversions < 60%, these samples mainly involve the hydrolysis of the amorphous portions. At 60% conversion, the crystalline portions would start to dominate the hydrolysis reactions for both 1 h and 4 h ball-milled samples. Therefore, a reduction in the selectivity of the high-DP glucose oligomers is shown in Figure 8-8, due to probably the same reasons as discussed for the cryogenic ball-milled sample.

Figure 8-8 also shows that for the 7 h ball-milled sample, the selectivity ratio always increases with DP. The selectivity ratios for high-DP glucose oligomers are significantly higher than 1. Table 8-1 shows that due to prolonged milling the sample is completely amorphous and there is no crystalline portion remaining in the sample. Therefore, in comparison to the raw cellulose, the hydrogen bonding networks within the 7 h ball-milled sample would be destroyed considerably and the length of the glucose chains would also be shorter, leading to the production of more high-DP glucose oligomers (see Figure 8-7). In addition, the short glucose chains would also be more easily and quickly removed during hydrolysis in HCW, reducing the probability of those chains to be further hydrolysed to produce lower-DP glucose oligomers. This is indeed shown in Figure 8-8 where the selectivities of those glucose oligomers are actually less than 1 and the effect is more significant at a high conversion (i.e. 60%).

### 8.5 Further Discussion on Mechanisms of Cellulose Hydrolysis in HCW

The above data and discussion lead to important knowledge on the mechanisms of cellulose hydrolysis in HCW. First of all, the maximal DP of the glucose oligomers in the primary liquid products is determined by the longest length of glucose chain within the cellulose, which is accessible by HCW. Weakening and destruction of the hydrogen bonding networks by ball milling can significantly increase the accessibility of long glucose chains in microcrystalline cellulose. The study in Chapter 5 showed that the maximal DP of glucose oligomers in the primary liquid products for the raw sample increases with temperature, from 23 at 230 °C to 28 at 270 °C. However, for the 7 h ball-milled cellulose sample in this study, the maximal

DP of glucose oligomers in the primary liquid product is 28 even at 230 °C. This further proves that the increase in the maximal DP with reaction temperature during the hydrolysis of microcrystalline cellulose is indeed due to increased accessibility of longer glucose chains as results of faster breaking of hydrogen bonds at higher temperatures. Secondly, the distribution of glucose oligomers in the primary liquid products is significantly influenced by the distribution of accessible glucose chains of various lengths. Such distributions are determined by key properties of cellulose, particularly hydrogen bonding pattern, length of chain segments, crystallinity and DP. Thirdly, the reaction rate of microcrystalline cellulose during hydrolysis in HCW is also determined by the accessibility of chain segments within the microcrystalline cellulose. An increase in reaction temperature can significantly increase the reaction rate as the crystalline cellulose becomes more accessible due to the faster breaking of hydrogen bonds at elevated temperatures. Ball milling also increases the reaction rate since ball milling significantly weakens or even destroys the hydrogen bonding networks within the microcrystalline cellulose. A reduction in particle size (e.g., via a 2-min cryogenic ball milling) only leads to a minor increase in the reaction rate, because the overall accessibility of glucose chain segments does not improve.

Therefore, the pattern of hydrogen bonding networks within microcrystalline cellulose plays an essential role in the hydrolysis behavior in HCW. There are at least two pretreatment methods which may be used to weaken and/or destroy the hydrogen bonds within microcrystalline cellulose. One is to pretreat the cellulose at high temperatures, which may lead to the crystalline-to-amorphous transformation of cellulose, as reported previously in HCW at ~300 °C.<sup>123</sup> The other is to pretreat the cellulose via ball milling. From the viewpoint of maximising sugar production, a low-temperature pretreatment condition is preferred in order to minimize the degradation of sugar products. Therefore, ball milling seems to be a good strategy for improving cellulose hydrolysis reactivity although energy consumption during ball milling should also be considered. Future studies are required to develop the efficient, effective and cheap pretreatment methods to break the hydrogen bonding networks within microcrystalline cellulose.

## 8.6 Conclusions

This study investigated the effect of ball milling as a pretreatment method on microcrystalline cellulose hydrolysis in HCW. The structural changes of microcrystalline cellulose after ball milling, as well as their liquid products during hydrolysis in HCW at different conversions, were characterised, respectively. After ball milling, the particle size distribution of cellulose sample shows a considerable reduction compared to that of raw sample, and the crystallinity of ball milled sample decreases significantly with ball milling time. It was also found that the specific reactivity of ball milled cellulose samples during hydrolysis in HCW increases with ball milling, mainly due to the structure changes during ball milling to make the microcrystalline cellulose more accessible, including the reduction in particle size, and the decrease in crystallinity due to the breaking of hydrogen bonding networks within microcrystalline cellulose, etc.

Further experiments using a cellulose sample with considerable reduction in particle size but little change in crystallinity by cryogenic ball milling for 2 min, indicate that particle size is not the limiting factor during hydrolysis of microcrystalline cellulose in HCW, because the specific reactivity only slightly increases after cryogenic ball milling. Therefore, the crystallinity of cellulose is likely to play an essential role in the hydrolysis behavior in HCW, due to the more accessible of microcrystalline cellulose samples with smaller crystallinity.

The liquid product analysis by HPAEC-PAD indicates that the distribution of glucose oligomer in the primary liquid products is affected by cellulose particle size, although the specific reactivity only slightly increases with particle size. The selectivities of glucose oligomers all increase when reducing the particle size, but the selectivity ratios of high-DP glucose oligomers decrease with DP, when comparing the cryogenic ball milled sample with raw sample at the same conversion. While for long time ball milled sample, the selectivity of glucose oligomers all increase at low conversions. At high conversion, the ball milled samples for 1 h and 4 h show the similar trend as those for cryogenic ball milled samples, because particle size starts to play an important role on glucose oligomer formation since cellulose samples become more crystalline at higher conversion. Further increasing the ball milling

time will completely destroy the crystalline cellulose, leading to the significant increasing formation of high-DP glucose oligomers.



## CHAPTER 9 CONCLUSIONS AND RECOMMENDATIONS

### 9.1 Introduction

This chapter concludes the present study by highlighting the main research findings. The present research has improved the present status of knowledge on cellulose hydrolysis in HCW. The development of a sampling and analytical method makes it possible to characterise the glucose oligomers in the liquid products and understand the formation of precipitate in the liquid products. The primary liquid products of cellulose hydrolysis in HCW, which were firstly reported in this field, are of great importance to elucidate the primary hydrolysis reactions of cellulose hydrolysis in HCW. The structural differences between amorphous and crystalline cellulose, as well as the evolution of structural changes with conversion during hydrolysis in HCW were also revealed. This study further estimated the effect of ball milling on the improvement in the performance of cellulose hydrolysis in HCW. The conclusions and evaluations of the present research have also led to some recommendations for future study in this area of research.

### 9.2 Conclusions

#### 9.2.1 Characteristics and Precipitation of Glucose Oligomers in the Fresh Liquid Products

- A high performance anion exchange chromatography with pulsed amperometric detection (HPAEC-PAD) was employed to determine the distribution of the glucose oligomers in liquid products collected from the hydrolysis of cellulose in HCW using a semi-continuous reactor system. The fresh liquid products were collected from the experiments and analyzed immediately. The HPAEC-PAD

chromatogram clearly demonstrates the presence of a wide range of glucose oligomers (with DPs up to 30) and their derivatives.

- Due to their low concentrations, none of those glucose oligomers in the fresh liquid products could be detected by a HPLC-ELSD. HPLC-ELSD was able to detect glucose oligomers with DPs up to 6 in the liquid solutions after being concentrated by 25 times via vacuum evaporation at 40 °C, during which a large amount of precipitate was also formed.
- Quantitative analysis was only carried out for analyzing glucose oligomers up to cellopentaose (DP = 5) as the standards for glucose oligomers with DPs > 5 are unavailable. The concentrations of glucose oligomers from glucose to cellopentaose analysed by both HPAEC-PAC and HPLC-ELSD were in good agreement, suggesting that these low-DP glucose oligomers do not contribute to the precipitate formation.
- That precipitation started as the fresh sample was collected. The precipitation was fast during the initial 8 hours but leveled off as the precipitation time increases further. The precipitation process did not complete until after 120 hours (5 days).
- The glucose oligomers with DPs > 5 and their derivatives, which are soluble in HCW but become supersaturated in the solutions at ambient solutions, are responsible for precipitate formation. The contribution of glucose oligomer to the precipitate formation clearly increases with DP as the solubility of glucose oligomer increases with decreasing DP.
- Most but not all of the glucose oligomers and their derivatives with DPs of 17 and more contribute to the precipitate formation as tiny peaks of these glucose oligomers could still be observed in the chromatograms, suggesting that these glucose oligomers have very low (but non-zero) solubilities in ambient water.

- The retentions of glucose oligomers increase substantially with the DP decreasing from 16 to 6, indicating that less percentage of lower-DP glucose oligomers contributed to the precipitate formation. The glucose oligomers from glucose (DP = 1) to cellopentaose (DP = 5) and their derivatives contribute little to the precipitate formation.
- The results indicate that the fresh liquid products from cellulose hydrolysis in HCW must be analyzed immediately after sample collection in order to avoid the effect of precipitation on oligomer analysis.

### 9.2.2 Primary Liquid Products at Various Reaction Temperatures

- Reaction temperature has a significant effect on cellulose conversion and the distribution of glucose oligomers in the primary liquid products.
- The primary hydrolysis reactions on the surface of reacting cellulose particles seem to proceed by the breaking of hydrogen bonds in the structure of microcrystalline cellulose and the random cleavage of the accessible glycosidic bonds in the cellulose, leading to the formation of glucose oligomers with a wide range of DPs.
- Thermal degradation reactions also occur randomly on the surface of cellulose particles, but to a much less extent in comparison to the primary hydrolysis reactions, leading to the production of derivative of glucose and glucose oligomers with a wide range of DPs.
- The hydrolysis reactions seem also be influenced by other parallel reactions such as the possible cross-linking reactions during hydrolysis, leading to the change of cellulose structure. The primary liquid products may further undergo secondary reactions in the aqueous phase, depending on the reaction temperature and the residence time.
- To collect primary liquid products hydrolysis, a semicontinuous reactor system is required and the reactions conditions must be optimised. The essential criteria

are: a) secondary reactions of liquid products in the aqueous phase are minimised; b) solubility of each glucose oligomer in the liquid products is not a limiting factor; and c) the interactions between liquid products and the reacting cellulose particle are minimized.

- The post hydrolysis of primary liquid products has also shown a high glucose yield of ~80% on a carbon basis, therefore the combined HCW and enzymatic hydrolysis seems to be promising to recover sugar from lignocellulose or biomass.

### 9.2.3 Different Behaviors between Amorphous and Crystalline Portions within Microcrystalline Cellulose

- This study has successfully demonstrated the significant differences in the hydrolysis behavior of the amorphous and crystalline portions within microcrystalline cellulose in HCW. Such differences are apparently due to these structural differences, such as chain length and hydrogen bonding pattern.
- Amorphous portion is much more reactive than crystalline portion within microcrystalline cellulose. Therefore, reaction of amorphous portion occurs earlier, leading to the considerable reduction of reactivity of microcrystalline cellulose in the initial stage during cellulose hydrolysis in HCW, particularly at lower temperatures less than 230 °C.
- Amorphous portion consists of various short chain segments with a wide range of chain lengths (as short as C4) and these short chain segments are possibly hinged in the microcrystalline cellulose via weak hydrogen bonds. Those short chain segments can be extracted or hydrolysed by HCW at relatively low temperatures (e.g., < 150 °C) without breaking the glycosidic bonds in the chain segments.
- The minimal temperature to break the glycosidic bonds in the amorphous portion is ~150 °C. However, the minimal temperature at which hydrolysis reactions of the crystalline portion start is ~180 °C, due to the strong intra- and inter-

molecule hydrogen bonds which prevent the glycosidic bonds in the long cellulose chains from being accessible to HCW.

- An increase in hydrolysis temperature leads to the formation of more and larger-DP glucose oligomers, apparently due to the enhanced accessibility of glycosidic bonds in the cellulose chains as results of increasing breaking of hydrogen bonds.
- These structural differences also have a large influence on the distribution of glucose oligomers in the primary liquid products from amorphous and crystalline cellulose during hydrolysis in HCW. Amorphous cellulose is more reactive hence producing more glucose monomer and oligomers at the same temperature, but the selectivity ratios of glucose oligomers in the primary liquid products from amorphous and crystalline cellulose do not show a monotonic trend with DP, partly resulting from the presence of shorter glucose chains in amorphous cellulose.

#### **9.2.4 Evolution of Primary Liquid Products and Evidence of in Situ Structural Changes with Conversion**

- The specific reactivity and primary liquid products dynamically evolves during the course of cellulose hydrolysis in HCW, suggesting the evolution of cellulose structure during conversion.
- The intrinsic heterogeneity of cellulose results in the selective consumption of reactive components at early conversions at low temperatures, e.g. 180-200 °C for amorphous cellulose and 230 °C for microcrystalline cellulose.
- Various parallel reactions, including hydrogen bond cleavage, degradation reactions and cross-linking reactions, also contribute to the cellulose structure evolution during hydrolysis in HCW.
- While enhanced hydrogen bond cleavage increases the production of glucose oligomers, degradation reactions and cross-linking reactions have the opposite effects.

- The effect of cross-linking reactions becomes dominant at higher temperatures, resulting in a structural condensation which significantly reduces both the specific reactivity of cellulose and the selectivities of glucose oligomers in the primary liquid products.

### 9.2.5 Effect of Ball Milling on the Hydrolysis of Microcrystalline Cellulose

- After ball milling, the particle size distribution of cellulose sample shows a considerable reduction compared to that of raw sample, and the crystallinity of ball milled sample decreases significantly with ball milling time.
- It was also found that the specific reactivity of ball milled cellulose sample during hydrolysis in HCW increases with ball milling, mainly due to the structure changes during ball milling to make the microcrystalline cellulose more accessible, including the reduction in particle size, and the decrease in crystallinity due to the breaking of hydrogen bonding networks within microcrystalline cellulose, etc.
- Further experiments using a cellulose sample with considerable reduction in particle size but little change in crystallinity by cryogenic ball milling for 2 min, indicate that particle size is not the limiting factor during hydrolysis of microcrystalline cellulose in HCW, because the specific reactivity only slightly increases after cryogenic ball milling. Therefore, the crystallinity of cellulose is likely to play an essential role in the hydrolysis behavior in HCW, due to the more accessible of microcrystalline cellulose samples with smaller crystallinity.
- The liquid product analysis by HPAEC-PAD indicates that the distribution of glucose oligomer in the primary liquid products is affected by cellulose particle size, although the specific reactivity only slightly increases with particle size. The selectivities of glucose oligomers all increase when reducing the particle size, but the selectivity ratios of high-DP glucose oligomers decrease with DP, when comparing the cryogenic ball milled sample with raw sample at the same conversion.

- For long time ball milled sample, the selectivity of glucose oligomers all increase at low conversions. At high conversion, the ball milled samples for 1 hour and 4 hours show the similar trend as those for cryogenic ball milled samples, because particle size starts to play an important role on glucose oligomer formation since cellulose samples become more crystalline at higher conversion. Further increasing the ball milling time will completely destroy the crystalline cellulose, leading to the significant increasing formation of high-DP glucose oligomers.

### 9.3 Recommendations

Based on our studies, various new gaps have also been identified, leading to the following recommendations for future research.

For the precipitation, it is still unknown about the process of precipitate formation from the glucose oligomer in the fresh liquid products. Some chemical reactions between the small organic molecules and the glucose oligomer derivatives may also lead to the precipitate formation. Although our current results prove that the glucose oligomers are mainly responsible for precipitate formation, and experience re-crystallization to cellulose II after drying. Further experimental study is required to clearly understand the precipitation process, including the nucleation and crystal growth during precipitation.

For the cellulose hydrolysis in HCW, although our research advances have greatly improved the understanding on the mechanisms of cellulose hydrolysis in HCW, there are still several important research gaps which require further investigation. Firstly, although we can identify the main glucose oligomers peaks in the IC chromatogram, we still do not know the exact compounds of the small peaks near the main glucose oligomers peaks in the IC chromatogram. Those compounds are also found to contribute to the precipitate formation. Once we know exactly what those peaks are, we can clearly understand other parallel primary reactions occurred during hydrolysis in HCW. Secondly, due to small sample loading used in our reactor system, we could not collect enough partially reacted cellulose sample for further characterisation. Therefore, future studies are required to design a reactor system to

collect enough solid residues for analysis. Then, some hypotheses proposed in this study can be confirmed, and the detailed reaction mechanism of cellulose hydrolysis can be clearly understood. Thirdly, it is still not clear about the secondary decomposition reactions when the residence time of primary liquid products is increased. It seems that the initial secondary reactions lead to the shift of high-DP glucose oligomers to low-DP glucose oligomers, but the further secondary reactions are still unknown. Once we understand the secondary reactions of primary liquid products during hydrolysis in HCW, we may be able to achieve a high yield of sugar monomers from cellulose or biomass. The secondary reactions are also important to understand the oil and char formation process from sugars products. We may be able to commercialize the oil production process directly from cellulose or biomass, if we can enhance of the oil yield and improve the oil quality in the future. Fourthly, we have proven that the primary liquid products from cellulose hydrolysis achieve a glucose selectivity of ~80% after post hydrolysis. This provides a two-step process to produce glucose from cellulose with a high yield. The first step is to collect the liquid products with secondary reactions minimized, while the second step is to produce glucose via further enzymatic hydrolysis. Since the cellulose has already been significantly broken into glucose oligomers, which can be easily attacked by enzyme, the combined HCW and enzymatic hydrolysis process will become very promising in the future. However, detailed and systematic studies on the optimization of reaction conditions for the combined HCW and enzymatic hydrolysis technology are required.

It also has been found that amorphous cellulose is much easier to be hydrolysed in HCW compared to crystalline cellulose, due to the relative weak hydrogen bonds in amorphous cellulose. Hydrolysis of amorphous cellulose can start at lower reaction temperatures hence reducing the decomposition of sugar products. High temperature hydrolysis is not preferable due to the increased other parallel reactions such as cross-linking reactions. The pre-treatment of ball milling has been studied, and it has been found that breaking of hydrogen bonds by pre-treatment is an important strategy to significantly increase the reaction rate as well as the sugar yields at relative low temperatures. However, ball milling process is an energy intensive process, which may reduce its economic feasibility to be used as a pretreatment method. Therefore, further research is required to find other efficient and cheap pre-



treatment methods to break the hydrogen bonding structure in crystalline cellulose therefore hydrolysis can occur at low reaction temperature. Some catalysts may be helpful to further reduce the reaction temperature and achieve a high yield of sugar products.

**REFERENCES**

1. Intergovernmental Panel on Climate Change (IPCC). <http://www.ipcc.ch> (accessed on December 10, 2009).
2. Demirbas, A., Biomass Resource Facilities and Biomass Conversion Processing for Fuels and Chemicals, *Fuel Process. Technol.* **2001**, *42*: 1357-1378.
3. Ramage, J.; Scurlock, J., *Biomass*, in *Renewable Energy-power for a Sustainable Future*, Bolye, G., Editor. 1996, Oxford University Press: Oxford.
4. European Commission (EC), Communication from the Commission: Energy for the Future: Renewable Energy Sources - White Paper for a Community Strategy and Action Plan, Technical Report Number COM(97)599, Brussels, **1997**.
5. International Energy Agency (IEA), World Energy Outlook 2006.
6. Ni, M.; Leung, D.Y.C.; Leung, M.K.H.; Sumathy, K., An Overview of Hydrogen Production from Biomass, *Fuel Process. Technol.* **2006**, *87*: 461-472.
7. Cooper, D.; Olsen, G.; Bartle, J.R., Capture of Agricultural Surplus Water Determines Productivity and Scale of New Low-rainfall Woody Crop Industries, *Aust. J. Exp. Agric.* **2005**, *45*: 1369-1388.
8. Clarke, C.J.; George, R.J.; Bell, R.W.; Hatton, T.J., Dryland Salinity in South-western Australia: its Origins, Remedies, and Future Research Directions, *Aust. J. Soil Res.* **2002**, *40*: 93-113.
9. Bartle, J.; Olsen, G.; Don, C.; Trevor, H., Scale of Biomass Production from New Woody Crops for Salinity Control in Dryland Agriculture in Australia, *Int. J. Global Energy Issues* **2007**, *27*: 115-137.
10. Sochacki, S.J.; Harper, R.J.; Smettem, K.R.J., Estimation of Biomass Production from a Short Rotation Bio-energy System in Semi-arid Australia, *Biomass Bioenerg.* **2007**, *31*: 608-616.
11. Wu, H.; Fu, Q.; Giles, R.; Bartle, J., Production of Mallee Biomass in Western Australia: Energy Balance Analysis, *Energy Fuels* **2008**, *22*: 190-198.
12. Yu, Y.; Bartle, J.; Wu, H., Production of Mallee Biomass in Western Australia: Life Cycle Greenhouse Emissions in *Chemeca 2008 Conference*. 28 Sep-1 Oct, 2008: Newcastle, Australia.
13. Yu, Y.; Bartle, J.; Li, C.Z.; Wu, H., Mallee Biomass as a Key Bioenergy Source in Western Australia: Importance of Biomass Supply Chain, *Energy Fuels* **2009**, *23*: 3290-3299.
14. Bartle, J.R.; Abadi, A., Toward Sustainable Production of Second Generation Bioenergy Feedstocks, *Energy Fuels* **2009**, DOI: 10.1021/ef9006438, in press.
15. Harper, R.J.; Sochacki, S.J.; Smettem, K.R.J.; Robinson, N., Bioenergy Feedstock Potential from Short-Rotation Woody Crops in a Dryland Environment, *Energy Fuels* **2009**, DOI: 10.1021/ef9005687 in press.
16. Wu, H.; Yip, K.; Tian, F.; Xie, Z.; Li, C.-Z., Evolution of Char Structure during the Steam Gasification of Biochars Produced from the Pyrolysis of

- Various Mallee Biomass Components, *Ind. Eng. Chem. Res.* **2009**, *48*: 10431-10438.
17. Garcia-Perez, M.; Wang, S.; Shen, J.; Rhodes, M.; Lee, W.J.; Li, C.Z., Effect of Temperature on the Formation of Lignin-Derived Oligomers during the Fast Pyrolysis of Mallee Woody Biomass, *Energy Fuels* **2008**, *22*: 2022-2032.
  18. Garcia-Perez, M.; Wang, X.S.; Shen, J.; Rhodes, M.J.; Tian, F.; Lee, W.J.; Wu, H.; Li, C.Z., Fast Pyrolysis of Oil Mallee Woody Biomass: Effect of Temperature on the Yield and Quality of Pyrolysis Products, *Ind. Eng. Chem. Res.* **2008**, *47*: 1846-1854.
  19. Abdullah, H.; Wu, H., Biochar as a Fuel: 1. Properties and Grindability of Biochars Produced from the Pyrolysis of Mallee Wood under Slow-Heating Conditions, *Energy Fuels* **2009**, *23*: 4174-4181.
  20. Mulligan, C.J.; Strezov, L.; Strezov, V., Thermal Decomposition of Wheat Straw and Mallee Residue Under Pyrolysis Conditions, *Energy Fuels* **2009**, DOI: 10.1021/ef9004797, in press.
  21. Asadullah, M.; Zhang, S.; Min, Z.; Yimsiri, P.; Li, C.-Z., Importance of Biomass Particle Size in Structural Evolution and Reactivity of Char in Steam Gasification, *Ind. Eng. Chem. Res.* **2009**, *48*: 9858-9863.
  22. Yip, K.; Tian, F.; Hayashi, J.-i.; Wu, H., Effect of Alkali and Alkaline Earth Metallic Species on Biochar Reactivity and Syngas Compositions during Steam Gasification, *Energy Fuels* **2009**, DOI: 10.1021/ef900534n, in press.
  23. Ragauskas, A.J.; Williams, C.K.; Davison, B.H.; Britovsek, G.; Cairney, J.; Eckert, C.E.; Frederick, W.J.; Hallett, J.P.; Leak, D.J.; Liotta, C.L.; Mielenz, J.R.; Murphy, R.; Templer, R.; Tschaplinski, T., The Path Forward for Biofuels and Biomaterials, *Science* **2006**, *311*: 484-489.
  24. Karimi, K.; Kheradmandinia, S.; Taherzadeh, M.J., Conversion of Rice Straw to Sugars by Dilute-Acid Hydrolysis, *Biomass Bioenerg.* **2006**, *30*: 247-253.
  25. Torget, R.W.; Kim, J.S.; Lee, Y.Y., Fundamental Aspects of Dilute Acid Hydrolysis/Fractionation Kinetics of Hardwood Carbohydrates. 1. Cellulose Hydrolysis, *Ind. Eng. Chem. Res.* **2000**, *39*: 2817-2825.
  26. U.S. Department of Energy, Energy Efficiency and Renewable Energy.
  27. Goldstein, I.S., *Organic Chemicals from Biomass*, in *Composition of Biomass*, Goldstein, I.S., Editor. 1981, CRC Press: Boca Raton, FL. p. 9-19.
  28. Bobleter, O., Hydrothermal Degradation of Polymers Derived from Plants, *Prog. Polym. Sci.* **1994**, *19*: 797-841.
  29. Coughlan, M.P., Enzymic Hydrolysis of Cellulose: An Overview, *Bioresour. Technol.* **1992**, *39*: 107-115.
  30. Sun, Y.; Cheng, J., Hydrolysis of Lignocellulosic Materials for Ethanol Production: a Review, *Bioresour. Technol.* **2002**, *83*: 1-11.
  31. Hamelinck, C.N.; Hooijdonk, G.v.; Faaij, A.P.C., Ethanol from Lignocellulosic Biomass: Techno-Economic Performance in Short-, Middle- and Long-Term, *Biomass Bioenerg.* **2005**, *28*: 384-410.
  32. Ando, H.; Sakaki, T.; Kokusho, T.; Shibata, M.; Uemura, Y.; Hatate, Y., Decomposition Behavior of Plant Biomass in Hot-Compressed Water, *Ind. Eng. Chem. Res.* **2000**, *39*: 3688-3693.
  33. Hashaiekh, R.; Fang, Z.; Butler, I.S.; Hawari, J.; Kozinski, J.A., Hydrothermal Dissolution of Willow in Hot Compressed Water as a Model for Biomass Conversion, *Fuel* **2007**, *86*: 1614-1622.

34. Sasaki, M.; Adschiri, T.; Arai, K., Kinetics of Cellulose Conversion at 25 MPa in Sub- and Supercritical Water, *AIChE J.* **2004**, *50*: 192-202.
35. Sasaki, M.; Kabyemela, B.; Malaluan, R.; Hirose, S.; Takeda, N.; Adschiri, T.; Arai, K., Cellulose Hydrolysis in Subcritical and Supercritical Water, *J. Supercrit. Fluids* **1998**, *13*: 261-268.
36. Bröll, D.; Kaul, C.; Krämer, A.; Krammer, P.; Richter, T.; Jung, M.; Vogel, H.; Zehner, P., Chemistry in Supercritical Water, *Angew. Chem. Int. Ed.* **1999**, *38*: 2998-3014.
37. Kashimura, N.; Hayashi, J.-i.; Chiba, T., Degradation of a Victorian Brown Coal in Sub-Critical Water, *Fuel* **2004**, *83*: 353-358.
38. Krammer, P.; Vogel, H., Hydrolysis of Esters in Subcritical and Supercritical Water, *J. Supercrit. Fluids* **2000**, *16*: 189-206.
39. Liu, C.; Wyman, C.E., Partial Flow of Compressed-Hot Water through Corn Stover to Enhance Hemicellulose Sugar Recovery and Enzymatic Digestibility of Cellulose, *Bioresour. Technol.* **2005**, *96*: 1978-1985.
40. Mosier, N.; Hendrickson, R.; Ho, N.; Sedlak, M.; Ladisch, M.R., Optimization of pH Controlled Liquid Hot Water Pretreatment of Corn Stover, *Bioresour. Technol.* **2005**, *96*: 1986-1993.
41. Feng, W.; van der Kooi, H.J.; de Swaan Arons, J., Biomass Conversions in Subcritical and Supercritical Water: Driving Force, Phase Equilibria, and Thermodynamic Analysis, *Chem. Eng. Process.* **2004**, *43*: 1459-1467.
42. Feng, W.; van der Kooi, H.J.; de Swaan Arons, J., Phase Equilibria for Biomass Conversion Processes in Subcritical and Supercritical Water, *Chem. Eng. J.* **2004**, *98*: 105-113.
43. Matsumura, Y.; Minowa, T.; Potic, B.; Kersten, S.R.A.; Prins, W.; van Swaaij, W.P.M.; van de Beld, B.; Elliott, D.C.; Neuenschwander, G.G.; Kruse, A.; Jerry Antal Jr, M., Biomass Gasification in Near- and Super-Critical Water: Status and Prospects, *Biomass Bioenerg.* **2005**, *29*: 269-292.
44. Matsumura, Y.; Sasaki, M.; Okuda, K.; Takami, S.; Ohara, S.; Umetsu, M.; Adschiri, T., Supercritical Water Treatment of Biomass for Energy and Material Recovery, *Combust. Sci. Technol.* **2006**, *178*: 509-536.
45. Osada, M.; Sato, T.; Watanabe, M.; Shirai, M.; Arai, K., Catalytic Gasification of Wood Biomass in Subcritical and Supercritical Water, *Combust. Sci. Tech.* **2006**, *178*: 537-552.
46. Klein, M.T.; Torry, L.A.; Wu, B.C.; Townsend, S.H.; Paspek, S.C., Hydrolysis in Supercritical Water: Solvent Effects as a Probe of the Reaction Mechanism, *J. Supercrit. Fluids* **1990**, *3*: 222-227.
47. Kruse, A.; Dinjus, E., Hot Compressed Water as Reaction Medium and Reactant: 2. Degradation Reactions, *J. Supercrit. Fluids* **2007**, *41*: 361-379.
48. Watanabe, M.; Iida, T.; Aizawa, Y.; Aida, T.M.; Inomata, H., Acrolein Synthesis from Glycerol in Hot-Compressed Water, *Bioresour. Technol.* **2007**, *98*: 1285-1290.
49. Mok, W.S.L.; Antal, M.J., Uncatalyzed Solvolysis of Whole Biomass Hemicellulose by Hot Compressed Liquid Water, *Ind. Eng. Chem. Res.* **1992**, *31*: 1157-1161.
50. Adschiri, T.; Hirose, S.; Malaluan, R.; Arai, K., Noncatalytic Conversion of Cellulose in Supercritical and Subcritical Water, *J. Chem. Eng. Jpn.* **1993**, *26*: 676-680.

51. Minowa, T.; Fang, Z.; Ogi, T.; Varhegyi, G., Decomposition of Cellulose and Glucose in Hot-Compressed Water under Catalyst-Free Conditions, *J. Chem. Eng. Jpn.* **1998**, *31*: 131-134.
52. Sasaki, M.; Fang, Z.; Fukushima, Y.; Adschiri, T.; Arai, K., Dissolution and Hydrolysis of Cellulose in Subcritical and Supercritical Water, *Ind. Eng. Chem. Res.* **2000**, *39*: 2883-2890.
53. Sakaki, T.; Shibata, M.; Sumi, T.; Yasuda, S., Saccharification of Cellulose Using a Hot-Compressed Water-Flow Reactor, *Ind. Eng. Chem. Res.* **2002**, *41*: 661-665.
54. Ehara, K.; Saka, S., A Comparative Study on Chemical Conversion of Cellulose between the Batch-Type and Flow-Type Systems in Supercritical Water, *Cellulose* **2002**, *9*: 301-311.
55. Ehara, K.; Saka, S., Decomposition Behaviour of Cellulose in Supercritical Water, Subcritical Water and Their Combined Treatments, *Jpn. Wood Res. Soc.* **2005**, *51*: 148-153.
56. Matsunaga, M.; Matsui, H.; Otsuka, Y.; Yamamoto, S., Chemical Conversion of Wood by Treatment in a Semi-Batch Reactor with Subcritical Water, *J. Supercrit. Fluids* **2008**, *44*: 364-369.
57. Xu, C.; Lad, N., Production of Heavy Oils with High Caloric Values by Direct Liquefaction of Woody Biomass in Sub/Near-critical Water, *Energy Fuels* **2007**, *22*: 635-642.
58. Yang, B.; Wyman, C.E., Characterization of the Degree of Polymerization of Xylooligomers Produced by Flowthrough Hydrolysis of Pure Xylan and Corn Stover with Water, *Bioresour. Technol.* **2008**, *99*: 5756-5762.
59. Kumar, S.; Gupta, R.B., Hydrolysis of Microcrystalline Cellulose in Subcritical and Supercritical Water in a Continuous Flow Reactor, *Ind. Eng. Chem. Res.* **2008**, *47*: 9321-9329.
60. Kumar, S.; Gupta, R.B., Biocrude Production from Switchgrass Using Subcritical Water, *Energy Fuels* **2009**, *23*: 5151-5159.
61. Yuan, X.Z.; Tong, J.Y.; Zeng, G.M.; Li, H.; Xie, W., Comparative Studies of Products Obtained at Different Temperatures during Straw Liquefaction by Hot Compressed Water, *Energy Fuels* **2009**, *23*: 3262-3267.
62. Zhao, Y.; Lu, W.-J.; Wang, H.-T., Supercritical Hydrolysis of Cellulose for Oligosaccharide Production in Combined Technology, *Chem. Eng. J.* **2009**, *150*: 411-417.
63. Zhao, Y.; Lu, W.-J.; Wang, H.-T.; Yang, J.-L., Fermentable Hexose Production from Corn Stalks and Wheat Straw with Combined Supercritical and Subcritical Hydrothermal Technology, *Bioresour. Technol.* **2009**, *100*: 5884-5889.
64. Zhao, Y.; Lu, W.-J.; Wang, H.-T.; Li, D., Combined Supercritical and Subcritical Process for Cellulose Hydrolysis to Fermentable Hexoses, *Environ. Sci. Technol.* **2009**, *43*: 1565-1570.
65. Rogalinski, T.; Ingram, T.; Brunner, G., Hydrolysis of Lignocellulosic Biomass in Water under Elevated Temperatures and Pressures, *J. Supercrit. Fluids* **2008**, *47*: 54-63.
66. Ingram, T.; Rogalinski, T.; Bockemuhl, V.; Antranikian, G.; Brunner, G., Semi-Continuous Liquid Hot Water Pretreatment of Rye Straw, *J. Supercrit. Fluids* **2009**, *48*: 238-246.

67. Cheng, L.; Ye, X.P.; He, R.; Liu, S., Investigation of Rapid Conversion of Switchgrass in Subcritical Water, *Fuel Process. Technol.* **2009**, *90*: 301-311.
68. Kruse, A.; Dinjus, E., Hot Compressed Water as Reaction Medium and Reactant: Properties and Synthesis Reactions, *J. Supercrit. Fluids* **2007**, *39*: 362-380.
69. Murphy, J.D.; McCarthy, K., Ethanol Production from Energy Crops and Wastes for Use as a Transport Fuel in Ireland, *Appl. Energy* **2005**, *82*: 148-166.
70. Liao, C.; Yan, Y.; Wu, C.; Huang, H., Study on the Distribution and Quantity of Biomass Residues Resource in China, *Biomass Bioenerg.* **2004**, *27*: 111-117.
71. Mohan, D.; Pittman, C.U.; Steele, P.H., Pyrolysis of Wood/Biomass for Bio-oil: A Critical Review, *Energy Fuels* **2006**, *20*: 848-889.
72. Huber, G.W.; Dumesic, J.A., An Overview of Aqueous-Phase Catalytic Processes for Production of Hydrogen and Alkanes in a Biorefinery, *Catal. Today* **2006**, *111*: 119-132.
73. Hearle, J.W.S., *The development of ideas of fine structure*, in *Fibre structure*, Butterworth, Editor. 1963, The Textile Institute: London-Manchester.
74. Paakkari, T.; Serimaa, R.; Fink, H.-P., Structure of Amorphous Cellulose, *Acta Polymerica* **1989**, *40*: 731-734.
75. Fink, H.-P.; Philipp, B.; Paul, D.; Serimaa, R.; Paakkari, T., The Structure of Amorphous Cellulose as Revealed by Wide-angle Xray Scattering, *Polymer* **1987**, *28*: 1265-1270.
76. Kondo, T.; Sawatati, C., A Fourier Transform Infra-red Spectroscopic Analysis of the Character of Hydrogen Bonds in Amorphous Cellulose, *Polymer* **1996**, *37*: 393-399.
77. Newman, R.H.; Hemmingson, J.A., Carbon-13 NMR Distinction between Categories of Molecular Order and Disorder in Cellulose., *Cellulose* **1995**, *2*: 95-110.
78. Hirai, A.; Horii, F.; Kitamura, R., Carbon-13 Spin-Lattice Relaxation Behaviour of the Crystalline and Noncrystalline Components of Native and Regenerated Celluloses, *Cell. Chem. Technol.* **1990**, *24*: 703-711.
79. Nishiyama, Y.; Chanzy, H.; Langan, P., Crystal Structure and Hydrogen-Bonding System in Cellulose I $\beta$  from Synchrotron X-ray and Neutron Fiber Diffraction, *J. Am. Chem. Soc.* **2002**, *124*: 9074-9082.
80. Nishiyama, Y.; Sugiyama, J.; Chanzy, H.; Langan, P., Crystal Structure and Hydrogen Bonding System in Cellulose I $\alpha$  from Synchrotron X-ray and Neutron Fiber Diffraction, *J. Am. Chem. Soc.* **2003**, *125*: 14300-14306.
81. Kumar, S.; Gupta, R.; Lee, Y.Y.; Gupta, R.B., Cellulose Pretreatment in Subcritical Water: Effect of Temperature on Molecular Structure and Enzymatic Reactivity, *Bioresour. Technol.* **2010**, *101*: 1337-1347.
82. Jarvis, M., Cellulose Stacks Up, *Nature* **2003**, *426*: 611-612.
83. Langan, P.; Nishiyama, Y.; Chanzy, H., X-ray Structure of Mercerized Cellulose II at 1 Å Resolution, *Macromolecules* **2001**, *2*: 410-416.
84. Wada, M.; Heux, L.; Isogai, A.; Nishiyama, Y.; Chanzy, H.; Sugiyama, J., Improved Structural Data of Cellulose III $_1$  Prepared in Supercritical Ammonia, *Macromolecules* **2001**, *34*: 1237-1243.
85. Zugenmaier, P., Conformation and Packing of Various Crystalline Cellulose Fibers, *Prog. Polym. Sci.* **2001**, *26*: 1341-1417.

86. Sarko, A.; Southwick, J.; Hayashi, J., Packing Analysis of Carbohydrates and Polysaccharides. 7. Crystal Structure of Cellulose III<sub>I</sub> and Its Relationship to Other Cellulose Polymorphs, *Macromolecules* **1976**, *9*: 857-863.
87. Wada, M.; Heux, L.; Sugiyama, J., Polymorphism of Cellulose I Family: Reinvestigation of Cellulose IV<sub>L</sub>, *Macromolecules* **2004**, *5*: 1385-1391.
88. Bridgwater, A.V., Biomass Fast Pyrolysis, *Thermal Sci.* **2004**, *8*: 21-49.
89. Glasser, W.G.; Northey, R.A.; Schultz, T.P., Lignin: Historical, Biological and Materials Perspectives, in *Lignin chemistry, technology and utilization: a brief history*, McCarthy, J.; A., I., Editors. 2000, American Chemistry Society: Washington, DC. p. 2-100.
90. Nimz, H.H., Chemistry of Potential Chromophoric Groups in Beech Lignin, *Tappi* **1973**, *56*: 124-124.
91. Lü, X.; Sakoda, A.; Suzuki, M., Decomposition of Cellulose by Continuous Near-Critical Water Reactions, *Chinese J. Chem. Eng.* **2000**, *8*: 321-325.
92. Kabyemela, B.M.; Takigawa, M.; Adschiri, T.; Malaluan, R.M.; Arai, K., Mechanism and Kinetics of Cellobiose Decomposition in Sub- and Supercritical Water, *Ind. Eng. Chem. Res.* **1998**, *37*: 357-361.
93. Minowa, T.; Zhen, F.; Ogi, T., Cellulose Decomposition in Hot-Compressed Water with Alkali or Nickel Catalyst, *J. Supercrit. Fluids* **1998**, *13*: 253-259.
94. Sasaki, M.; Adschiri, T.; Arai, K., Production of Cellulose II from Native Cellulose by Near- and Supercritical Water Solubilization, *J. Agric. Food Chem.* **2003**, *51*: 5376-5381.
95. Sasaki, M.; Furukawa, M.; Minami, K.; Adschiri, T.; Arai, K., Kinetics and Mechanism of Cellobiose Hydrolysis and Retro-Aldol Condensation in Subcritical and Supercritical Water, *Ind. Eng. Chem. Res.* **2002**, *41*: 6642-6649.
96. Khajavi, S.H.; Kimura, Y.; Oomori, T.; Matsuno, R.; Adachi, S., Kinetics on Sucrose Decomposition in Subcritical Water, *LWT - Food Sci. Technol.* **2005**, *38*: 297-302.
97. Kabyemela, B.M.; Adschiri, T.; Malaluan, R.; Arai, K., Degradation Kinetics of Dihydroxyacetone and Glyceraldehyde in Subcritical and Supercritical Water, *Ind. Eng. Chem. Res.* **1997**, *36*: 2025-2030.
98. Kabyemela, B.M.; Adschiri, T.; Malaluan, R.M.; Arai, K., Kinetics of Glucose Epimerization and Decomposition in Subcritical and Supercritical Water, *Ind. Eng. Chem. Res.* **1997**, *36*: 1552-1558.
99. Mochidzuki, K.; Sakoda, A.; Suzuki, M., Measurement of the Hydrothermal Reaction Rate of Cellulose Using Novel Liquid-Phase Thermogravimetry, *Thermochimi. Acta* **2000**, *348*: 69-76.
100. Mochidzuki, K.; Sakoda, A.; Suzuki, M., Liquid-Phase Thermogravimetric Measurement of Reaction Kinetics of the Conversion of Biomass Wastes in Pressurized Hot Water: a Kinetic Study, *Adv. Environ. Res.* **2003**, *7*: 421-428.
101. Rogalinski, T.; Liu, K.; Albrecht, T.; Brunner, G., Hydrolysis Kinetics of Biopolymers in Subcritical Water, *J. Supercrit. Fluids* **2008**, *46*: 335-341.
102. Kamio, E.; Takahashi, S.; Noda, H.; Fukuhara, C.; Okamura, T., Liquefaction of Cellulose in Hot Compressed Water under Variable Temperatures, *Ind. Eng. Chem. Res.* **2006**, *45*: 4944-4953.
103. Matsumura, Y.; Yanachi, S.; Yoshida, T., Glucose Decomposition Kinetics in Water at 25 MPa in the Temperature Range of 448-673 K, *Ind. Eng. Chem. Res.* **2006**, *45*: 1875-1879.

104. Kamio, E.; Sato, H.; Takahashi, S.; Noda, H.; Fukuhara, C.; Okamura, T., Liquefaction Kinetics of Cellulose Treated by Hot Compressed Water under Variable Temperature Conditions, *J. Mater. Sci.* **2008**, *43*: 2179-2188.
105. Kamio, E.; Takahashi, S.; Noda, H.; Fukuhara, C.; Okamura, T., Effect of Heating Rate on Liquefaction of Cellulose by Hot Compressed Water, *Chem. Eng. J.* **2008**, *137*: 328-338.
106. Akiya, N.; Savage, P.E., Roles of Water for Chemical Reactions in High-Temperature Water, *Chem. Rev.* **2002**, *102*: 2725-2750.
107. Buhler, W.; Dinjus, E.; Ederer, H.J.; Kruse, A.; Mas, C., Ionic Reactions and Pyrolysis of Glycerol as Competing Reaction Pathways in Near- and Supercritical Water, *J. Supercrit. Fluids* **2002**, *22*: 37-53.
108. Weast, R.C., *CRC Handbook of Chemistry and Physics*. 1991, Cleveland, OH: CRC Press. C727.
109. Townsend, S.H.; Abraham, M.A.; Huppert, G.L.; Klein, M.T.; Paspek, S.C., Solvent Effects during Reactions in Supercritical Water, *Ind. Eng. Chem. Res.* **1988**, *27*: 143-149.
110. Kruse, A.; Gawlik, A., Biomass Conversion in Water at 330-410 °C and 30-50 MPa. Identification of Key Compounds for Indicating Different Chemical Reaction Pathways, *Ind. Eng. Chem. Res.* **2003**, *42*: 267-279.
111. Savage, P.E., Organic Chemical Reactions in Supercritical Water, *Chem. Rev.* **1999**, *99*: 603-622.
112. Watanabe, M.; Sato, T.; Inomata, H.; Smith, R.L.; Arai, K.; Kruse, A.; Dinjus, E., Chemical Reactions of C1 Compounds in Near-Critical and Supercritical Water, *Chem. Rev.* **2004**, *104*: 5803-5822.
113. Bobleter, O.; Bonn, G., The Hydrothermolysis of Cellobiose and Its Reaction Product D-Glucose, *Carbohydr. Res.* **1983**, *124*: 185-193.
114. Sakaki, T.; Shibata, M.; Miki, T.; Hirose, H.; Hayashi, N., Decomposition of Cellulose in Near-Critical Water and Fermentability of the Products, *Energy Fuels* **1996**, *10*: 684-688.
115. Sakaki, T.; Shibata, M.; Miki, T.; Hirose, H.; Hayashi, N., Reaction Model of Cellulose Decomposition in Near-Critical Water and Fermentation of Products, *Bioresour. Technol.* **1996**, *58*: 197-202.
116. Sasaki, M.; Iwasaki, K.; Hamaya, T.; Adschiri, T.; Shibata, M., Super-Rapid Enzymatic Hydrolysis of Cellulose with Supercritical Water Solubilisation Pretreatment, *Kobunshi Ronbunshu* **2001**, *58*: 527-532.
117. Varhegyi, G.; Szabo, P.; Mok, W.S.-L.; Antal, M.J., Kinetics of the Thermal Decomposition of Cellulose in Sealed Vessels at Elevated Pressures. Effects of the Presence of Water on the Reaction Mechanism, *J. Anal. Appl. Pyrolysis* **1993**, *26*: 159-174.
118. Antal, M.J.; Mok, W.S.L.; Richards, G.N., Mechanism of Formation of 5-(Hydroxymethyl)-2-Furaldehyde from D-Fructose and Sucrose, *Carbohydr. Res.* **1990**, *199*: 91-109.
119. Antal, M.J.; Mok, W.S.L.; Richards, G.N., Four-Carbon Model Compounds for the Reactions of Sugars in Water at High Temperature, *Carbohydr. Res.* **1990**, *199*: 111-115.
120. Antal, M.J.; Allen, S.G.; Schulman, D.; Xu, X.; Divilio, R.J., Biomass Gasification in Supercritical Water, *Ind. Eng. Chem. Res.* **2000**, *39*: 4040-4053.



121. Malaluan, R.M., *A Study on Cellulose Decomposition in Subcritical and Supercritical Water*. 1995, Tohoku University: Sendai, Japan.
122. Deguchi, S.; Tsujii, K.; Horikoshi, K., Cooking Cellulose in Hot and Compressed Water, *Chem. Commun.* **2006**: 3293-3295.
123. Deguchi, S.; Tsujii, K.; Horikoshi, K., Crystalline-to-Amorphous Transformation of Cellulose in Hot and Compressed Water and Its Implications for Hydrothermal Conversion, *Green Chem.* **2008**, *10*: 191-196.
124. Fang, Z.; Minowa, T.; Smith, R.L.; Ogi, T.; Kozinski, J.A., Liquefaction and Gasification of Cellulose with Na<sub>2</sub>CO<sub>3</sub> and Ni in Subcritical Water at 350°C, *Ind. Eng. Chem. Res.* **2004**, *43*: 2454-2463.
125. Minowa, T.; Fang, Z., Hydrogen Production from Cellulose in Hot Compressed Water using Reduced Nickel Catalyst: Production Distribution at Different Reaction Temperatures, *J. Chem. Eng. Jpn.* **1998**, *31*: 488-491.
126. Minowa, T.; Fang, Z.; Ogi, T.; Varhegyi, G., Liquefaction of Cellulose in Hot Compressed Water using Sodium Carbonate: Products Distribution at Different Reaction Temperatures, *J. Chem. Eng. Jpn.* **1997**, *30*: 186-190.
127. Minowa, T.; Ogi, T., Hydrogen Production from Cellulose Using a Reduced Nickel Catalyst, *Catal. Today* **1998**, *45*: 411-416.
128. Minowa, T.; Ogi, T.; Yokoyama, S.Y., Hydrogen Production from Wet Cellulose by Low Temperature Gasification Using a Reduced Nickel Catalyst, *Chem. Lett.* **1995**, *10*: 937-938.
129. Minowa, T.; Kondo, T.; Sudirjo, S.T., Thermochemical Liquefaction of Indonesian Biomass Residues, *Biomass Bioenerg.* **1998**, *14*: 517-524.
130. Aida, T.M.; Sato, Y.; Watanabe, M.; Tajima, K.; Nonaka, T.; Hattori, H.; Arai, K., Dehydration of D-glucose in High Temperature Water at Pressures up to 80 MPa, *J. Supercrit. Fluids* **2007**, *40*: 381-388.
131. Aida, T.M.; Tajima, K.; Watanabe, M.; Saito, Y.; Kuroda, K.; Nonaka, T.; Hattori, H.; Smith Jr., R.L.; Arai, K., Reactions of D-fructose in Water at Temperatures up to 400 °C and Pressures up to 100 MPa, *J. Supercrit. Fluids* **2007**, *42*: 110-119.
132. Kabyemela, B.M.; Adschiri, T.; Malaluan, R.M.; Arai, K., Glucose and Fructose Decomposition in Subcritical and Supercritical Water: Detailed Reaction Pathway, Mechanisms, and Kinetics, *Ind. Eng. Chem. Res.* **1999**, *38*: 2888-2895.
133. Kabyemela, B.M.; Adschiri, T.; Malaluan, R.M.; Arai, K.; Ohzeki, H., Rapid and Selective Conversion of Glucose to Erythrose in Supercritical Water, *Ind. Eng. Chem. Res.* **1997**, *36*: 5063-5067.
134. Sasaki, M.; Goto, K.; Tajima, K.; Adschiri, T.; Arai, K., Rapid and Selective Retro-Aldol Condensation of Glucose to Glycolaldehyde in Supercritical Water, *Green Chem.* **2002**, *4*: 285-287.
135. Sinag, A.; Kruse, A.; Rathert, J., Influence of the Heating Rate and the Type of Catalyst on the Formation of Key Intermediates and on the Generation of Gases During Hydrolysis of Glucose in Supercritical Water in a Batch Reactor, *Ind. Eng. Chem. Res.* **2004**, *43*: 502-508.
136. Sinag, A.; Kruse, A.; Schwarzkopf, V., Key Compounds of the Hydrolysis of Glucose in Supercritical Water in the Presence of K<sub>2</sub>CO<sub>3</sub>, *Ind. Eng. Chem. Res.* **2003**, *42*: 3516-3521.
137. Sinag, A.; Kruse, A.; Schwarzkopf, V., Formation and Degradation Pathways of Intermediate Products Formed during the Hydrolysis of Glucose as a

- Model Substance for Wet Biomass in a Tubular Reactor, *Eng. Life Sci.* **2003**, 3: 469-473.
138. Srokol, Z.; Bouche, A.-G.; van Estrik, A.; Strik, R.C.J.; Maschmeyer, T.; Peters, J.A., Hydrothermal Upgrading of Biomass to Biofuel: Studies on Some Monosaccharide Model Compounds, *Carbohydr. Res.* **2004**, 339: 1717-1726.
139. Watanabe, M.; Aizawa, Y.; Iida, T.; Aida, T.M.; Levy, C.; Sue, K.; Inomata, H., Glucose Reactions with Acid and Base Catalysts in Hot Compressed Water at 473 K, *Carbohydr. Res.* **2005**, 340: 1925-1930.
140. Watanabe, M.; Aizawa, Y.; Iida, T.; Levy, C.; Aida, T.M.; Inomata, H., Glucose Reactions within the Heating Period and the Effect of Heating Rate on the Reactions in Hot Compressed Water, *Carbohydr. Res.* **2005**, 340: 1931-1939.
141. Watanabe, M.; Aizawa, Y.; Iida, T.; Nishimura, R.; Inomata, H., Catalytic Glucose and Fructose Conversions with TiO<sub>2</sub> and ZrO<sub>2</sub> in Water at 473 K: Relationship between Reactivity and Acid-Base Property Determined by TPD Measurement, *Appl. Catal. A Gen.* **2005**, 295: 150-156.
142. Watanabe, M.; Inomata, H.; Arai, K., Catalytic Hydrogen Generation from Biomass (Glucose and Cellulose) with ZrO<sub>2</sub> in Supercritical Water, *Biomass Bioenerg.* **2002**, 22: 405-410.
143. Yang, B.Y.; Montgomery, R., Alkaline Degradation of Glucose: Effect of Initial Concentration of Reactants, *Carbohydr. Res.* **1996**, 280: 27-45.
144. Mok, W.S.; Antal, M.J.; Varhegyi, G., Productive and Parasitic Pathways in Dilute Acid-Catalyzed Hydrolysis of Cellulose, *Ind. Eng. Chem. Res.* **1992**, 31: 94-100.
145. Watanabe, M.; Iida, T.; Aizawa, Y.; Ura, H.; Inomata, H.; Arai, K., Conversions of Some Small Organic Compounds with Metal Oxides in Supercritical Water at 673K, *Green Chem.* **2003**, 5: 539-544.
146. Watanabe, M.; Inomata, H.; Smith, R.L.; Arai, K., Catalytic Decarboxylation of Acetic Acid with Zirconia Catalyst in Supercritical Water, *Appl. Catal. A Gen.* **2001**, 219: 149-156.
147. Watanabe, M.; Osada, M.; Inomata, H.; Arai, K.; Kruse, A., Acidity and Basicity of Metal Oxide Catalysts for Formaldehyde Reaction in Supercritical Water at 673 K, *Appl. Catal. A Gen.* **2003**, 245: 333-341.
148. Saka, S.; Ueno, T., Chemical Conversion of Various Celluloses to Glucose and Its Derivatives in Supercritical Water, *Cellulose* **1999**, 6: 177-191.
149. Sakanishi, K.; Ikeyama, N.; Sakaki, T.; Shibata, M.; Miki, T., Comparison of the Hydrothermal Decomposition Reactivities of Chitin and Cellulose, *Ind. Eng. Chem. Res.* **1999**, 38: 2177-2181.
150. Sumi, T.; Sakaki, T.; Ohba, H.; Shibata, M., Application of Matrix-Assisted Laser Desorption/Ionization Time-of-Flight Mass Spectrometry to Insoluble Glucose Oligomers in Decomposed Cellulose, *Rapid Commun. Mass Spectrom.* **2000**, 14: 1823-1827.
151. Ogihara, Y.; Smith, R.L.J.; Inomata, H.; Arai, K., Direct Observation of Cellulose Dissolution in Subcritical and Supercritical Water over a Wide Range of Water Density (550-1000 kg/m<sup>3</sup>), *Cellulose* **2005**, 12: 595-606.
152. Kim, I.-C.; Park, S.-D.; Kim, S., Effects of Sulfates on the Decomposition of Cellobiose in Supercritical Water, *Chem. Eng. Process.* **2004**, 43: 997-1005.

153. Kim, S.T.; Park, Y.S.; Kim, H.J., Effect of Copper Addition on Corrosion Resistance of Austenite Stainless Steel in Highly Concentrated Sulphuric Acid Solution, *J. Corr. Sci. Soc. Korea* **1999**, *28*: 281-294.
154. Onda, A.; Ochi, T.; Yanagisawa, K., Selective Hydrolysis of Cellulose into Glucose over Solid Acid Catalyst, *Green Chem.* **2008**, *10*: 1033-1037.
155. Suganuma, S.; Nakajima, K.; Kitano, M.; Yamaguchi, D.; Kato, H.; Hayashi, S.; Hara, M., Hydrolysis of Cellulose by Amorphous Carbon Bearing SO<sub>3</sub>H, COOH, and OH Groups, *J. Am. Chem. Soc.* **2008**, *130*: 12787-12793.
156. Jacobsen, S.E.; Wyman, C.E., Xylose Monomer and Oligomer Yields for Uncatalyzed Hydrolysis of Sugarcane Bagasse Hemicellulose at Varying Solids Concentration, *Ind. Eng. Chem. Res.* **2002**, *41*: 1454-1461.
157. Lavarack, B.P.; Griffin, G.J.; Rodman, D., The Acid Hydrolysis of Sugarcane Bagasse Hemicellulose to Produce Xylose, Arabinose, Glucose and Other Products, *Biomass Bioenerg.* **2002**, *23*: 367-380.
158. Kumar, R.; Wyman, C.E., The Impact of Dilute Sulfuric Acid on the Selectivity of Xylooligomer Depolymerization to Monomers, *Carbohydr. Res.* **2008**, *343*: 290-300.
159. Sasaki, M.; Hayakawa, T.; Arai, K.; Adichiri, T. Measurement of the Rate of Retro-Aldol Condensation of D-xylose in Subcritical and Supercritical Water. in *Proc. 7th International Symposium on Hydrothermal Reactions*. 2003.
160. Goto, M.; Obuchi, R.; Hirose, T.; Sakaki, T.; Shibata, M., Hydrothermal Conversion of Municipal Organic Waste into Resources, *Bioresour. Technol.* **2004**, *93*: 279-284.
161. Kobayashi, N.; Okada, N.; Hirakawa, A.; Sato, T.; Kobayashi, J.; Hatano, S.; Itaya, Y.; Mori, S., Characteristics of Solid Residues Obtained from Hot-Compressed-Water Treatment of Woody Biomass, *Ind. Eng. Chem. Res.* **2009**, *48*: 373-379.
162. Khajavi, S.H.; Kimura, Y.; Oomori, T.; Matsuno, R.; Adachi, S., Degradation Kinetics of Monosaccharides in Subcritical Water, *J. Food Eng.* **2005**, *68*: 309-313.
163. Oomori, T.; Khajavi, S.H.; Kimura, Y.; Adachi, S.; Matsuno, R., Hydrolysis of Disaccharides Containing Glucose Residue in Subcritical Water, *Biochem. Eng. J.* **2004**, *18*: 143-147.
164. Lu, X.; Yamauchi, K.; Phaiboobsilpa, N.; Saka, S., Two-Step Hydrolysis of Japan Beech as Treated by Semi-Flow Hot-Compressed Water, *Jpn. Wood Res. Soc.* **2009**, *55*: 367-375.
165. Allen, S.G.; Kam, L.C.; Zemann, A.J.; Antal, M.J., Fractionation of Sugar Cane with Hot, Compressed, Liquid Water, *Ind. Eng. Chem. Res.* **1996**, *35*: 2709-2715.
166. Sasaki, M.; Adschiri, T.; Arai, K., Fractionation of Sugarcane Bagasse by Hydrothermal Treatment, *Bioresour. Technol.* **2003**, *86*: 301-304.
167. Nakata, T.; Miyafuji, H.; Saka, S., Enzymatic Saccharification of Water-Soluble Portion after Hot-Compressed Water Treatment of Japanese Beech with Xylanase and  $\beta$ -Xylosidase, *Jpn. Wood Res. Soc.* **2009**, *55*: 209-214.
168. Nakata, T.; Miyafuji, H.; Saka, S., Ethanol Production with  $\beta$ -Xylosidase, Xylose Isomerase, and *Saccharomyces Cerevisiae* from the Hydrolysate of Japanese Beech after Hot-Compressed Water Treatment, *Jpn. Wood Res. Soc.* **2009**, *55*: 289-294.

169. Nakata, T.; Miyafuji, H.; Saka, S., Process Integration of Ethanol Production from Japanese Beech as Treated with Hot-Compressed Water Followed by Enzymatic Treatment, *Jpn. Wood Res. Soc.* **2009**, *55*: 295-301.
170. Pérez, J.A.; Ballesteros, I.; Ballesteros, M.; Sáez, F.; Negro, M.J.; Manzanares, P., Optimizing Liquid Hot Water Pretreatment Conditions to Enhance Sugar Recovery from Wheat Straw for Fuel-Ethanol Production, *Fuel* **2008**, *87*: 3640-3647.
171. Thomsen, M.H.; Thygesen, A.; Thomsen, A.B., Hydrothermal Treatment of Wheat Straw at Pilot Plant Scale Using a Three-Step Reactor System Aiming at High Cemicellulose Recovery, High Cellulose Digestibility and Low Lignin Hydrolysis, *Bioresour. Technol.* **2008**, *99*: 4221-4228.
172. Dogaris, I.; Karapati, S.; Mamma, D.; Kalogeris, E.; Kekos, D., Hydrothermal Processing and Enzymatic Hydrolysis of Sorghum Bagasse for Fermentable Carbohydrates Production, *Bioresour. Technol.* **2009**, *100*: 6543-6549.
173. Suryawati, L.; Wilkins, M.R.; Bellmer, D.D.; Huhnke, R.L.; Maness, N.O.; Banat, I.M., Effect of Hydrothermolysis Process Conditions on Pretreated Switchgrass Composition and Ethanol Yield by SSF with *Kluyveromyces Marxianus* IMB4, *Process Biochem.* **2009**, *44*: 540-545.
174. Lee, J.M.; Shi, J.; Venditti, R.A.; Jameel, H., Autohydrolysis Pretreatment of Coastal Bermuda Grass for Increased Enzyme Hydrolysis, *Bioresour. Technol.* **2009**, *100*: 6434-6441.
175. Petchpradab, P.; Yoshida, T.; Charinpanitkul, T.; Matsumura, Y., Hydrothermal Pretreatment of Rubber Wood for the Saccharification Process, *Ind. Eng. Chem. Res.* **2009**, *48*: 4587-4591.
176. Nagamori, M.; Funazukuri, T., Glucose Production by Hydrolysis of Starch under Hydrothermal Conditions, *J. Chem. Technol. Biotechnol.* **2004**, *79*: 229-233.
177. Miyazawa, T.; Funazukuri, T., Noncatalytic Hydrolysis of Guar Gum under Hydrothermal Conditions, *Carbohydr. Res.* **2006**, *341*: 870-877.
178. Amin, S.; Reid, R.C.; Modell, M. Reforming and Decomposition of Glucose in An Aqueous Phase. in *Intersociety Conference on Environmental Systems*. 1975. San Francisco, CA: The American Society of Mechanical Engineers (ASME): New York.
179. Bobleter, O.; Pape, G., Hydrothermal Decomposition of Glucose, *Monatsh. Chem.* **1968**, *99*: 1560-1567.
180. Converse, A.O., Simulation of a Cross-Flow Shrinking-Bed Reactor for the Hydrolysis of Lignocellulosics, *Bioresour. Technol.* **2002**, *81*: 109-116.
181. Lee, Y.Y.; Wu, Z.; Torget, R.W., Modeling of Countercurrent Shrinking-Bed Reactor in Dilute-Acid Total-Hydrolysis of Lignocellulosic Biomass, *Bioresour. Technol.* **2000**, *71*: 29-39.
182. Kim, K.H.; Tucker, M.; Nguyen, Q., Conversion of Bark-Rich Biomass Mixture into Fermentable Sugar by Two-Stage Dilute Acid-Catalyzed Hydrolysis, *Bioresour. Technol.* **2005**, *96*: 1249-1255.
183. Duff, S.J.B.; Murray, W.D., Bioconversion of Forest Products Industry Waste Cellulosics to Fuel Ethanol: A Review, *Bioresour. Technol.* **1996**, *55*: 1-33.
184. Fang, L.T.; Gharpuray, M.M.; Lee, Y.H., *Cellulose Hydrolysis Biotechnology Monographs*. 1987, Berlin: Springer. 55.

185. Reese, E.T.; Siu, R.G.H.; Levinson, H.S., The Biological Degradation of Soluble Cellulose Derivatives and Its Relationship to the Mechanism of Cellulose Hydrolysis, *J. Bacteriol.* **1950**, *59*: 485-497.
186. Mosier, N.; Wyman, C.; Dale, B.; Elander, R.; Lee, Y.Y.; Holtzapple, M.; Ladisch, M., Features of Promising Technologies for Pretreatment of Lignocellulosic Biomass, *Bioresour. Technol.* **2005**, *96*: 673-686.
187. Patel-Predd, P., Overcoming the Hurdles to Producing Ethanol from Cellulose, *Environ. Sci. Technol.* **2006**, *40*: 4052-4053.
188. Kim, S.; Holtzapple, M.T., Lime Pretreatment and Enzymatic Hydrolysis of Corn Stover, *Bioresour. Technol.* **2005**, *96*: 1994-2006.
189. Kim, T.H.; Lee, Y.Y., Pretreatment and Fractionation of Corn Stover by Ammonia Recycle Percolation Process, *Bioresour. Technol.* **2005**, *96*: 2007-2013.
190. Lloyd, T.A.; Wyman, C.E., Combined Sugar Yields for Dilute Sulfuric Acid Pretreatment of Corn Stover Followed by Enzymatic Hydrolysis of the Remaining Solids, *Bioresour. Technol.* **2005**, *96*: 1967-1977.
191. Teymouri, F.; Laureano-Perez, L.; Alizadeh, H.; Dale, B.E., Optimization of the Ammonia Fiber Explosion (AFEX) Treatment Parameters for Enzymatic Hydrolysis of Corn Stover, *Bioresour. Technol.* **2005**, *96*: 2014-2018.
192. Wyman, C.E.; Dale, B.E.; Elander, R.T.; Holtzapple, M.; Ladisch, M.R.; Lee, Y.Y., Coordinated Development of Leading Biomass Pretreatment Technologies, *Bioresour. Technol.* **2005**, *96*: 1959-1966.
193. Ghosh, P.; Pamment, N.B.; Martin, W.R.B., Simultaneous Saccharification and Fermentation of Cellulose: Effect of  $\beta$ -Glucosidase Activity and Ethanol Inhibition of Cellulases, *Enzyme Microb. Technol.* **1982**, *4*: 425-430.
194. Kim, C.H.; Rhee, S.K., Process Development for Simultaneous Starch Saccharification and Ethanol Fermentation by *Zymomonas Mobilis*, *Process Biochem.* **1993**, *28*: 331-339.
195. Saha, B.C.; Iten, L.B.; Cotta, M.A.; Wu, Y.V., Dilute Acid Pretreatment, Enzymatic Saccharification and Fermentation of Wheat Straw to Ethanol, *Process Biochem.* **2005**, *40*: 3693-3700.
196. Wyman, C.E.; Spindler, D.D.; Grohmann, K., Simultaneous Saccharification and Fermentation of Several Lignocellulosic Feedstocks to Fuel Ethanol, *Biomass Bioenerg.* **1992**, *3*: 301-307.
197. Aden, A.; Ruth, M.; Ibsen, K.; Jechura, J.; Neeves, K.; Sheehan, J.; Wallace, B., Lignocellulosic Biomass to Ethanol Process Design and Economics Utilizing Co-current Dilute Acid Prehydrolysis and Enzymatic Hydrolysis for Corn Stover. June 2002, National Renewable Energy Laboratory: Golden, CO.
198. Román-Leshkov, Y.; Chheda, J.N.; Dumesic, J.A., Phase Modifiers Promote Efficient Production of Hydroxymethylfurfural from Fructose, *Science* **2006**, *312*: 1933-1937.
199. Chheda, J.N.; Dumesic, J.A., An Overview of Dehydration, Aldol-Condensation and Hydrogenation Processes for Production of Liquid Alkanes from Biomass-Derived Carbohydrates, *Catal. Today* **2007**, *123*: 59-70.
200. Cortright, R.D.; Davda, R.R.; Dumesic, J.A., Hydrogen from Catalytic Reforming of Biomass-Derived Hydrocarbons in Liquid Water, *Nature* **2002**, *418*: 964-967.

201. Davda, R.R.; Shabaker, J.W.; Huber, G.W.; Cortright, R.D.; Dumesic, J.A., Aqueous-Phase Reforming of Ethylene Glycol on Silica-Supported Metal Catalysts, *Appl. Catal. B Environ.* **2003**, *43*: 13-26.
202. Davda, R.R.; Shabaker, J.W.; Huber, G.W.; Cortright, R.D.; Dumesic, J.A., A Review of Catalytic Issues and Process Conditions for Renewable Hydrogen and Alkanes by Aqueous-Phase Reforming of Oxygenated Hydrocarbons Over Supported Metal Catalysts, *Appl. Catal. B Environ.* **2005**, *56*: 171-186.
203. Elliott, D.C.; Hart, T.R.; Neuenschwander, G.G., Chemical Processing in High-Pressure Aqueous Environments. 8. Improved Catalysts for Hydrothermal Gasification, *Ind. Eng. Chem. Res.* **2006**, *45*: 3776-3781.
204. Elliott, D.C.; Neuenschwander, G.G.; Hart, T.R.; Butner, R.S.; Zacher, A.H.; Engelhard, M.H.; Young, J.S.; McCready, D.E., Chemical Processing in High-Pressure Aqueous Environments. 7. Process Development for Catalytic Gasification of Wet Biomass Feedstocks, *Ind. Eng. Chem. Res.* **2004**, *43*: 1999-2004.
205. Elliott, D.C.; Neuenschwander, G.G.; Phelps, M.R.; Hart, T.R.; Zacher, A.H.; Silva, L.J., Chemical Processing in High-Pressure Aqueous Environments. 6. Demonstration of Catalytic Gasification for Chemical Manufacturing Wastewater Cleanup in Industrial Plants, *Ind. Eng. Chem. Res.* **1999**, *38*: 879-883.
206. Elliott, D.C.; Phelps, M.R.; Sealock, L.J.; Baker, E.G., Chemical Processing in High-Pressure Aqueous Environments. 4. Continuous-Flow Reactor Process Development Experiments for Organics Destruction, *Ind. Eng. Chem. Res.* **1994**, *33*: 566-574.
207. Elliott, D.C.; Sealock, L.J.; Baker, E.G., Chemical Processing in High-Pressure Aqueous Environments. 2. Development of Catalysts for Gasification, *Ind. Eng. Chem. Res.* **1993**, *32*: 1542-1548.
208. Elliott, D.C.; Sealock, L.J., Jr.; Baker, E.G., Chemical Processing in High-Pressure Aqueous Environments. 3. Batch Reactor Process Development Experiments for Organics Destruction, *Ind. Eng. Chem. Res.* **1994**, *33*: 558-565.
209. Sealock, L.J.; Elliott, D.C.; Baker, E.G.; Butner, R.S., Chemical Processing in High-Pressure Aqueous Environments. 1. Historical Perspective and Continuing Developments, *Ind. Eng. Chem. Res.* **1993**, *32*: 1535-1541.
210. Sealock, L.J.; Elliott, D.C.; Baker, E.G.; Fassbender, A.G.; Silva, L.J., Chemical Processing in High-Pressure Aqueous Environments. 5. New Processing Concepts, *Ind. Eng. Chem. Res.* **1996**, *35*: 4111-4118.
211. Huber, G.W.; Iborra, S.; Corma, A., Synthesis of Transportation Fuels from Biomass: Chemistry, Catalysts, and Engineering, *Chem. Rev.* **2006**, *106*: 4044-4098.
212. Sluiter, A.; Hames, B.; Ruiz, R.; Scarlata, C.; Sluiter, J.; Templeton, D.; Crocker, D., Determination of Structural Carbohydrates and Lignin in Biomass, Technical Report NREL/TP-510-42618.
213. Alltech, Carbohydrate Analysis - Prevail Carbohydrate ES HPLC Columns and ELSD, Brochure #467A.
214. Agblevor, F.A.; Hames, B.R.; Schell, D.; Chum, H.L., Analysis of Biomass Sugars Using a Novel HPLC Method, *Appl. Biochem. Biotechnol.* **2007**, *136*: 309-326.

215. Dionex, Analysis of Carbohydrates by High-Performance Anion-Exchange Chromatography with Pulsed Amperometric Detection (HPAE-PAD), Technical Note 20.
216. Dionex, Optimal Setting for Pulsed Amperometric Detection of Carbohydrates Using the Dionex ED40, Technical Note 21.
217. Shimadzu, Total Organic Carbon Analyzer TOC-V Series, Instruction Manual.
218. Segal, L.; Creely, J.J.; Martin Jr., A.E.; Conrad, C.M., An Empirical Method for Estimating the Degree of Crystallinity of Native Cellulose Using the X-Ray Diffractometer, *Text. Res. J.* **1959**, *29*: 786-794.
219. Li, X.; Converse, A.O.; Wyman, C.E., Characterization of Molecular Weight Distribution of Oligomers from Autocatalyzed Batch Hydrolysis of Xylan, *Appl. Biochem. Biotechnol.* **2003**, *105-108*: 515-522.
220. Liu, C.; Wyman, C.E., The Effect of Flow Rate of Compressed Hot Water on Xylan, Lignin, and Total Mass Removal from Corn Stover, *Ind. Eng. Chem. Res.* **2003**, *42*: 5409-5416.
221. Bradbury, A.G.W.; Sakai, Y.; Shafizadeh, F.J., A Kinetic Model for Pyrolysis of Cellulose, *J. Appl. Polym. Sci.* **1979**, *23*: 3271-3280.
222. Ito, T.; Hirata, Y.; Sawa, F.; Shirakawa, N., Hydrogen Bond and Crystal Deformation of Cellulose in Sub/Super-critical Water, *Jpn. J. Appl. Phys.* **2002**, *41*: 5809-5814.
223. Watanabe, A.; Morita, S.; Ozaki, Y., Study on Temperature-Dependent Changes in Hydrogen Bonds in Cellulose I $\beta$  by Infrared Spectroscopy with Perturbation-Correlation Moving-Window Two-Dimensional Correlation Spectroscopy, *Biomacromolecules* **2006**, *7*: 3164-3170.
224. Watanabe, A.; Morita, S.; Ozaki, Y., Temperature-Dependent Changes in Hydrogen Bonds in Cellulose I $\alpha$  Studied by Infrared Spectroscopy in Combination with Perturbation-Correlation Moving-Window Two-Dimensional Correlation Spectroscopy: Comparison with Cellulose I $\beta$ , *Biomacromolecules* **2007**, *8*: 2969-2975.
225. Chaiwat, W.; Hasegawa, I.; Kori, J.; Mae, K., Examination of Degree of Cross-Linking for Cellulose Precursors Pretreated with Acid/Hot Water at Low Temperature, *Ind. Eng. Chem. Res.* **2008**, *47*: 5948-5956.
226. Chaiwat, W.; Hasegawa, I.; Tani, T.; Sunagawa, K.; Mae, K., Analysis of Cross-Linking Behavior during Pyrolysis of Cellulose for Elucidating Reaction Pathway, *Energy Fuels* **in press**.
227. Zhang, S.; Wilson, D.B.J., Surface Residue Mutations which Change the Substrate Specificity of Thermomonospora Fusca Endoglucanase E2, *J. Biotechnol.* **1997**, *57*: 101-113.
228. Zhang, Y.-H.P.; Lynd, L.R., Toward an Aggregated Understanding of Enzymatic Hydrolysis of Cellulose: Noncomplexed Cellulase Systems, *Biotechnol. Bioeng.* **2004**, *88*: 797-824.
229. Paakkari, T.; Serimaa, R.; Fink, H.P., Structure of amorphous cellulose, *Acta Polymerica* **1989**, *40*: 731-734.
230. Mazeau, K.; Heux, L., Molecular Dynamics Simulations of Bulk Native Crystalline and Amorphous Structures of Cellulose, *J. Phys. Chem. B* **2003**, *107*: 2394-2403.

231. Zhao, H.; Kwak, J.H.; Wang, Y.; Franz, J.A.; White, J.M.; Holladay, J.E., Effects of Crystallinity on Dilute Acid Hydrolysis of Cellulose by Cellulose Ball-Milling Study, *Energy Fuels* **2006**, *20*: 807-811.

**Every reasonable effort has been made to acknowledge the owners of copyright material. I would be pleased to hear from any copyright owner who has been omitted or incorrectly acknowledged.**